Analysis of the Spindle Assembly Checkpoint in Vertebrates

Helen Dodson

Ph.D. Thesis

Wellcome Trust Centre for Cell Biology
Institute of Cell and Molecular Biology
University of Edinburgh

February 2003

I declare that all the work presented in this thesis is my own except where stated otherwise, and it has been entirely composed by myself.

Helen Dodson

Acknowledgements

Firstly, I would like to thank my supervisor Bill Earnshaw for all his help and encouragement during my Ph.D.

Also, I would like to thank all the members of the Earnshaw lab, past and present, who made me welcome, helped and encouraged me. Ana, Anca, Ciaran, Chih-Jui, Damien, Fiona, Helder, Kumiko, Liz, Mar, Nadia, Paola, Richard, Reto, Sally, Sander, Sandrine, Sarah and Steffi – a big thank you to you all.

In particular, I would like to thank Ciaran Morrison for his role as day to day supervisor for a good part of my Ph.D. Thanks for your continued support and encouragement and for the many wise words you spoke.

A special thank you to Damien, Nadia, Liz, Sander and Sarah for taking the time to read my thesis and helping me with ideas and corrections.

I would also like to thank Richard Adams and Andreas Merdes for help with the frogs.

A special thanks to my good friends, Nadia, for always knowing and understanding what I was feeling, it has been great to 'go through it together'. Damien, for always answering my stupid questions, and Sandrine, for her help and patience.

Thanks to my parents and my brother, Iain, for their continued love, support and encouragement in everything I do.

Finally, thanks to Bob, not only for his help in the preparation of this thesis, but for his love and encouragement.

Abbreviations

λ	bacteriophage lambda
°C	degrees Celsius
µF	microfarad
A	ampere
APS	ammonium persulphate
ATP	adenosine-5′-triphosphate
BLAST	basic local alignment search tool
bp	base pair(s)
BSA	bovine serum albumin
Bsr	blasticidin resistance cassette
cDNA	complementary DNA
CIP	calf intestinal alkaline phosphatase
CLAP	chymostatin, leupeptin, antipain, pepstatin A
Coomassie	Coomassie Brilliant Blue R
CREST	calcinosis/Raynaud's phenomenon/esophageal dysmotility/telangiectasia variant of scleroderma
DAPI	4′,6-diamidino-2-phenylindole
database	NCBI sequence database
DEPC	diethylpyrocarbonate
dH_2O	de-ionised water
DMSO	dimethylsulfoxide
DNA	deoxyribonucleic acid
dNTPs	deoxyribonucleotide-5′-triphosphate
Drosophila	*Drosophila melanogaster*
DTT	1,4-dithiothreitol
E. coli	*Escherichia coli*
ECL	enhanced chemiluminescence
EDTA	ethylenediaminetetraacetic acid
EST	expressed sequence tag
FBS	fetal bovine serum
FITC	fluorescein isothiocyanate
g	gram
g	gravity
HEPES	*N*-[2-Hydroxyethyl]piperazine-*N*′-[2-ethanesulfonic acid]
HisD	histidinol resistance cassette
Hyg	hygromycin resistance cassette
GST	glutathione S transferase
hCG	human chorionic gonadotropin
HRP	horseradish peroxidase
IPTG	isopropyl β-D-thiogalactopyranoside
J	joule
l	litre(s)
kb	kilobase pair(s)
KDa	kilodaltons
KOV1	knock out vector 1
KOV2	knock out vector 2
LB	Luria-Bertani medium
M	molar, (moles/litre)
mRNA	messenger RNA
NGS	normal goat serum

OD	optical density
phage	bacteriophage λ
PBS	phosphate buffered saline
PBS-T	PBS with 0.05% tween-20
PCR	polymerase chain reaction
pfu	plaque forming unit
PMSF	phenylmethylsulfonyl fluoride
PMSG	pregnant mare serum gonadotropin
PTX-BSA	2.5% BSA solution in PBS with 0.2% Triton X-100
Puro	puromycin resistance cassette
RNA	ribonucleic acid
RNAi	RNA interference
RNase	ribonuclease
rpm	revolutions per minute
RT-PCR	reverse transcriptase PCR
SDS	sodium dodecyl sulphate
SDS-PAGE	SDS polyacrylamide gel eletrophoresis
TAE	tris acetate EDTA
TEMED	*N,N,N′,N′* - tetramethylethylenediamine
Tris	Tris (hydroxymethyl)aminomethane
TRIzol	Total RNA Isolation Reagent
UTR	untranslated region
UV	ultraviolet
V	volt
w/v	weight/volume
w/w	weight/weight
XB	extract buffer
Xenopus	*Xenopus laevis*

Standard prefixes used:

k	kilo (10^{3})
m	milli (10^{-3})
μ	micro (10^{-6})
n	nano (10^{-9})
p	pico (10^{-12})

Table of Contents

List of Figures

Abstract

At mitosis, chromosomes must be accurately partitioned between the two newly forming daughter cells. To ensure that no vital genetic information is lost, this must happen with the utmost accuracy and to this end the process is controlled and monitored by a mechanism known as the spindle assembly checkpoint. This mechanism is highly conserved throughout eukaryotes. The proteins of this checkpoint are located at the kinetochore, a proteinaceous structure that overlies the centromeric DNA. The checkpoint functions by sensing attachment and/or tension of the microtubules at the kinetochore and halting the progression of the cell cycle. This is achieved by inhibiting the anaphase promoting complex, an E3 ubiquitin ligase that triggers the onset of anaphase by targeting key proteins for degrading.

One such checkpoint protein localised to the kinetochore in vertebrate cells is BubR1. I have cloned the chicken *BubR1* cDNA and raised antibodies to the protein. The protein is highly conserved when compared to other vertebrate BubR1s with 55% identity and 70% similarity to human. The antibody recognises a protein of approximately 150 kDa and stains the kinetochores of chicken cells during prometaphase with the signal disappearing as they become attached to microtubules, a localisation typical of spindle checkpoint proteins. In order to further characterise the function of this protein in vertebrates, I have attempted to generate a chicken DT40 cell line conditionally null for *BubR1*. I have successfully targeted one allele of the *BubR1* locus in DT40 cells. *BubR1* (+/-) cells grow normally and have an intact checkpoint. Since I expect *BubR1* to be essential, the gene must be expressed under the control of the tetracycline operator in the heterozygote cells. Attempts to target the second allele have failed thus far, although the expected targeting frequency is 1/20 clones. It appears that expression of exogenous BubR1 is detrimental to these cells and they shut off expression when possible. It seems that expression levels of this essential checkpoint component are critical to avoid problems within the cell.

In addition to this study in chicken cells I have cloned two other vertebrate checkpoint components from *Xenopus laevis*. The proteins Zw10 and Rod were initially identified in *Drosophila* and since no homologues have been identified in yeast these are considered as metazoan-specific components of the spindle assembly checkpoint. In order to study the checkpoint and the kinetochore, I have cloned partial *Xenopus* cDNA for *Zw10* and *Rod* and raised antibodies to these proteins. Zw10 is localised to the kinetochores of metaphase *Xenopus* cells and along with Rod is present in a complex of approximately 11S in *Xenopus* egg extracts. The cloning and generation of antibodies to these proteins in *Xenopus* will hopefully be the basis of further study into this complex, other interactors and the vertebrate kinetochore complex.

Chapter 1

Introduction

1.1 Overview

For the continuation of life, be it multiplication of a single celled organism, development of a fertilised embryo or regeneration of a tissue, cells must accurately replicate their DNA and then equally segregate it between the two newly forming daughter cells. This process is known as the cell cycle and is controlled by the activation or inactivation of members of a conserved family of proteins known as cyclin-dependant kinases. Various checkpoints are present throughout the cell cycle to ensure that mistakes are minimised. The classical definition of a cell cycle checkpoint is a point which the cycle cannot proceed beyond until certain criteria have been met. In the case of the spindle assembly checkpoint, anaphase cannot ensue until all chromosomes are attached in a biorientated fashion and are under tension.

The spindle assembly checkpoint is the mechanism which ensures that the newly replicated DNA is segregated accurately between the two new daughter cells. This checkpoint is highly conserved and regulated by a number of different proteins that form multiple complexes. This checkpoint works by sensing tension and/or attachment of microtubules to the kinetochore and sends an inhibitory 'wait anaphase' signal to the APC/C (Anaphase Promoting Complex or Cyclosome). The APC/C is a multi-subunit complex which targets proteins for ubiquitination and hence degradation. Once the spindle assembly checkpoint is satisfied, the APC/C is activated. One key event leading to the progression of the cell cycle is the cleavage of a molecule called securin, which in turn leads to the activation of separase which cleaves Scc1, a component of the cohesin complex. The cohesin complex is required for sister chromatid pairing and holds the chromosomes together, once Scc1 is cleaved this releases the cohesion at the centromeres allowing the cell to progress into anaphase.

Errors in this checkpoint lead to aberrant segregation, which can lead to aneuploidy. At meiosis this can cause birth defects such as Down's Syndrome and at mitosis has been implicated in the progression of cancer (tumour progression).

1.2 Cell cycle progression

The cell cycle is divided into four phases, G1, S phase where DNA replication occurs, G2 and M (mitosis or cell division), G1 and G2 are gap phases between replication and division. Figure 1.1 shows a schematic representation of the cell cycle indicating the changes in the DNA, which occur, and the various checkpoints.

Figure 1.1. Schematic representation of the cell cycle

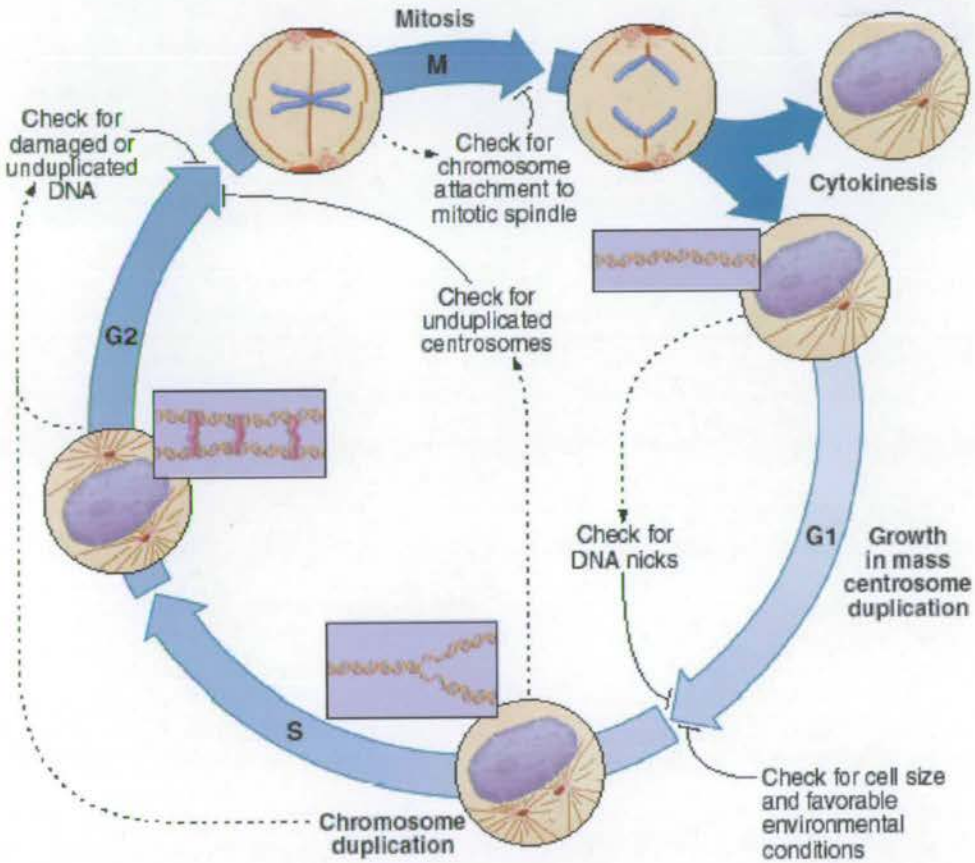

Schematic representation of the cell cycle, showing the various stages and the checkpoints. As discussed in the text the G1 checkpoint or restriction point, DNA damage checkpoint and spindle assembly checkpoint are indicated. Diagram adapted from Cell Biology by Pollard and Earnshaw.

CDK (cyclin dependant kinases) require the binding of a cyclin for activity. In addition to the regulation of these kinases by cyclin binding the CDK must also be phosphorylated and there are known specific cyclin-CDK inhibitors. More than ten cdks, which control various stages of the cell cycle, have been identified in vertebrates. For example cdk1 is known to control the G2 to M transition, cdk2 plays

a role in both G1 to S and G2 to M transition and cdk4 and cdk6 play a role in the restriction point. The restriction point is a checkpoint in the G1 phase of the cycle, which ensures that a cell does not go into replication unless the size and state of the cell are appropriate (for review see (Zetterberg *et al.*, 1995; Planas-Silva & Weinberg, 1997)).

There are 16 human cyclins, which although being diverse proteins share a core structure. The complex of cyclin and cdk regulates the cell cycle along with many other activators and inhibitors which alter the phosphorylation and localisation state of these proteins.

1.3 Chromosome structure

In order that the DNA can fit into the nucleus of a eukaryotic cell it must condense and compact enormously. Estimates for an average human cell are that the 6.6×10^9 base pairs of DNA, which stretch up to 2 metres must be packaged into the human cell nucleus of 5 - 20 μm in diameter. The precise details of this compaction still remain to be fully elucidated. However, it is known that the DNA associates with proteins to form a structure known as chromatin. The main proteins involved in the compaction of the DNA are the histones. DNA wraps around a complex of histone molecules to form a structure known as a nucleosome, resulting in a 7-fold compaction of the naked DNA (Kornberg, 1974). In turn the nucleosomes are compacted further to form the 30 nm fibre, which results in a 40 fold shortening. The next stage of compaction, and perhaps the highest order of packaging of the interphase nucleus, has been identified as a fibre of between 100-300 nm in diameter, which has been termed the chromonema fibre. This structure appears to be organised into loop domains where specific regions of the DNA may anchor to the chromosome scaffold thus forming loops (Marsden & Laemmli, 1979).

Upon entry into mitosis the chromosomes must condense further in order that they can become attached to the apparatus of the mitotic spindle and be segregated. During anaphase the chromosomes must move a distance of 5 – 20 μm, and therefore must be highly compacted in order that this movement can occur. This condensation process begins at prophase before nuclear envelope breakdown. The process of condensation is still poorly understood. However, it is clear that a complex known as condensin is required for this process. The two most abundant non-histone protein

components of the metaphase chromosomes are topoisomerase II and the condensin complex. Topoisomerase II is an ATP-dependant DNA strand-passing enzyme. Presumably, it is required in abundance on the mitotic chromosomes to help untangle the DNA as it is organised into a highly condensed state. The condensin complex was initially isolated from *Xenopus* egg extracts (Hirano & Mitchison, 1994) and is composed of five subunits, which are conserved from yeast to humans. This complex organises condensation by altering the topology of DNA loops, since it is able to introduce positive writhe (Kimura *et al.*, 1999), and positive supercoiling into DNA molecules (Kimura & Hirano, 1997; Kimura *et al.*, 2001). The five subunit complex is composed of two SMC (Structural Maintenance of Chromosomes, SMC2 and SMC4) proteins, which form a V-shaped dimer. Each SMC molecule is composed of two antiparallel, coiled-coil arms with a flexible hinge. The most recent model for the dimerisation is that this is mediated by a hinge-hinge interaction between self-folded monomers (Hirano & Hirano, 2002). The SMC components are associated with the regulatory subcomplex consisting of three non-SMC proteins namely, XCAP-D/Cnd1, XCAP-H/Cnd2 and XCAP-G/Cnd3. It is known that the interaction between the regulatory subcomplex and the SMC components increases the DNA binding and ATPase activity of the complex (Kimura & Hirano, 2000). The most recent model proposed by (Bazett-Jones *et al.*, 2002), suggests that the complex introduces positive supercoils into the DNA resulting in a compacted structure. It is known that condensation is absolutely required for chromosome segregation, since yeast mutants in components of this complex fail to segregate their chromosomes resulting in a 'cut' phenotype (Saka *et al.*, 1994; Strunnikov *et al.*, 1995; Sutani *et al.*, 1999; Freeman *et al.*, 2000). In addition, work in *Caenorhabditis elegans* has shown that the condensin complex is required for chromosome condensation and segregation (Hagstrom *et al.*, 2002). Also, a study in DT40 cells shows that the condensin subunit SMC2 is required for some lateral condensation of the chromosome. However, the main defect is the failure in anaphase (D. Hudson, personal communication). This along with other data from *Drosophila* (Steffensen *et al.*, 2001) has led to the hypothesis that condensation is required for overall chromosome structure and segregation.

1.4 Chromosome cohesion and segregation

Cohesion between sister chromatids is established during replication and this cohesion must be reversed in order that the chromosomes can separate at anaphase. The complex required to keep sister chromatids together is known as the cohesin complex. Like the condensin complex it is composed of SMC and non–SMC proteins (Losada *et al.*, 1998; Darwiche *et al.*, 1999). The SMC proteins, SMC1 and SMC3, form a V- shaped heterodimer. Each protein is folded back on itself at the hinge region and the hinge region is the point of interaction forming a V-shaped molecule (Haering *et al.*, 2002). SMC1 and SMC3 interact with Scc1, which bridges the two head domains resulting in the formation of a loop. It has been proposed that the replicated DNA may be trapped within this proteinaceous ring (Haering *et al.*, 2002). This therefore led to a proposed model where the DNA strands are held together by topological rather than chemical means. Scc1 is the protein whose cleavage by separase triggers anaphase allowing the chromatids to move apart to the spindle poles (Uhlmann *et al.*, 1999; Rao *et al.*, 2001). The dissociation of cohesin from the chromosomes occurs in two distinct stages in eukaryotes. The first stage occurs during prophase in tandem with the association of the condensin complex onto the mitotic chromosomes (Sumara *et al.*, 2000; Waizenegger *et al.*, 2000). At this stage, cohesin is lost from the chromosome arms but remains associated at the centromere regions. It is known that this dissociation is, at least in part, regulated by polo-like kinase (PLK) (Alexandru *et al.*, 2001; Sumara *et al.*, 2002). Cohesin remains at the centromere regions until the onset of anaphase. The dissociation is prevented by the spindle assembly checkpoint, as discussed previously, until all the kinetochores are properly aligned on the metaphase plate with microtubule attachments to each pole and under tension. At this time the APC/C is activated leading to the degradation of securin (Pds1p) (Cohen-Fix *et al.*, 1996), which releases activated separase (Esp1p) (Ciosk *et al.*, 1998), resulting in the cleavage of Scc1 (Uhlmann *et al.*, 1999) and dissociation of the sister chromatids.

1.5 Chromosomal Passenger Proteins

The chromosome passengers are a group of proteins recognised by their distinctive localisation during mitosis, whereby they move from the chromosome arms during prometaphase to the centromeres and then to the spindle midzone during anaphase.

This group of proteins consists of three members, namely, INCENP, AuroraB and Survivin.

INCENP was the first of these proteins to be characterised and before any knockout study or RNAi an indication of its role came from studies of a deletion mutant, 1-405. Expression of the deletion mutant results in the mislocalisation of the endogenous INCENP and causes defects in chromosome congression, segregation and cytokinesis (Mackay *et al.*, 1998). Knocking out INCENP in mouse resulted in very early embryonic lethality, with embryos only surviving to the 32 - 64 cell stage with defects in cytokinesis and abnormal bundling of microtubules (Cutts *et al.*, 1999).

Initial indications in yeast (Kim *et al.*, 1999), which were subsequently confirmed *in vivo* from *Xenopus* egg extracts, identified a complex formed between INCENP and AuroraB kinase (Adams *et al.*, 2000). The Aurora kinases were initially identified in yeast (Chan & Botstein, 1993) and subsequently in *Drosophila* as genes which regulate the structure and function of the mitotic spindle (Glover *et al.*, 1995). Different organisms have different members of this family of proteins, for example three in human, two in *Drosophila* and *C. elegans* and only one, Ipl1, in yeast. The Aurora family of protein kinases are implicated in human cancers with aurora-A being amplified in several human cancers and aurora-B and C being overexpressed in many human cancer cell lines.

Survivin is also now known to be a component of the passenger complex in *Xenopus* (Bolton *et al.*, 2002), *C. elegans* (Kaitna *et al.*, 2000; Speliotes *et al.*, 2000) and human (Wheatley *et al.*, 2001). This is a small protein containing a BIR (baculovirus IAP repeat) domain. Other known IAP proteins bind and inhibit caspases and therefore play a role in apoptosis. Survivin's role, if any, in apoptosis is controversial. Its main role appears to be in mitosis. As with the other passengers Survivin regulates chromosome movement and spindle events. The function of Survivin has been investigated by gene disruption in mouse, this resulted in embryonic lethality at day 4.5 with the cells having disrupted microtubule formation and becoming polyploid (Uren *et al.*, 2000). INCENP (Sli15), Aurora-B (Ipl1) and Survivin (Bir1), have been shown to be physically associated in budding yeast (Cheeseman *et al.*, 2002).

1.6 Centromere/kinetochore

The centromere is the specialised region of the chromosome where the microtubules attach. It is a nucleoprotein structure requiring both DNA and protein to function. What constitutes a centromere and how the position is faithfully maintained through cell division is still under active investigation, although a growing number of facts are now known. The kinetochore is a proteinaceous structure, which is embedded in the surface of the centromeric heterochromatin, and more precisely is the region where microtubules attach and the movements of the chromosome are directed.

1.6.1 Centromere Structure

The centromeric DNA varies in size between different organisms, ranging from just 125 bp in the yeast *Saccharomyces cerevisiae* to megabases in humans. The DNA sequence of the centromere has been fully characterised in the model organism *S. cerevisiae*, budding yeast, which has 16 chromosomes. A consensus sequence, with three DNA elements, has been defined in this organism and these elements are referred to as CDEI, CDEII and CDEIII. It seems that these sequences specify protein binding sites and that they are sufficient to act as a centromere. This has been demonstrated by experiments where the centromere elements have been introduced into plasmid DNA which as a result, becomes mitotically stable and segregates as if chromosomal.

In *S. cerevisiae* a 125 bp region of DNA is sufficient to direct segregation of the chromosomes. In stark contrast to this, the structure of the centromere of the yeast, *Schitzosaccharamyces pombe*, fission yeast, spans a region of 35,000 - 110,00 bp. This organism has three chromosomes, which are larger than those of *S. cerevisiae*. In addition, the centromere DNA is strikingly different. In *S. pombe* the centromeres have a central core of 4 – 7 kb of unique sequence, which is flanked by complex arrays of repeated sequence. It is also known that the centromeric DNA of this organism is heterochromatic since genes in the centromere are repressed (Allshire *et al.*, 1995). Investigation of the centromeric DNA sequences has also been carried out in higher organisms. In *Drosophila melanogaster* the centromeres investigated are larger, around 420 kb, and are rich in simple satellite DNA sequences and transposable elements (Murphy & Karpen, 1995). No sequences were found to be in common with yeast centromeres and interestingly none of the sequence was unique

to the centromere region: all sequence found could also be found on the chromosome arms of *Drosophila*. The structure of mammalian centromere DNA has also been investigated and is mainly composed of satellite DNA sequences. Satellite DNA is composed of repeated copies of short DNA sequences clustered together in head to tail arrays. The main constituent of primate centromere DNA is alpha satellite which consists of 171 bp monomers organised into high order repeats. Some monomers have 17 bp CENP-B boxes contained within them, which function to bind the centromeric protein CENP-B.

1.6.2 Constitutive centromere components

A number of constitutive centromere proteins have been identified and these appear to be conserved throughout eukaryotes. One such protein is CENP-A, which is a Histone H3 variant (Shelby *et al.*, 1997). The histones are proteins involved in wrapping up the naked DNA into its functional chromatin form. It has been discovered that, at centromeres, histone H3 is replaced by CENP-A which presumably plays some role in defining the centromeric DNA and allows it to function in a specific manner (Vafa & Sullivan, 1997). CENP-A is essential for life (Howman *et al.*, 2000), and is required for the targeting of another centromeric protein CENP-C. Orthologues of CENP-A have also been found in yeast, *S. cerevisae* and *S. pombe* and are called CSE4p and spCENP-A/Cen1 respectively (Meluh *et al.*, 1998; Takahashi *et al.*, 2000).

Another constitutive centromere protein is CENP-B. This protein is highly conserved and binds to specific sequences of DNA known as CENP-B boxes which are present in centromeric DNA (Masumoto *et al.*, 1989). The role of CENP-B within the centromere is not clearly understood and one striking observation is that mice null for CENP-B are viable and have no obvious defects in centromere function (Hudson *et al.*, 1998; Kapoor *et al.*, 1998; Perez-Castro *et al.*, 1998). Recently, it has been shown that both CENP-B boxes and alphoid DNA sequence are required for *de novo* mammalian artificial chromosome formation (Ohzeki *et al.*, 2002). In addition it has been noted that the vertebrate Y chromosome contains little or no CENP-B boxes (Kipling & Warburton, 1997), nor does the centromeric DNA of African green monkey cells (Goldberg *et al.*, 1996). CENP-B shares homology with a transposable element of the pogo superfamily and for many years the link between transposable

elements and centromeres was unclear. Recent evidence has shown that components of the RNAi machinery are somehow involved in centromere function, primarily in silencing of the chromatin (Volpe *et al.*, 2002). RNAi or RNA interference is a mechanism by which genes are post-transcriptionally silenced in a sequence specific manner by double stranded RNA (for review see (Hammond *et al.*, 2001)). It has been suggested, from evidence in *Drosophila* and *C.elegans* (Ketting *et al.*, 1999; Aravin *et al.*, 2001) that RNAi may have evolved in order to immobilise transposable elements. This may therefore be a clue towards answering questions as to CENP-B's role at the centromere.

CENP-C, another constitutive centromere component, is a DNA binding protein concentrated at the inner plate of the kinetochore. It is known that this protein is essential for the viability of vertebrate cells (Fukagawa & Brown, 1997; Kalitsis *et al.*, 1998), and is involved in the assembly and functioning of the kinetochore (Tomkiel *et al.*, 1994; Fukagawa & Brown, 1997). Like CENP-A, orthologues of CENP-C have been identified in yeast, namely mif2 in *S. cerevisae* (Meeks-Wagner *et al.*, 1986; Meluh & Koshland, 1995) and Cnp3 in *S. pombe* (R. Allshire, Personal Communication).

CENP-G is a protein localised to the inner kinetochore plate which associates with alpha- satellite DNA (He *et al.*, 1998). It is known to be associated with neocentromeres and the inactive centromere (Gimelli *et al.*, 2000). CENP-G has not been cloned and little further is known about it.

In recent years two other constitutive centromere proteins have been identified, namely CENP-H and CENP-I. CENP-H was initially identified in mouse as a 33 kDa centromere associated protein with a coiled-coil domain (Sugata *et al.*, 1999). Subsequently, it has been identified in human (Sugata *et al.*, 2000). It is localised to the inner kinetochore plate alongside CENP-A and CENP-C during both interphase and mitosis and has been shown to be present at neocentromeres but not at inactive centromeres. In addition, CENP-H can bind to itself and to the mitotic centromere associated kinesin, MCAK (Sugata *et al.*, 2000). A conditional DT40 knockout of CENP-H has been generated and this revealed that the protein is necessary for the progression of the cell cycle since null cells arrest at metaphase (Fukagawa *et al.*, 2001). In addition CENP-H is required for the targeting of CENP-C, but not CENP-A, to the kinetochore.

CENP-I has also been identified as a constitutive centromere component in vertebrate cells and, in a manner similar to CENP-H, the function has been analysed by the generation of a conditionally null DT40 cell line (Nishihashi *et al.*, 2002). CENP-I has homology to the *S. pombe* centromere protein Mis6 and co-localises with CENP-A, CENP-C and CENP-H throughout the cell cycle. As is the case with CENP-H, CENP-I is required for the localisation of CENP-C to the kinetochore, but not for the localisation of CENP-A. In addition cells lacking CENP-I arrested in prometaphase without misaligned chromosomes. It has been shown in *S. pombe* that Mis6 is required for the recruitment of CENP-A to the kinetochore (Takahashi *et al.*, 2000).

Recently, Mis12 was identified as a novel kinetochore protein family which is conserved from yeast to human and essential for equal chromosome segregation (Goshima *et al.*, 2003). The human homologue is localised to a region indistinguishable from CENP-A. Depletion of Mis12 in human cells by RNAi resulted in a number of defects including misaligned metaphase chromosomes, lagging anaphase chromosomes, and an abnormally long metaphase spindle length (Goshima *et al.*, 2003). Table 1.1 summarises the current understanding of the constitutive centromere proteins.

Table 1.1. Summary of centromere associated proteins

Centromere protein	Comments and key references
CENP-A	• Histone variant (Shelby *et al.*, 1997), which marks and allows the formation of a centromere (Vafa & Sullivan, 1997) • Essential for life and required for targeting of CENP-C (Howman *et al.*, 2000) • Found at neocentromeres, active centromeres but not inactive centromere (du Sart *et al.*, 1997) • Inner kinetochore plate protein (Warburton *et al.*, 1997)
CENP-B	• Binds CENP-B boxes (Masumoto *et al.*, 1989) • Significance of this not understood since Y- chromosome (Kipling & Warburton, 1997) and African green monkey cells (Goldberg *et al.*, 1996) lack them at the centromere • CENP-B mice are viable (Hudson *et al.*, 1998; Kapoor *et al.*, 1998; Perez-Castro *et al.*, 1998) • Not found at neocentromeres, but localised to both the active and inactive centromere (Earnshaw *et al.*, 1989)
CENP-C	• Inner kinetochore protein required for assembly and function (Tomkiel *et al.*, 1994) • Essential for viability (Fukagawa & Brown, 1997; Kalitsis *et al.*, 1998) • Found at neocentromeres, active centromeres but not inactive centromere (Earnshaw *et al.*, 1989)
CENP-E	• Kinesin like motor protein (Yen *et al.*, 1992; Wood *et al.*, 1997) • Not a constitutive centromere protein, but localised to the kinetochore during prometaphase (Yen *et al.*, 1991) • Plays a role in the spindle assembly checkpoint in vertebrates (Abrieu *et al.*, 2000)
CENP-F	• 400 kDa outer kinetochore protein (Rattner *et al.*, 1993) • Not a constitutive centromere protein, but localised to the kinetochore from prophase to anaphase (Liao *et al.*, 1995) • Modified by farnesylation (Hussein & Taylor, 2002)
CENP-G	• A constitutive inner kinetochore plate protein (He *et al.*, 1998) • Associates with neocentromeres and inactive centromeres (Gimelli *et al.*, 2000)
CENP-H	• Inner kinetochore plate protein which interacts with MCAK (Sugata *et al.*, 2000) • Required for cell cycle progression and targeting of CENP-C, but not CENP-A to the kinetochore (Fukagawa *et al.*, 2001) • Present at the active centromere only (Sugata *et al.*, 2000)
CENP-I	• S. *cerevisae* Mis6 homologue • Inner kinetochore plate protein required for cell cycle progression and targeting of CENP-C, but not CENP-A to the kinetochore (Nishihashi *et al.*, 2002) • Required for CENP-A targeting In *S. pombe* (Takahashi *et al.*, 2000)

It is becoming increasingly obvious that the position and heritability of the centromere is regulated in an epigenetic manner i.e. not totally controlled by the DNA sequence. The study of neocentromeres and dicentric chromosomes has been particularly useful in defining what is required to make a functional centromere. A neocentromere can form *de novo* on a chromosome at a site which is not normally centromeric in terms of the DNA sequence. The best studied neocentromere is mardel (10), which can recruit the appropriate proteins and function as a centromere (Voullaire *et al.*, 1993). The sequence of this neocentromere has been investigated and found to be identical to normal chromosome 10 (du Sart *et al.*, 1997; Lo *et al.*, 2001), indicating that the sequence does not define centromere function. It is interesting to note that the constitutive centromere proteins CENP-A and CENP-C are localised to neocentromeres, but CENP-B is not, presumably due to the lack of CENP-B boxes.

In nature, dicentric chromosomes also occur by chromosome rearrangement. However, for the chromosome to be mitotically stable, one of these centromeres must be inactivated and cannot function. It is known that CENP-A and CENP-C (Earnshaw *et al.*, 1989; Sullivan & Schwartz, 1995) are found only at the active centromere, whereas CENP-B is found at both (Earnshaw *et al.*, 1989), again putting into question the role of CENP-B at the centromere. The study of neocentromeres and artificial centromeres has increased the knowledge about centromeres but still it remains to be answered what truly defines a centromere. It is clearly some combination of the centromeric sequence and proteins associated and recruited in the normal situation. However, in the aberrant situation of a neocentromere, the proteins are enough to define the centromere and this in turn can be inherited.

The kinetochore is a proteinaceous structure which lies above the centromeric DNA. The structure of the kinetochore has been studied in vertebrate cells where it is described as a trilaminar plate (Brinkley & Stubblefield, 1966; Jokelainen, 1967; McEwen *et al.*, 1998) with three domains where different proteins are localised (Figure 1.3). The regions are the inner plate, where DNA associated proteins such as CENP-A and CENP-B can be found; the outer plate, where checkpoint molecules such as BubR1 are located; and the fibrous corona, where motor proteins such as CENP-E reside. In addition to these locations, a new domain has been described with the localisation of the microtubule-associated protein CLASP/MAST/orbit outside

the fibrous corona (H. Maiato, personal communication). The function of the kinetochore is two fold, firstly as the specific site of attachment of the microtubules to the chromosome and, secondly as the location of checkpoint proteins which assess the attachment and tension of the microtubules. The relationship between the centromere and the kinetochore is illustrated in Figure 1.2. The localisation of a number of kinetochore associated proteins is indicated.

Figure 1.2. Relationship between centromere and kinetochore.

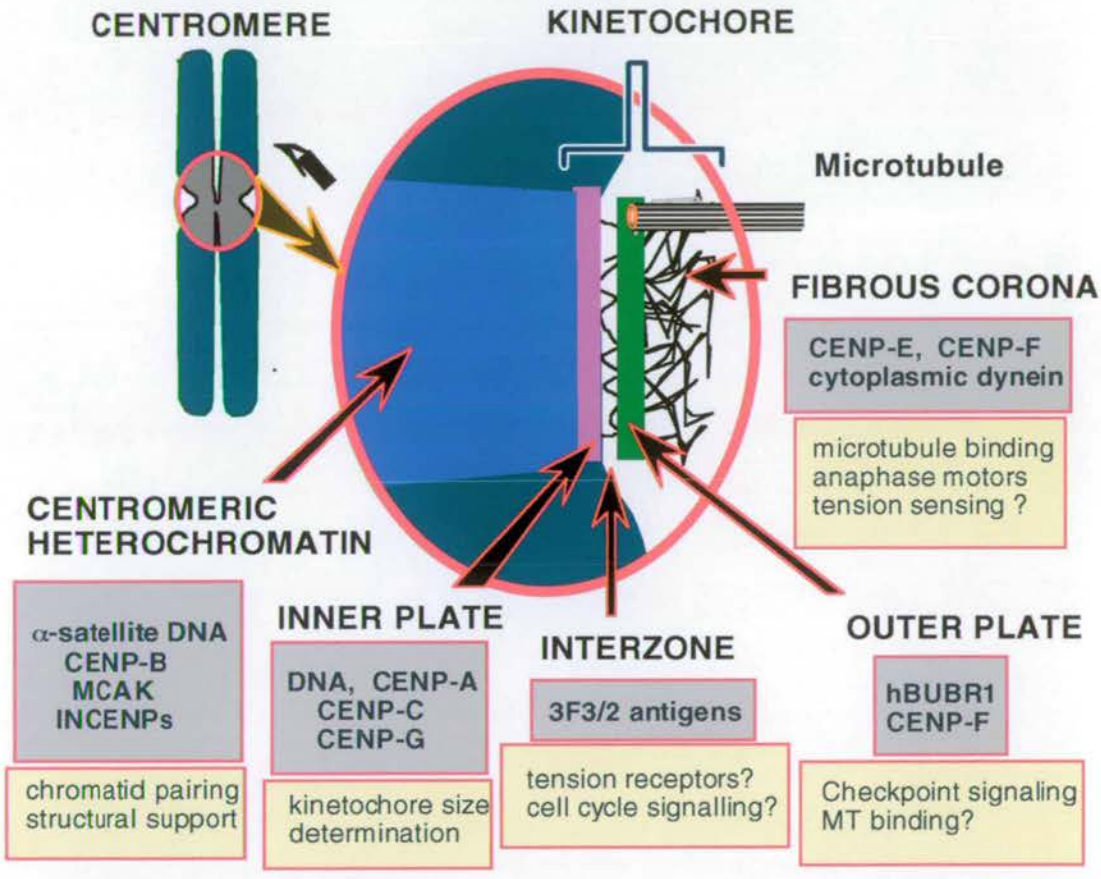

Schematic representation of the kinetochore indicating the various zones and the localisation of some kinetochore-associated proteins. (Diagram from W. C. Earnshaw).

Figure 1.3 shows the trilaminar plate structure of the kinetochore as identified by electron microscopy.

Figure 1.3. The kinetochore is a trilaminar plate

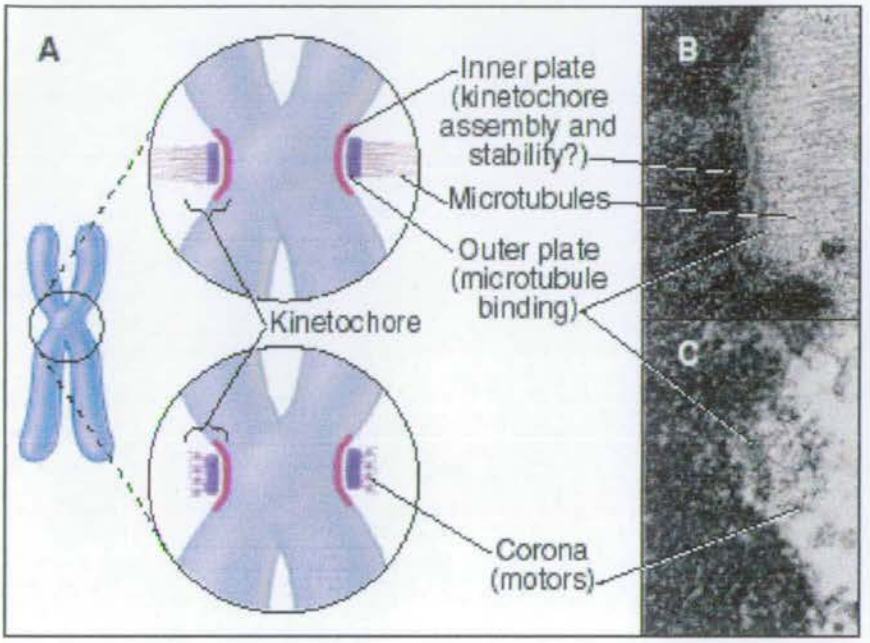

Diagram showing the structure of the kinetochore in relation to the electron microscopy images. Diagram adapted from Cell Biology by Pollard and Earnshaw.

1.7 Spindle assembly

The mitotic spindle is required to pull the chromosomes to opposite poles of the cell during anaphase. It is nucleated from the centrosome or microtubule organising centre (MTOC), referred to as the spindle pole body in yeast. The spindle also plays a role in determining the position and orientation of the cleavage furrow and regulating exit from mitosis (Khodjakov & Rieder, 2001; Piel & Bornens, 2001). The centrosome is a complex structure composed of a number of different proteins. Each centrosome is assembled around two barrel shaped centrioles. The centrioles themselves are composed of 9 triplets of short microtubules that are embedded in the pericentriolar matrix (PCM) (Dutcher, 2001). The PCM contains the γ-tubulin ring complex (γ-TURC), which is essential for nucleation of the microtubules (Bobinnec *et al.*, 1998). The centrosome must be replicated before cell division occurs. As in the case of DNA replication, centrosome duplication occurs in a semi-conservative manner. A number of processes constitute the centrosome cycle, namely, duplication, maturation, separation and disorientation. These processes are regulated by phosphorylation and proteolysis of key cell cycle regulators such as cdk2/cyclinE

(Lacey *et al.*, 1999; Hinchcliffe & Sluder, 2002). In addition to the centrosomes' role in nucleating and organising the mitotic spindle, it is known to play a key role in the regulation of cell cycle progression. This was defined by experiments where the centrosome of vertebrate cells was destroyed by laser ablation (Khodjakov *et al.*, 2000). Surprisingly cells with one or no functional centrosomes were able to form a bipolar spindle and progress through mitosis presumably by a centrosome independent pathway. Subsequently, it was shown that these cells had a higher failure rate in cytokinesis and did not enter a subsequent S phase (Khodjakov & Rieder, 2001). Similar experiments in African green monkey cells where the centrosomes were microsurgically removed also resulted in cells entering and completing mitosis, however, they were unable to enter the next S phase, these experiments lead to the conclusion that there are components of the centrosome not needed for the progression from G2 to M, but essential for the G1 to S transition (Hinchcliffe *et al.*, 2001). It is hardly surprising, therefore, that centrosome amplification can lead to chromosome instability and in turn to tumour development (Reviewed by (D'Assoro *et al.*, 2002)).

1.8 Spindle assembly checkpoint

The spindle assembly checkpoint is active when a kinetochore is either unattached or not under tension and sends a signal to inhibit the APC/C, preventing it from degrading key cell cycle regulators such as cyclin B and securin. This highly sensitive checkpoint requires a number of proteins, which form multiple complexes, in order to sense and transmit the 'wait anaphase' signal. Figure 1.4 shows an overview of the checkpoint indicating that anaphase onset is blocked by the inactivation of the APC. A vast body of literature now exists exploring the checkpoint in many different organisms. Since the spindle assembly checkpoint is the main subject of this thesis the components and mechanisms will be discussed in some detail.

Figure 1.4 Overview of spindle assembly checkpoint activation

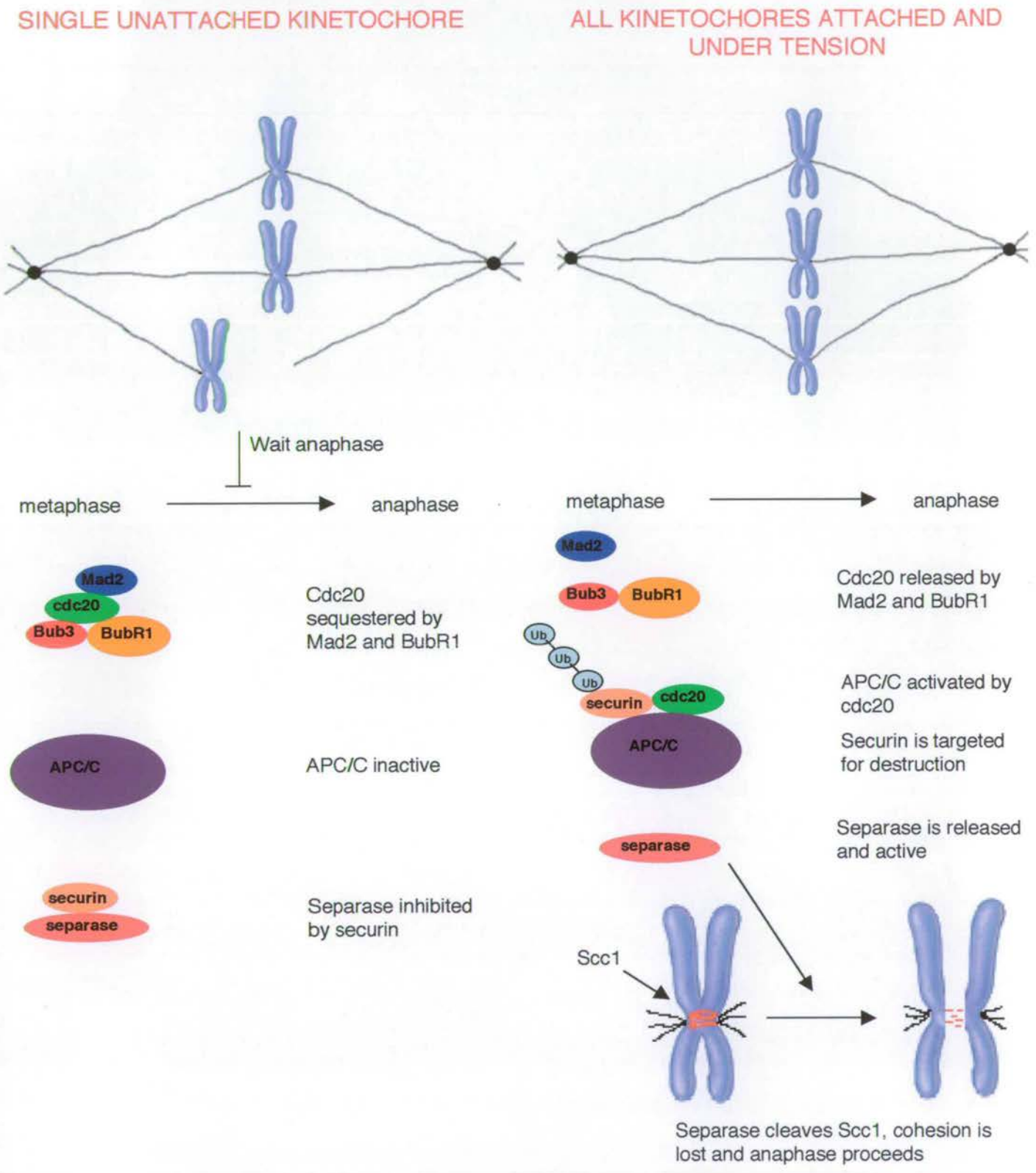

Figure 1.4 Spindle assembly checkpoint inhibits the metaphase to anaphase transition. The metaphase to anaphase transition is blocked by activation of the spindle assembly checkpoint when one or more kinetochores are unattached or not under tension. The checkpoint proteins BubR1 and Mad2 sequester cdc20 and prevent activation of the APC/C. Once all kinetochores are attached or under tension the checkpoint is somehow inactivated and cdc20 is released. This results in activation of the APC/C. Securin, which normally binds and inactivates separase is targeted for destruction by the APC/C. Active separase cleaves Scc1, a subunit of the cohesin complex, cohesion is lost and the chromatids move apart.

Components of the spindle assembly checkpoint were initially identified as budding yeast mutants which failed to arrest in the presence of spindle damage. These were classed as either Mad (Mitotic Arrest Deficient) (Li & Murray, 1991), or Bub (Budding uninhibited by benzimidazole) mutants (Hoyt *et al.*, 1991). Initially Mad1, 2 and 3 and Bub1, 2 and 3 were identified. Subsequently, Mps1p has been identified as an additional component of the checkpoint in yeast (Weiss & Winey, 1996) and vertebrates (Abrieu *et al.*, 2001) and Bub2 has been redefined as having a role in mitotic exit (Fesquet *et al.*, 1999; Fraschini *et al.*, 1999; Li, 1999).

The sensitivity of the spindle checkpoint and specifically the role of the kinetochore in generating the signal to block anaphase onset was described in a series of groundbreaking experiments, which showed that a single unattached kinetochore was sufficient to activate the checkpoint and prevent the cells from proceeding into anaphase (Rieder *et al.*, 1994). Using laser irradiation to destroy the kinetochore on the last mono-orientated chromosome, Rieder and colleagues showed that this relieved the checkpoint and cells entered anaphase (Rieder *et al.*, 1995). This work showed that the signal to delay the cell cycle is generated by the kinetochore and once the kinetochore was destroyed the cell reacted as if the checkpoint had been satisfied.

The fact that the spindle checkpoint senses both attachment of microtubules and tension across the kinetochore was investigated in the spermitids of praying mantis. In this experiment, tension was applied to an improperly attached kinetochore using a micromanipulation needle. In a manner similar to the laser ablation studies, this tension, artificially applied, resulted in the cell proceeding into anaphase as though the checkpoint had been satisfied (Li & Nicklas, 1995). Further evidence of a tension sensing mechanism was established by the observation that the phosphoepitope specific monoclonal antibody 3F3/2 preferentially stains kinetochores that are not under tension (Gorbsky & Ricketts, 1993). When this antibody was microinjected into cells it caused a delay in the metaphase to anaphase transition (Campbell & Gorbsky, 1995). This has been further investigated by experiments in grasshopper spermatocytes where the kinetochore attachment was disrupted using a microneedle. This resulted in 3F3/2 staining at the kinetochores, which remained until the kinetochores were brought artificially under tension (Nicklas *et al.*, 1995). This knowledge that the checkpoint signal was generated by the kinetochore and that this

signal was related to the tension generated by microtubule attachment to the kinetochore laid the groundwork for more detailed studies of the proteins and complexes involved, as discussed below.

1.8.1 Bub1

Cloning and identification of budding yeast Bub1 revealed that it is a kinase able to autophosphorylate and phosphorylate Bub3 *in vitro* (Roberts *et al.*, 1994), and interact physically with Bub3. Subsequently, vertebrate homologues of this checkpoint protein were identified (Pangilinan *et al.*, 1997) and in particular the mouse protein was studied in depth (Taylor & McKeon, 1997). It was found that the N-terminal domain was required for kinetochore localisation, and that this domain expressed in HeLa cells had a dominant negative effect, causing a failure of cells to arrest in mitosis in the presence of spindle damage. The localisation of Bub1 is slightly different to that observed for the checkpoint components Mad1 and Mad2 since Bub1 seems to be retained for longer at the kinetochores after stable attachments have been established (Sharp-Baker & Chen, 2001). This was seen particularly for the *S. pombe* homologue of Bub1 where it remained at the kinetochores until telophase, perhaps suggesting another role for Bub1 after the metaphase to anaphase transition (Bernard *et al.*, 1998). The dependency of the checkpoint upon Bub1 was confirmed by a study in *Xenopus* where Bub1 was immunodepleted (Sharp-Baker & Chen, 2001). This led to inactivation of the checkpoint and failure of Mad1, Mad2, Bub3 and CENP-E to bind the kinetochore, indicating that Bub1 plays a role upstream in the checkpoint, presumably being responsible for targeting of components to the kinetochore. Intriguingly, this study also revealed that the kinase domain of Bub1 was not required for the checkpoint, a point which will be re-iterated upon discussion of the metazoan specific Bub1 related protein, BubR1.

1.8.2 Bub2

Bub2 was initially identified and cloned from the screen which identified the Bub components of the spindle assembly checkpoint (Hoyt *et al.*, 1991). In more recent years it has become apparent that Bub2 plays a different role to other components of the checkpoint and is part of an independent pathway regulating exit from mitosis, known as the mitotic exit network (MEN) (Fesquet *et al.*, 1999; Fraschini *et al.*,

1999). Bub2 prevents premature exit from mitosis when anaphase is inhibited (Alexandru *et al.*, 1999). It does this by interacting with Bfa1 to form a GTPase activating protein, which inhibits the G protein Tem1 and prevents cells from exiting mitosis when the checkpoint is active (Bloecher *et al.*, 2000).

1.8.3 Bub3

Bub3 was cloned and described in the initial characterisation of the spindle checkpoint (Hoyt *et al.*, 1991). Subsequently, Bub3 has been identified in a number of organisms including mouse (Martinez-Exposito *et al.*, 1999; Kalitsis *et al.*, 2000), *Aspergillus nidulas* (Efimov & Morris, 1998), *Drosophila* (Basu *et al.*, 1998) and human (Taylor *et al.*, 1998). Identification of *Drosophila* Bub3 confirmed its role in the spindle assembly checkpoint in metazoans (Basu *et al.*, 1998). This study revealed that the localisation of Bub3 was disrupted by mutations in the Bub1[1] (BubR1) gene. However, Bub3 localisation was unaffected in flies mutant for the checkpoint proteins Zw10 and Rod, indicating that these proteins are in distinct pathways. Identification of human Bub3 reinforced the notion that Bub1 and Bub3 interact, since expression of Bub1 altered the localisation of Bub3 (Taylor *et al.*, 1998). The domain of Bub1 required for this interaction was identified and found to be the same as that required for kinetochore localisation, indicating a role for Bub3 in the localisation of Bub1 to the kinetochores (Taylor *et al.*, 1998). This study also led to the identification of the mammalian homologue of Mad3 (BubR1) as a component of the checkpoint which interacted with Bub3. The requirement for complex formation between Bub3 and BubR1 was demonstrated by the fact that ectopically expressed BubR1 was only able to localise to the kinetochores of BHK (baby hamster kidney) cells when Bub3 was overexpressed in the same cell. This, therefore, leads to the hypothesis that Bub3 is required for the kinetochore localisation of both Bub1 and BubR1 in order for the checkpoint to function in vertebrate cells. The essential role of Bub3 in the spindle assembly checkpoint was further defined by the targeted disruption of this gene in mouse (Kalitsis *et al.*, 2000). The disruption caused embryonic lethality with the animals failing to survive beyond day 6.5 - 7.5 pc. The embryos were found to develop normally until day 3.5 and then between days 4.5 – 6.5 accumulated a number of mitotic defects. These

---

[1] Drosophila Bub1 is more closely related to BubR1 from other species.

included chromatin bridging, lagging chromosomes, micronuclei and irregular nuclear morphology. The authors also showed that these cells were unable to activate the spindle assembly checkpoint, since embryos treated with microtubule depolymerising agents failed to arrest in metaphase (Kalitsis *et al.*, 2000).

It has been noted that Bub3 shares extensive sequence homology with a protein called RAE1 (GLE2) which binds to the nuclear pore complex component NUP98 (Wang *et al.*, 2001). RAE1 binds to NUP98 by way of a motif called GLEBS (GLE2p binding sequence). Both Bub1 and BubR1 have a motif with a high degree of similarity to the GLEBS motif, and this is the region with which they interact with Bub3. At present, the significance, if any, of this sequence similarity between components of the spindle assembly checkpoint and the nuclear pore complex remains unknown. However, it is interesting to note that in addition, Mad1 and Mad2 have been found at nuclear core complexes (Campbell *et al.*, 2001). These observations could indicate either multiple cellular roles for checkpoint components or that the nuclear pore complex plays some role in the spindle assembly checkpoint. An interesting hypothesis suggested by these workers, is that localisation at the nuclear pore may play some role in loading checkpoint components onto the kinetochore in order that they can fulfil their role once the nuclear envelope has broken down. This idea is based upon observations that interphase centromeres associate with the nuclear envelope (Moroi *et al.*, 1981; Haaf & Schmid, 1989; Ochs & Press, 1992).

1.8.4 Mad1

Mad1 was initially identified in budding yeast and was shown to be hyperphosphorylated when cells were arrested in mitosis. This hyperphosphorylation of Mad1 was defective in Mad2, Bub1 and Bub3 mutant backgrounds, but not in the Mad3 background (Hardwick & Murray, 1995). Subsequently, Mad1 and Mad2 have been found in tight association in budding yeast throughout the cell cycle. This association is considered critical for checkpoint function and the hyperphosphorylation of Mad1 (Chen *et al.*, 1999). Mad1 was also identified in *Xenopus* in a complex with Mad2. Mad1 was found to be necessary for the establishment and maintenance of the checkpoint in *Xenopus* egg extracts and the idea was postulated that Mad1 was required to recruit Mad2 to unattached kinetochores (Chen *et al.*, 1998). Mad1 has also been found to facilitate the

localisation and hyperphosphorylation of BubR1 in *Xenopus* egg extracts (Chen, 2002).

1.8.5 Mad2

Mad2, as with the other checkpoint components, is conserved and has been identified and cloned from a number of organisms including budding yeast (Chen *et al.*, 1999), human (Li & Benezra, 1996) and fission yeast (Ikui *et al.*, 2002). Mad2 forms complexes with Mad1 (Chen *et al.*, 1999), which results in hyperphosphorylation of Mad1, and also with the activating subunit of the APC/C, Cdc20 (Fang *et al.*, 1998; Kallio *et al.*, 1998; Wassmann & Benezra, 1998; Sironi *et al.*, 2001). Mad2's complex formation with Cdc20 sequesters the latter; therefore preventing both its association with the APC/C and inactivation until the spindle checkpoint is satisfied (Chen *et al.*, 1998; Kallio *et al.*, 1998). It has been established that Mad1 is required for the kinetochore localisation of Mad2 (Chen *et al.*, 1998; Sironi *et al.*, 2001; Luo *et al.*, 2002), and that Mad2 is required both at the kinetochore to sense activation of the spindle checkpoint (Waters *et al.*, 1998) and to send an inhibitory signal to the APC by way of binding and inhibiting Cdc20 (Fang *et al.*, 1998; Kallio *et al.*, 1998; Wassmann & Benezra, 1998).

A novel human kinetochore associated protein, Hec1, was identified as an interactor of Mad1 in a yeast two hybrid screen (Chen *et al.*, 1997). Hec1 is a coiled-coil protein, which is the putative homologue of the budding yeast kinetochore component Ndc80 (Martin-Lluesma *et al.*, 2002). RNAi depletion analysis in human cells revealed that Hec 1 is required for the recruitment of Mps1 and the Mad1/Mad2 complex to the kinetochore. In addition, depletion of Hec1 resulted in persistent activation of the spindle assembly checkpoint, although significant amounts of Mad1 and Mad2 were not present at the kinetochore (Martin-Lluesma *et al.*, 2002). These results suggest that Mad2 does not need to be retained at the kinetochore for the spindle assembly checkpoint to be activated.

The first mechanistic insights into the workings of the spindle assembly checkpoint have been established recently by solving the structure of Mad2 interacting with both Mad1 and Cdc20. It has been revealed that Mad2 undergoes a major conformational change upon binding of either Mad1 or Cdc20 (Luo *et al.*, 2002; Sironi *et al.*, 2002). In addition a Mad2 binding motif has been identified in common with both the Mad1

and Cdc20 sequence (Luo *et al.*, 2002). It is becoming increasing clear that the Mad1-Mad2 interaction is a priming step, which alters the conformation of Mad2 so that it is ready for the crucial role of binding Cdc20 and hence inhibiting the APC until all kinetochores are attached. However, questions still remain regarding where these interactions take place and how Mad1 is able to release Mad2 for binding Cdc20. The complex between Mad1 and Mad2 has been found to be very strong and Mad1 binds Mad2 in a competitive manner, actually inhibiting the Cdc20 interaction (Sironi *et al.*, 2001; Sironi *et al.*, 2002).

It is not entirely clear as to where the Cdc20-Mad2 interaction takes place, although Cdc20 has been reported to localise to the kinetochore (Fang *et al.*, 1998; Kallio *et al.*, 1998). Once all the kinetochores are attached to microtubules, Mad2 must release Cdc20 in order that the APC can be activated. How this release of Cdc20 occurs is still unknown although it has been proposed that microtubule attachment alters the structure of the kinetochore (Rieder & Salmon, 1998; Howell *et al.*, 2000). This structural alteration may be the signal for Mad2 to release Cdc20 and for Mad2 itself to leave the kinetochore. Mad2 is known to leave the kinetochore and translocate to the spindle pole by way of spindle fibres, with anaphase onset occurring 10 minutes later in PtK cells (Howell *et al.*, 2000), presumably this is the length of time needed for the dissociation of the Mad2/Cdc20 complex, activation of the APC/C and the destruction of key proteins.

Since Mad2 plays a role downstream in the checkpoint, inhibiting the function of the APC/C, it is interesting to address what happens when the gene is disrupted or removed. A Mad2 knockout mouse has been generated which is embryonic lethal at day 6.5-7.5 pc (Dobles *et al.*, 2000). The embryos grow normally until 5.5 pc, but are unable to arrest in the presence of spindle damage. By 6.5 pc there is chromosome missegregation and apoptosis. In addition, it has been discovered that Mad2 is haploinsufficient, since deletion of one Mad2 allele in the human colon carcinoma cell line, Hct-116 results in a defective checkpoint, premature sister chromatid separation and an increase in chromosome missegregation (Michel *et al.*, 2001). In addition, embryonic fibroblasts from the Mad2 +/- mice showed premature sister chromatid separation and an increase in the number of aneuploid cells.

Strikingly, the heterozygous mice had a high frequency of papillary lung adenocarcinomas by the age of 18-19 months. This is a very rare tumour, and the

development time is fairly long, presumably indicating that other co-operative mutations of oncogenes or tumour suppressors must have occurred in order to drive this transformation (Michel *et al.*, 2001). In another study, it was shown that human breast tumour line T47D, which is sensitive to taxol and nocodazole, had reduced Mad2 expression, and the cells failed to arrest after nocodazole treatment (Li & Benezra, 1996).

An interaction between the oestrogen receptor β and Mad2 was identified by yeast two hybrid screen and confirmed by GST pulldown (Poelzl *et al.*, 2000). Oestrogen receptors are ligand-activated transcription factors that regulate gene expression and cell growth, with ER-β being involved in the regulation of cellular proliferation. The specific role of an interaction or complex formation between these two proteins is currently unknown.

Mad2 has also found to interact with the cytoplasmic domain of the insulin receptor (O'Neill *et al.*, 1997) and the ubiquitin-like protein, FAT10 (Liu *et al.*, 1999). Neither of these interactions has been explained in terms of Mad2's role in the spindle checkpoint. These observations do, however, emphasise the idea, as discussed for Bub3 and BubR1, that components of the spindle checkpoint may have multiple roles within the cell.

1.8.6 Mad3/ BubR1

Initial identification of human BubR1 classed it as a human Bub1 related protein (Cahill *et al.*, 1998; Jablonski *et al.*, 1998; Taylor *et al.*, 1998). Indeed Bub1 and BubR1 share a considerable degree of homology at both the N-terminus and within the kinase domain. However, subsequently by sequence analysis and functional studies, others have argued that BubR1 should be classed as the functional homologue of budding yeast Mad3 (Hardwick *et al.*, 2000) and fission yeast Mad3 (Millband & Hardwick, 2002). The most striking difference between these proteins being that yeast Mad3 does not contain a kinase domain. However, since the requirement of BubR1's kinase domain within the checkpoint is somewhat controversial, this issue may be unimportant (Tang *et al.*, 2001) (Fang, 2002).

Initially identified as a gene mutated in human colorectal cancer cell lines (Cahill *et al.*, 1998), it is now becoming apparent that BubR1 is an important component of the

vertebrate checkpoint that interacts with a number of other proteins, senses kinetochore attachment and/or tension and inhibits the APC/C. Here I will discuss the known involvement of BubR1 in the checkpoint, including the complexes it forms, and speculations concerning how BubR1 actually senses unattached kinetochores and relays that signal to the APC/C.

Cloning of the budding yeast checkpoint component Mad3 revealed that it has two domains at the N-terminus with a high degree of similarity to Bub1 (Hardwick *et al.*, 2000). Mad3 interacts with Bub3, Mad2 and Cdc20 and it is known that the regions of homology to Bub1 are crucial for these interactions (Hardwick *et al.*, 2000). Figure 1.5 illustrates these domains, region I and region II in addition to the Bub3 binding domain.

Figure 1.5. Sequence comparisons between BubR1, Bub1 and Mad3

A

Region I

Region II

B

A, Homology regions I and II, as described by Hardwick *et al.*, 2000. Key to Clustal symbols, * - amino acid fully conserved, : strong group fully conserved, STA, NEQK, NHQK, NDEQ, QHRK, MILV, MIL, HY, FYW, . Weaker group fully conserved CSA, ATV, SAG, STNK, STAP, SGND, SNDEQK, NDEQHK, NEQHRK, FVLIM, HFY. Colouring of Clustal alignment Blue: AFILMVW, Purple: ED, Green: NQST, Yellow: P, Orange: G, Red:KR, Turquoise: YH, Salmon: C. **B**, Schematic representation of Bub1 related proteins, indicating the conserved homology domain in red, the Bub3 binding domain in pale blue and the kinase domain in dark blue. Diagram adapted from Taylor *et al.*, 1998.

Identification of the fission yeast Mad3 has allowed the dependency for kinetochore localisation of Mad3 to be determined (Millband & Hardwick, 2002). The authors showed that Mad3 localisation is dependant upon Bub1, Bub3 and Mph1 (fission yeast Mps1), but not Mad1 or Mad2. In addition Mad3 was shown to co-immunoprecipitate with Bub3, Mad2 and Cdc20. Fission yeast Mad3 is required for Mad2 to inhibit the APC/C (Millband & Hardwick, 2002).

The first ever mutational analysis of a spindle assembly checkpoint component in a multi-cellular organism came from work on BubR1 in *Drosophila* (Basu *et al.*, 1999). The gene mutated in this analysis was initially named *Drosophila* Bub1. However, subsequent analysis of this sequence reveals that it is more similar to vertebrate BubR1 proteins identified, and therefore should be renamed BubR1 (M. Goldberg, personal communication). This study revealed that flies with a P-element mutation (a near null), die during late larval stages. This death is due to severe mitotic abnormalities including accelerated exit from mitosis with chromosomes that are both mis-segregated and fragmented. In addition, an increase in levels of apoptosis was observed in these 'BubR1' mutant flies (Basu *et al.*, 1999).

Several studies have focussed on addressing the fact that metazoans have two Bub1 related proteins involved in the spindle checkpoint and on attempting to identify what different roles, if any, they play. It is known that both proteins are localised to the kinetochore with slightly different timing, with Bub1 localising first at early

prophase onto the kinetochores in human cells (Jablonski *et al.*, 1998). Studies on the Bub1a and Bub1b proteins in mouse show that they have different timing of expression, with Bub1b (BubR1 homologue) expression being delayed by 6 hours relative to Bub1a (Bub1 homologue) (Davenport *et al.*, 1999). In addition it is known that BubR1 contains a putative destruction box, which targets proteins for degradation via the APC, and Bub1 does not, presumably implying that the degradation of the proteins may be regulated differently. Both proteins form a number of complexes. However, to date only BubR1 has been shown to bind Cdc20, in order to directly inhibit the APC/C (Wu *et al.*, 2000; Sudakin *et al.*, 2001; Tang *et al.*, 2001). It therefore seems that Bub1 and BubR1 have distinct roles within the checkpoint. Bub1 may act upstream, forming a complex with Bub3 and Mad1 that may allow the binding of BubR1 and Mad2 to the kinetochore in order to sense microtubule attachment and/or tension.

The question as to whether BubR1 and Mad2 sense specific signals still remains somewhat controversial. It is known that a single unattached kinetochore is able to halt cell cycle progression (Rieder *et al.*, 1994), and that the lack of tension and attachment signals to the checkpoint (Li & Nicklas, 1995). Experiments using taxol (which suppresses microtubule dynamics) revealed that the Mad2 signal depends upon microtubule attachment and not tension (Waters *et al.*, 1998). In this case, taxol was used to generate a state where the tension is lost at the kinetochore, as judged by the lack of 3F3/2 signal. 3F3/2 is a phosphorylated epitope present at kinetochores, which are not under tension (Gorbsky & Ricketts, 1993). Cells in this situation had no Mad2 signal, indicating that Mad2 is unable to sense the lack of tension and does not bind to the kinetochore and activate the checkpoint (Waters *et al.*, 1998). These cells however, are still halted in the checkpoint indicating that something is able to sense lack of tension. Increasingly, it is being hypothesised that this is the function of BubR1 (Skoufias *et al.*, 2001; Taylor *et al.*, 2001; Zhou *et al.*, 2002). This was also shown using a compound called vinblastine which when used at nanomolar concentrations causes a loss of tension at the kinetochore while they are still attached to microtubules. In these treated cells, BubR1 was recruited to the kinetochores but Mad2 was not (Skoufias *et al.*, 2001). At higher vinblastine concentrations when microtubules disassemble and attachment becomes affected, Mad2 was then recruited.

Whether the Mad2 and BubR1 sensing mechanisms are independent or part of the same pathway has been addressed by a recent paper studying PtK1 cells. In this study, it is shown that, if the growth temperature for these cells is decreased from 37°C to 23°C, the time taken for anaphase can increase from 20 minutes to 100 minutes (Shannon *et al.*, 2002). It was shown that this delay is checkpoint dependant by the injection of the checkpoint inhibitor GST-Mad1F10, which subsequently alleviated the anaphase delay. GST-Mad1F10 (amino acids 321-556) contains both the Mad1 oligomerisation domain and the Mad2 binding domain and has been shown to induce premature anaphase specifically in a dominant negative manner by inhibiting the ability of Mad2 to inactivate Cdc20/APC (Canman *et al.*, 2002; Canman *et al.*, 2002). The authors of this paper, (Shannon *et al.*, 2002), then went on to show that the kinetochores at metaphase were under 24% less tension at 23°C than 37°C and that there were increased levels of 3F3/2, Bub1 and BubR1 associated with the kinetochores. Injection of anti-BubR1 antibodies also alleviated the delay, indicating that the BubR1 protein is also required for this temperature sensitive delay. In addition the authors were able to show that although Mad2 and BubR1 may sense distinct signals, they are part of the same pathway. By using both GST-Mad1F10 to inhibit Mad2 and anti-BubR1 they showed that the delay was decreased by the same amount of time if these inhibitors were used independently or together.

Recently, a connection between the chromosomal passenger protein, Survivin, and the spindle assembly checkpoint has been identified in human cells following RNAi depletion of Survivin (Carvalho et al., Personal Communication). This study has shown that Survivin is required for the proper function of the checkpoint, but only in response to lack of tension. Cells, which have been depleted for Survivin, can exit mitosis after treatment with taxol, however, after treatment with nocodazole they are blocked in mitosis. Although BubR1 can bind to the kinetochores in Survivin depleted cells it is not maintained for extended periods. These results further emphasise the notion that there are two arms to the checkpoint pathway one, which involves BubR1, and the other Mad2.

An interaction between the kinetochore motor protein CENP-E and BubR1 was initially identified by yeast two hybrid screen and was subsequently confirmed by immunoprecipitation from HeLa cells (Chan *et al.*, 1998). This work gave initial insight into how a checkpoint protein may actually be able to sense the presence or

attachment of the microtubule at the kinetochore. BubR1 is also known to interact with the checkpoint component Bub3, as discussed previously (Taylor *et al.*, 1998; Tang *et al.*, 2001; Chen, 2002) with the likely role of Bub3 being to correctly localise BubR1 to the kinetochore. BubR1 is also known to interact with the activating subunit of the APC/C, Cdc20 (Wang *et al.*, 2000; Sudakin *et al.*, 2001; Fang, 2002), and, in a manner similar to Mad2, it sequesters this protein, preventing the activation of the APC/C. It seems therefore, that BubR1 is a checkpoint component that may have a central role in both directly sensing the microtubule-kinetochore status and then transducing this signal to the APC by way of interaction with Cdc20.

As discussed previously, the necessity of BubR1's kinase domain for the function of the checkpoint has been thrown into doubt by the work of two groups. In human cells it was shown that a complex between BubR1 and Bub3 exists and that this interacts with Cdc20 (Tang *et al.*, 2001). In that study, it was shown that the kinase domain is not required for BubR1 to inhibit the APC. An additional study in human cells also showed that both BubR1 and Mad2 interacted with Cdc20 (Fang, 2002). The complex formed between BubR1 and Cdc20 was of higher affinity than that between Mad2 and Cdc20 alone. However, it was shown that these proteins act synergistically and each promotes the other's binding to Cdc20. The inhibition of the APC by BubR1 was again shown to be independent of its kinase activity (Fang, 2002). In further agreement with these studies it has been shown that the kinase activity of BubR1 is not essential for checkpoint activity in *Xenopus* (Chen, 2002). In the latter study, immunodepletion of BubR1 from egg extracts reduced the kinetochore localisation of Bub1, Bub3, Mad1, Mad2 and CENP-E and impaired the interaction between Mad2 and Cdc20. These checkpoint defects could be rescued by addition of either wild type BubR1, kinase dead or a kinase domain truncation, indicating that the kinase domain is not essential.

1.8.7 CENP-E

CENP-E was initially identified as a human centromere protein when HeLa chromosome scaffold preparations were used to generate monoclonal antibodies (Yen *et al.*, 1991). One such monoclonal antibody recognised a protein that had a localisation somewhat distinct from CENP-A, CENP-B and CENP-C in that it was not seen at the centromere during interphase, but associated with the centromeres at prometaphase and then redistributed to the spindle midzone as anaphase began (Yen

et al., 1991). This initial study recognised that CENP-E was involved in the transition of cells from metaphase to anaphase, since injection of antibodies to the protein blocked cells and caused a delay in anaphase. CENP-E is a kinesin-like, microtubule-dependant motor protein (Yen *et al.*, 1992; Wood *et al.*, 1997). Subsequently, CENP-E has been implicated as a component of the vertebrate spindle assembly checkpoint that is phosphorylated by MAPK (Zecevic *et al.*, 1998) and interacts with BubR1 (Chan *et al.*, 1998), as mentioned previously. There are two *Drosophila* CENP-E proteins, CENP-meta and CENP-ana (Yucel *et al.*, 2000). CENP-meta has a different cell cycle distribution compared to vertebrate CENP-E, in that it remains localised to the centromere at all stages of the cell cycle. A P-element disruption of CENP-meta leads to incomplete chromosome alignment at metaphase, indicating that this motor protein is required for chromosome congression. Its role in the spindle assembly checkpoint has been defined in both *Xenopus* and mammalian cells. In *Xenopus*, CENP-E has been found to be required for both establishing and maintaining the checkpoint, since extracts immunodepleted of this protein fail to arrest in the presence of spindle damage (Abrieu *et al.*, 2000). Since an increase in the levels of Mad2 can overcome this block, it has been argued that CENP-E is upstream of Mad2 in the checkpoint pathway. The authors hypothesise that CENP-E acts as a kinetochore attachment sensor, which is capable of activating or silencing the checkpoint as required (Abrieu *et al.*, 2000). Further insight into how CENP-E affects chromosome movements were revealed by depleting CENP-E levels in human cells using antisense oligonucleotides. It was found that CENP-E was required for the stable, biorientated attachment of chromosomes to the spindle and for the development of tension across the kinetochore (Yao *et al.*, 2000). Recently, a mouse knockout of CENP-E has been generated (Putkey *et al.*, 2002). Since no homozygous null embryos were detected at embryonic day 7.5 – 8.5 it was concluded that they did not survive beyond implantation. In order to determine the phenotype resulting from disruption of CENP-E Cre/loxP technology was employed. Selective disruption was carried out both in cultured primary fibroblast and in the mouse liver. Primary fibroblasts were treated with Cre recombinase by adenovirus infection. 90% of these cells lacked detectable levels of CENP-E and had a high frequency of mitotic abnormalities. Liver regeneration was studied in the absence of CENP-E, firstly by injection of Cre adenovirus, which is absorbed by the liver, then by injection of the toxin carbon tetrachloride, which induces liver damage. It was

found that the livers were able to recover normally in animals infected with the Cre adenovirus, but that mitotic abnormalities were observed including misaligned and lagging chromosomes (Putkey *et al.*, 2002).

1.8.8 Mps1

Mps1 was initially identified as a gene essential for spindle pole body duplication in budding yeast (Winey *et al.*, 1991). Subsequently, it was identified as a component of the spindle assembly checkpoint with kinase activity (Weiss & Winey, 1996). Recent identification of vertebrate homologues of Mps1 has raised questions concerning the potential dual role of this kinase in vertebrates (Abrieu *et al.*, 2001; Fisk & Winey, 2001; Stucke *et al.*, 2002). Overexpression of Mps1p in budding yeast constitutively activated the spindle assembly checkpoint, causing hyperphosphorylation of Mad1 (Hardwick *et al.*, 1996). Phosphorylation of Mad1 by Mps1p is required for Mad1 and Mad2 to associate with each other (Chen *et al.*, 1999), and also for the Bub1/Bub3 complex to form (Brady & Hardwick, 2000). The fission yeast homologue of Mps1p, called Mph1, is capable of complementing both the checkpoint and SPB duplication defect in budding yeast lacking Mps1p. Surprisingly, however, fission yeast Mph1 mutants show only checkpoint defects (He *et al.*, 1998).

Mps1 kinases share extensive sequence homology in the C-terminal kinase domain but have little or no homology at the N-terminus. In order to address the question as to whether the dual or multiple roles of yeast Mps1 are conserved, the vertebrate homologues are now being studied. Identification of *Xenopus* Mps1 revealed that it is a kinetochore-associated kinase that is required both to establish and maintain the spindle assembly checkpoint (Abrieu *et al.*, 2001). In addition, this study established that Mps1 is upstream of Mad2 in the signalling pathway, since overexpression of Mad2 can overcome the checkpoint defect in extracts, which have been depleted of Mps1. Mps1 is also required for the recruitment and retention of the kinetochore motor protein CENP-E at the kinetochores in *Xenopus* (Abrieu *et al.*, 2001). CENP-E localisation is in turn required for Mad1 and Mad2 to be localised to the kinetochore. Human Mps1 was initially identified and named TTK/PYT (Mills *et al.*, 1992; Hogg *et al.*, 1994). Mouse Mps1, initially named ESK, has been shown to regulate centrosome duplication (Fisk & Winey, 2001). In contrast to this, investigation of the human Mps1 using both antibody injection and siRNA technology showed that

this protein is indeed required for the spindle assembly checkpoint to function but not for centrosome duplication (Stucke *et al.*, 2002).

1.8.9 MAPK

MAPK (mitogen activated protein kinase) has been implicated as a component of the spindle assembly checkpoint in a number of systems. Immunofluorescence has shown that active MAPK is present at the kinetochores of vertebrate cells during prometaphase and that the signal intensity diminishes as the kinetochores become lined up on the metaphase plate and under tension (Shapiro *et al.*, 1998; Zecevic *et al.*, 1998). This localisation is observed for components of the checkpoint and is the pattern seen with the phosphoepitope recognised by the monoclonal antibody 3F3/2 (Gorbsky & Ricketts, 1993), as discussed previously. In addition it has been shown that MAPK can phosphorylate the kinetochore motor protein CENP-E, which is known to have a role in the checkpoint, at sites known to be involved in microtubule interaction (Zecevic *et al.*, 1998). Further indications that MAPK may play a role in the checkpoint have come from work in *Xenopus* egg extracts. Initially it was shown that extracts treated with nocodazole, not only showed an increase in cdc2/cyclinB levels indicative of a cell cycle block, but also an increase in MAP kinase activity (Minshull *et al.*, 1994). Subsequently, it has been shown that extracts immunodepleted of MAPK fail to arrest the cell cycle in the presence of microtubule poisons (Takenaka *et al.*, 1998). In order to address the question as to whether MAPK has a role in somatic cells, XTC cells were injected with the MAPK phosphatase, XCL100, with the result that the cells failed to arrest after treatment with nocodazole (Wang *et al.*, 1997). This seemed to indicate therefore that MAPK plays a crucial role in the function of the spindle assembly checkpoint in somatic cells. However, in the light of more recent work on the p38 kinase it may be that the inhibitor is not specific to MAPK and that additional or other proteins play a role in the checkpoint. p38 (also known as MPK2, CSBP or HOG1) is a component of the MAPK superfamily. In a study addressing the role of MAPK family members in the checkpoint of somatic cell cycles, it was found that specifically p38 was activated in NIH 3T3 cells that had been arrested in mitosis by the addition of nocodazole (Takenaka *et al.*, 1998). Cultured cells treated with a specific inhibitor of p38, SB203580, and subjected to nocodazole treatment had compromised checkpoint activity. In addition, when activated p38 was injected into two-cell *Xenopus*

embryos these failed to develop normally and arrested early in development with high histone H1 kinase activity (Takenaka *et al.*, 1998), indicative of a mitotic arrest. It therefore seems that the activity of p38 is required for the spindle assembly checkpoint to function in somatic cells.

1.8.10 Complexes and checkpoint activation

Illuminating work identifying multiprotein complexes in *S. cerevisae* (Brady & Hardwick, 2000), and human cells (Sudakin *et al.*, 2001; Tang *et al.*, 2001) allows a model to be drawn up that brings all this information together. In addition, a study in *S. pombe* regarding the timing, order and dependency of the checkpoint components helps in the formulation of this model (Millband & Hardwick, 2002). In *S. cerevisae* it has been shown that a complex between Mad1-Bub1-Bub3 forms which is required for the checkpoint function and that this requires both Mad2 and Mps1 for formation (Brady & Hardwick, 2000). In human cells two complexes have been identified. The first, with APC/C inhibitory activity, has been named the mitotic checkpoint complex (MCC) and consists of BubR1, Bub3, Cdc20 and Mad2 (Sudakin *et al.*, 2001). It was found that this is a pre-formed complex present and active in interphase cells but that only APC/C purified from mitotic cells was sensitive to inhibition. This complex is capable of inhibiting mitotic APC/C 3,000-fold more efficiently than recombinant Mad2.

In another study, a 500 kDa complex was purified from mitotic HeLa cells which was composed of BubR1, Bub3 and Cdc20, but not Mad2 (Tang *et al.*, 2001). As with the MCC complex, this has the ability to inhibit the APC/C, but in a Mad2 independent manner. It is known from budding yeast that a complex of Mad1-Bub1 and Bub3 forms and is present at the kinetochores and that the formation of this complex is dependant upon Mad2 and Mps1 (Brady & Hardwick, 2000). It has been suggested by Millband and Hardwick (2002), that this complex may act as a 'landing pad' for Mad3, and, when this is associated with the kinetochore, it interacts or assists Mad2 in binding to Cdc20 and hence inhibits the APC. This model, however, does not take into account that BubR1 is known to interact with CENP-E and rather than being a downstream effector may in addition sense microtubule attachment or tension through this motor protein. It has, however, been shown that BubR1 becomes localised to the kinetochores later than Bub1 in both human (Jablonski *et*

al., 1998) and mouse cells (Davenport *et al.*, 1999). Insights into the mechanism of checkpoint activation have been obtained from studies of the structure of Mad2 interacting with both Mad1 and Cdc20 and it appears that the interaction with Mad1 is required as a priming step. The model is consistent with Mad2 being recruited later, interacting with Mad1 already present at the kinetochore and then with Cdc20.

Although there is a considerable amount of information about the spindle assembly checkpoint from both *in vitro* and *in vivo* studies from a number of different organisms, many questions still remain unanswered. In particular, how the checkpoint is turned off so rapidly once all kinetochores become properly attached, and how the signal from just one unattached kinetochore is enough to inhibit the APC/C throughout the whole cell. The checkpoint maybe inactivated by a redistribution of proteins away from the kinetochore, as is seen with Mad2, which moves along microtubules away from the kinetochore to the spindle poles (Howell *et al.*, 2000). Although a picture is beginning to emerge as to how the various complexes interact at the kinetochore, the specific roles of individual components still remains to be fully elucidated. In addition, it remains to be fully determined if there are additional components of the checkpoint in metazoans as opposed to yeast. With such a large number of components it may also be interesting to determine if there is any redundancy in the system. Figure 1.6 is a proposed model based on the current understanding of how the checkpoint complexes may be recruited to the kinetochore to halt the progression from metaphase to anaphase until such time as all kinetochores have proper bipolar attachments.

1.8.11 APC/C

The anaphase promoting complex or cyclosome is a 20S complex consisting of between 10 and 12 subunits in vertebrates. It has E3 ubiquitin ligase activity and acts to target proteins for destruction by the 26S proteasome. The APC/C plays a key role in cell cycle progression as it targets key components for destruction at specified times in the cycle. Key molecules such as A and B type cyclins (Glotzer *et al.*, 1991) and securin (Cohen-Fix *et al.*, 1996) are targeted by the APC/C, leading to the inactivation of cdk1 kinase and mitotic exit. The process of ubiquitination involves a number of protein activities, the first of which is an E1 ubiquitin activating enzyme, which activates ubiquitin so that it can be transferred to an E2 ubiquitin conjugating

enzyme. The E2 can either then add ubiquitins directly to targets or transfer them to an E3 such as the APC/C. Transfer to the E3 adds a further level of specificity to the process. The proteins that APC/C targets, are recognised by specificity factors such as Cdc20 and Cdh1, which recognise specific sequences within proteins and hence target them for destruction. Cdc20 recognises a motif called the destruction box with the consensus RxxLxxxxN (Glotzer *et al.*, 1991), whereas Cdh1 recognises either the destruction box or KEN box, which has the consensus KENxxxN/D (Pfleger & Kirschner, 2000). APC/C Cdc20 is replaced as the specificity factor for APC/C by cdh1 later in mitosis, when cdk1 activity drops. The discovery that cdh1 also recognises a specific sequence came from observations (Pfleger & Kirschner, 2000) that Cdc20 is itself targeted for degradation by the APC when the specificity changes from Cdc20 to Cdh1, leading to the identification of a KEN box.

Figure 1.6 Proposed model of Spindle Assembly Checkpoint

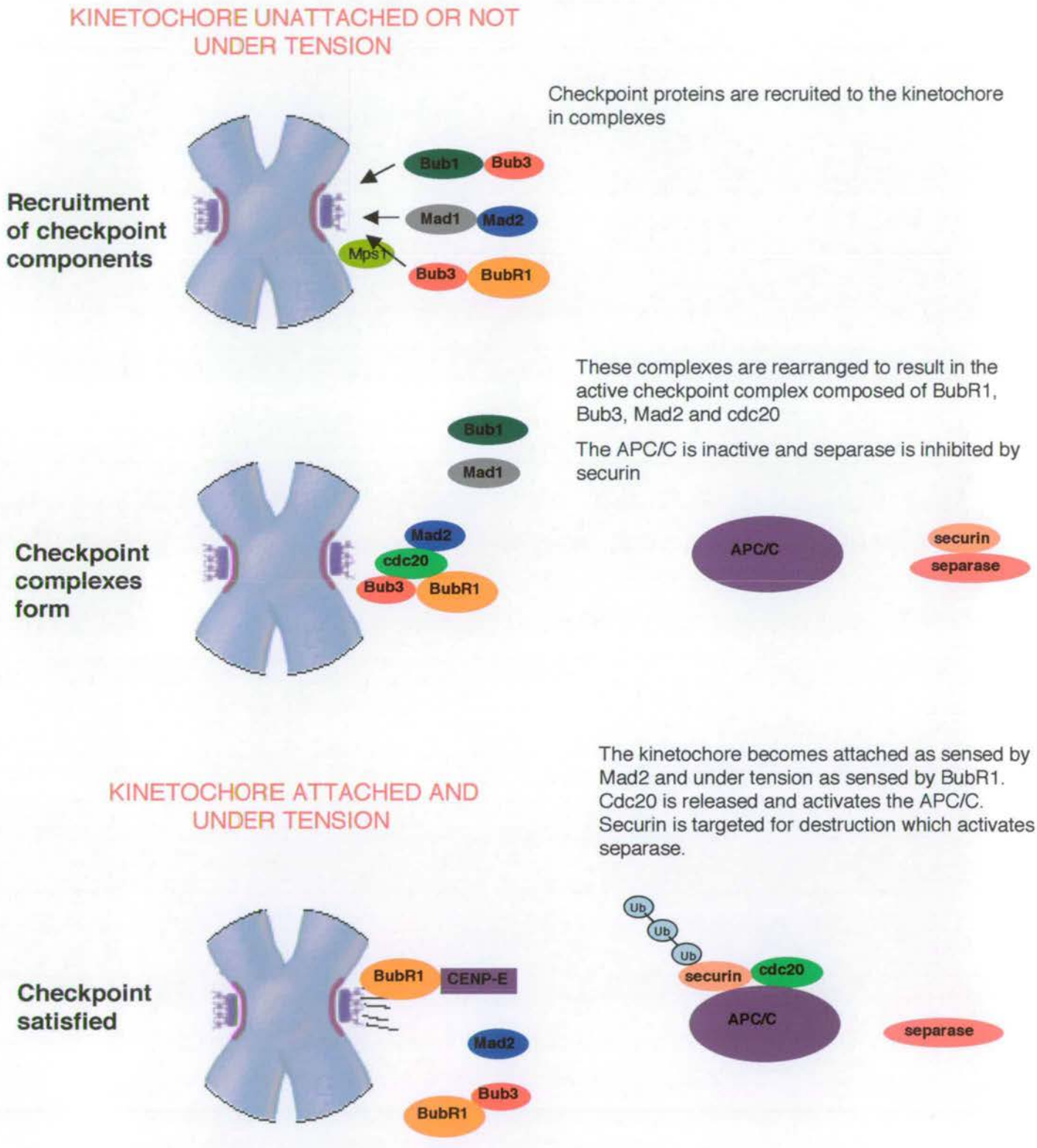

Figure 1.6 proposed model of spindle assembly checkpoint. Model for spindle assembly checkpoint activation based on a number of model organisms. The checkpoint proteins are recruited to the kinetochore in a number of complexes as discussed in the text. These must be rearranged to form the mitotic checkpoint complex (Sudakin *et al.*, 2001) which results in inhibition of the APC. Once the checkpoint is satisfied cdc20 activates the APC, securin is degraded and separase is active to cleave Scc1.

1.9 Zw10 and Rod

The gene *Zeste White 10 (zw10)* was identified in *Drosophila melanogaster* in a screen for mitotic mutants (Gatti & Goldberg, 1991) and similarly *rough deal (rod)* was identified as a gene required for the faithful transmission of chromosomes to daughter cells at mitosis (Karess & Glover, 1989). The intriguing, dynamic mitotic distribution of the proteins encoded by these genes led to their subsequent identification as components of the spindle assembly checkpoint in both *Drosophila* and human cells. Both proteins are localised to the kinetochores early in mitosis, and have essentially the same distribution throughout mitosis. During prometaphase they become concentrated at the kinetochores, and as the cells progresses towards metaphase the proteins become redistributed to the kinetochore microtubules, both are then re-localised specifically at the kinetochores during early anaphase and maintain that localisation until telophase (Williams & Goldberg, 1994; Scaerou *et al.*, 1999). Although these proteins appear to co-localise throughout the cell cycle there is some discrepancy in the literature regarding the timing of localisation of human Rod and Zw10. Chan *et al.*, show that in early prophase some kinetochores are positive for Rod but not Zw10 (Chan *et al.*, 2000), whereas Scaerou *et al.*, show the opposite in that these kinetochores at an early stage of prophase only have Zw10 present (Scaerou *et al.*, 2001).

Initial indications that these proteins act together came from a study which revealed that Zw10 was mislocalised in *rough deal (rod)* and *abnormal anaphase resolution (aar)* mutants (Williams & Goldberg, 1994). Subsequently, these two proteins have been identified in other multicellular organisms. However, no orthologues of either have been identified in yeast. This has therefore lead to the postulation that these proteins add an increased level of complexity to the spindle assembly checkpoint, presumably due to the increased complexity of the kinetochore structure and the functions which it must orchestrate in metazoans. Zw10 has been identified in a number of organisms (Starr *et al.*, 1997) which, shared a common ancestor around 1 billion years ago (Doolittle *et al.*, 1996) and have quite diverse kinetochore structures. These organisms include *Drosophila*, *C. elegans* with holokinetochores, *Arabidopsis* with the ball and cup kinetochore structure (for review see (Yu *et al.*, 2000)), mouse and human. These results appear to indicate that Zw10 at least is

evolutionarily conserved. To date, Rod has also been identified in human and *C. elegans* (Scaerou *et al.*, 1999).

Classically, the definition of a component of the spindle assembly checkpoint is a mutant that fails to arrest in metaphase in the presence of spindle damage. It has been shown that both Rod and Zw10 fall into this category and both are therefore now thought to contribute in some manner to the spindle assembly checkpoint in *Drosophila* (Basto *et al.*, 2000) and human cells (Chan *et al.*, 2000). Controversy still remains as to how these proteins interact, if at all, with the Mad and Bub components of the checkpoint and what particular function they carry out. It has been shown that Mad and Bub components are still able to localise to the kinetochores in *Drosophila* Zw10 and Rod mutants (Basto *et al.*, 2000) and in human cells following injection of Rod and Zw10 antibodies (Chan *et al.*, 2000). It is now known that these proteins are part of a multisubunit complex in both human (Chan *et al.*, 2000) and *Drosophila* cells (Scaerou *et al.*, 2001). This complex is approximately 19S or 700-900 kDa in *Drosophila.*

Additional information about the function of this complex has been gleaned from the fact that these proteins are required for the targeting of cytoplasmic dynein to the kinetochore (Starr *et al.*, 1998). Cytoplasmic dynein is a microtubule motor protein with a number of roles during mitosis, including movement of the spindle, movement of the chromosomes and trafficking of proteins along the spindle microtubules (for review see (Banks & Heald, 2001)). *Drosophila zw10* mutants prevent the association of the dynein heavy chain with the kinetochore and this is thought to be due to an interaction between Zw10 and dynamitin (the p50 subunit of the dynactin complex) (Starr *et al.*, 1998). In addition to this, it has been shown that the rate of poleward chromosome movement is reduced in *Drosophila zw10* and *rod* mutants (Savoian *et al.*, 2000), suggesting that this complex contributes to poleward chromosome motion, presumably through interaction with the dynein/dynactin complex.

Zwint (Zw10-interacting protein) interacts in a yeast two hybrid screen with human Zw10 (Starr *et al.*, 2000). Zwint is a 43 kDa protein with a coiled-coil domain which has been postulated to target Zw10 to the kinetochore during prometaphase, since it is localised before Zw10. It has also been shown to localise to neocentromeres and

the active centromere of dicentric chromosomes (Starr *et al.*, 2000). To date, no orthologues of Zwint have been identified in any organism outside the mammals.

The main questions remaining unanswered about these proteins are how Zw10 and Rod actually function within the spindle checkpoint and the relevance of their interaction with the motor cytoplasmic dynein. It has been shown that dynein migrates from the kinetochores to the poles during prometaphase and metaphase and carries with it cargo, including the checkpoint protein Mad 2 (Howell *et al.*, 2001) and Rod (Wojcik *et al.*, 2001). It would appear therefore that this could be a mechanism to shut off the spindle assembly checkpoint to let anaphase proceed, and that Zw10 and Rod contribute to this somehow through interactions with cytoplasmic dynein. Figure 1.7 shows a model which has been proposed for how Zw10 and Rod interact at the kinetochore (Starr *et al.*, 1998).

Figure 1.7. Zw10 and Rod at the kinetochore.

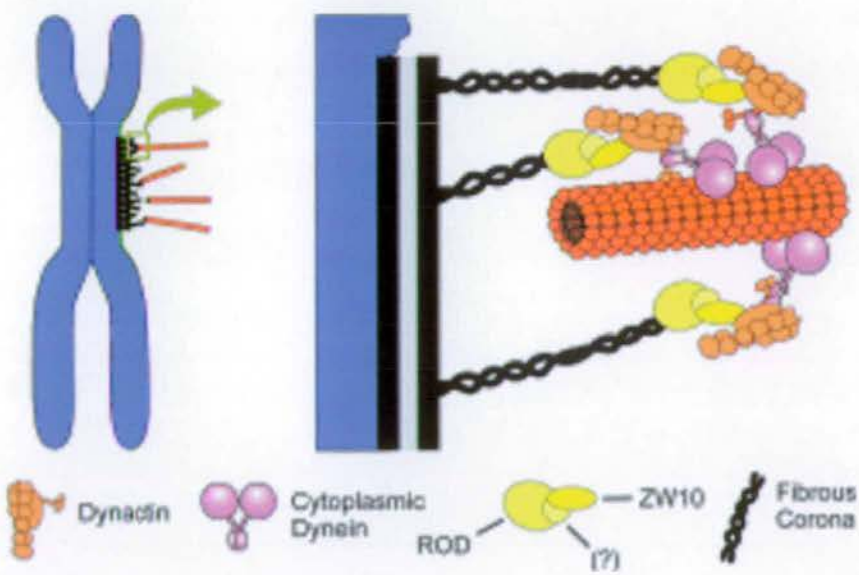

Model of how Zw10 and Rod may interact with cytoplasmic dynein and dynactin at the kinetochore. Diagram taken from Starr *et al.*, 1998.

Table 1.2 summarises the components of the spindle assembly checkpoint which have been discussed.

Table 1.2. Summary of spindle assembly checkpoint proteins, their roles and interactions.

Protein	Comments and key references
Mad1	*In budding yeast;* • Binds and recruits Mad2 to the checkpoint (Brady & Hardwick, 2000) • hyperphosphorylated upon checkpoint activation (Hardwick & Murray, 1995) • Binds Bub1 and Bub3 upon checkpoint activation (Brady & Hardwick, 2000) *In human;* • Binds Bub1 and Bub3 *in vitro* (Seeley *et al.*, 1999)
Mad2	*In budding yeast;* • Binds to Mad1, Mad3 and Cdc20 (Hardwick *et al.*, 2000) *In vertebrates;* • Identified complex with Mad1, BubR1 and Cdc20 (Sudakin *et al.*, 2001) • Mouse knockout is embryonic lethal (Dobles *et al.*, 2000), with heterozygous animals being developing lung tumours indicating haploinsufficiency (Michel *et al.*, 2001) • Inhibits the APC by binding and sequestering Cdc20 (Chen *et al.*, 1998; Kallio *et al.*, 1998) • Structures of Mad2-Cdc20 (Luo *et al.*, 2000) and Mad1-Mad2 (Luo *et al.*, 2002) interactions solved by NMR
Mad3/BubR1	*Mad3*; • Interacts with Mad2 and Cdc20 (Hardwick *et al.*, 2000) • Constitutively bound to Bub3 (Millband & Hardwick, 2002) • Kinetochore recruitment requires Bub1, Bub3, and Mps1 (Millband & Hardwick, 2002) *BubR1;* • Shares homology regions with both Bub1 and Mad3, looks more similar to Mad3 but contains a kinase domain (Hardwick *et al.*, 2000) • Binds motor protein CENP-E (Chan *et al.*, 1999; Yao *et al.*, 2000) • Identified in complexes with Bub3, Mad2 and cdc20 (Sudakin *et al.*, 2001) and Bub3 and Cdc20 only (Tang *et al.*, 2001) • Kinase domain not required for checkpoint function (Tang *et al.*, 2001; Chen, 2002)
Bub1	*Budding yeast;* • Binds Bub3 (Roberts *et al.*, 1994) Binds Mad1 when checkpoint is active (Brady & Hardwick, 2000) *Xenopus;* • Kinase domain not required for the checkpoint (Sharp-Baker & Chen, 2001) • Required for kinetochore localisation of Mad1, Mad2, Bub3 and CENP-E (Sharp-Baker & Chen, 2001)
Bub3	*Budding yeast;* • Binds Mad1 when checkpoint is active (Brady & Hardwick, 2000) Binds Mad1 and Bub1 during a normal cell cycle (Brady & Hardwick, 2000) *Vertebrates;* • Identified in complexes with BubR1, Mad2 and Cdc20 (Sudakin *et al.*, 2001) BubR1 and Cdc20 only (Tang *et al.*, 2001) • Mouse knockout is embryonic lethal (Kalitsis *et al.*, 2000)
Mps1	*Budding yeast;* • Phosphorylates Mad1 *in vitro* (Hardwick *et al.*, 1996) Kinase with essential role in spindle pole body duplication (Weiss & Winey, 1996) *Xenopus;* • Required for recruitment of CENP-E, Mad1 and Mad2 to the kinetochores (Abrieu *et al.*, 2001)
CENP-E	• Kinesin like microtubule motor with no obvious yeast homologue (Yen *et al.*, 1992; Wood *et al.*, 1997) • Interacts with BubR1 (Chan *et al.*, 1999; Yao *et al.*, 2000)

Zw10	• Identified as *Drosophila* mutant which failed to arrest in the presence of spindle damage (Gatti & Goldberg, 1991; Basto *et al.*, 2000) • No yeast homologue identified • Required for the kinetochore localisation of cytoplasmic dynein (Starr *et al.*, 1998) • Interacts with Zwint (Starr *et al.*, 2000) and found in complex with Rod (Scaerou *et al.*, 2001)
Rod	• Identified as *Drosophila* mutant which failed to arrest in the presence of spindle damage (Karess & Glover, 1989; Basto *et al.*, 2000) • No yeast homologue identified • Interacts with dynein (Wojcik *et al.*, 2001) and found in complex with Zw10 (Scaerou *et al.*, 2001)

(The table was adapted from the review by Millband *et al.*, 2002)

1.10 Spindle assembly checkpoint and cancer

For a number of years, it has been known that tumours are associated with chromosomal instabilities and aneuploidy (Lengauer *et al.*, 1997). The molecular basis of this instability is largely unclear. However, there is a growing body of evidence that abnormalities in the function of the spindle assembly checkpoint may in some way contribute to the resulting aneuploidy and, more specifically, mutations in components of the checkpoint have been identified in some human tumours. The first identification of the human orthologues of the yeast spindle checkpoint components Bub1 and Mad3 was described in a study by (Cahill *et al.*, 1998) which, showed mutations in these genes in human colorectal cancers. Colorectal cancers can be defined as having either microsatellite instability (MIN) defects or chromosomal instability (CIN) defects. The molecular basis of the CIN defect was of interest since the cell lines derived from tumours were unable to arrest in metaphase in the presence of the microtubule disrupting drug nocodazole, indicating defects in the spindle assembly checkpoint. Two somatic mutations of human Bub1 were identified in tumours but not present in neighbouring healthy tissue. Both these mutations were found to have a dominant negative effect when transfected into cells. In addition, two mutations of the human BubR1 were identified in this study, the significance of which still remains to be determined. In contrast to the results reported by Cahill et al., a subsequent report has shown that CIN cell lines do actually undergo mitotic arrest in response to spindle damage, although the checkpoint may be somewhat compromised (Tighe *et al.*, 2001).

Numerous studies have been carried out to try and determine the prevalence of mutations in spindle checkpoint proteins in tumours and the subsequent consequences of these mutations. The results of these studies make it very hard to

conclude what impact, if any, mutations in components of the spindle assembly checkpoint have on the progression of human cancers.

An additional study addressing the question of mutations in checkpoint genes arising in human colorectal cancers, found a new mis-sense mutation in *Bub1*, however no mutations in the coding region of *BubR1* (Shichiri *et al.*, 2002). Moreover, it was found that in a number of tumours there was a significant decrease in the expression levels of both Bub1 and BubR1 and that these correlated with lymph node metastasis and shorter relapse-free survival after the patients had undergone surgery. A study into adult T cell leukaemia/lymphoma (ATLL), which is associated with severe chromosome abnormalities, revealed mutations or deletions of Bub1 or BubR1 in 4 out of 10 cases studied (Ohshima *et al.*, 2000), suggesting that mutations in these genes might contribute to the chromosomal abnormalities in this cancer. In addition, a study into nasopharyngeal carcinoma, which is very common in south east Asia, showed that some cells lines derived from these tumours had a defective mitotic checkpoint co-incident with abberantly reduced expression of Mad2 (Wang *et al.*, 2000).

In contrast to those mentioned above, a number of studies have failed to find any significant mutations in components of the spindle checkpoint. For example, a study into glioblastomas revealed only silent mutations or polymorphisms of Bub1, BubR1 and Bub3 (Reis *et al.*, 2001). Studies into lung cancers yielded similar results with no mutations, rearrangements or deletions in Bub1 or BubR1 (Sato *et al.*, 2000), no mutations in Bub1, BubR1 or Bub3 (Haruki *et al.*, 2001) and no mutations in Mad2 or its downstream interactor p55CDC (Takahashi *et al.*, 1999). Thyroid cancers have also been investigated (Ouyang *et al.*, 2002) and although a high number of these have aberrant checkpoints as judged by treatment with nocodazole, this does not correlate with mutations in Bub1 or BubR1. A very thorough study of hepatocellular carcinomas, (Saeki *et al.*, 2002) showed that although the spindle checkpoint was impaired, no mutations were found in Bub1, BubR1, Bub3, Mad2 or Cdc20.

One possible reason for the fact that mutations were not discovered in some of these cancers with aberrant spindle assembly checkpoints may simply be that the wrong genes were being investigated. It is apparent that the spindle assembly checkpoint is very complicated, involving a number of different proteins and complexes which are conserved from yeast to human and that the checkpoint is even more complex and

highly regulated in metazoans by the assistance of Zw10 and Rod, CENP-E and MAPK. Most studies of human cancers have focussed on Bub1 and BubR1 as potential targets for mutation and have neglected the other components of the checkpoint, Mad1, Mad2, Bub3, Zw10 and Rod. Although it appears that Bub1 and BubR1 mutations do not play a significant role in many types of cancer, one or more of the other components may be doing so. As discussed previously Mad2 +/- mice develop papillary lung adenocarcinomas by the age of 18-19 months, indicating a role for this checkpoint protein in tumour progression (Michel *et al.*, 2001). It is obvious that chromosome instabilities and aneuploidy are a common feature of a number of cancer types and that this evidently leads to progression of the disease and subsequent genetic abnormalities within the cells. For now, it remains controversial as to what effect mutations in components of the spindle assembly checkpoint have on the progression of human cancers.

A further intriguing finding linking the spindle assembly checkpoint with colorectal cancer is the interaction between the Adenomatous Polyposis Coli (APC) protein and the Bub proteins. It is known that mutations in the APC gene are responsible for some forms of colon cancer (for review see (Kinzler & Vogelstein, 1996)). A number of roles are known for APC including regulation of the degradation of β-catenin in the Wnt signalling pathway (for review see (McCartney & Peifer, 2000; Peifer & Polakis, 2000)), stabilisation of microtubules (Nathke *et al.*, 1996; Mimori-Kiyosue *et al.*, 2000) and regulation of the cytoskeleton (McCartney *et al.*, 1999). A recent study by Kaplan and colleagues has shown that cells with a truncated version of the APC gene are defective in chromosome segregation. APC is a plus end microtubule binding protein, which is embedded in the kinetochore. In addition it was shown that immunoprecipitates of APC from mitotic HeLa cells contained Bub1 and Bub3 and that recombinant complexes of Bub1-Bub3, BubR1-Bub3 and immunoprecipitated Bub1 could efficiently and specifically phosphorylated APC (Kaplan *et al.*, 2001). No specific role for APC in the spindle assembly checkpoint has yet been defined since cells mutant for the protein are able to arrest in the presence of nocodazole. However, it seems that APC's role as a kinetochore-microtubule binding protein may contribute to the chromosomal instability observed in colorectal cancer through its interactions and regulation by the Bub components of the spindle assembly checkpoint.

A further intriguing observation is the link between Brca2 and BubR1. Brca2 is known to have a function in DNA repair and to bind to the Rad51 protein, a RecA orthologue that is involved in homologous recombination and double strand break repair (Shinohara *et al.*, 1992; Baumann *et al.*, 1997). One defective copy of the Brca2 gene pre-disposes to breast cancer (Wooster *et al.*, 1995; Tavtigian *et al.*, 1996), and usually two defective copies occur in the tumour (Collins *et al.*, 1995). Therefore this gene is defined as a tumour suppressor.

Tumours from mice that are homozygous mutant for Brca2 have a dysfunctional spindle assembly checkpoint, and this is often accompanied by mutations in Bub1, BubR1 and p53 (Lee *et al.*, 1999). In addition to the observation that the spindle assembly checkpoint is dysfunctional in these tumours, a direct link between Brca2 and the checkpoint has been identified in the form of an interaction between Brca2 and BubR1. This interaction was identified in a yeast two-hybrid screen (Futamura *et al.*, 2000). Furthermore, BubR1 can phosphorylate Brca2 *in vitro*. Moreover, stimulation of the checkpoint by treating the cells with vincristine, which disrupts microtubules, increased the expression of both BubR1 and Brca2 (Futamura *et al.*, 2000). The authors of this paper conclude that Brca2 may have a role in the spindle assembly checkpoint. However, it has been shown in both human and the *Xenopus* system that the kinase domain of BubR1 is dispensable for its function in the checkpoint (Tang *et al.*, 2001; Chen, 2002), so it could be worth considering the potential role of BubR1, and in particular its kinase activity, in other pathways such as DNA repair (Brca2) and signalling (APC).

The involvement of p53 in the spindle assembly checkpoint remains somewhat controversial. Observations that cells from p53-null mouse embryos failed to arrest in metaphase in the presence of spindle damage induced by either nocodazole or colcemid led Cross *et al.*, to conclude that, in mouse at least, the spindle assembly checkpoint was dependant upon p53 (Cross *et al.*, 1995). This phenomenon has subsequently been investigated in human cells as it is known that some p53 missense mutations have a dominant gain of function activity, which leads to genetic instability. Fibroblasts from patients with Li-Fraumeni syndrome, which have one mutant copy of p53, were exposed to spindle damaging agents and polyploid cells were generated, indicating that the spindle assembly checkpoint failed to arrest the cells in mitosis (Gualberto *et al.*, 1998). The same phenotype was observed with the

expression of a mutant allele of p53, $p53^{RSC}$ (relaxed spindle checkpoint). However, when p53 levels were decreased in human cells by a number of means including retroviral infection and anti-sense techniques and then the cells challenged with spindle disrupting agents, the spindle assembly checkpoint was maintained and the cells arrested. In order to extend these results, Gualberto *et al.*, repeated the mouse experiments of Cross *et al.*, and again found that, in the case of mouse the spindle checkpoint was dependant upon p53 function. Finally, human tumours lacking p53 were tested but found to have a functional checkpoint. It therefore seems that a dominant mutant form of p53 affects the spindle checkpoint and can play a role in human tumourogenesis. Around 40% of p53 mutations identified in tumours fall into this category.

1.11 Perspectives

This thesis is divided into three results chapters which aim to address some of the issues raised concerning the spindle assembly checkpoint and the vertebrate kinetochore. More specifically, Chapter 3 focuses on the identification and characterisation of chicken BubR1. The cDNA was cloned from a library and sequenced, revealing that it had a high degree of similarity to other vertebrate BubR1 proteins. Subsequently, a polyclonal antibody was generated so that the localisation and function of this protein could be investigated in chicken cell lines.

Chapter 4 focuses on the generation of a DT40 cell line with a targeted disruption of BubR1. DT40 is a hyper-recombinogenic chicken cell line which is a useful tool with which to investigate essential genes, since conditional cell lines can be generated. The first stage of this project was cloning the chicken genomic locus in order that targeting vectors could be generated. Once the first allele was targeted, attempts were made to express the rescue construct within these cells.

The work in Chapter 5 aims to further the understanding of the vertebrate kinetochore and the spindle checkpoint by using *Xenopus* egg extracts. This system is a powerful tool with which to study cell cycle complexes. In particular the checkpoint components Zw10 and Rod were cloned from a *Xenopus* cDNA library and antibodies were raised to them. Preliminary work with these antibodies has

identified a complex, in *Xenopus* egg extracts, of approximately 11S which contains Zw10 and Rod. Hopefully, the reagents generated in this study will be of use in the future in order to further investigate the vertebrate kinetochore.

Chapter 2

Materials and Methods

2.1 Materials

2.1.1 Chemicals and Solutions

All solutions were prepared using Milli-Q synthesis water (Millipore) and, where appropriate were autoclaved before use. All solutions used for RNA work were treated with 0.1% diethyl pyrocarbonate (DEPC), supplied by Sigma. Chemicals used were purchased from Sigma, BDH or Fisher.

Acids, alcohols and solvents were supplied by Sigma, BDH or Fisher. Radioisotopes were supplied by Amersham and oligodeoxynucleotides primers were supplied by Sigma-Genosys.

Table 2.1. Genotype of Eschericia coli strains used in this thesis

Strain	Genotype	Use
Top 10	F⁻ mcrA Δ(mrr-hsdRMS-mcrBC) ϕ80lacZΔM15 ΔlacX74 deoR recA1 araD139 Δ(ara-leu)7697 galU galK rpsL(Str^R) endA1 nupG	General cloning
XL-1 Blue	recA1 endA1 gyrA96 thi-1 hsdR17 supE44 relA1 lac [F' proAB $lacI^q$ ZΔ M15 Tn10 (Tet^r)]	Site-directed mutagenesis
XL-1 Blue MRF'	Δ(mcrA)183 Δ(mcrCB-hsdSMR-mrr)173 endA1 supE44 thi-1 gyrA96 relA1 lac [F'proAB $lacI^q$ ZΔM15 Tn10 (Tet^r)]	λ-ZAP chicken cDNA library screen
XL-1 Blue MRA-P2	Δ(mcrA)183 Δ(mcrCB-hsdSMR-mrr)173 endA1 supE44 thi-1 gyrA96 relA1 lac (P2 lysogen)	λFixII chicken genomic library screen
SOLR	e14⁻(McrA⁻) Δ(mcrCB-hsdSMR-mrr)171 sbcC recB recJ uvrC umuC::Tn5 (Kan^r) lac gyrA96 relA1 thi-1 endA1 λ^R [F'proAB $lacI^q$ ZΔM15 Tn10 (Tet^r)]^c	*In vivo* excision from λ-ZAP cDNA library
C600	*Sup*E44 *hsdR thi-1 thr-1 leuB6 lacY1 tonA21 hflA150 [chr::Tn10 (tet^r)]*	*Xenopus* library screen λgt10
BL21	*hsdS gal (λcIts*857 *ind1 Sam7 nin5* lacUV5- T7 gene *1*	Expression of recombinant fusion proteins

Table 2.2. Antibodies used in this thesis

Antibody	Working dilution	Reference
AuroraB	1:500	Earnshaw laboratory
BubR1	1:500	This thesis
CENP-C	1:500	Ciaran Morrison
INCENP	1:500	Earnshaw laboratory
Monoclonal anti – HA (12CA5)	western 1:1000	Cell line from Earnshaw laboratory
	IF 1:500	
Monoclonal anti-tubulin (B512)	western 1:10000	Sigma
	IF 1:2000	
ZW10	1:500	This thesis
Rod	1:500	This thesis
Texas Red and FITC conjugated secondary antibodies for immunofluorescence (IF)	1:200	Jackson Labs
HRP-conjugated secondary antibodies for ECL	1:10000	Amersham

Table 2.3. Common reagents and buffers

Reagent or buffer	Details	Notes
10 x DNA loading dye	20% Ficoll, 0.1 M EDTA, pH 8.0, 1% SDS, 0.25% Bromophenol blue, 0.25% xylene cyanol.	Add to DNA sample before running agarose gel.
20 x XB salts	2 M KCl, 20 mM $MgCl_2$, 2 mM $CaCl_2$.	Filter sterilised and stored at 4°C.
3 x sample buffer	150 mM Tris:HCl pH 6.8, 45% sucrose, 6 mM K-EDTA pH 7.4, 9% SDS, 0.03% bromophenol blue.	Add β-mercaptoethanol to 10% final concentration just prior to use.
Aprotinin	Sigma A-6279	1,000 x
Church buffer	0.5 M NaPi/ 7% SDS/ 1 mM EDTA	For Southern hybridisation.
CLAP	Chymostatin (Sigma C-7268) Leupeptin (Calbiochem 108975) Antipain (Sigma A-6191) Pepstatin A (Sigma P-4265)	All 1 mg/ml in DMSO 1,000 x stock.
Coomassie Brilliant Blue R	0.5% Coomassie in methanol	5 x stock
CSF Energy Mix	150 mM creatine phosphate, 20 mM ATP, 20 mM $MgCl_2$	stored aliquoted at -20°C.
CSF Extract buffer (CSF-XB)	100 mM KCl, 0.1 mM $CaCl_2$, 1 mM $MgCl_2$, 10 mM potassium HEPES, pH 7.7, 50 mM sucrose, 5 mM EGTA, pH 7.7	Made from 20 x XB salts filter sterilised and stored at 4°C.
Cytoskeleton buffer	137 mM NaCl, 5 mM KCl, 1.1 mM Na_2HPO_4, 0.4 mM KH_2PO_4, 2 mM $MgCl_2$, 2 mM EGTA, 5 mM PIPES, 5.5 mM glucose, pH'd to 6.1 and filter sterilised	For IF of microtubules.
Dejellying solution	1x XB salts, 2% w/v cysteine.	Made up within 1 hour of use and titrated to pH 7.8 with NaOH.

Diluent	35% methanol, 14% acetic acid	To dilute Coomassie to 1 x
Extract Buffer (XB)	100 mM KCl, 0.1 mM $CaCl_2$, 1 mM $MgCl_2$, 10 mM potassium HEPES, pH 7.7, 50 mM sucrose,	Made from 20 x XB salts filter sterilised and stored at 4°C.
Gerace buffer	5 x stock; 250 mM triethanolamine:HCl pH7.4, 500 mM NaCl, 10 mM K-EDTA pH 7.4, 2.5% Triton-X-100, 0.5% SDS	For blotting with Protein A-^{125}I.
KB	10 mM Tris :HCl pH 8.5, 0.2 mM EDTA, 25 mM NaCl	For IF of metaphase spreads.
KCM	120 mM KCl, 20 mM NaCl, 10 mM Tris pH 8.0, 0.5 mM EDTA pH 8.0, 0.1% Triton-X-100	For IF.
LB (Luria-Bertani Medium)	1% tryptone, 0.5% yeast extract, 1% NaCl, pH adjusted to 7.0 with 5N NaOH.	Prepared by the Media staff.
MMR	100 mM NaCl, 2 mM KCl, 1 mM $MgCl_2$, 2 mM $CaCl_2$, 0.1 mM EDTA, 5 mM HEPES, pH 7.8.	10 x stock prepared and titrated to pH 7.8 with NaOH.
NaPi	$Na_2HPO_4 \bullet H_2O$	1 M stock, pH adjusted to 7.2 with H_3PO_4
PBS	137 mM NaCl, 2.7 mM KCl, 10 mM Na_2HPO_4, 2 mM KH_2PO_4.	General use
PMSF	Sigma P-7626	100 mM in ethanol, 10,000 x stock.
Running buffer	25 mM Tris, 250 mM glycine, 0.1% SDS	For running SDS-PAGE gels.
SDS-PAGE gel buffer	1.5 M Tris pH 8.8	Lower gel
SDS-PAGE stacking gel buffer	0.5 M Tris pH 6.8	Stacking buffer
Slow destain	10% methanol, 7% acetic acid	To destain Coomassie.
SM buffer	For 1 L, 5.8 g NaCl, 2 g $MgSO_4 \bullet 7H_2O$, 50 ml 1 M Tris-Cl , pH 7.5, 5 ml 2% gelatin solution. Sterilise by autoclaving	For the dilution of bacteriophage λ stocks.
SSC	10 x stock,1.5 M NaCl/ 0.15 M sodium citrate, adjust pH to 7.0 with citric acid	General use
Super broth	5 g tryptone, 20 g yeast extract, 5 g NaCl per litre. pH adjusted to 7.5 with 5 M NaOH.	For recombinant protein expression, prepared by the media staff.
TAE	For 1 L of 50 x stock, 242 g Tris base, 57.1 ml glacial acetic acid and 100 ml 0.5 M EDTA, pH 8.0.	For agarose gels.
Tail buffer	50 mM Tris pH 8.8, 100 mM EDTA, 100 mM NaCl, 1% SDS	For the preparation of genomic DNA.
TEEN	1 mM triethanolamine:HCl pH8.5, 0.2 mM EDTA, 25 mM NaCl	For IF.
TfbI	30 mM KAc, 100 mM $RbCl_2$, 10 mM $CaCl_2$, 50 mM$MnCl_2$, 15% glycerol. pH to 5.8 with dilute HAc, filter sterilise and store at 4°C.	For the preparation of chemical competent *E. coli.*
TfbII	10 mM MOPS, 75 mM $CaCl_2$, 10 mM $RbCl_2$, 15% glycerol. pH to 6.5 with KOH, filter sterilise and store at 4°C.	For the preparation of chemical competent *E. coli.*
Transfer buffer	48 mM Tris, 39 mM glycine, 20% methanol and 0.0375% SDS	For transferring SDS-PAGE gels.

2.2 Methods

2.2.1 Plasmid DNA preparation

Small scale plasmid DNA preparations were performed using the Ultraclean Plasmid miniprep kit from MoBio laboratories Inc. according to manufacturer's instructions. Cultures of *E.coli* (2 ml) were grown overnight in the presence of antibiotics at 37°C with shaking. Larger midi (50 ml) or maxi (100 ml) preparations were performed using Qiagen Midi/MaxiPrep kit according to manufacturer's instructions.

2.2.2 Agarose gel electrophoresis

Unless otherwise stated, 1% agarose gels were prepared using Invitrogen electophoresis grade agarose in TAE buffer and contained 0.3 µg/ml ethidium bromide. These were elecrophoresed using Hybaid tanks in 1 x TAE according to manufacturer's instructions. Gels were analysed using a UV light box and photographed with a digital camera.

2.2.3 Purification of DNA from agarose gels

After gel electrophoresis bands were excised from the gel using a razor blade and placed in a 1.5 ml eppendorf tube. DNA was extracted using Qiagen Qiaquick Gel Extraction Kit according to manufacturer's instructions, and eluted from the column in de-ionised water (dH_20).

2.2.4 Restriction digestion of DNA

In general, restriction digests were performed using enzymes from New England Biolabs. The enzymes were used with the 10x buffer provided and BSA (0.1 mg/ml) or any other required supplement. The digest was performed at the required temperature for 2-16 hours depending on the amount and type of DNA being digested. If appropriate, the enzyme was inactivated by heating to 65°C for 15 minutes.

2.2.5 Generation of blunt ended DNA fragments

T4 DNA polymerase, which has both 5′→3′ polymerase activity and 3′→5′ exonuclease activity, was used to blunt both 5′ and 3′ overhangs left after restriction digestion. T4 DNA polymerase was obtained from New England Biolabs, the reaction was carried out in the presence of 10x buffer and supplemented with BSA (0.1 mg/ml) and dNTPs (100 μM). 5U of enzyme/μg DNA was used and the reaction incubated at 37°C for 5 minutes and then heat inactivated at 75°C for 15 minutes.

2.2.6 Dephosphorylation of 5' DNA ends

Vectors for sub-cloning fragments were treated with Calf Intestinal Alkaline Phosphatase (CIP) after restriction digestion and prior to ligation in order to reduce the self-ligation of empty vector. CIP was obtained from New England Biolabs and was used with any restriction enzyme buffer. CIP was used at a concentration of 1U per pmol of DNA, the reaction was carried out at 37°C for 1hr.

2.2.7 Ligation of DNA fragments

Ligations were performed using T4 DNA ligase from New England Biolabs supplemented with the provided buffer. A vector:insert ratio of 1:3 was used where possible, and the reaction incubated at 18°C overnight or 25°C for 5 hours before transformation into competent *E. coli.*

2.2.8 Preparation of chemical competent *E. coli* and transformation

E. coli were grown in LB at 37°C to λ nm A_{600} 0.5, then transferred to ice for 5 minutes. Cells were pelleted by centrifugation at 3300 g in the Heraeus benchtop megafuge for 15 minutes and then re-suspended in TfbI (40 ml per 100 ml culture, see Table 2.3). Thereafter, cells were pelleted, re-suspended in TfbII (4 ml per initial 100 ml culture, see Table 2.3) and incubated on ice for 15 minutes.

In order to make highly efficient competent cells it is important to keep the cells as cold as possible during aliquoting. This was therefore carried out in the cold

room with all pipettes, tip and eppendorfs pre-chilled. The cells were snap frozen in liquid nitrogen and stored at -80°C.

For transformations, 100 µl of cells were thawed on ice prior to the ligation reaction mixture being added, and the mixture was then incubated on ice for 20 minutes. This was then heat shocked at 42°C for 90 seconds and chilled on ice for 2 minutes. 0.5 ml of LB was added and the cells incubated for 40 minutes at 37°C. The cells were then pelleted by spinning at 600 g for 5 minutes. The majority of the supernatant was removed and the pellet re-suspended in 100 µl. This was spread on agar plates containing the appropriate antibiotic selection.

2.2.9 DNA Sequencing

Samples were prepared for the ICMB (Institute of Cell and Molecular Biology, University of Edinburgh) sequencing facility to run on the ABI 3100 sequencing machine.

200-250 ng of mini or midi prep DNA or phage DNA was used per reaction. This was mixed with 3.2 pmol primer and 4 µl of ABI big dye mix (Applied Biosystems) and the reaction volume was adjusted to 10 µl with dH_2O. PCR cycling was carried out as described below on the Personal Cycler (Biometra).

Table 2.4. ABI sequencing reaction.

Step	Conditions	Cycle
1	95°C - 1 minute	
2	95°C - 1 minute 50°C – 15 seconds 60°C – 4 minutes	25

The DNA pellet was then precipitated at room temperature for 15 minutes by adding 1 µl 3M sodium acetate and 25 µl 100% ethanol per reaction. The DNA was then spun at 20,000 g for 15 minutes, washed with 70% ethanol and then re-spun. The pellet was either air dried or dried under vacuum.

Sequences were analysed using computer programs including Editview (ABI Prism, Perkin Elmer), Gene Jockey (BioSoft) and Sequencher (Gene Codes Corporation). Plasmid maps were constructed using DNA Strider.

2.2.10 Polymerase Chain Reaction (PCR)

Polymerase chain reaction (PCR) was carried out on either a Personal Cycler (Biometra) or Robocycler Gradient 40 (Stratagene), depending upon the experiment being undertaken. Different polymerases were used depending on template and the experiment. Below is a summary of these polymerases, the primer and dNTP concentration used and an example of a programme. Differences to these methods are indicated in the text.

2.2.10.1 Taq polymerase (Roche)

0.25 µM primers
100 µM dNTP's
0.5 µl enzyme per 50 µl reaction

Table 2.5. PCR using Taq polymerase

Step	Conditions	Cycle
1	95°C – 2 minutes	
2	95°C – 1 minute 55°C – 1 minute 72°C – 1 minute per kb	25 - 30
3	72°C – 10 minutes	

2.2.10.2 Vent polymerase (NEB)

As above for Taq polymerase.

2.2.10.3 *PfuTurbo* (Stratagene)

0.25 µM primers
250 µM dNTP's
2 µl enzyme per 50 µl reaction

Table 2.6. PCR using PfuTurbo

Step	Conditions	Cycle
1	95°C – 2 minutes	
2	95°C – 1 minute 55°C – 1 minute 76°C – 2 minute per kb	25 - 30
3	76°C – 10 minutes	

2.2.10.4 TaKaRA LA Taq (Takara Shuzo Co., Ltd.)

0.25 µM primers

Buffer, $MgCl_2$ and dNTP's supplied with kit and reaction carried out according to manufacturer's instructions. Typical cycle as above for Taq polymerase.

2.2.10.5 Using phage library clones as a template for PCR

This method was used for the rapid amplification of library insert DNA in order that it could be cloned and sequenced. The *Xenopus* cDNA library used was cloned into the λgt10 vector. High titre stocks were prepared from phage purified through a tertiary screen as described in section 2.20. The DNA was extracted from these stocks by phenol/chloroform extraction. Initially 500 µl of phage stock was heated to 95°C for 2 minutes, 500 µl of phenol/chloroform/ isoamyl alcohol (25:24:1) was then added and the sample centrifuged for 5 minutes at 20, 000 *g*. The top aqueous phase was removed to a fresh tube and 1/10 volume of 3M sodium acetate was added together with an equal volume of isopropanol. After inversion, this was centrifuged again at 20,000 *g* for 5 minutes. The DNA pellet was then washed twice in 70% ethanol and air dried. It was then resuspended in 100 µl dH_2O. This DNA was used as a template for the PCR using the λgt10 forward and reverse primers. The PCR products were cloned into pGEM-T and sequenced.

2.2.11 Reverse Transcriptase – PCR (RT-PCR)

cDNA synthesis was carried out using the Superscript First-Strand Synthesis for RT-PCR kit from Invitrogen (Cat. #11904-018). RNA was prepared as described in section 2.18. cDNA was generated using oligo dT and synthesised according

to the manufacturer's instructions. PCR was carried out as described in section 2.2.10.

2.2.12 5′ Rapid amplification of cDNA ends (5′ RACE)

Rapid amplification of cDNA ends was carried out using a kit obtained from GibcoBRL (cat. #18374-041, 5′ RACE system for rapid amplification of cDNA ends v.2) according to the manufacturer's instructions. This method allows the isolation and cloning of mRNA sequences where the 5′ end is unknown. Initially RNA is reverse transcribed using a gene-specific primer. A homopolymeric tail is then added to this cDNA using terminal deoxynucleotide transferase. The unknown sequence can then be amplified using an additional gene-specific primer and an anchor primer, which contains sequence complementary to the homopolymeric tail together with an adapter region.

2.2.13 Site Directed Mutagenesis

Site directed mutagenesis was carried out using the QuikChange Site-Directed Mutagenesis kit (Cat. #200519) obtained from Stratagene, according to manufacturer's instructions. This method involves designing a primer with the mutation in it. Both a forward and reverse primer are required and the template is amplified using *PfuTurbo,* resulting in the incorporation of the mutation into the PCR product. The PCR reaction is then digested with the enzyme *DpnI,* which will digest only the methylated non-mutated parental DNA, leaving the newly synthesised mutated DNA to be transformed into bacteria.

Table 2.7. Constructs used in this project, description of cloning, use and reference to main text.

Construct	Description of cloning	Description and reference
pBluescriptKS-ggBubR1	*In vivo* excision from λ ZAP library	Chicken BubR1 cDNA used throughout this thesis.
pGex-4T-1 ggBubR1 653-778	PCR with primers HD1 and HD2, cloned *Eco*R 1/blunt into *Eco*R 1/*Xho* 1(blunt) sites of pGEX-4T-1.	N-terminal GST fusion for the generation of chicken BubR1 specific rabbit polyclonal antibodies. Section 3.2.3
pEGFP-C1-ggBubR1	PCR of the 5′ end of ggBubR1 with primers HD3 and HD4, cloned into pEGFP-C1. *Acc* 1/ *Kpn* 1 fragment cut from pbsKS-ggBubR1, cloned into pEGFP-C1 with 5′ end.	N-terminal GFP fusion of full length chicken BubR1.
pUHG10.3-ggBubR1	PCR to fuse the STOP codon to the polyA signal and remove 356 bp of 3′ UTR. PCR with HD5 and HD6, *Nco* I/*Kpn* I removed from pbsKS-ggBubR1 and replaced by smaller fragment with mutated 3′ UTR.	Rescue construct (3'UTR mutated for RT-PCR screening purposes). Tet operator sequence upstream of CMV promoter, allows the conditional expression of the cDNA once co-transfected with tTA plasmid. Section 4.2.5
pZeo-ggBubR1-HA-His	PCR to remove STOP codon using HD10 and HD11. Cloned into pZeoSV2HA-His with 5′ fragment cut *Sma* I/*Spe* I from pbsKSggBubR1.	C-terminal HA-His tag on full length chicken BubR1. Section 3.2.4
KOV1 (Bsr, HisD, Puro)	see chapter 4 section 4.2.2 for description of cloning.	Vector for targeted disruption of the BubR1 locus in DT40 cells. Section 4.2.2
KOV2 (Bsr, HisD, Hyg, Puro)	see chapter 4 section 4.2.2 for description of cloning.	Vector for targeted disruption of the BubR1 locus in DT40 cells. Section 4.2.2
pGEM-T-xlZw10 (3′ end)	200 bp PCR product generated using primers HD12 and λGT10 –R and cloned into pGEM-T.	200 bp PCR product from 3′ end of *Xenopus* Zw10 used to screen a *Xenopus* oocyte cDNA library. Section 5.2.5
pGex-xlXw10 (most C-terminal 50 amino acids)	200 bp PCR product generated with primers HD13 and HD14, cloned into pGEX-4T-1 EcoR1/Xho1.	N-terminal GST fusion of most C-terminal 50 aa of *Xenopus* Zw10 in order to generate rabbit polyclonal antibodies. Section 5.2.5
pGem-T -xlRod (3-4)	1.5 kb PCR product generated using primers HD15 and HD16 and cloned into pGEM-T.	1.5 kb PCR product of *Xenopus* Rod used to screen *Xenopus* oocyte cDNA library. Section 5.2.6
pGex-xlRod (most C-terminal 126 amino acids)	500bp PCR product generated using primers HD17 and HD18, cloned into pGEX-4T-1 EcoR1/Xho1.	N-terminal GST fusion of C-terminal 126 amino acids of *Xenopus* Rod in order to generate rabbit polyclonal antibodies.

Table 2.8. Primers used for cloning as described in Table 2.4

Primer name	Sequence 5′ - 3′	Use
HD1	GGGGAATTCAGTGTTCTAAAGGAAGAC	For cloning peptide for BubR1 GST fusion
HD2	GGGGGATCCCTCCAAATGAAAATGTGG	
HD3	CCCAAGCTTAGATGTCACGGGACGGTGAC	5′ end of BubR1 for pEGFP-C1
HD4	CTTTCTGTAGACTTCAGC	
HD5	GATTGTCCATGGAGATCTGAG	To fuse the stop codon to the polyA signal for rescue of BubR1 KO.
HD6	CGGGGTACCTATCAAGATACAACTTTATTATCAGAA CTTCTCCAAGAAGAAAC	
HD7	CCGGGTACCATGTCACGGGACGGTGACGAT	5′ arm from KOV1
HD8	CGCGGATCCCTGATTTCTGATTCGAATTCT	
HD9	CGCGGATCCGATCCAAGGGTTCATTACAGC	5′ arm for KOV2
HD10	GTTATTTTACTAGTTGTTTAT	To remove stop codon for BubR1-HA-His fusion
HD11	ATAGTTTAGCGGCCGCCTGTGAAAACAGAACTTCTC	
HD12	TATGCAGGCCAGCTTGCAGGA	To clone 3′ end of *Xenopus* Zw10 from λGT10 library
λGT10-R	CTTATGAGTATTTCTTCCAGGGTA	
HD13	CCGGAATTCATGCAGGCCAGCTTGCAG	C-terminal 50 amino acids of *Xenopus* Zw10 as GST fusion
HD14	CCGCTCGAGTTTGATCTTTGCCAGGGC	
HD15	CCCAAAGTAAAGCCGGAAGATC	Fragment of *Xenopus* Rod.
HD16	TGAGTGGGCTGCAGCTATTGCT	
HD17	CCGCTCGAGATTTAAAAAGGCCTTTAC	C-terminal 126 amino acids of *Xenopus* Rod as GST fusion.
HD18	CCGGAATTCTTGTTAATTTCCCACATG	
HD19	ATGGAGGCAGCGGAGACAGAGG	For RT-PCR of human Zwint
HD20	TCATGGCAAATTTACATCTCCA	
HD21	CAGGCCTTCTGTCAAAACTG	5′ External probe for targeting
HD22	CTTCAAGCTCTGCGTGATTA	

2.2.14 Preparation of genomic DNA from tissue culture cells

Genomic DNA was prepared from DT40 cells in order to screen colonies for targeting events by Southern hybridisation. DT40 cell colonies were picked from 96 wells into 3 ml of medium (see Table 2.10) and grown for 2-3 days until the cells were confluent, half for freezing and half for DNA preparation. The cells (1.5 ml) were pelleted by centrifugation at 240 g for 5 minutes. The cells were then lysed in 0.5 ml tail buffer (50 mM Tris pH 8.8, 100 mM EDTA, 100 mM NaCl, 1% SDS) containing 0.5 mg/ml proteinase K and incubated overnight at 37°C. The samples were shaken vigorously for 1-2 minutes then 200 µl of 6 M (saturated) NaCl was added and the shaking repeated. The samples were

centrifuged at 20, 000 *g* for 10 minutes. The supernatant was transferred to a fresh tube and 1 volume of isopropanol was added to precipitate the DNA. The samples were centrifuged again at 20, 000 *g* for 10 minutes, and the DNA pellet washed in 70% ethanol and spun again at 20, 000 *g* for 10 minutes. The DNA pellet was air dried and re-suspended in 70 µl dH_20.

2.2.15 Southern Blot

DNA was digested as described in section 2.2.4. In the case of genomic DNA this was always carried out in a volume of 50 µl with the addition of RNase (10 µg/ml) and BSA, and the reaction was incubated overnight at 37°C. Digested DNA was electrophoresed on a 0.8% agarose gel as described in section 2.2.2 and photographed alongside a fluorescent ruler in order to calculate the size of bands after blotting. The gel was then depurinated in 0.25 M HCl for 20 minutes and denatured in 0.5 M NaOH/ 1.5 M NaCl for 20 minutes. The gel was transferred onto nylon membrane (Amersham Hybond-N), in 10 x SSC (see Table 2.3), by upwards capillary transfer (Russel, 2001). After transfer, the membrane was UV crosslinked with 0.12 J using the UV Stratalinker 2400 (Stratagene), prior to hybridisation (section 2.2.17) with a radiolabelled probe (section 2.2.16).

2.2.16 Random priming with ^{32}P

Random priming and incorporation of radiolabelled α-^{32}P-dCTP was carried out using the Megaprime DNA labelling kit (Amersham, Cat. No. RPN1607), according to manufacturer's instructions.

2.2.17 Hybridisation

Membranes previously UV crosslinked were pre-hybridised in church buffer (see Table 2.3) with salmon sperm DNA for at least 1 hour at 65°C prior to the addition of radiolabelled probe. The membranes were then hybridised at 65°C overnight. Membranes were washed (40 mM NaPi/ 1% SDS) at 65°C until the desired signal remained. Generally this was 1 x 5 minutes, 1 x 20 minutes and 1 x 10 minutes. The membranes were exposed to photographic film at -80°C for the appropriate length of time depending on the strength of the signal. In some

cases the signal was visualised using the phosphoimager (Storm 860, Molecular Dynamics).

2.2.18 RNA preparation

RNA was prepared from tissue culture cells using TRIzol (Total RNA Isolation Reagent) obtained from Invitrogen and carried out according to the manufacturer's instructions. If 1.5 x 10^6 DT40 cells were used, the pellet was re-suspended in 20 µl DEPC- treated water (0.1%) and heated to 50°C for 10 minutes to re-suspend.

2.2.19 Bacteriophage lambda techniques

In all, three bacteriophage lambda (λ) libraries were screened, DT40 genomic library (Earnshaw laboratory), DU249 cDNA library (Earnshaw laboratory) and *Xenopus* cDNA library (Rabagliati et al., 1985). The techniques used for screening these libraries were identical, with the only difference being the bacterial cells used as shown in Table 2.9.

Table 2.9. Cells used for library screens

Library	Cells
Genomic DT40 (chicken cells)	MRA-P2
cDNA DU249 (chicken cells)	XL1-Blue MRF'
	SOLR (for *in vivo* excision)
cDNA *Xenopus* oocyte	C600

To plate the library, 4 LB agar texas (22 cm x 22 cm) plates were prepared with 5 x 10^5 pfu of phage on each. These were then incubated at 37°C until separated plaques had formed – generally this took around 8 hours.

Plating cells were grown with the addition of $MgSO_4$ (10 mM) and maltose (0.2%) to an OD_{600} = 0.5 prior to being spun down and re-suspended in 10 mM $MgSO_4$ to an OD of 0.5. Plating cells (200 µl) were mixed with the phage and incubated at 37°C for 15 minutes. Normally, various dilutions of the phage stock were required and these were diluted in SM buffer (see Table 2.3) prior to incubation with the cells. To this, 3 ml of top agarose, previously melted and kept at 50°C until required, was added and the mixture poured quickly onto an LB agar plate, which had been previously dried and warmed at 37°C.

To titre phage, 6 x 10 fold serial dilutions of phage were prepared in SM buffer, using 1 µl of undiluted, and then serial 10 fold dilutions, and plated out as described above.

Plaque lifts were performed using nylon membranes. In the case of library screens, two membranes were lifted from each plate. This was to ensure the validity of any plaques picked by choosing only those that appeared on both membranes, 'double positives'. The membranes were placed on the plates for 2 minutes, during which time marks were made with ink in order to orientate the membranes with the plates after hybridisation. The membranes were then transferred through denaturation (1.5 M NaCl, 0.5 M NaOH), neutralisation (1.5 M NaCl, 0.5 M Tris-HCl pH 8.0) and rinse solution (0.2 M Tris, 2 x SSC). The DNA on the membrane must first be denatured in order that the probe can hybridise and then subsequently it is neutralised. The membranes were then bloted dry on Whatmann paper before UV crosslinking (see section 2.15). Hybridisation was carried out as described in section 2.2.16 and 2.2.17.

Positive plaques were picked from plates using a cut pipette tip. The plaques were put into 500 µl SM buffer plus 30 µl chloroform and vortexed. These were stored at 4°C for at least three hours to let the phage diffuse out of the plugs before plating.

High titre stocks were prepared by scraping the top agar from a plate that had a high concentration of plaques and mixing this with an equal volume, (3 ml) of SM buffer, and 200 µl of chloroform. After being incubated at 4°C for 3 hours, this was centrifuged at 3300 g for 15 minutes and the clarified solution was divided and stored both at 4°C and in 7% DMSO at -80°C.

2.2.20 Tissue culture techniques

Various cultured cells were grown, Table 2.10 indicates these cell types and how they were cultured. All cells were grown in Iwaki plasticware. Cells were frozen down for both -80°C and liquid nitrogen storage in FBS + 10% DMSO.

Table 2.10. Tissue culture media

Media	Supplier
RPMI-1640	Gibco BRL
L15	Sigma
Trypsin	Gibco BRL
Glutamine	Gibco BRL
PBS-EDTA	Prepared in lab, Dulbeco's PBS plus 5 mM EDTA
Fetal Bovine Serum (FBS)	Sigma
Chicken Serum	Gibco BRL
Optimem	Gibco BRL

Table 2.11. Cell types and growth conditions

Cell type	Description	Medium	Culture conditions
HeLa	Human, cervical cancer	RPMI + 10% FBS	37°C, 5% CO_2
DU249	Chicken, embryonic hepatoma cell line	RPMI + 10% FBS	37°C, 5% CO_2
MSB-1	Chicken, lymphoblastoid cell line	RPMI + 10% FBS	37°C, 5% CO_2
DT40	Chicken, B - cell lymphoma	RPMI + 10% FBS + 1% chicken serum	39°C, 5% CO_2
A6	*Xenopus*, normal kidney	L15 medium supplemented with 10% FBS and glutamine	25°C, sealed flask

Table 2.12. Drugs used for DT40 selection

Drug	Final concentration for DT40 selection
G418 (Invitrogen)	2 mg/ml
Histidinol (Sigma)	1 mg/ml
Hygromycin B (Calbiochem, info)	2.5 mg/ml
Puromycin (Calbiochem)	0.5 µg/ml
Blasticidin (Calbiochem)	25 µg/ml
Zeocin (Invitrogen)	400 µg/ml

2.2.21 Transient transfections

Transient transfections were carried out using FuGENE 6 reagent (Boeringer Mannheim) according to the manufacturer's instructions. In summary, cells were plated out in 6 well plates and 97 µl of serum free medium was mixed with 3 µl FuGENE 6 per well of cells to be transfected, and this was incubated for 5 minutes at room temperature. This diluted FuGENE was then added dropwise to a separate tube containing 1-1.5 µg of DNA and incubated at room temperature for 15 minutes. The DNA-FuGENE mix was then added dropwise to the cells. The cells were fixed after 24 hours to assess the phenotype by microscopy.

2.2.22 Stable transfections

DT40 stably transfected cell lines were generated by electroporation. 10 mls of approximately 1 x 10^6 cells per ml were centrifuged at 300 *g* for 5 minutes and then washed in either PBS or Optimem depending on the protocol to be followed. The protocol using Optimem resulted in a larger number of colonies being generated in the transfection. The cells were then centrifuged again at 300 *g* for 5 minutes, re-suspended in 0.5 ml of either PBS or Optimem, and transferred to an electroporation cuvette (Bio-Rad, 0.4 cm). 20-25 µg of linearised DNA was added to the cells and incubated on ice for 10 minutes, before being electroporated using the Gene Pulsar apparatus from Bio-Rad. If PBS was used, the electroporation conditions were, 550 V and 25 µF on the bacterial plug. If Optimem was used, the electroporation conditions were 300 V and 950 µFD on the mammalian plug. The electroporated cells were then placed on ice for 10 minutes before diluting them in 10 ml of medium, plating them in a dish and incubating at 39°C for 24 hours.

After 24 hours, the transfected cells were plated out in selective media at the concentrations shown in Table 2.9. 200 µl of cells were put into each well of 4 x 96 well plates and then incubated at 39°C until the colonies were visible through the bottom of the plate. The colonies were then picked into 3 ml of medium without the addition of selective drugs and incubated at 39°C until confluent.

2.2.23 Immunofluorescence

Many different cell types were fixed and stained for immunofluorescence using a range of different antibodies. Below is a summary of the protocols used.

2.2.23.1 Paraformaldehyde fixation

Generally, cells to be stained for microtubules were fixed with 4% paraformaldehyde in cytoskeleton buffer (see Table 2.3 (Wheatley & Wang, 1998)) in order to maintain the best morphology of the microtubules. The cytoskeleton buffer was preheated to 37°C before fixing cells for 10 minutes at room temperature. The cells were then washed 3 times in PBS and permeabilised in 0.15% Triton X-100 (Bio-Rad) in cytoskeleton buffer for 2 minutes at room temperature. Again the cells were washed 3 times in PBS and

then blocked in 1% BSA (Sigma) in PBS for 1 hour at room temperature or overnight at 4°C. This fixation could also be carried out using PBS instead of CB. Both primary and secondary antibodies were diluted to the appropriate concentration (see Table 2.2) in 1% BSA in PBS and incubated at 37°C for 1 hour. The DNA was then stained with DAPI (1 µg/ml final) by incubation at room temperature for 10 minutes. The cells were mounted using Vectashield mounting medium (Vector). The cells were visualised using the NA 1.4 100 x, oil immersion lens on the Ziess Axioplan2 microscope and images captured using the Princeton camera and the IP Lab software. The images were then formatted using Adobe Photoshop. Where stated, the Deltavision deconvolution microscope was used.

2.2.23.2 Staining *Xenopus* cells

Two *Xenopus*-specific protocols were attempted in order to stain A6 cells with anti-Zw10.

Fixation with methanol

This protocol was used to successfully stain *Xenopus* cells with anti-Mad2 antibodies. Initially the coverslips were rinsed in MMR (see Table 2.3), and then the cells fixed in a solution of 50% acetone/50% methanol at room temperature for 2 minutes. These were then rinsed in PBS four times before blocking and antibody incubation as described above.

Fixation with paraformaldehyde

This protocol was used to successfully stain *Xenopus* cells with anti-Bub3 antibodies. As above, initially the coverslips were rinsed in MMR, then the cells were swollen in Hanks' Balanced salts (GibcoBRL cat. #24020-091) at room temperature for 10 minutes. The cells were then fixed in a 3% paraformaldehyde solution diluted in MMR for 10 minutes at room temperature. The cells were then rinsed twice in PBS before permeabilisation in 0.5% Triton X-100 in PBS for 2 minutes at room temperature. The cells were then washed 4 times in PBS before blocking and antibody incubation as described above.

2.2.23.3 Permeabilisation before fixation using TEEN buffer.

This staining procedure was used in order to permeabilise the cells before fixation. In some cases this allowed the partial unmasking of antigens so they could be recognised by the antibody. The cells were initially treated with a permeabilisation solution of 0.5% triton in TEEN buffer (see Table 2.3) for 5 minutes at room temperature. After washing 3 times in TEEN buffer the cells were then fixed in 4% PFA diluted in TEEN for 10 minutes at room temperature. The cells were then washed in PBS then blocked and incubated with primary and secondary antibodies as described in section 2.2.23.1.

2.2.23.4 Methanol fixation

Cells were washed in PBS (prewarmed to 37°C) and then plunged into 95% methanol with 5 mM EGTA (pre-chilled to -20°C) and incubated for 10 minutes. Thereafter the cells were washed 3 times in PBS and then blocked and processed with antibodies as described in section 2.2.23.1.

2.2.23.5 Metaphase Spreads

To block the cells in metaphase, cultures were treated with colcemid (Sigma, 0.1 µg/ml final) for 2-3 hours. During this time a 3:1 methanol:acetic acid fixative mix was chilled to -20°C and 75 mM KCl was warmed to 37°C. 10 ml of cells were spun down at 300 g for 10 minutes, the medium removed carefully and the cells re-suspended in an equal volume (10 ml) of 75 mM KCl. The cells were then incubated at room temperature to swell for 8-10 minutes. It should be noted that changing this time can be crucial to the amount of swelling. The cells were then spun down again at 300 g for 5 minutes and the supernatant removed. A few drops of the fixative mix were added and the tube vortexed in order to re-suspend the cells with no clumps. The volume was then made up to the starting volume (10 ml) with fixative mix and incubated at room temperature for 15 minutes. The cells were then centrifuged again at 300 g for 5 minutes, after which time most of the fix was removed, leaving only 0.5 ml in the bottom of the tube in which to re-suspend the cells. Cells were spread onto ethanol washed slides by dropping from a height of 10-20 cm. The spreads were checked under the microscope before staining. The cells could be kept stored in fixative at -20°C.

After dropping the cells onto the slides, they were left to dry briefly before being washed in PBS for 5 minutes. The cells were then treated with 1 x TEEN (see Table 2.3) supplemented with 0.1% Triton X-100 and 1% BSA 3 times for 1 minute each. The primary antibodies were diluted in this buffer at the appropriate concentration (as shown in Table 2.2) and incubated at 37°C for 30 minutes. The slides were then washed with KB^- (see Table 2.3) for 2, 5 and 3 minutes, prior to incubation with the secondary antibody which was diluted in KB^- and incubated at 37°C for 30 minutes. The wash was repeated as above and the cells stained with DAPI and mounted as described in section 2.2.23.1.

2.2.23.6 Cytospin and KCM staining

The cells were collected by mitotic shake off and centrifuged at 300 g for 8 minutes. The medium was removed and the cells re-suspended in 10 ml of KCl (pre-warmed to 37 °C) and incubated at room temperature for 10 minutes. The cells were then centrifuged again at 300 g for 8 minutes and re-suspended in 4 ml KCl. 500 µl of cells were used per slide for cytospining (Shandon, Cytospin 3) at 800 rpm for 5 minutes. The cells on the slide were circled with a pen before incubating in KCM solution (see table 2.3) for 10 minutes. The primary antibody was diluted (see Table 2.2) in KCM with 10% Normal Goat Serum (NGS) and incubated at 37°C for 30 minutes. The cells were then washed 3 times 5 minutes with KCM. The secondary antibody was also diluted in KCM with 10% NGS and incubated at 37°C for 30 minutes. After washing, 3 times for 5 minutes each in KCM, the cells were fixed in 4% PFA in KCM for 10 minutes at room temperature. They were then washed, 3 times for 5 minutes in KCM, DAPI stained and mounted in Vectashield as described in section 2.2.23.1.

2.2.24 SDS-Polyacrylamide gel electrophoresis (SDS-PAGE)

Equipment – large gels 14 x 14 cm (Hoeffer SE 400 Sturdier Vertical Units).
small gels 8 x 10 cm (Biorad Mini-PROTEAN II cell).

The recipe for 20 ml of lower gel acrylamide mix is shown in Table 2.13. 30% acrylamide/ bis acrylamide stock was purchased from Severn Biotech Ltd. The recipe for 10 ml of stacking gel, containing urea is shown in Table 2.14.

Table 2.13. Lower gel mix for SDS-PAGE

	7.5%	10%	12.5%	13%	13.5%	15%	16%
1.5 M Tris pH 8.8	5 ml	5	5	5	5	5	5
30% acrylamide/bis stock	5.4	6.7	8.3	8.65	9	10	10.3
20% SDS	0.1	0.1	0.1	0.1	0.1	0.1	0.1
H_2O	9.4	8.1	6.5	6.15	5.8	4.8	4.5
100 mM EDTA	0.2	0.2	0.2	0.2	0.2	0.2	0.2
10% APS	0.2	0.2	0.2	0.2	0.2	0.2	0.2
TEMED	0.02	0.02	0.02	0.02	0.02	0.02	0.02

All volumes are in ml.

Table 2.14. Stacking gel mix for SDS-PAGE

	10ml
Urea	4.8 g
0.5 M Tris pH 6.8	2.5
30% acrylamide/bis stock	1.34
20% SDS	0.05
H_2O	6
100mM EDTA	0.1
10% APS	0.1
TEMED	0.01

All volumes are in ml.

Cell extracts were prepared by centrifuging at 240 *g* for 5 minutes, washed in PBS and centrifuging again. The cell pellet was then re-suspended in sample buffer with β-mercaptoethanol (see Table 2.3) and the sample sonicated 3 times for 10 seconds each using the micro-tip on setting 3 (Ultrasonic Processor, Misonix Incorporated). If to be stored, the samples were heated to 95°C for 5 minutes and then stored at -20°C. All samples were heated to 95°C for 5 minutes before loading on the gel and clarified by centrifugation if necessary. Protein markers, (Broad Range, 2-212 kDa) and prestained protein markers, (Broad range, 6-175 kDa), obtained from New England Biolabs, were loaded on all gels.

Mini gels were generally run at 200 V for around 45 minutes in running buffer (see Table 2.3). Large gels were generally run for a total of 90 mA hours, but this varied depending upon the percentage of the gel and the size of the protein to be analysed.

2.2.25 Coomassie Brilliant Blue R Staining

In order to visualise proteins in the gel they were stained with Coomassie Blue R. A 5 x stock solution of 0.5% Coomassie Blue in methanol was diluted to 1 x in diluent (see Table 2.3) before use. The 1 x solution was added to the gel directly after running for 30 minutes or more on a rocking platform. The gel was then de-stained (see Table 2.3) for as long as necessary. For best results, the de-stain was changed a number of times and a piece of exposed autoradiography film was used to soak up the Coomassie. In order to prevent the gel from cracking, during drying, it was immersed in a 10% glycerol solution for 15 minutes. Gels were air-dried using the BioRad GelAir Dryer system.

2.2.26 Western Blotting

SDS-polyacrylamide gels were transferred to nitrocellulose membrane (Amersham ECL). This was carried out using both wet and semi-dry transfer depending upon the experiment. Wet transfer was performed using the Biorad Trans-Blot Cell in transfer buffer (see Table 2.3) for 3.5 hours at 400 mA at 4°C.

Semi-dry transfer was carried out using the same buffer in the Hoefer Semiphor Semi-dry transfer unit according to manufacturer's instructions. After blotting, in order to visualise the protein, the membrane was rinsed three times in dH_2O before adding Ponceau S (0.1% Ponceau S, 5% acetic acid) for approximately 5-10 minutes, after which time the membrane was rinsed in dH_2O. The addition of Ponceau was repeated as necessary in order to clearly see the protein markers. Finally, the Ponceau was rinsed off and the membrane either stored dry or prepared for antibody incubation.

2.2.26.1 Antibody detection by Enhanced Chemiluminescence (ECL)

In order to decrease background, the membranes were first blocked with a 10% milk solution (dried skimmed milk purchased from Safeway) in PBS-Tween 20 (0.05%), (PBS-T), for 30 minutes - 1 hour on a rocking platform at room temperature. Antibodies were diluted at the concentrations as shown in Table 2.2. Different percentages of milk were used depending on the antibody ranging from 0.5% - 5%. This is due to the fact that some of the polyclonal antibodies used recognise non-specific bands and the addition of more milk during the

antibody incubation can help to decrease this background. In general, membranes were incubated with antibodies for 1 hour at room temperature and any differences to this are indicated in the text. The membranes were then washed with PBS-T, 3 times for 5 minutes each at room temperature, before the addition of secondary antibody. All secondary antibodies used for ECL detection were horseradish peroxidase (HRP) conjugated, diluted in PBS-T (see Table 2.2) and incubated with the membrane for 45 minutes at room temperature. The membranes were then washed again, as above, before visualizing with ECL (Amersham), according to the manufacturer's instructions and exposure to autoradiograph film.

2.2.26.2 Antibody detection by protein A -^{125}I

Some of the antibodies used required detection using protein A -^{125}I rather than ECL. The membranes were initially blocked in PTX-BSA, (2.5% BSA solution in PBS + 0.2% Triton X-100), for 20 minutes at room temperature. The primary antibody, diluted in PTX-BSA, was added as described in section 2.26.1. The membrane was then washed 5 times for 3 minutes with Gerace buffer (see Table 2.3). After this, the membrane was rinsed briefly in PTX, then a minimal amount of PTX-BSA was added and incubated at room temperature for 5 minutes. The protein A -^{125}I was diluted 1:1000 into this solution and incubated with the membrane at room temperature for 30 minutes. The membrane was then washed 5 times for 3 minutes each with Gerace buffer, dried thoroughly on Whatmann paper and exposed to autoradiograph film at –80°C for the desired length of time.

2.2.27 Expression of recombinant proteins in *Eschericia coli*

This protocol was used for the expression of tagged fusion proteins in *E. coli* following induction with IPTG.

Following successful cloning into an expression vector, the plasmid was then transformed into competent BL21 cells following the protocol described in section 2.8. A single colony was then grown overnight at 37°C. The following day this culture was diluted 1:100 in superbroth medium and grown at 37°C to an OD_{600} of 0.5. At this time, a 1ml sample was collected for analysis of the expression pattern before the induction by IPTG. Expression was then induced

by the addition of IPTG to the culture followed by growth of the culture for a further 3-4 hours at 30°C. In order to optimise the expression of the recombinant protein, the concentration of IPTG used (range 0.05 – 1 mM), the temperature (18 - 37°C), and the time of induction can be varied. After induction, a further 1 ml sample was collected and the remainder of the cells centrifuged at 3,300 g for 15 minutes, the supernatant removed and stored frozen at -80°C if required.

2.2.28 Purification of GST fusion protein

In order to purify recombinant GST fusion proteins from bacterial cells glutathione agarose beads were used.

The bacterial cell pellet from a 50 ml culture was re-suspended in 600 µl of TEN (100 mM NaCl, 2 mM Na-EDTA, 20 mM Tris pH8.0), which was supplemented with the protease inhibitors, CLAP, PMSF and aprotinin in order to reduce proteolysis, and vortexed until easily pipettable. 200 µl of lysozyme (5 mg/ml diluted in TEN) solution was then added and incubated on ice for 30 minutes. The cells were then sonicated 3 times for 10 seconds at setting 3 on the micro-tip. Triton X-100 was then added to 1% final concentration and the cells centrifuged at 10,000 *g* for 5 minutes to remove the cell debris from the cytosolic extract. The supernatant was transferred to a fresh tube and glutathione agarose beads (glutathione agarose 4B, Amersham) were added. 50 µl of a 50% slurry (according the to manufacturer's instructions) was mixed with 200 µl supernatant and this was incubated on a rotating wheel for 1 hour at 4°C. After this time, the beads were washed 3 times with TEN + 0.5% Triton-X 100. The fusion protein could then be eluted from the beads by boiling in sample buffer or eluted with 10 mM glutatione in TEN with the pH adjusted to 8.0, the same bead volume was added and 4 elutions were collected.

The eluted protein was then quantitated using the BioRad Protein Assay (Dye Concentrate cat# 500-0006) at OD_{595} and, if necessary, concentrated by spin column (Ultrafree concentrator devices purchased from Millipore cat# UFV5 BGC25).

2.2.29 Preparation of recombinant protein as antigen for immunisation

Recombinant protein was purified as described in section 2.2.28 and run on an SDS-polyacrylamide gel. A comb with only one wide tooth was used so the largest possible amount of protein could be run. Initially the gel was washed in dH_2O, 3 times for 10 minutes each. The gel was then stained with aqueous Coomassie blue (0.1% Coomassie in 1 x running buffer without SDS (section 2.2.24). After visualisation of the band, the gel was de-stained with running buffer without the addition of SDS. The protein band was then cut out using a scalpel and ground up in liquid nitrogen using a pestle and mortar. The gel band was ground to a powder fine enough that it could pass through a syringe so that it could be injected into the rabbit. The ground powder was then placed in a tube and an equal volume of PBS was added. This was stored at -80°C until required.

2.2.30 Affinity purification of antibody from serum

2.2.30.1 Purification against specific peptide

This was carried out in order to increase antibody specificity. The fusion protein used to generate the antibody was run on an SDS-polyacrylamide gel as described in section 2.2.30. This was then transferred to nitrocellulose membrane and stained with Ponceau S as described in section 2.2.27. The band was then cut from the membrane and blocked in 5% milk PBS-T as described in section 2.2.27. After washing the membrane with PBS the nitrocellulose was cut into small pieces and transferred to a 2 ml eppendorf tube. The membrane was then incubated with undiluted serum from the immunised rabbit for 2 hours at room temperature, the serum was then removed and kept to test the level of depletion from the serum. The membranes were then washed with PBS to remove the serum. The washes were later assayed for the decrease in protein concentration indicative of the serum being removed. Once washed, the protein was eluted twice in 100 mM glycine, pH 3.0 for 20 minutes at room temperature. This was then neutralised with Tris pH 8.8, and the protein concentration assayed by Bio-Rad assay as described in section 2.2.29. If necessary, this was concentrated using a spin column as described in section 2.2.29. The antibody was then stored at 4 °C or diluted 1 x in glycerol and stored at –80°C.

2.2.30.2 Purification of antibody using Protein A

In some cases it was found that purification of serum from an immunised rabbit over a protein A column decreased the background signal of the antibody. 1 ml of Affi-Prep Protein A matrix (Bio-Rad #156-0005) was added to a column. This was then washed with 5 x column volumes of 100 mM Tris, pH8.0. 1/10 volume of 1M Tris, pH 8.0 was added to the rabbit serum (1 ml) and this was then passed over the column 5 times. The column was then washed with 5 x column volumes of 100 mM Tris, pH 8.0 and 5 x column volumes of 10 mM Tris, pH 8.0. The antibody was then eluted with 100 mM glycine, pH 3.0 in small aliquots (200 ml) into eppendorf tubes containing 1/10 volume 1M Tris, pH 8.0 in order to neutralise the antibody. The protein concentration was then determined by Bio-Rad assay and concentrated using a centrifugal concentrator if necessary. The antibody was stored at 4°C or diluted 1 x in glycerol and stored at –80°C.

2.2.31 Making *Xenopus laevis* egg extracts

Xenopus laevis extracts were made according to protocols (Murray, 1991). The solutions required and a brief description of the procedure are described below.

PMSG – Pregnant Mare Serum Gonadotropin
HCG – Human Chorionic Gonadotropin
Cytochalasin B – 10mg/ml in DMSO stored at -80°C.

The frogs were primed for ovulation by injection of PMSG, 50 units on day 1 and 25 units on day 3. They were then induced to ovulate between day 5 to day 12 with 150 units HCG. At this time, the frogs were placed in containers with 1x MMR and kept at 16°C. Generally, the frogs took around 14 hours to lay. Both laid and squeezed eggs were used, however, freely laid eggs were checked in case lysis had begun to occur and discarded if necessary. The eggs were then washed several times in MMR to remove any skin or other contaminants.

Initially, the eggs were incubated in dejellying solution, which was changed several times until all eggs were dejellied and packed tightly together. The eggs were then washed 4 times in XB, then 2 times in CSF-XB with the addition of protease inhibitors, PMSF and CLAP mix (see Table 2.3). The eggs were next

transferred to a centrifuge tube using a cut pipette tip in order to prevent disrupting the eggs. CSF-XB with CLAP and cytochalasin B at 100 µg/ml were added, in order to depolymerise the actin cytoskeleton. A packing spin at 1000 rpm for 1 minute and 2000 rpm for 30 seconds was performed in the Heraeus benchtop megafuge 1.0R. The CSF-XB was removed from on top of the eggs, which were then centrifuged at 10,000 rpm in the SW55 rotor of the Beckman ultracentrifuge for 10 minutes in order to crush them. This resulted in 3 layers, bottom-yolk, middle-cytoplasm and top-lipid. The cytoplasmic layer was then collected by inserting a needle and syringe at the bottom of the straw-coloured cytoplasmic layer. CLAP (1000x), cytochalasin B (10 µg/ml final) and 1/20 volume CSF energy mix were then added to the extract and it was kept on ice or stored at -80°C. This was the starting material for both SDS-polyacrylamide gels and immunoprecipitation. For sucrose gradients it was necessary to centrifuge at 70,000 rpm for 30 minutes at 4°C to generate a purified high speed supernatant.

2.2.32 Immunoprecipitation from *Xenopus* egg extracts

Immunoprecipitation (IP) from *Xenopus* egg extracts was performed using protein A agarose beads (Biorad). These were initially washed in PBS and then in CSF-XB (with protease inhibitors, CLAP, PMSF and aprotinin, see Table 2.3). The antibody or control pre-immune serum was bound to the beads by incubation with rotation for 1 hour at 4°C. Generally, 20 µl beads was mixed with 5 µl of serum. The beads were washed 3 x with CSF-XB to remove the unbound antibody. 40 µl of extract was added to the beads, and the total volume made up to 100 µl with CSF-XB (plus protease inhibitors). The beads and extract were then incubated together on a rotating wheel for 1 hour at 4°C, after which the beads were washed, 3 x with XB, 1 x with XB + 0.2% Triton X-100, 1 x XB + 0.5 M NaCl. Sample buffer was then added to the beads, boiled and loaded on an SDS-polyacrylamide gel. In order to assess the effectiveness of the immunoprecipitation, the starting extract, supernatant after binding to the beads and the washes were also loaded on the gel.

In addition to the protocol set out above, some changes were made to the buffers used. In some experiments the extract was incubated with the beads in RIPA buffer (PBS with 1% NP40, 0.5% sodium deoxychlorate and 0.1% SDS), and

then washed in either XB as described above, or a Tris Buffer (50 mM Tris pH 7.4 and 500 mM NaCl). In other experiments, the extract was incubated with the beads in XB buffer and then washed in either XB or Tris buffer.

In an additional modification of the protocol the antibody was first incubated with the extract in the presence of protease inhibitors for 30 minutes at 4°C on the rotating wheel. The protein A beads were then added and incubated for 1 hour at 4°C. The protein A beads were then washed with XB as described above.

2.2.33 Sucrose Gradients

To examine whether proteins were present in a complex, *Xenopus* egg extracts were separated on sucrose gradients and then blotted to discover if proteins were present in the same fractions.

A stock solution of 66% sucrose in water was prepared, the appropriate weight of this was then diluted in 1 x CSF-XB with CLAP. Table 2.15 shows the weight of 66% sucrose need to make 10 ml of each solution.

Table 2.15. Weight of 66% sucrose need for 10 ml of solution.

Final % w/w sucrose solution	Weight of 66% sucrose in grams
2%	0.31
5%	0.76
8%	1.25
10%	1.57
12.5%	1.99
15%	2.4
17%	2.78
20%	3.26
22%	3.57
25%	4.18
35%	6.08
42%	7.54

5-20% sucrose gradients were prepared in two different ways, the first used 5, 10, 15 and 20% solutions which were layered underneath, i.e, 5% first, then 10% underneath, etc. 2 ml gradients were formed, by allowing them to diffuse for 1 hour, 50 minutes at room temperature and the last 10 minutes at 4°C.

The second method involved using the sucrose solutions shown in Table 2.16, to make either 5 – 20 or 10 – 40% gradients. The volumes used are shown to make a 2 ml gradient. As above the solutions were layered underneath. These gradients were left to form for 16 hours at 4°C. 100 µl of clarified high speed supernatant from *Xenopus* extract (see section 2.31) was loaded on each gradient and then spun in the Beckman Ultrtacentrifuge, rotor TLS 55 at 53,000 rpm for 4 to 5.5 hours at 4°C depending on the gradient and experiment being carried out. Protein standards, BSA (4S) and catalase (11S), were also run on a parallel gradient.

Table 2.16. Volume of sucrose solution needed for indicated gradient

5-20%	**Volume**	**10-40%**	**Volume**
2%	0.4 ml	8%	0.4 ml
12.5%	0.6 ml	25%	0.6 ml
17%	0.6 ml	35%	0.6 ml
22%	0.4 ml	42%	0.4ml

Chapter 3

Cloning and Characterisation of Chicken BubR1

3.1 Introduction

BubR1 is a mitotic checkpoint kinase that has been identified in a number of species including human, *Drosophila* and *Xenopus*. The aim of this work was to identify and clone the cDNA of this kinase in chicken (*Gallus gallus*), in order that antibodies could be generated and used for biochemical experiments in chicken cells. More specifically the aim was to generate a stable MSB1 (chicken) cell line that expressed BubR1 with a C-terminal HA-His fusion and then use this to investigate the kinetochore structure in vertebrates. BubR1 is localised to the outer plate of the kinetochore (Jablonski *et al.*, 1998) and therefore would be an ideal tool for purification of kinetochore-associated proteins by affinity chromatography or immunoprecipitation. A number of approaches could be used, such as immunoprecipitation with anti-BubR1 or with anti-HA antibodies or nickel chelate chromatography using the His tag to pull down complexes after crosslinking BubR1 to other kinetochore components.

Chicken BubR1 cDNA was cloned and sequenced and a rabbit polyclonal antibody was raised for immunolocalisation and biochemical studies. Sequencing of this cDNA revealed that chicken BubR1 has a high degree of sequence similarity to other vertebrate BubR1 proteins. In addition the antibody raised revealed that BubR1 localises in a manner typical of other checkpoint proteins in chicken cells.

3.2 Results

3.2.1 Cloning chicken *BubR1* from a cDNA library

Initially an EST was obtained from the Buerstedde DT40 (chicken cell) database designated dkfz426-4hz with the annotation mad3l/bub1a (in the database[2]

[2] In this Thesis the term database refers to the NCBI sequence database unless otherwise stated.

human BubR1 is also called Mad3L (Mad3 Like) and Bub1a. The EST received in the Laboratory[3] was cloned into the pSPORT vector with an insert size of 1.8kb. This EST was sequenced, as outlined section 2.2.9, and a small restriction map determined by digestion with *Not* I, *Sal* I, *Hin*d III and *Pst* I (not shown). Sequencing revealed that this plasmid contained the 3' end of chicken BubR1 and restriction mapping revealed that a 0.6 kb *Hind* III/*Eco*R I fragment was the most 5' sequence available. This fragment was therefore used as a probe to screen a cDNA library. The cDNA library used was made from DU249 cells, and cloned into λZAPII bacteriophage, and the screen was carried out as described in section 2.2.19. In total, 2 million phage were screened. From the primary screen, 44 phage were identified as positive on duplicate membranes; 10 of these were subsequently taken through to a secondary, and 9 to the tertiary screen before *in vivo* excision was carried out. This resulted in the cDNAs being recovered as pBluescript phagemid vector inserts. These cDNAs were initially investigated by restriction digest as shown in Figure 3.1. Digestion with the enzymes *EcoR* I and *Xho* I present in the polylinker of pBluescript released the cloned inserts. By adding up the sizes of the bands generated after digestion, it was possible to determine that four were potentially full length, C1-15, C3-5, C3-9 and C4-16. Since the human and mouse full length cDNAs in the database are in the region of 3.5 kb it seemed reasonable to estimate that the cDNA clone would be approximately 3.5 kb in length.

Initially the 5' and 3' ends of these four clones were sequenced using the T3 and T7 primers. Although all clones contained the 3' end of the gene, as expected, not all were the same in their 5' region. Sequencing of clones C1-15, C3-5, C3-9 and C4-16 revealed that they were all either full length or nearly full length. In order to establish if the most 5' end of the gene had indeed been cloned, 5' RACE (rapid amplification of cDNA ends) was carried out, (see Figure 3.2A for explanation). Initially this was carried out on DT40 (chicken cell line) RNA and a band of approximately 300 bp was generated (Figure 3.2Bi). This was the expected size according to the region where the primers had been designed and based on the fact that the clones identified from the library screen were indeed full length. This PCR product was cloned and sequenced and found to be identical to the longest clones from the library, when compared to the human

[3] In this Thesis the term Laboratory refers to the Laboratory of Professor William Earnshaw Wellcome Centre for Cell Biology, ICMB, University of Edinburgh.,

BubR1 sequence at the 5' end it can be noted that this sequence is shorter by 14 amino acids (Figure 3.2C). In order to further verify whether this was the ATG, the 5' RACE experiment was repeated on DT40 cells and in addition on two other chicken cell lines, MSB1 and DU249. As shown in Figure 3.2Bii, a similar size product was generated from all three cell lines and upon sequencing these were all found to be identical. A comparison of the 5' UTR sequences from human, mouse, *Xenopus* and chicken is shown in Figure 3.2C, and although these differ in length, the clustal alignment shows that certainly the chicken and *Xenopus* sequences are very similar in this region. In addition the Kozak sequence was investigated. This is the sequence immediately upstream of the initiation codon which acts as a signal for the initiation of translation. The work of Kozak (1987), identified a consensus sequence of GCCA/GCCATGG, with the most conserved nucleotide being at position –3, which is nearly always a purine and most commonly alanine (Kozak, 1987). From the data shown in Figure 3.2C it can be seen that although the sequences do not conform closely to the consensus they all have A at position –3. In conclusion the ATG of chicken *BubR1* was identified as shown.

The full length cDNA sequence of chicken BubR1 was determined and found to be 3711 bp in length with the ATG-STOP being 3264 bp, the ATG at position 48 in the sequence (start of transcription is zero) and the polyadenylation signal at position 3660 as indicated. This sequence is shown in Appendix 1. The sequence has been deposited in the NCBI database with the accession number AY245433.

Figure 3.1

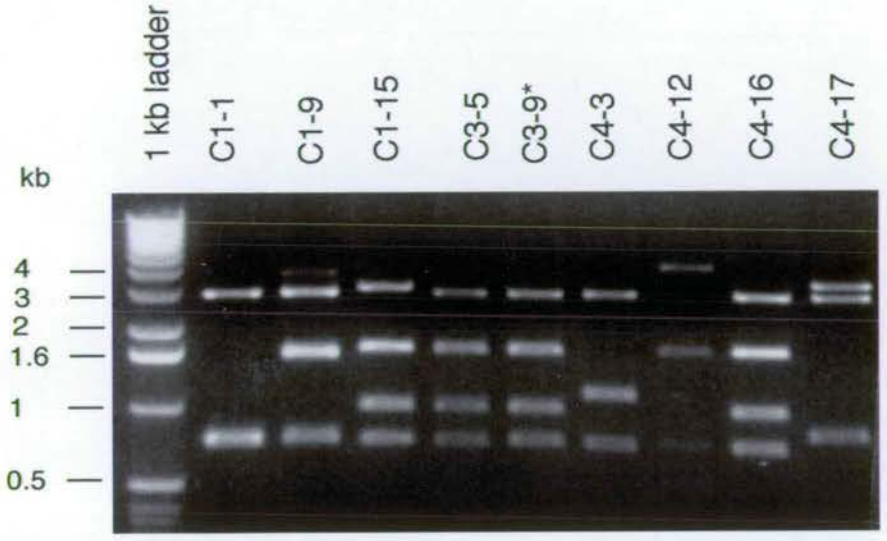

Figure 3.1 cDNA library screen for chicken BubR1. Nine clones isolated from cDNA screen were digested with *EcoR* I and *Xho* I and run on a 1% agarose gel in order to determine the insert size of the clones. These clones were subsequently sequenced in order to determine which clones were full length. * Clone C3-9 was found to be full length and is referred to as chicken BubR1 cDNA from here on.

Figure 3.2

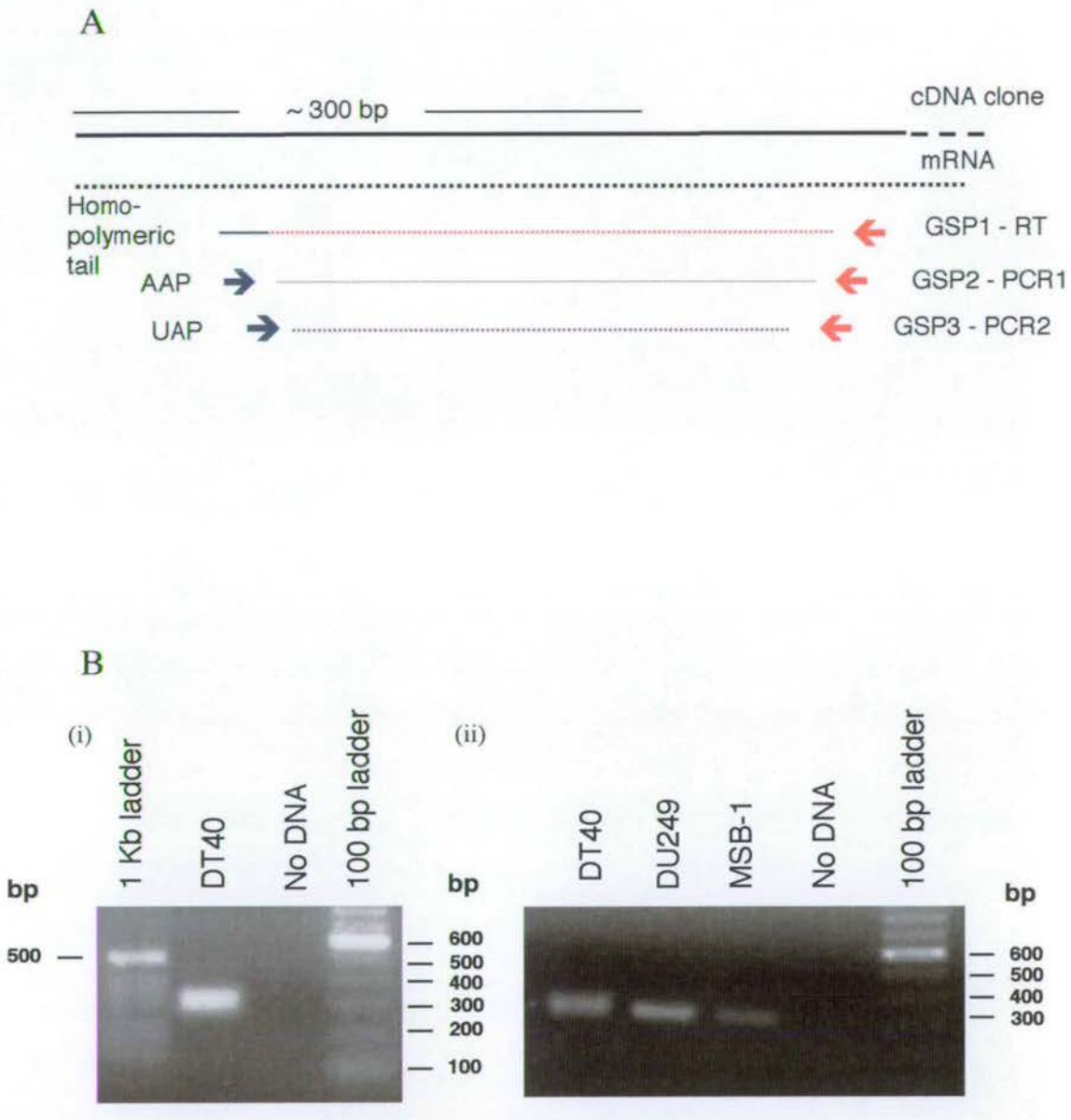

Figure 3.2. 5´RACE and identification of the ATG of chicken BubR1. **A,** Schematic representation of 5´ RACE reaction. Firstly cDNA is synthesised from RNA using reverse transcriptase from a gene specific primer (GSP1). This cDNA is then tailed and this tailed product can be amplified by PCR using GSP2 and a primer to the homopolymeric tail. A second round of amplification was then carried out using GSP3 in order to generate a visible product. **B**, 5´ RACE was carried out on DT40 cells, resulting in a PCR product of around 300 bp (i), subsequently this was repeated on DT40 cells and two other chicken cell lines, CHEPS and MSB-1. All cell lines gave a similar sized product (ii), and when sequenced were found to be identical.

Figure 3.2 Continued

C

Chicken BubR1

```
TTC GCG CGG TCG CCT CAG AGC TGG GGC TGC GGC GCT CAG AGC TTG AAG ATG TCA CGG GAC
F   A   R   S   P   Q   S   W   G   C   G   A   Q   S   L   K   M   S   R   D

GGT GAC GAT GAG TGG GAG CTG AGC AAG GAG AAC GTG CAG CCG CTG CGG CAG GGC CGG GTC
G   D   D   E   W   E   L   S   K   E   N   V   Q   P   L   R   Q   G   R   V
```

Human BubR1

```
TTG TTA GGG AGT CGT GTG CGT GCC TTG GTC GCT TCT GTA GCT CCG AGG GCA GGT TGC
L   L   G   S   R   V   R   A   L   V   A   S   V   A   P   R   A   G   C

GGA AGA AAG CCC AGG CGG TCT GTG GCC CAG AGG AAA GGC CTG CAG CAG GAC GAG GAC CTG
G   R   K   P   R   R   S   V   A   Q   R   K   G   L   Q   Q   D   E   D   L

AGC CAG GAA TGC AGG ATG GCG GCG GTG AAG AAG GAA GGG GGT GCT CTG AGT GAA GCC ATG
 S   Q   E   C   R   M   A   A   V   K   K   E   G   G   A   L   S   E   A   M

TCC
S
```

Mouse BubR1

```
GAA CTT GGC GGC CCT TGC GTG ATG GGG CGT GAG GTG GCT ATT CTG AGA AGG AGT CGG ATG
E   L   G   G   P   C   V   M   G   R   E   V   A   I   L   R   R   S   R   M

CGT GGT TTT GTT TAG GAG CAC GGG GTG ACG ATC TTC GCA GCT CCA GAG CCA GCT GAA GGT
R   G   F   V   *   E   H   G   V   T   I   F   A   A   P   E   P   A   E   G

TGA GGG GGG CTC AGT TAG CAC TCG GAG GAT AAA GGT CTG CGG AAG GGC GAG AGC AAG TAT
*   G   G   L   S   *   H   S   E   D   K   G   L   R   K   G   E   S   K   Y

TGG GAA TGC AGG ATG GCG GAG GCG AGT GAA GCC ATG TGC CTG GAG GGA GCA GAG TGG GAG
W   E   C   R   M   A   E   A   S   E   A   M   C   L   E   G   A   E   W   E
```

Xenopus BubR1

```
GGAG TTT GAA TGT GCC GAA AGC GGG CGA GAC GGA GGA CAG TGG CGA AGT GTT AGA GTA CCT
 E   F   E   C   A   E   S   G   R   D   G   G   Q   W   R   S   V   R   V   P

GAC CGG AGT TTG AAT GTG CCG AAA GCG GGC GAG ACG GAG GAC AGT GGC GAA GTG TTA GAG
D   R   S   L   N   V   P   K   A   G   E   T   E   D   S   G   E   V   L   E

TAC CTG ACC ATG GCA CAA GCT GGA GAT GAA TGG GAG CTA AGC AAA GAA AAT GTG CAA CCC
Y   L   T   M   A   Q   A   G   D   E   W   E   L   S   K   E   N   V   Q   P
```

D

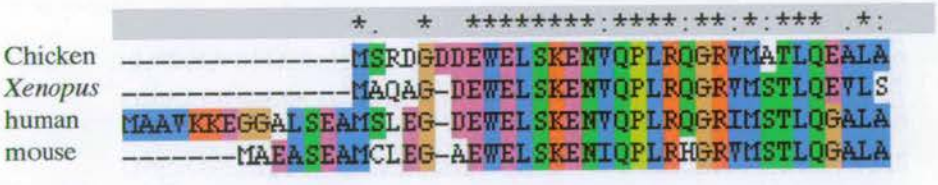

Figure 3.2 Continued. **C,** Sequence comparison between the 5′ UTR sequence of chicken, human, mouse and *Xenopus* is shown, with the Kozak sequence underlined and ATG indicated in red **D,** A clustal alignment of the amino acids at the N-terminus of BubR1 are shown, indicating that chicken is most similar to the *Xenopus* protein in this region. Key to Clustal symbols, * - amino acid fully conserved, : strong group fully conserved, STA, NEQK, NHQK, NDEQ, QHRK, MILV, MIL, HY, FYW, . Weaker group fully conserved CSA, ATV, SAG, STNK, STAP, SGND, SNDEQK, NDEQHK, NEQHRK, FVLIM, HFY. Colouring of Clustal alignment Blue: AFILMVW, Purple: ED, Green: NQST, Yellow: P, Orange: G, Red:KR, Turquoise: YH, Salmon: C.

3.2.2 Chicken BubR1 shows sequence similarity to other vertebrate BubR1's.

Cloning and sequencing revealed that the chicken *BubR1* cDNA encodes a protein of 1085 amino acids. Sequence analysis reveals that the protein is highly homologous to other vertebrate BubR1s over its entire length. The clustal sequence alignment between human and chicken BubR1 shows that the proteins are 52% identical and 79% similar (Figure 3.3A). It was possible to identify various domains within the chicken sequence as indicated in Figure 3.3B. These were the putative destruction box, the putative nuclear localisation signal and the kinase domain, with the active site. In addition a putative KEN box has been identified at amino acid position 13. This motif has a function similar to the destruction box, which signals proteins for destruction by the APC (Pfleger & Kirschner, 2000), the difference being that the cdc20 activating subunit recognises the destruction box, whereas cdh1 recognises the KEN box, as discussed in Section 1.8.10. It is known that BubR1 contains a putative destruction box as shown in Figure 3.3, which is not present in Bub1. A comparison between these two Bub1 proteins in mouse and how they may be targeted for destruction is discussed by Davenport *et al.*,. The authors conclude that Bub1b (BubR1) in mouse may be targeted for destruction by the APC/C after it is released from the chromosomes, but since Bub1 does not contain a destruction box it must be degraded by other means (Davenport *et al.*, 1999).

Since it is known, that in organisms ranging from *Drosophila* to humans two closely related proteins, Bub1 and BubR1, are present, it was also important to demonstrate that the cDNA cloned did indeed encode for chicken BubR1 rather than Bub1. Sequence comparison revealed that the overall sequence similarity between the proteins was 21% for the gene cloned versus human Bub1 and 52% versus human BubR1. This evidence, along with a detailed comparison between the known homology domains of BubR1 as shown in Figure 3.4, led to the conclusion that the cloned cDNA does indeed encode for chicken BubR1 rather than Bub1.

Figure 3.3

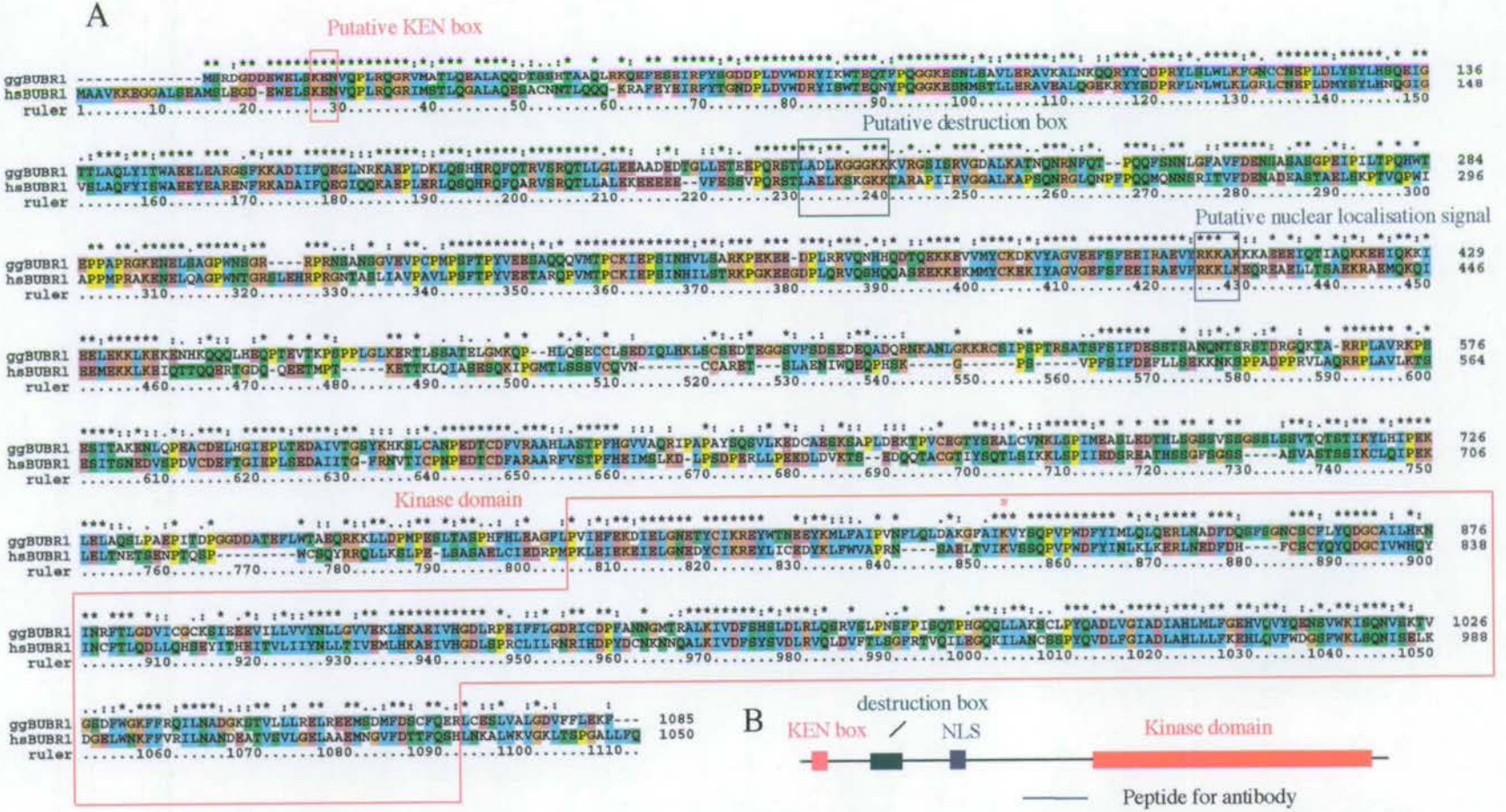

Figure 3.3 Comparison of human and chicken BubR1 sequence. **A,** Clustal alignment of human (hs) and chicken (gg) BubR1 sequence, overall similarity is 79% and identity is 52%. The putative KEN box is shown at position 13, putative destruction box at position 214, and putative nuclear localisation signal at position 403, all these domains are conserved as compared to the human sequence. The kinase domain with the active site, lysine 830, is indicated (red asterix).**B**, Diagram showing the domains as in A, including the region used to generate the polyclonal antibody is also (aa653-778). Key to Clustal symbols, * - amino acid fully conserved, **:** strong group fully conserved, STA, NEQK, NHQK, NDEQ, QHRK, MILV, MIL, HY, FYW, **.** Weaker group fully conserved CSA, ATV, SAG, STNK, STAP, SGND, SNDEQK, NDEQHK, NEQHRK, FVLIM, HFY. Colouring of Clustal alignment Blue: AFILMVW, Purple: ED, Green: NQST, Yellow: P, Orange: G, Red:KR, Turquoise: YH, Salmon: C.

As mentioned previously BubR1 is also referred to as Mad3L, due to the fact that it shares regions of homology with the *S. cerevisae* protein Mad3. Figure 3.4 shows a comparison of chicken BubR1 in the homology regions 1 and 2 as described by Hardwick et al., 2000, and it can be seen that chicken BubR1 is more similar to Mad3 than it is to human Bub1.

3.2.3 Generation of an antibody to chicken BubR1

To further characterise chicken BubR1, polyclonal rabbit antibodies were raised to the protein. Since Bub1 and BubR1 have a high degree of sequence homology within some domains, (Figure 3.4 and the kinase domain), it was important to raise the antibody against a region of the protein that was not within these domains, in order to avoid cross reactivity (Figure 3.3). A fragment encoding amino acids 653-778 was therefore cloned into the vector pGEX-4T-1, which creates an N-terminal GST fusion protein. This cloning was carried out using primers HD1 and HD2 as outlined in Tables 2.7 and 2.8. After inducing the expression of this protein using IPTG in Bl21 cells the fusion protein was purified over glutathione agarose beads as described in Section 2.2.27 and 2.2.28. The fusion protein expresses well as a protein of approximately 45 kDa (20 kDa for BubR1 peptide plus 25 kDa for GST), as shown in Figure 3.5A.

This protein was then prepared as described in Section 2.2.29 for injection into two rabbits. The bleeds were tested initially on immunoblots of whole cell lysates from chicken cells using ECL, as described in Section 2.2.26. A clear band of approximately 140 kDa can be seen by immunoblot on chicken MSB1 cells (Figure 3.5B) and DT40 cells (Figure 3.6B), which is not seen with the pre-immune serum. The predicted molecular weight of chicken BubR1 is 122 kDa, however, human BubR1 migrates at 120 kDa and *Xenopus* migrates at 145 kDa. Subsequently, the antisera were also tested by immunfluorescence on various chicken cell lines including, MSB1 (Figure 3.7C), DU249 and DT40 (Figure 3.5C), as described in section 2.2.23. The antibody worked well for immunofluorescence on chicken cells, in particular DT40 cells, as shown in Figure 3.5C.

Figure 3.4

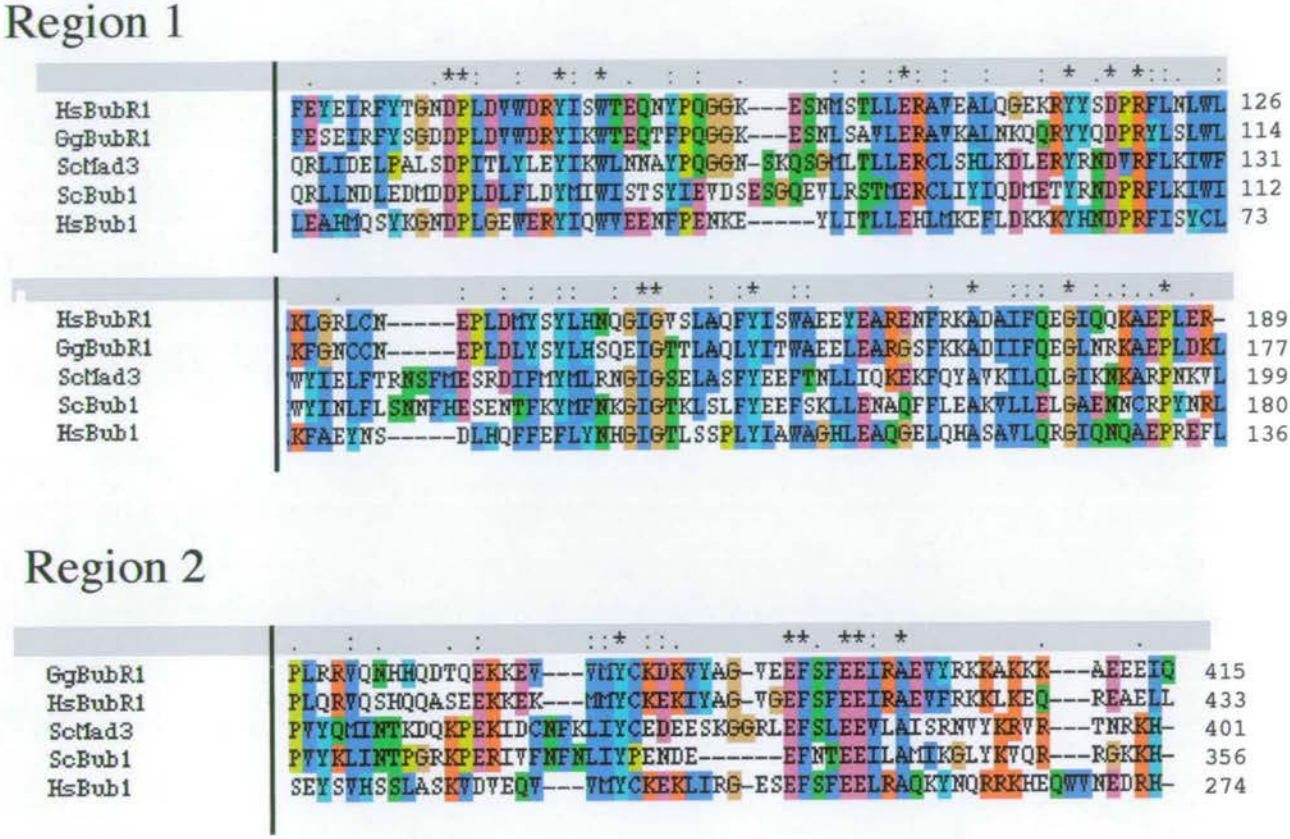

Figure 3.4 Sequence alignment of chicken BubR1. **A,** Clustal sequence alignment showing homology regions 1 and 2 (Hardwick et al., 2000) compared to chicken BubR1 sequence. See Figure 3.2 for Clustal alignment symbol and colour explanation.

BubR1 localises at the kinetochores of cells in prometaphase and remains at this location until the kinetochores become attached to microtubules, at which time the signal can no longer be seen at any particular cellular location, but remains diffuse throughout the cell.

To characterise this antibody further I was interested to address the question as to what happened to BubR1 after treatment of cells with the microtubule depolymerising drug colcemid and the microtubule stabilising drug taxol (paclitaxel). To this end DT40 cells were treated with these drugs and the cells fixed and stained for BubR1, in addition the cell extracts were immunoblotted. As shown in Figure 3.6A, cells treated with colcemid arrest at metaphase with unattached kinetochores that stain brightly for BubR1. This result is as expected based on the known localisation and role of BubR1 in human cells (Chan *et al.*, 1998; Jablonski *et al.*, 1998; Taylor *et al.*, 1998). In the case of taxol treatment, the cells look very similar, with cells blocked in metaphase and kinetochores stained brightly for BubR1. Current models propose that Mad2 senses spindle attachment whereas BubR1 senses tension at the kinetochore (Skoufias *et al.*, 2001). In the case of taxol treatment, the result is as expected, because although the microtubules are stabilised rather then depolymerised they are unable to generate tension at the kinetochore. Cells treated with the drugs were also subjected to immuoblotting using the anti-BubR1 antibody (Figure 3.6B). A protein of increased molecular weight can be detected in DT40 cells after the addition of these drugs and presumably activation of the spindle assembly checkpoint. This higher molecular weight protein could be a phosphorylated form of BubR1, which has been previously reported in other systems once the spindle assembly checkpoint is activated (Taylor *et al.*, 2001; Chen, 2002; Fang, 2002). This is therefore further evidence that the antibody generated does indeed recognise BubR1 and also that it is able to recognise the phosphorylated form.

Figure 3.5

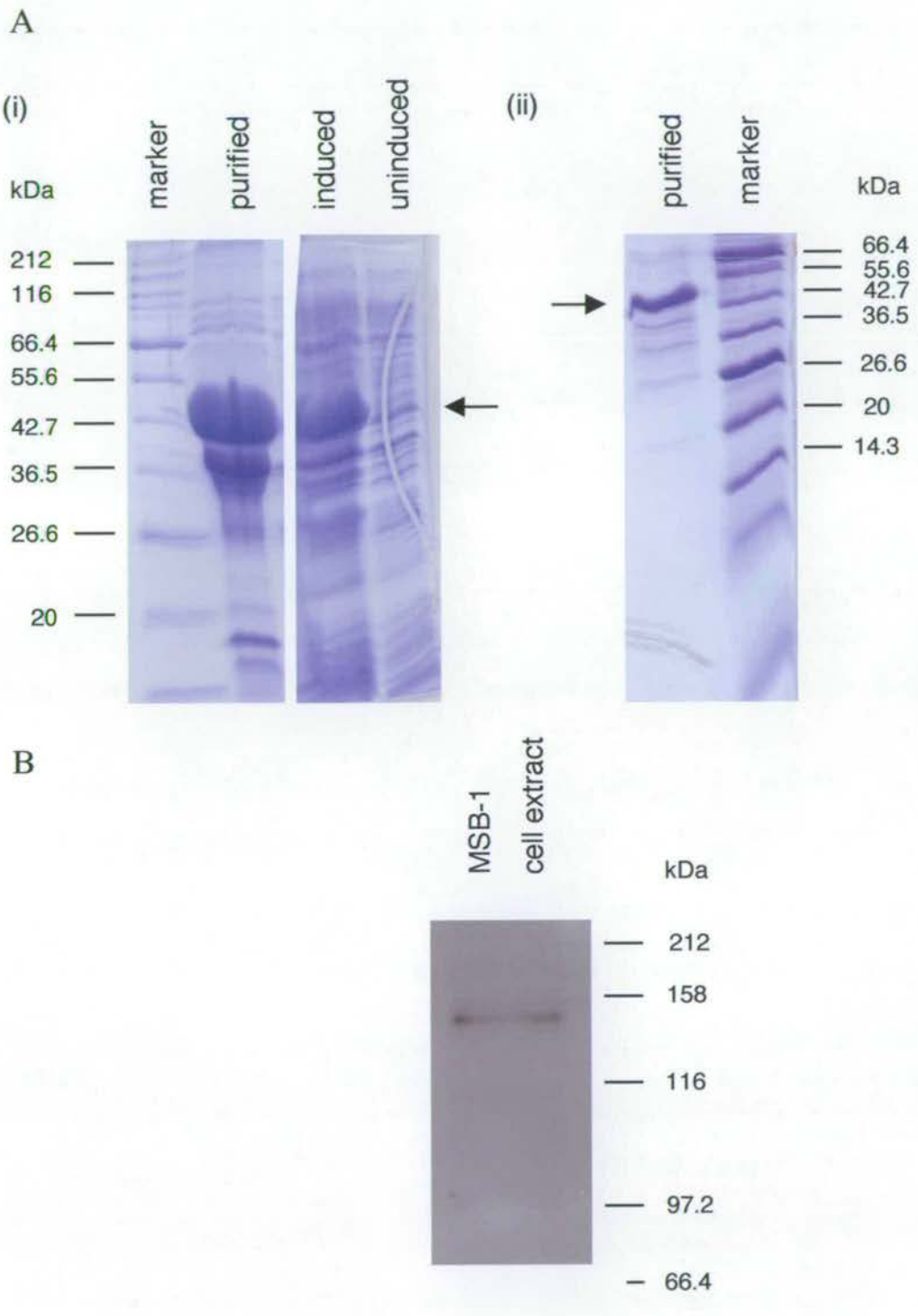

Figure 3.5. Generation of an antibody to chicken BubR1. **A**, Expression and purification of amino acids 653-778 of chicken BubR1 fused to GST. This purified protein is shown here run on a 12.5% SDS-polyacrylamide gel and stained with Coomassie blue, (i) initial purification, (ii) subsequent improved purification procedure. **B**, MSB-1 cell extracts were subjected to 10% SDS-PAGE, transferred to nitrocellulose and blotted with anti-BubR1, the signal was detected using ECL. The antibody recognised a protein of approximately 140 kDa.

Figure 3.5 Continued

C

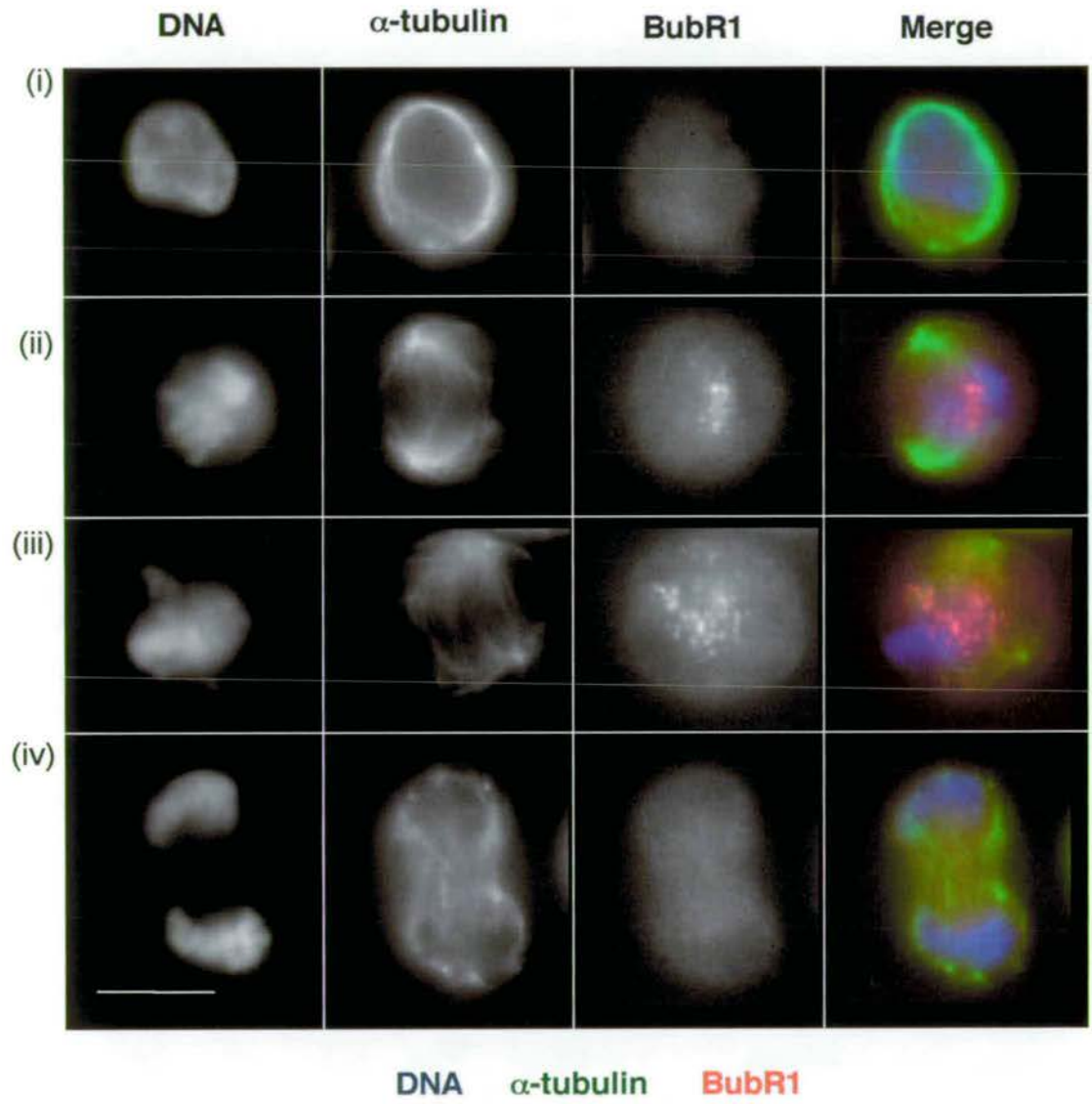

Figure 3.5 Continued. **C,** DT40 cells were fixed with paraformaldehyde and stained with anti-BubR1 (red) and anti-alpha tubulin (green). The DNA was stained with DAPI (blue). Scale bar is 10μm. Anti-BubR1 stains these cells in a manner typical of other spindle assembly components with little or no staining in interphase (i), kinetochore localisation in prometaphase (ii) and (iii) and then diffusely throughout the cell during anaphase (iv).

Figure 3.6

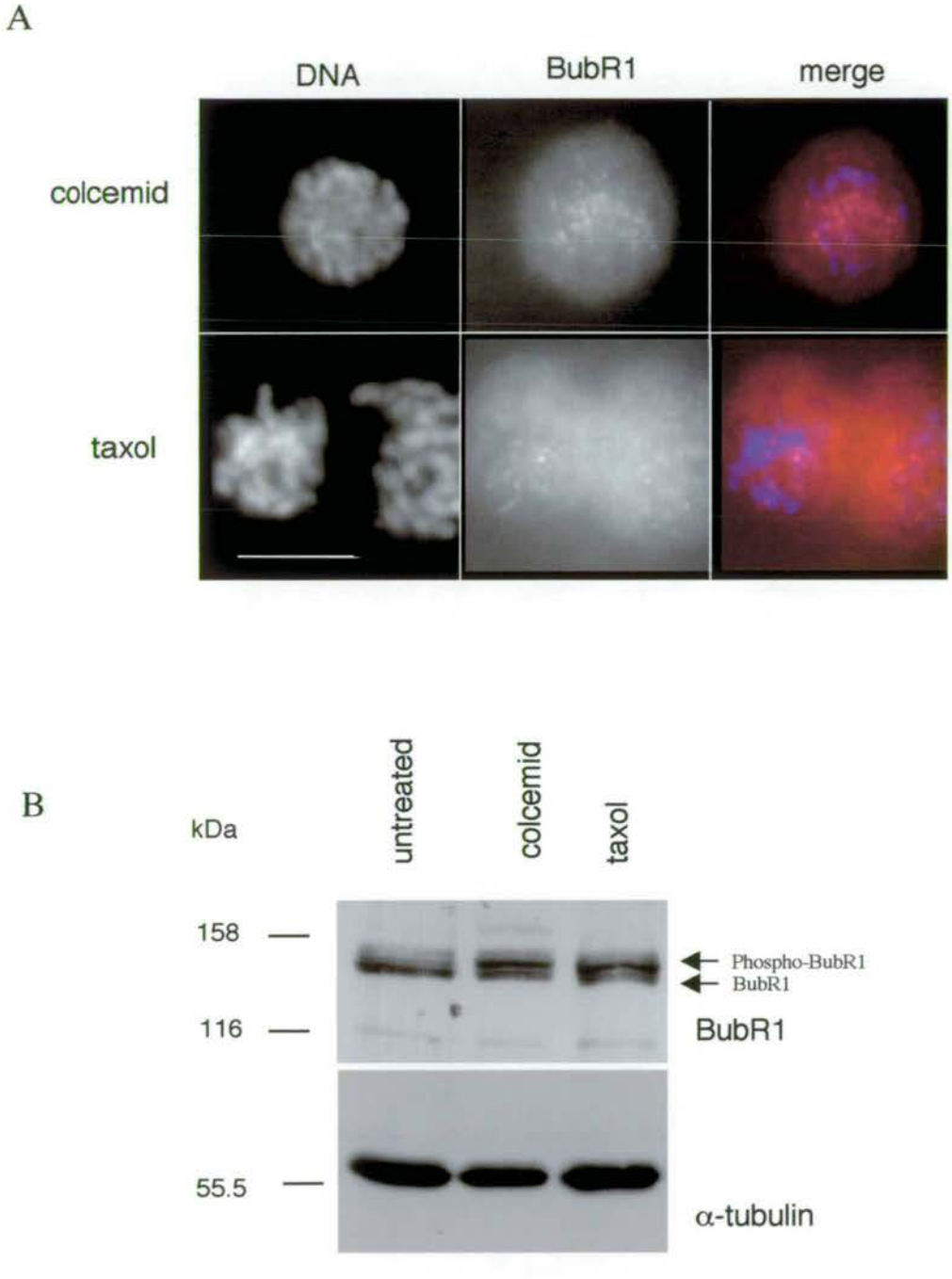

Figure 3.6 Chicken DT40 cells treated with colcemid or taxol. DT40 cells were either untreated or treated with 10 μM taxol or colcemid (0.1 μg/ml) for 3 hours. **A,** The cells were then fixed and stained for BubR1 (red) and the DNA stained with DAPI (blue). Scale bar is 10 μm. **B,** Cell lysates were subjected to 10% SDS-PAGE, transferred to nitrocellulose and blotted with anti-BubR1. The signal was detected using ECL.

This antibody to chicken BubR1 proved to be useful in a recent study. A novel constitutive centromere protein CENP-I was identified in chicken and disrupted in DT40 cells by gene targeting (Nishihashi *et al.*, 2002). The work showed that this protein is essential for centromere function and its absence caused cells to arrest at prometaphase with misaligned chromosomes. After a substantial delay the cells were able to exit mitosis without cytokinesis having occurred. Using the antibody I generated it was possible to show that BubR1 was no longer associated with the metaphase chromosomes 60 - 72 hours after the addition of tetracycline (to shut off the expression of the rescue). This may explain why the cells were able to exit mitosis; either because the spindle assembly checkpoint was turned off, or because the compromised structure of the centromere was no longer able to bind checkpoint proteins. In addition, by using the BubR1 antibody it was possible to show more specifically the localisation of CENP-I within the kinetochore. BubR1 has been localised to the outer kinetochore plate by immunoelectron microscopy (Jablonski *et al.*, 1998), so it was possible to state that CENP-I is localised in or near the inner plate since the signal for CENP-I was inside that of BubR1.

3.2.4 Expression of tagged recombinant BubR1 in chicken MSB1 cells.

As mentioned in the introduction, the main aim of the identification of the chicken orthologue of BubR1 was to use it as a tool to investigate the structure of the kinetochore in chicken cells. The cell line of choice was MSB1, a chicken lymphoblastoid line, which grows easily and rapidly in culture since the cells grow in suspension rather than by adhering. It is possible to obtain a highly synchronous population of cells in mitosis by treating them with microtubule depolymerising drugs such as colcemid. Chromosomes can then be prepared from these cells and used as a starting material to purify kinetochore-associated proteins. Another additional advantage to studying the kinetochore in chicken cells is that the chicken karyotype consists of around 80 chromosomes meaning that there are more kinetochores per cell than in other cell lines. The aim of this project was to tag chicken BubR1 with the HA-His epitopes, generate stable cell lines in which the expressed recombinant protein localised appropriately to the kinetochore, and then use biochemical means to purify the recombinant protein and other co-purifying components. The reason for using BubR1 as the 'handle' for this study was that it has been shown previously that BubR1 is localised to

the outer plate of the kinetochore by immunoEM (Jablonski *et al.*, 1998). The initial plan was to chemically cross-link the tagged BubR1 to proteins in physical proximity to it at the kinetochore. The chromosomes would then be run over a nickel column, under denaturing conditions, which would bind the His tag. After the reversal of cross-linking the proteins eluted from the column would be identified by mass spectroscopy.

Full length BubR1 (with the stop codon removed) was cloned into the vector pZeo SV2HA-His (constructed by S. Kandels-Lewis), which resulted in a C-terminal tagged protein. This cloning was carried out using primers HD10 and HD11 as described in Table 2.7 and 2.8. This plasmid was transfected into MSB1 cells and initially resistant clones were screened by immunoblot using an antibody to the HA tag (monoclonal anti-HA 12CA5). Figure 3.7A shows the comparison of two cell lines, H4 and H22 which were expressing the HA tagged transgene to the control cell line M6 and wild type MSB1 cells. The M6 cell line was generated by Ciaran Morrison and expresses the constitutive centromere protein CENP-C with a C-terminal HA-His tag. The expected size for tagged CENP-C is around 100 kDa as shown in Figure 3.7A. In total, 24 cell lines were screened and 11 found to be positive by immunoblot (not shown). Subsequently, the cells positive by immunoblot were screened by immunofluorescence to determine if the tagged BubR1 was indeed localised correctly and had integrated into the kinetochore structure. Both chromosome spreads and colcemid treated cells were stained. As shown in Figure 3.7B, the cell lines H4 and H22 did not show clear kinetochore localisation of the HA tag as in the control line M6. It was also determined that the HA antibody cross-reacts with the centrosome of wild-type MSB1 cells, as shown in Figure 3.7C(i). A further example of clone H4 is shown in Figure 3.7D. However, although the endogenous BubR1 could be detected at centromeres (Figure 3.7C(ii)), no specific kinetochore staining was seen with the HA-antibody. Unfortunately, I was unable to find any MSB1 cell lines which had kinetochore localisation of the HA signal.

Figure 3.7

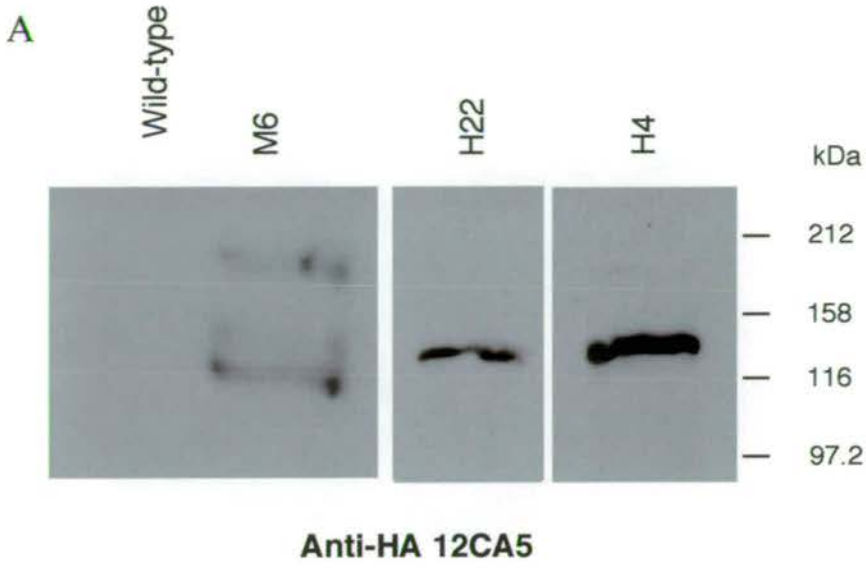

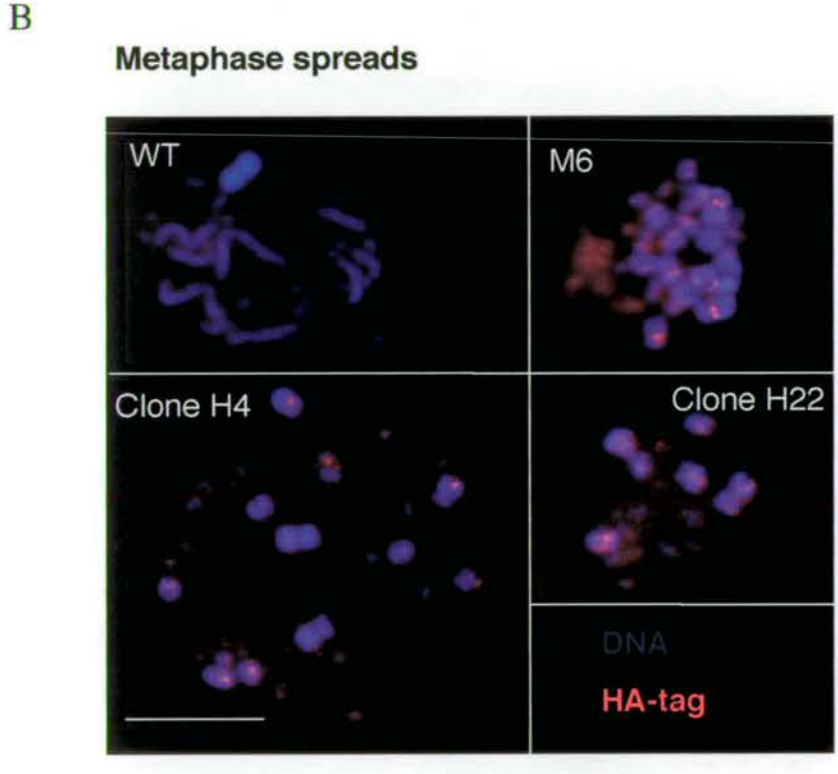

Figure 3.7 Generation of an MSB-1 cell line expressing chicken BubR1 with a C-terminal HA-His tag. **A,** Western blot showing the expression of the BubR1 fusion protein as judged by anti-HA antibody, M6 is a control cell line expressing chicken CENP-C with an HA-His tag. **B**, Immunofluorescence on metaphase spreads prepared from these two cell lines using the anti-HA antibody, again M6 and wild type are shown as controls, scale bar is 10 μm.

Figure 3.7 Continued

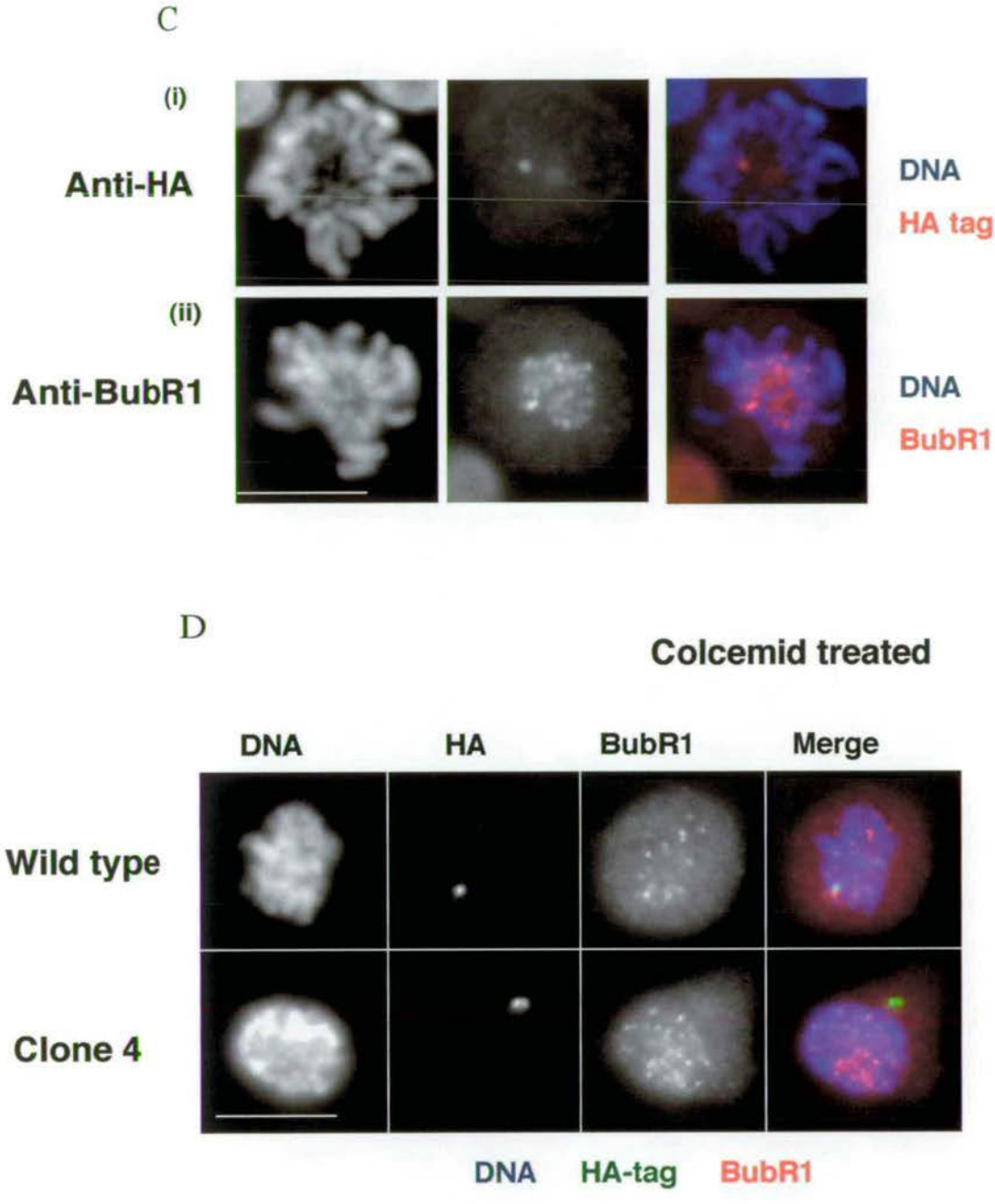

Figure 3.7 continued. **C,** Immunoflourescence on wild type MSB-1 cells showing that the anti-HA antibody cross reacst with the centrosomes (i), and anti-BubR1 stains the kinetochores (ii). **D,** The HA tagged fusion protein cannot be detected at the kinetochores of colcemid treated H4 cells (green), although endogenous BubR1 can (red). Scale bar is 10 μm.

Figure 3.7 Continued

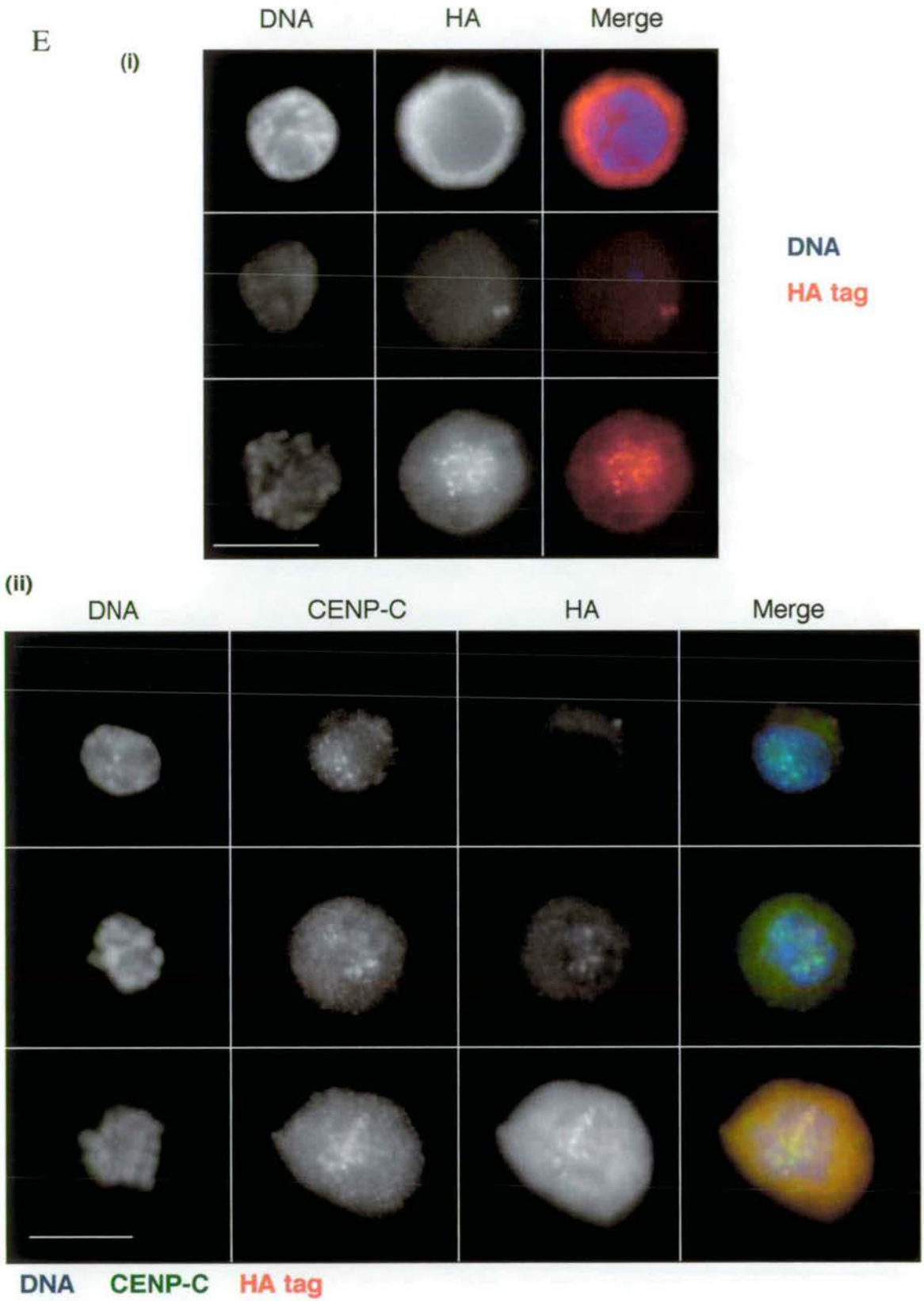

Figure 3.7 continued. **E,** DT40 cell line transfected with chicken BubR1-HA-His construct. **(i)** Immunofluorescence with anti-HA showing kinetochore localisation. **(ii)** Double staining with the kinetochore marker CENP-C shows that the transgene does indeed localise specifically to the kinetochore. Scale bar is 10 μm.

To further explore why no BubR1-HA-His MSB1 cell line with the tagged BubR1 correct localisation was generated, I used this construct in a different cell line. Subsequently, I have shown that this tagged BubR1 construct is able to localise to the kinetochore in chicken DT40 cells, so it seems that the problem did not arise from the construct *per se*. A DT40 cell line stably transfected with the same BubR1-HA-His construct shows localisation at the kinetochore region as determined by the anti-HA staining (Figure 3.7E(i)) and co-localisation with CENP-C (Figure 3.7E(ii)), confirming that tagged BubR1 can localise to the kinetochore.

3.3 Discussion

3.3.1 Cloning chicken BubR1

Cloning the BubR1 cDNA from the DU249 cDNA library was successful, and it appeared that of the nine clones taken to the tertiary screen four of these were full length. Sequencing of these clones revealed that the human cDNA is longer by 42 bp (14 amino acids) and initially this prompted the investigation of the 5' end of the gene further by 5' RACE. Analysis of three chicken cell lines, DU249, MSB1 and DT40 revealed that the cDNA length and the position of the ATG was as initially predicted, and it appears that the human sequence is indeed longer at the 5' end (Figure 3.2D). It is also encouraging to note the similarity between the chicken and *Xenopus* sequence which has recently been published (Chen, 2002). The genomic sequence upstream of the ATG was also analysed in order to identify a possible Kozak sequence (Figure 3.2C). These observations, in conjunction with that of the 5' RACE, lead to the conclusion that the ATG of chicken BubR1was correctly determined. Two other possible ways to determine the ATG would be primer extension or RNase protection. The RNase protection would only address however, if this was a potential ATG, rather than whether it was the actual ATG used. The most striking piece of evidence that this is the full length sequence is that the expressed protein was able to localise to the kinetochore of chicken cells (Figure 3.7E). As described in Section 3.2.4, the cDNA was tagged with HA-His at the C-terminus and this was transfected into cells. Although the MSB1 cell lines generated appeared to mislocalise tagged BubR1, when this experiment was subsequently repeated with DT40 cells, the recombinant protein appeared to localise correctly to the centromere. The

expression in DT40 cells was carried out as part of a separate study as outlined in Chapter 4.

3.3.3 Sequence alignments of chicken BubR1 protein

Sequencing of the chicken cDNA allowed the comparison of this sequence to other related proteins in the database. As mentioned in the introduction, BubR1 (Bub1 related) is also referred to as Mad3-like, as it was noticed that it shares homology domains with yeast Mad3 in addition to yeast Bub1 (see Figure 1.5). BubR1 is more similar to Mad3 in some domains, with the main difference between these two proteins being that Mad3 has no kinase domain. Comparison of the sequence similarity between the sequence that I cloned and the database sequences for human Bub1 and human BubR1 reveals that we can conclude this to be chicken BubR1 since it not only has a higher degree of homology, but also shares several distinguishing features, including the putative destruction box, putative nuclear localisation signal and putative KEN box (Figure 3.3). In addition, comparison of the *Drosophila* Bub sequences that are now present in the database, reveals that the *Drosophila* sequence initially referred to in (Basu *et al.*, 1999) is actually a BubR1 orthologue rather than Bub1, as named (not shown).

3.3.4 Generation of an antibody to chicken BubR1

An N-terminal GST fusion on amino acids 653-778 was expressed and purified in order to raise polyclonal antibodies to chicken BubR1. Since BubR1 has a closely related homologue in vertebrates, Bub1, it was important to raise a specific antibody by avoiding conserved domains. The resulting antibody recognises a protein of approximately 140 kDa by immunoblot of chicken cells. In addition, an upper band, which is likely to be the phosphorylated form of the protein appears after activation of the spindle assembly checkpoint by treatment of cells with microtubule poisons. The antibody stains the centromere region of chicken cells at prometaphase, when they have unaligned or unattached kinetochores. As these kinetochores become attached and the cell proceeds from metaphase into anaphase, the specific kinetochore staining is lost. This localisation is typical for spindle assembly checkpoint components. DT40 cells were treated with colcemid and taxol in order to determine how the antibody would respond under conditions of checkpoint activation. As discussed, the

phosphorylated form of the protein could be detected by immunoblot (Figure 3.6B), as previously shown in human (Taylor *et al.*, 2001; Fang, 2002) and *Xenopus* (Chen, 2002) studies. After treatment with both of these drugs, the antibody brightly stained the kinetochore regions (Figure 3.6A), indicating that BubR1 responds to spindle damage generated by both colcemid and taxol, and then contributes to the block in cell cycle progression. Current models suggest that BubR1 and Mad2 recognise distinct signals at the kinetochore, with Mad2 sensing attachment and BubR1 sensing tension at the kinetochore (Skoufias *et al.*, 2001). Since colcemid depolymerises microtubules and taxol stabilises them, both these drugs lead to a situation where the kinetochores are not under tension. Therefore both would be expected to recruit BubR1to kinetochores, as is the case here. If an antibody were available to chicken Mad2, it would be possible to test the hypothesis that these proteins recognise distinct signals. However, an antibody to chicken Mad2 has not been raised, and the published human antibodies remain to be tested on chicken cells. These results demonstrate that my antibody recognises BubR1 and that the localisation and behaviour of this protein is similar to that published previously for human BubR1 and other spindle assembly checkpoint proteins.

3.3.5 Expression of BubR1-HA-His construct

The initial aim of cloning chicken BubR1 was so that it could be used in biochemical studies of the vertebrate kinetochore structure. Unfortunately, it was not possible to generate an MSB1 cell line with the appropriate localisation of the tagged BubR1 and therefore this project was not undertaken. One possible reason that this construct did not localise correctly was that the cDNA was not full length. However, subsequent experiments with this construct in DT40 cells show that the protein it encodes can localise properly. Therefore, an alternative explanation is required to explain why it was not possible to generate the line in MSB1 cells. It may simply be that not enough colonies were screened to detect this localisation. In addition, other work on the overexpression of recombinant BubR1 in chicken cells has shown that it can be toxic or in some way detrimental to the cell (as discussed in Chapter 4). It may be that the stable cell lines were downregulating the BubR1-HA-His expression so as to not have this effect. This biochemical approach was undertaken with a very similar strategy by a co-worker Ciaran Morrison, using the constitutive centromere protein CENP-C as

the 'handle'. A stable cell line was generated called M6 and the experiments as outlined above carried out. Unfortunately, those experiments did not yield promising results due to the fact that CENP-C was difficult to solubilise (Ciaran Morrison, personal communication). The crosslinking reagent used was sodium tetrathionate and this could potentially be further optimised. In addition the starting material of Percoll purified chromosomes rather than clusters may be a better approach. In order to solubilise the proteins from the chromosomes so they can be analysed by chromatography either treatment of the chromosomes with dextran sulphate and heparin or sodium chloride could be used.

Since this cell line could not be generated it was decided to adopt alternative approaches in order to investigate the kinetochore structure and spindle assembly checkpoint in vertebrate cells. Two approaches were under taken, firstly to answer questions regarding the vertebrate spindle assembly checkpoint and in particular the role of BubR1, attempts were made to generate a conditionally null chicken DT40 cell line as described in Chapter 4. Secondly, the kinetochore structure was investigated by turning to the *Xenopus* egg extract system as described in Chapter 5.

Chapter 4

Generation of BubR1 +/- DT40 cells

4.1 Introduction

In order to further define the role of BubR1 in mitosis the aim was to generate a chicken DT40 cell line that has a targeted disruption of the *BubR1* gene.

One of the most powerful methods for analysing the function of a gene is to disrupt it or knock it out. In higher eukaryotic cells this technology is hampered by the fact that the homologous recombination frequency is usually low, although the length of homology greatly affects the efficiency of targeting (Hasty *et al.*, 1991; Deng & Capecchi, 1992). For a number of years the analysis of gene function in mammals has been made possible by knocking out genes in mouse. In this model system one copy of the mouse gene is targeted by homologous recombination in ES (embryonic stem) cells and then germ line chimeras are generated by injection of targeted stem cells into blastocysts. The chimeric mice are then bred to homozygosity. However, if a gene function is essential, then this results in embryonic lethality, and analysis of any phenotype can be limited and difficult. In this case Cre-*loxP* technology can be used in order to conditionally knockout a gene in one particular tissue of the mouse (reviewed by (Porter, 1998)). The targeting construct is flanked by *loxP* sites, and once the homozygous mice are generated they are crossed with a mouse containing the recombinase, Cre, under the control of a tissue specific promoter (for review see (Kuhn & Torres, 2002)). The resulting mouse then has the essential gene knocked out in one particular tissue and the phenotype can be analysed.

A different approach to analyse the role of genes with essential, ubiquitous cell cycle functions is targeted disruption in cultured cells. For example, genes have been disrupted in several human cells lines, including the fibrosarcoma cell line, HT1080, (Itzhaki *et al.*, 1997) and the colorectal adenocarcinoma line, HCT116, (Chan *et al.*, 1999). Although human cell lines are perhaps the best system with which to study the roles of genes involved in human disease, few laboratories have successfully generated these cell lines, presumably partly due to the fact that homologous recombination frequencies are so low.

4.1.1 DT40 cells

The favoured model system in this laboratory for generating genetic knockouts is the chicken DT40 cell line. DT40 cells are chicken cells derived from an avian leukosis virus (AVL)-induced bursal lymphoma. The tumour was twice transplanted *in vivo* before culturing (Baba & Humphries, 1984; Baba *et al.*, 1985). DT40 cells continue to undergo gene conversion of the light chain variable region and for this reason the cells have the unique feature of very high levels of homologous recombination (Buerstedde & Takeda, 1991; Arakawa *et al.*, 2002), with the targeted to random DNA integration ratio of more than 1:2. The result is vertebrate cells that can be used for gene targeting experiments, and, in addition essential genes can be targeted by using the tetracycline regulated promoter, recently reviewed by (Hudson *et al.*, 2002).

The technology of knocking out genes in DT40 cells has been particularly useful in the investigation of two fields of cell biology, namely DNA repair (for review see (Morrison & Takeda, 2000)) and apoptosis (for review see (Lahti, 1999)). The system is now being used to investigate genes important for centromeres, chromosomes and cell cycle progression. Genes essential for cell viability, studied to date include, CENP-C (Fukagawa & Brown, 1997), Rad21 (Sonoda *et al.*, 2001), CENP-H (Fukagawa *et al.*, 2001), CENP-I (Nishihashi *et al.*, 2002), Cyclin D1 (Lahti *et al.*, 1997) and SMC2 (D. Hudson, personal communication).

DT40 cells have on average 80 chromosomes, 11 autosomes, the ZW sex chromosomes (female) and 67 microchromosomes (Sonoda *et al.*, 1998). This is two more than in chicken (*Gallus gallus*), due to trisomy of chromosome two and one additional microchromosome (Smith & Burt, 1998; Sonoda *et al.*, 1998). In some cases this means that three (Lyn, (Takata *et al.*, 1994) CENP-H, (Fukagawa *et al.*, 2001)) or even four copies of the gene (Cbl, (Yasuda *et al.*, 2000)) must be targeted.

Homologous recombination of targeting vectors in mouse ES cells can range from 10^{-2} to 10^{-5} whereas DT40 cells are capable of undergoing homologous recombination at several orders of magnitude higher, with the typical frequency of homologous recombination with a disruption vector being between 10% and 80% (Hudson *et al.*, 2002)

Initially gene disruptions in this cell line focussed on non-essential genes, for example Rag-2, required for V(D)J recombination, (Takeda *et al.*, 1992) and HMG-17 required for splicing of pre-mRNAs (Li & Dodgson, 1995). The technology was then developed to create conditionally null cell lines using the tetracycline operator system (Gossen & Bujard, 1992). This technology allows the cDNA of the essential gene being disrupted, to be expressed under the control of the tetracycline operator. The cells are transfected with both the cDNA under the control of the tet operator and the tetR fused to the VP16 minimal domain. The result is a cell line where the expression of the transgene can be repressed by the addition of tetracycline, or the more potent analogue doxycycline, to the cell. Initial conditional knockouts were rescued with the human cDNA, as in the case of ASF/SF2 (Wang *et al.*, 1996) and Rad51 (Sonoda *et al.*, 1998) and subsequent studies have rescued using the chicken cDNA. These include CENP-C, (Fukagawa & Brown, 1997), Rad21 (Sonoda *et al.*, 2001), CENP-H (Fukagawa *et al.*, 2001) and CENP-I (Nishihashi *et al.*, 2002). Additional technology using the counter-selectable marker HRPT and Cre/*loxP* techniques is being developed in DT40 cells (Fukagawa *et al.*, 1999). Presently there are seven selectable markers, which can be used in these cells allowing for multiple knockouts to be performed in the same cell. However, *loxP* flanked markers are also available so that this will not be the limiting step in the construction of multiple knockout lines. Other advantages to DT40 cells are that they grow in suspension with a doubling time of 8-10 hours at 39°C. They have no need for fibroblast feeder layers or LIF (Leukemia inhibitory factor) as ES cells do, and therefore are easier to culture, transfect and subclone. In addition, the cells can be grown between the temperatures of 34°C to 43°C, so can be used in the generation of TS (temperature sensitive) mutants (Fukagawa *et al.*, 2001). There is a rapidly expanding database of chicken sequences now available, which makes the identification of chicken homologous of genes easier (http://genetics.hpi.uni-hamburg.de/dt40.html).

4.1.2 Tetracycline Operator System

The tetracycline operator system can be used in order to assess the phenotypes generated by the removal of essential genes from DT40 cells. The tetracycline system is based on the regulatory elements of the *E.coli* tetracycline resistance operon (Tn10) in which the transcription of the resistance-mediating genes is negatively regulated by the tetracycline repressor (*tetR*). In the presence of tetracycline, *tetR* does not bind to its operators located within the promoter of the

operon, and therefore allows trranscription. A hybrid transactivator (tTa) was generated which fuses *tetR* (amino acids 1-207) with the negatively charged C-terminal activation domain (130 amino acids) of VP16 from HSV, which is known to be essential for the transcription of immediate early viral genes (Gossen & Bujard, 1992). The *tetR* moiety targets the tTa to the tet operator sequence, and then the VP16 domain recruits polymerase. The tTa stimulates minimal promoters fused to tet operator sequences and is virtually silent in the presence of low concentrations of tetracycline or doxycycline because the tTa is prevented from binding to the *tetO* sequences. The system is represented schematically in Figure 4.1A, which shows that in a cell containing the tTa and the transgene under the control of the tet operator, this will be expressed until doxycycline is added.

The system has been further modified to allow different levels of transcriptional activity by modification of the VP16 domain of the tTA vector. The tTa 2/3/4 plasmids express tetracycline-controlled transactivators containing minimal VP16 activation domains (Baron *et al.*, 1997). The minimal domains are shortened VP16 moieties composed of different combinations of 13 amino acid repeats which differ at one amino acid in the repeat. The repeat is PADALDDXDLDML with the variant amino acid **X**. tTa 2 has three copies of the repeat with F at this position. tTa 3 has two copies with F at this position, and tTa4 has three copies each with a different amino acid at position X; G, F and Y. These mutated VP16 domains do not bind as efficiently to the target thus reducing the relative transient activation to 98%, 39% and 14% for tTa 2, 3 and 4 respectively. This is represented schematically in Figure 4.1B. In addition the transient protein level is shown, this reflects the stability of the protein.

Figure 4.1

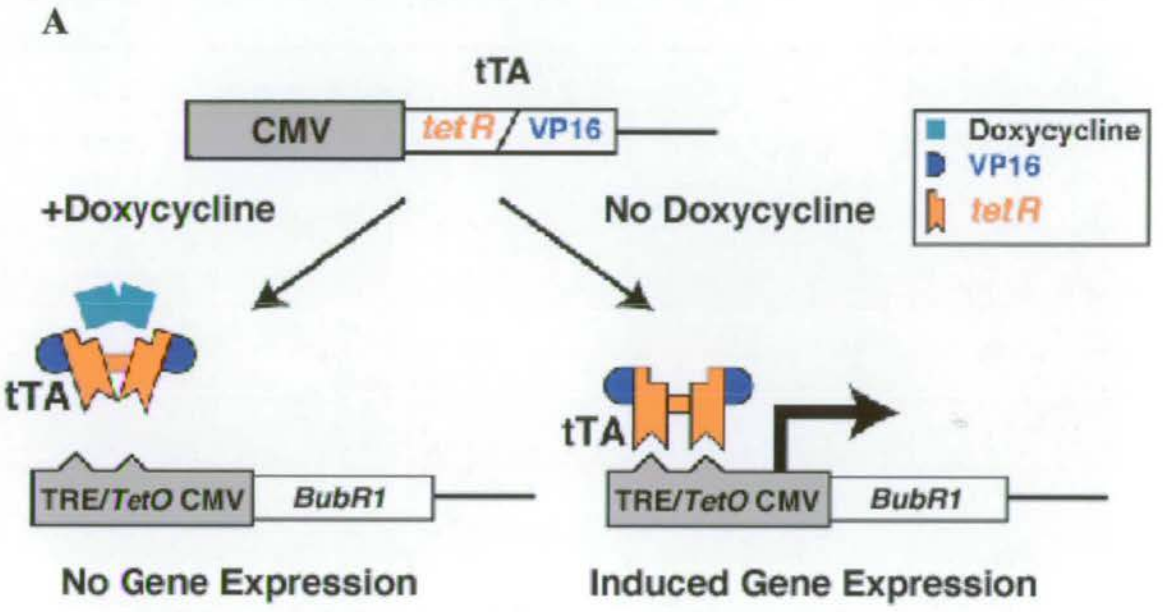

B

	VP16 activation domain	Transient protein level	Relative transient activation (%)
pTet-Off	F	1x	100
ptTA2	F F F	3x	98
ptTA3	F F	5x	39
ptTA4	G F Y	9x	14

Figure 4.1 Tetracycline system **A**, Diagram of Tet Off system, see text for further details, (adapted from http://gweb1.ucsf.edu/labs/conklin/Technical/Tetinmice.html). **B** Wild type tTA is a fusion of amino acids 1-207 of TetR and the negatively charged C-terminal activation domain (130 aa) of the VP16 protein of the herpes simplex virus. The shortened VP16 moieties in the VP16 minimal domain vectors are composed of different combinations of 13-amino acid repeats that differ at one amino acid in the repeat. tTA is expressed from the strong immediate early promoter of cytomegalovirus (pCMV IE). The transient protein level and relative activation are shown, (adapted from Clonetech information on plasmids tTa2/3/4).

DT40 cells seemed to be an ideal system in order to study the role of a checkpoint protein such as BubR1, which is predicted to be essential based on the data from other checkpoint proteins, namely Bub3 and Mad2, which are essential in mouse. The analysis of the phenotype of disrupting these proteins in mouse was severely hampered by the early embryonic lethality, and, it was therefore hoped that the DT40 system would permit a clear analysis of the effect of disruption of BubR1 on the progression of the cell cycle, the function of the checkpoint, the structure of the kinetochore and the effect on other checkpoint components including Zw10 and Rod. In addition, the system allows for the analysis of the domains of a protein by use of the tet system. For example, once the gene is removed then a kinase dead or otherwise mutant construct could be introduced into the cells and the phenotype analysed, following repression of the transgene.

Initially, this project required the isolation of the chicken BubR1 genomic locus in the form of a genomic phage, so that targeting vectors for this gene could be generated. Since I predicted the gene to be essential, the aim was to generate a conditionally null cell line. With the cDNA expressed under the control of the tetracycline promoter this could be switched off once both alleles of the gene have been disrupted, thus allowing a window of opportunity in which to investigate the phenotype of cells null for this central player in the spindle assembly checkpoint.

4.2 Results

4.2.1 Isolation of chicken BubR1 genomic phage

A total of two million phage were screened from the λ Fix II DT40 genomic library using the probe described in section 3.2.1 and diagrammed in Figure 4.2B. Eleven phage were identified in the primary screen as double positives and these were taken through a secondary and a tertiary screen. After the successful cloning of the full-length chicken *BubR1* cDNA as described in section 3.2.1, these phage were then screened with a 5′ probe, as shown in Figure 4.2. This led to the identification of phage 3B3, which was found to contain a 5′ portion of the BubR1 gene. Subsequently the library was screened again using the very 5′ portion of this phage as a probe, which is just upstream of the ATG, and again the two positive clones identified were the same as 3B3, suggesting that phage containing the region upstream of the BubR1 genomic locus may not

exist in this library. Fig 4.2B shows a partial restriction map of phage 3B3 and the probes used for library screens.

Partial mapping and sequencing of the ends of this phage revealed an approximately 18 kb insert that contains the ATG near its 5′ end. It terminates in an exon encoding amino acid 703 (the full length cDNA is 1085 amino acids). In all, 8 exons were identified, five at the 5′ end of the phage and three at the 3′ end (exon I -48 to -8, exon II -9 to 144, exon III 145 to 202, exon IV 203 to 348, exon V 349 to 375, exon X 1586 to 1672, exon Y 1673 to 1775, exon Z 1776 to 2062). Human BubR1 contains 23 exons and spans a genomic distance of 59.5kb. Comparison of the some of the human intron/exon boundaries with those identified here in chicken reveals that there is a high level of synteny between these genes, with the only difference being the size of the introns. As shown in Table 4.1 the introns are smaller in chicken, which has led me to suggest that the chicken BubR1 genomic locus is likely to be in the order of 30-40kb.

Table 4.1 Analysis of synteny between human and chicken BubR1

Human Exon	Exon length (base pairs)	Intron length (base pairs)	Chicken exon	Exon length (base pairs)	Intron length (base pairs)
1	**34**		**I**	**40**	
		3798			93
2	**143**		**II**	**153**	
		4866			undetermined
3	**59**		**III**	**57**	
		416			268
4	**144**		**IV**	**145**	
		5796			865
5	**196**		**V**	26* not full length	
13	**60**		**X**	**86**	
		124			undetermined
14	**105**		**Y**	**82**	
		3490			308
15	**274**		**Z**	**286**	

Figure 4.2

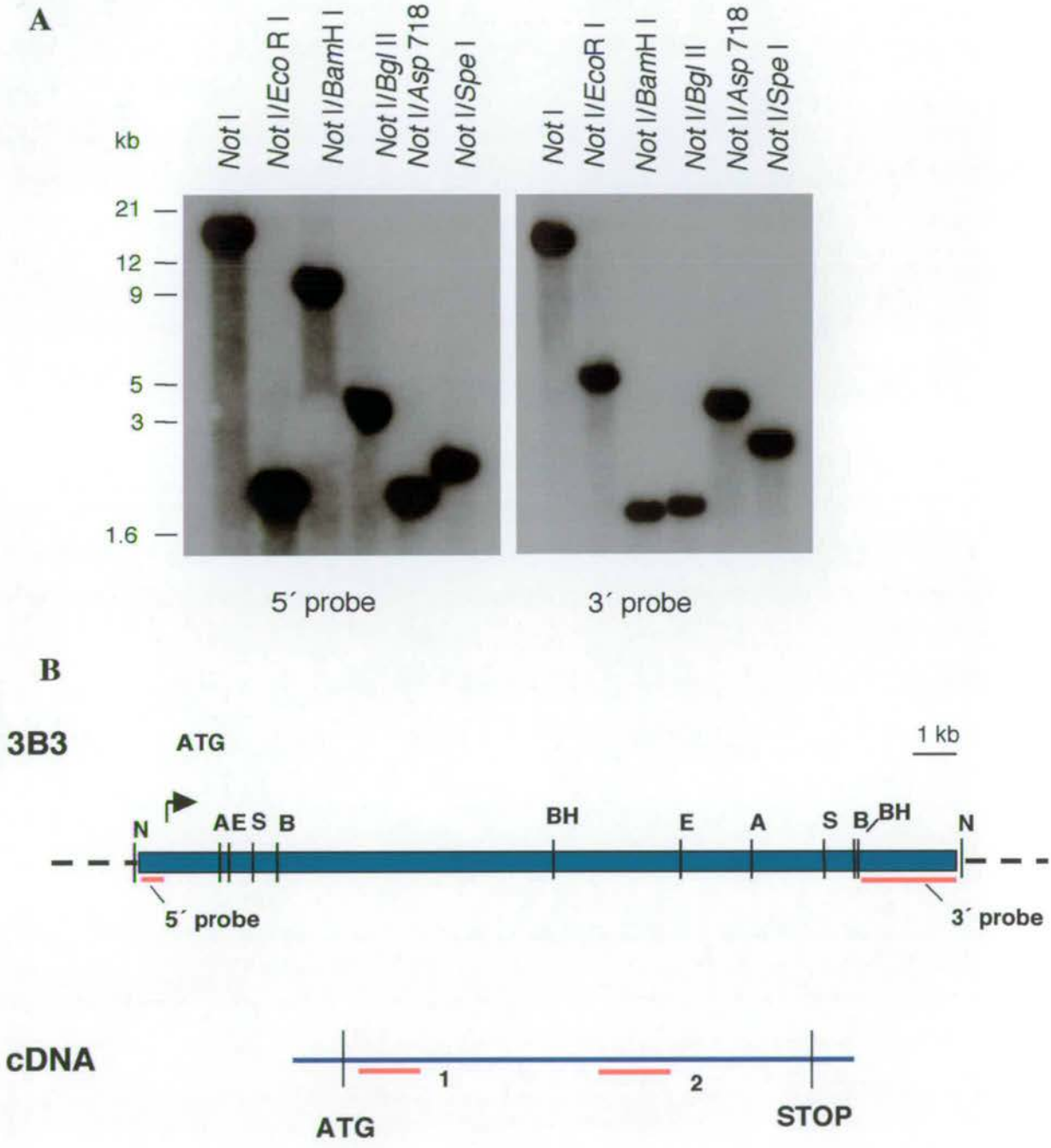

Figure 4.2 Mapping of genomic phage 3B3. **A,** Southern blots using 5´ and 3´ probes as indicated in B. Digestion with Not I releases the cloned insert from the phage arms. **B,** The restriction map was generated from the Southern blots in A. The probes 1 and 2, used for library screen are shown. The 5´ probe used for the final screen is indicated on the 3B3 map. Key; A - *Asp* 718, B - *Bgl* II, BH - *Bam*H I, E - *Eco*R I, S - *Spe* I, N - *Not* I.

A basic restriction digest map was generated from phage 3B3 by Southern blotting, as detailed in sections 2.2.15-2.2.17, using double digests with *Not* I, and probes to both the 3′ and 5′ ends (Fig 4.2A). In parallel, the DT40 *BubR1* genomic locus was also mapped, using Southern blotting (Fig. 4.3A). There are some slight differences in the sizes of the fragments between the phage 3B3 and the genomic locus, however, these are small and seem to be within the range of inaccuracy in the sizes as determined from the Southern blots.

In conclusion, the phage 3B3 and the *BubR1* genomic locus in DT40 cells have been mapped using the same 5′ and 3′ probes and it can be concluded that that they are isogenic. Therefore phage 3B3, was used as the basis of the targeting vector for the disruption of the *BubR1* genomic locus in DT40 cells.

4.2.2 Construction of targeting vectors

The sequence contained within phage 3B3 was used to generate both a 5′ and 3′ targeting arm and both 5′ and 3′ external probes for mapping the targeted locus. Initially a 5 kb *Not I/Eco*R I fragment from the 3′ end of the phage was cloned into pBluescript. This was then used to generate both the 3′ targeting arm and the 3′ external probe. A convenient *Bam*H I site cut this into 3 kb and 2 kb, with the 3 kb being cloned into pBluescript as the 3′ targeting arm and the 2 kb fragment to be used as the 3′ probe.

Figure 4.3

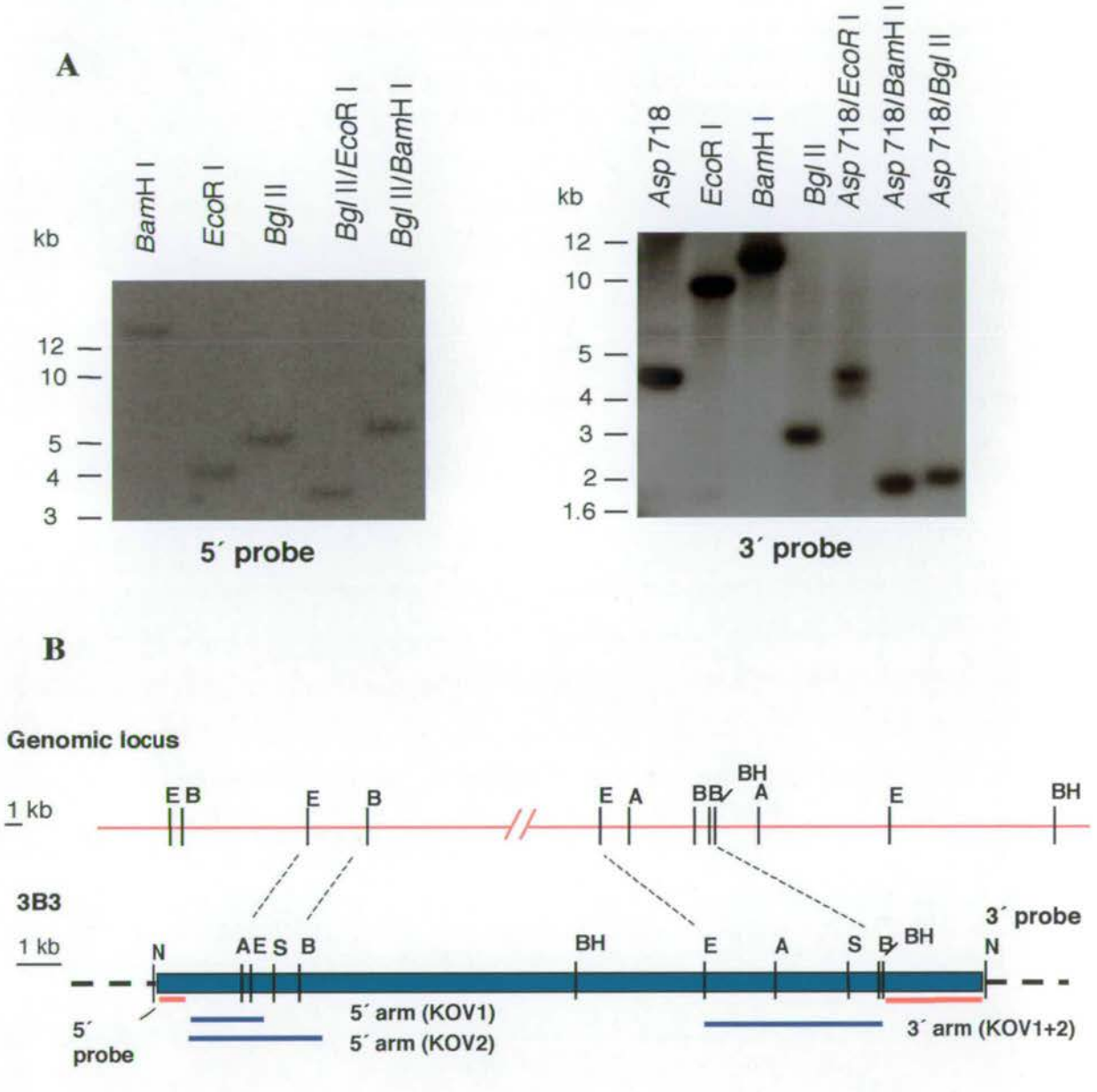

Figure 4.3 BubR1 genomic locus. **A,** Southern blots of DT40 genomic DNA digested as indicated and probed with 5´ and 3´ probes as indicated in B. **B,** A map of the genomic locus was constructed and compared to that of 3B3. Key; A - *Asp* 718, B - *Bgl* II, BH - *Bam*H I, E - *Eco*R I, S - *Spe* I, N - *Not* I.

To generate the 5′ external probe and the 5′ targeting arm, a PCR approach was adopted. A 383 bp PCR product corresponding to the most 5′ region was generated, using primers HD21 and HD22 (Table2.8). This sequence terminated at the ATG and was used as the 5′ external probe. This probe was then cloned into the pGEM-T vector. PCR primers were then designed to several sequences within the cDNA in order to generate a large enough fragment for the 5′ targeting arm. A limitation to this method was that since this DNA region was not sequenced, the PCR products generated would be of unknown size. This PCR was carried out using TAKaRa taq, as described in the section 2.2.10, which is a mixture of Taq and the proof reading polymerase Pfu. In this case it was necessary to minimise the introduction of mistakes, since these may decrease the targeting efficiency of the construct. A product of 1.6 kb was successfully generated using primers HD7 and HD8 (Table 2.8), and cloned into the pBluescript vector already containing the 3′ targeting arm. It was then necessary to clone the resistance cassette between these arms into the *Bam*H 1 site. Both Puromycin (Puro) resistant and Histidinol (HisD) resistant vectors were generated. This vector was named KOV1 (knockout vector 1), as shown in Figure 4.4.

Since phage 3B3 does not cover the entire gene and only contains a small portion upstream of the ATG the vector will not remove the entire open reading frame of BubR1. This construct will delete a region from amino acid 67 to 529, removing in the order of 10.5 kb of genomic DNA. Figure 4.4 shows this targeting vector, the genomic locus and the screening strategy using the 5′ external probe

The targeting vectors containing the puromycin resistance cassette and histidinol cassette were transfected into wild type DT40 cells (Cl18), and the resistant colonies screened using a *Bgl* II digest and the 5′ external probe. Table 4.2 shows the results of this initial screen.

Table 4.2 Initial screen with KOV1

KOV1	Number of clones screened	Apparent number of +/- clones
HisD	80	3
Puro	86	5

Figure 4.4

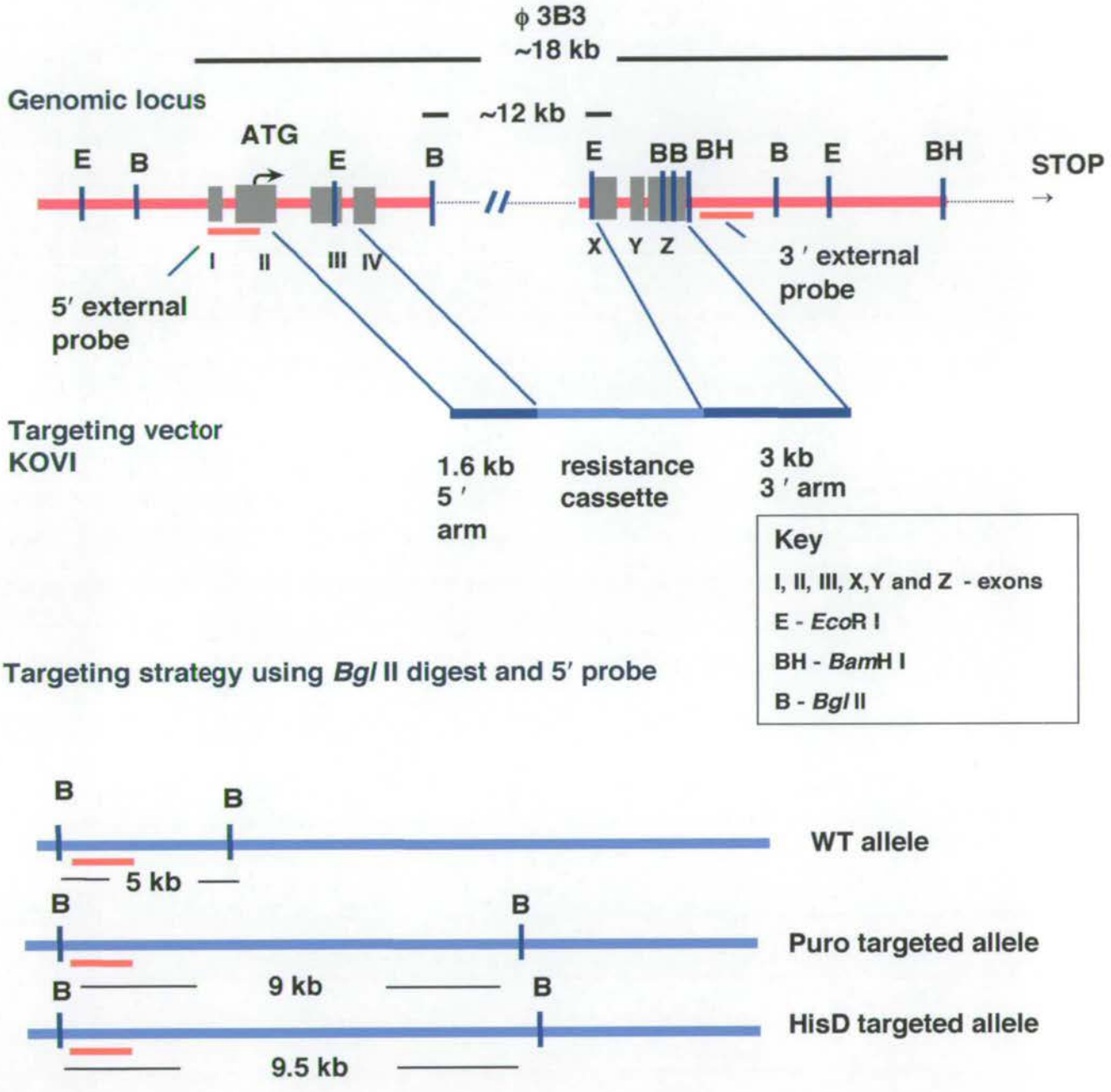

Figure 4.4 Knockout vector 1. Schematic representation of phage 3B3 including the exons identified, I-IV at 5′ end and X, Y, Z at 3′ end. This phage was the basis for knockout vector 1 (KOV1) as shown. Two knockout vectors were constructed one with the Puromycin and one with the Histidinol resistance cassette. The screening strategy from these vectors is shown using a *Bgl* II digest and 5′ external probe.c

It can be seen from Table 4.2 that, in all, eight cell lines were generated which appeared to be targeted at the *BubR1* locus. An example of one of these clones, 215, targeted with the puromycin vector is shown in Figure 4.5A. In order to further verify that these clones were heterozygote for the locus, the cells were thawed from -80°C, DNA prepared from them and then re-genotyped using the same strategy. The results of the Southern blots however, indicated that there was a problem or error since the cells no longer appeared heterozygote as shown in Figure 4.5B. One potential source of this problem was that the probe might spuriously hybridise to another DNA species and give a false result (Figure 4.5A). In order to check this, the targeting vectors were transferred to membrane and hybridised with the probe. Indeed the probe hybridised very strongly to these vectors (Figure 4.5C). One potential reason for this could be that the full length probe recognises some vector sequence. To make the probe more specific, it was cut in two by digestion with *Pst* I, generating a 5′ 212 bp fragment and a 3′ 171 bp fragment. These smaller probes were then labelled and tested to see if they hybridised to the vector (Figure 4.5D).

These both hybridised, but to a lesser degree than the full length probe. It seemed possible, therefore, that the problem was due to some cross reactivity between probe and vector sequence. Since the probe was cloned into pGEM-T it was being prepared for labelling by digestion and then extraction from an agarose gel. Although the contamination of uncut DNA containing polylinker sequences should have been removed by this protocol, this may be one explanation for this cross hybridisation. In order to avoid this problem, the probe was generated again by PCR, then gel extracted and labelled. A comparison was made between these two probe preparations as shown in Figure 4.5E. This led to the conclusion that the probe cut from the pGEM-T vector hybridises to the integrated targeting vectors in the clones which were apparently identified as heterozygotes in the initial screen. In the case of the smaller probes, the cleaner result may arise from the fact that a further digestion and gel purification has been carried out. When the membrane shown in Figure 4.5A was stripped and re-hybridised with the probe generated by PCR rather than digestion it was seen that the upper, 'targeted' band disappeared as shown in Figure 4.5F. It is theoretically possible that multiple arrays of the targeting vector could be integrated randomly in the genome and when cut by *Bgl* II result in a band of approximately 9.5 kb as illustrated in Figure 4.5G. This may also explain why the band is unstable and not present in Figure 4.5B, when the cells have been 'thawed and DNA prepared.

Figure 4.5

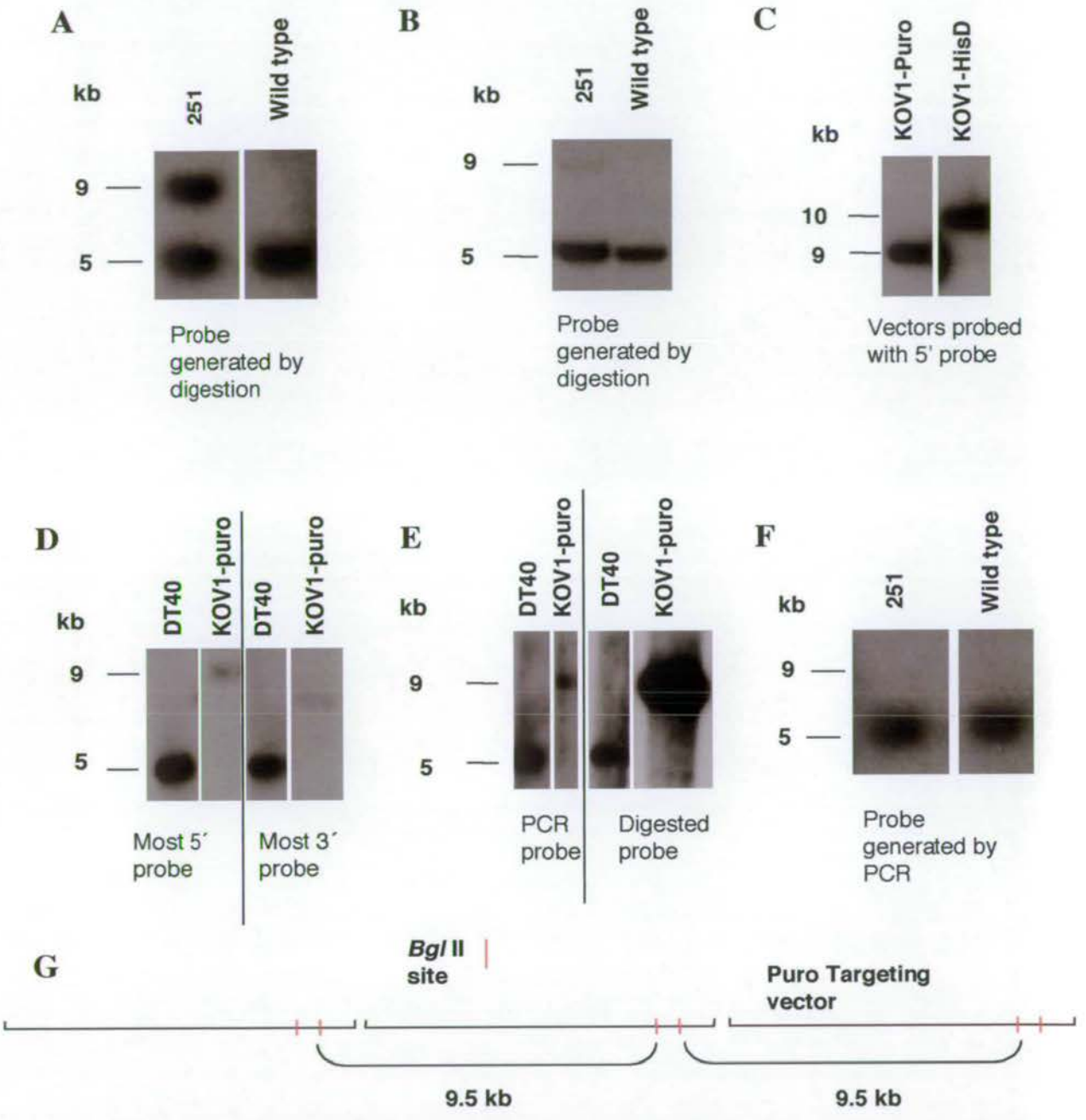

Figure 4.5 Investigation of cell line 251 **A**, Southern blot showing wild type and targeted allele (251) using 5′ probe and *Bgl* II digest as indicated in Figure 4.4. **B**, Southern blot showing that clone 251 appears to have a different pattern of bands on another blot using the same probe. **C,** Southern blot of linearised targeting vectors (10 ng), HisD and Puro, probed with 5′ probe. **D**, Southern blot of wild type DT40 DNA and Puro targeting vector digested with *Bgl* II and probed with the two portions of original 5′ probe, 5′ most (left) and 3′ most (right), generated by PCR and then digested with *Pst* I to make 212 and 171 bp fragments **E,** Southern blot of wild type DT40 DNA and Puro targeting vector, probed with the 5′ probe generated by either PCR or digestion from pGEM-T plasmid. **F**, Southern blot as in A which has been stripped and re-probed with the 5′ probe generated by PCR rather than digestion. **G**, Model indicating possible tandem integration of Puro targeting vector and the resulting 9.5 kb band after *Bgl* II digestion.

4.2.2.1 Generation of a Rescue construct

Since it now appeared that it had not been possible to target the *BubR1* locus with KOV1 several possible reasons were investigated. One possible reason could be that there is only one copy of *BubR1* in DT40 cells because it is located on the Z chromosome, (chicken sex chromosomes are designated Z and W and DT40 cells are female = ZW) and that the gene is essential. To potentially overcome the problem of disrupting an essential single copy gene, a rescue construct can be expressed in wild type cells before targeting. The rescue construct to be used in this case was the full length, untagged chicken BubR1 cDNA. In order to regulate the expression of this cDNA, it was cloned into the pUHG-10.3 plasmid under the control of the tetracycline operator (Figure 4.1).

Since the encoded protein was untagged it was necessary to design a strategy to differentiate between the exogenous and endogenous expression. To achieve this, the 3′ UTR of chicken BubR1 was mutated such that the STOP codon was fused to the polyadenylation signal. This construct was generated by PCR using one primer to a region 500 bp upstream of the STOP codon and another primer, which was a fusion between the sequence around the stop codon and the sequence at the polyadenylation signal (see Figure 4.6A). The difference between the endogenous and exogenous transcript was detected using an RT-PCR strategy with primer 1 and primer 2, designed to the polyadenylation signal which would therefore amplify a product of 839 bp for the endogenous transcript and 507 bp for the rescue transcript (see Figure 4.6B).

Wild type DT40 cells were transfected with the rescue construct described above and the transactivator tTa 2 as described in the introduction to this chapter. In order to determine if the expressing clones were able to switch off BubR1 expression, they were treated with 2 µg/ml doxycycline, the more stable analogue of tetracycline, for 48 hours. Figure 4.6B shows RT-PCR analysis of two such clones, which expressed BubR1 and were repressed by the addition of doxycycline. It is curious to note that in cell lines 4 and 10, before the addition of doxycycline a PCR band corresponding to the rescue construct is preferentially amplified. In this case, the wild type band is not detected until after the expression of the rescue construct is repressed. In other experiments, both the endogenous and rescue bands could be detected by RT-PCR (Figure 4.10A). Cell lines 4 and 10 were also analysed by immunoblot using the chicken BubR1

antibody described in Chapter 3. Indeed, the overexpression and repression could also be clearly seen using the antibody (Figure 4.6C). Notably, these clones were expressing quite a high level of BubR1 as compared to the wild type cells.

Based on these results, clones 4 and 10 were then used in targeting experiments. KOV1 was transfected into these two lines and the results of these experiments are shown in Table 4.3.

Table 4.3 Numbers of colonies screened with KOV1 in a rescued background.

Cell line	Resistance marker	Number of clones screened	Number of targeted clones
4	HisD	47	0
4	Puro	41	0
10	HisD	67	0
10	Puro	67	0

Since no targeting was observed even in the presence of a rescue construct, the final possibility was that the targeting vector contained too small a region of homology to efficiently target this size of genomic region. In order to overcome this problem a new vector was constructed with a longer 5′ targeting arm. Again, this longer 5′ homology arm was generated by PCR using phage 3B3 as the template and primers designed to the cDNA sequence. A fragment of 3 kb was successfully generated by PCR using primers HD7 and HD9 (Table 2.8), and cloned into the targeting vector in place of the shorter 5′ arm. This vector now had a total homology length of 6 kb, and would remove amino acids 125 to 529 of the protein. This vector was generated with four different resistant cassettes, Blasticidin (Bsr), Hygromycin (Hyg), Histidinol (HisD and Puromycin (Puro). The new vector was designated KOV2 and the screening strategy using both a 5′ and 3′ external probe is shown in Figure 4.7.

Figure 4.6

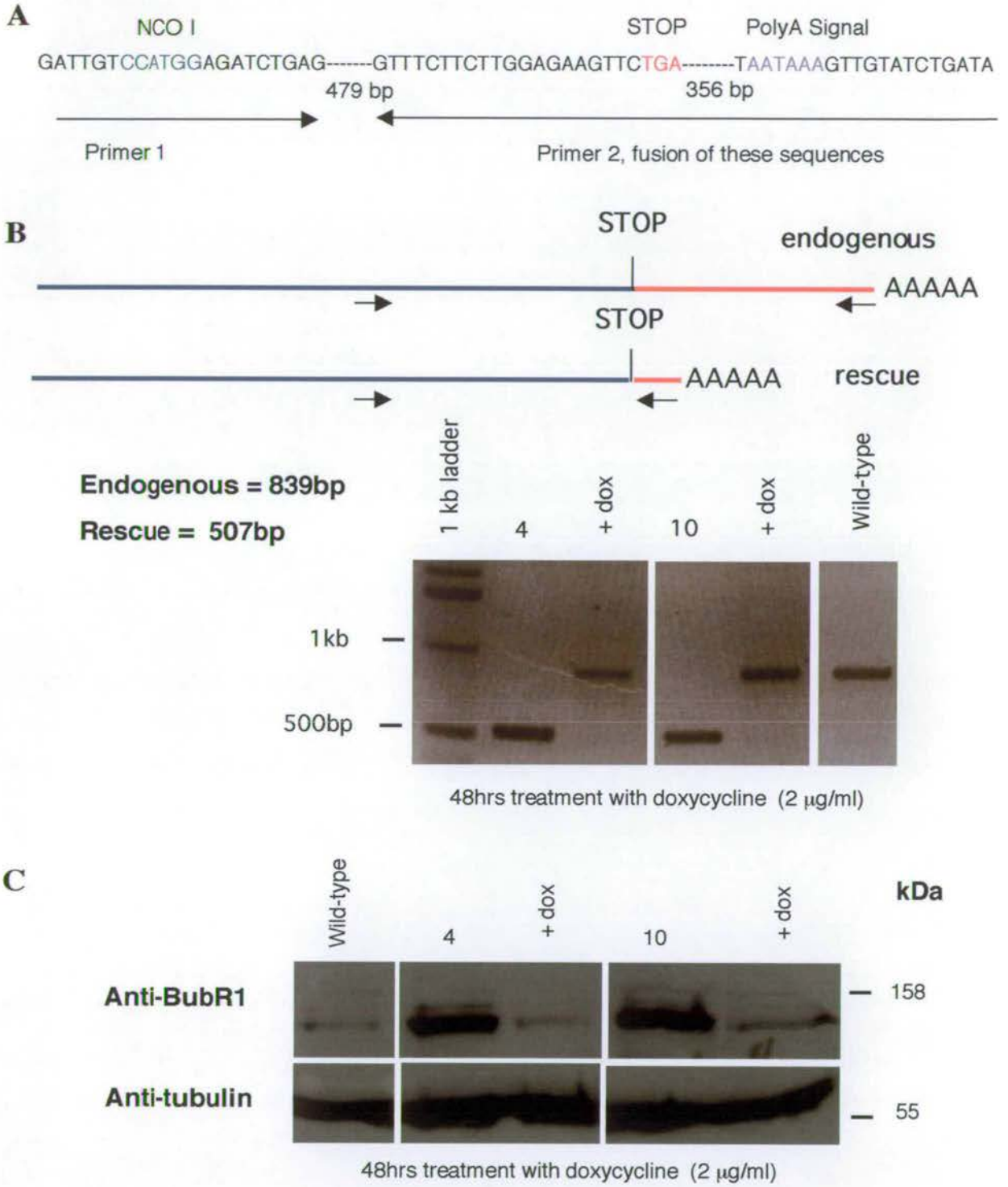

Figure 4.6 Rescue Strategy. **A**, Cloning strategy of rescue construct. Primers 1 and 2 were used to generate a PCR product, which was cloned into the cDNA from which the original 3′ end had been removed. **B**, RT-PCR strategy to determine if the rescue construct is expressed and repressed. +dox indicates treatment with 2 μg/ml doxycycline for 48 hours. Two repressing cell lines, 4 and 10, are shown alongside wild type cells. **C**, Western blot showing expression and repression of the rescue construct in clones 4 and 10 after treatment with 2 μg/ml doxycycline for 48 hours. Anti-tubulin was used as a loading control.

Figure 4.7

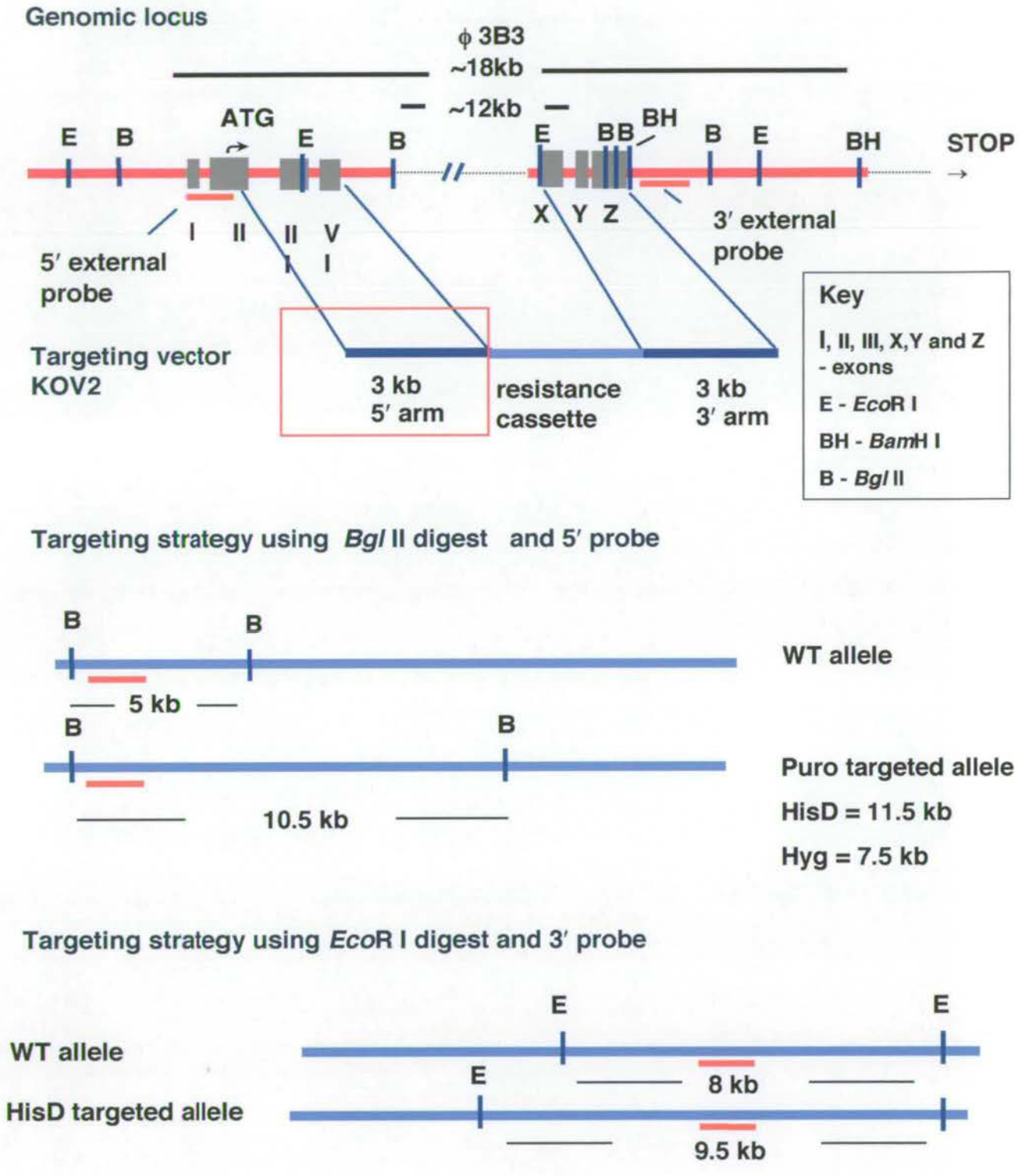

Figure 4.7 Knockout vector 2. A longer 5′ arm was cloned in order to generate knockout vector 2 (KOV2) with a longer region of homology than KOV1. The screening strategy using a *Bgl* II digest and 5′ external probe is shown. In addition the 3′ strategy using an *Eco*R I digest and 3′ external probe is shown.

4.2.3 Generation of +/- DT40 cells

KOV2 was transfected into wild-type DT40 cells, and also into clone 4 and clone 10, which express the rescue construct as discussed in section 4.2.2. The resistant colonies were screened using a *Bgl* II digest and the 5′ external probe. Targeting with KOV2 was successful and four different heterozygote cell lines were generated (Table 4.4). Three of these +/- cells were in the wild type background, and one was in the clone 4 background, which was previously transfected with the rescue construct.

As shown in Figure 4.8A, the 5′ external probe strategy clearly shows that clones 433, 511, 812 and 821 have been targeted, resulting in two bands after digestion with *Bgl* II. In order to confirm that the locus was targeted at both the 5′ and 3′ ends the clones were also screened using the 3′ external probe and an *EcoR* 1 digest. The Puro-targeted clones 812 and 821 have an additional *Eco*R 1 band as shown in Figure 4.8B. The *Eco*R 1 strategy and the 3′ probe is unsuitable for the HisD and Hyg targeted clones since these resistance cassettes all have an *Eco*R 1 site at the 3′ ends which is very close to the location of the genomic *Eco*R I that was removed by the cloning of the 3′ arm (Figure 4.7). In this case an alternative strategy is needed to check the targeting at the 3′ end of the locus. This may be possible by using a different digest or by using a PCR strategy. A number of digests and double digests were attempted in order to further map the 3′ end, however it was not possible to design another strategy with the information available. The PCR strategy was not attempted for these clones.

Table 4.4 Screen with KOV2

Background	Resistance marker	Number of clones screened	Number of targeted clones
Wild type (Cl18)	Bsr	26	0
	HisD	63	2 (#812, #821)
	Hyg	70	0
	Puro	20	1 (#511)
Clone 4	Bsr	73	0
	Hyg	85	1 (#433)
	Puro	12	0
Clone 10	Bsr	74	0
	Puro	55	0

Since one heterozygote clone, namely 433 was targeted with the Hyg resistance cassette in the rescue clone 4 background, this seemed to be a suitable cell line in which to attempt targeting of the second allele. From the initial Southern blotting analysis, which identified 433 as a targeted clone, (Figure 4.8A), it can be seen that the intensity of the wild type and targeted bands were unequal, which was not the case for clones, 511, 812 and 821. This is potentially due to a mixed population of cells. There is always a possibility when picking the resistant clones from 96 well plates after selection that two colonies will be present. Every effort is made to minimise this chance by carefully picking single colonies at the correct stage, however, one could be much larger than the other and obscure the small colony. The cells were subcloned by limiting dilution and re-genotyped by Southern blot. As can be seen in Figure 4.8C all the subcloned cells again had an unequal intensity of wild type and targeted bands indicating that this was not a result of a mixed population of cells. In the meantime the original clone 433 cells were targeted with KOV2 Puro and the result was that the puro vector was able to both replace the hygromycin marker (not shown) and target a further allele, giving rise to three bands of equal intensity on the Southern blot (Figure 4.8D). This result was most unexpected and may suggest that BubR1 is present in three copies in DT40 cells. Although the karyotype of DT40 cells is near diploid it is known that they have one extra copy of the macrochromosome 2 and one extra microchromosome. However, this difference in band intensity seen for clone 433 was not seen with the other +/- cell lines 511, 812 and 821, leading to the speculation that some rearrangement or change in the karyotype had occurred in this particular cell line. From the known role of BubR1 in the spindle assembly checkpoint and maintenance of the stability of the genome, it can be hypothesised that disruption of one allele caused the cell to rearrange its genotype and retain an extra copy of the chromosome containing BubR1. In the future, the number of copies of the *BubR1* locus could be determined by FISH.

In addition to the problems with the number of copies of BubR1 in clone 433 there also appeared to be problems with the expression of the rescue construct in these cells. The overexpression could no longer be detected by RT-PCR or immunoblot, and it appeared that with time the expression of the exogenous cDNA had been lost. This was the first observation that expression of BubR1 in DT40 cells may in some way be toxic or detrimental and that there may be a problem with stable expression of the protein.

Figure 4.8

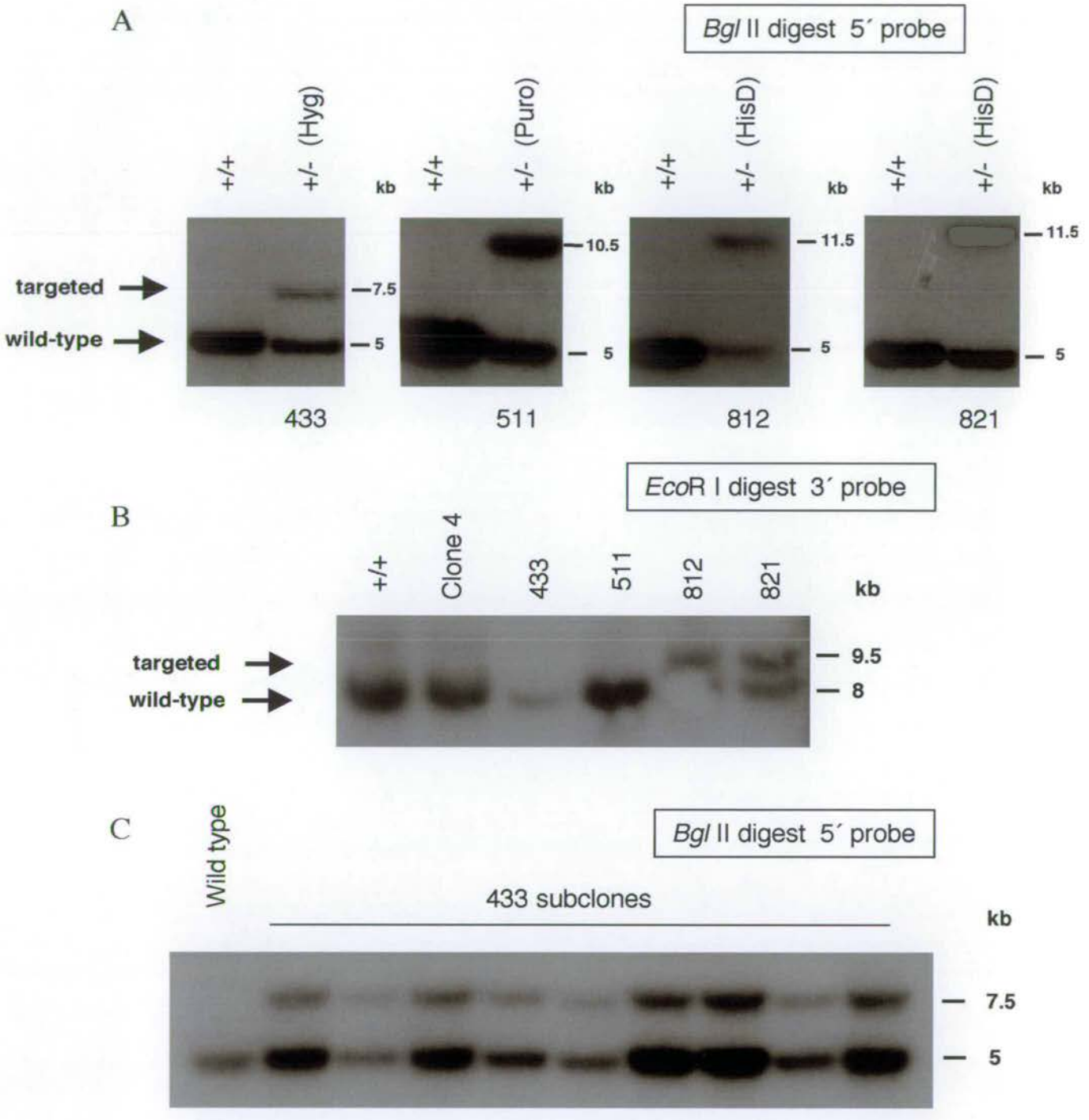

Figure 4.8 Generation of BubR1 +/- DT40 cells. **A**, Southern blot showing targeting at the 5´ end of the BubR1 locus as judged by *Bgl* II digest and 5´ external probe. **B**, Southern blot showing targeting of the 3´ end of the BubR1 locus as judged by *Eco*R I digest and 3´ external probe. It is impossible to determine if cell lines 433 and 511 are targeting using this strategy since there is an *Eco*R I site present at the end of the resistance cassettes very close to the location of the genomic *Eco*R I site. **C**, Southern blot showing subcloning of cell line 433. This cell line remains at an unequal band intensity after subcloning.

Figure 4.8 Continued

D

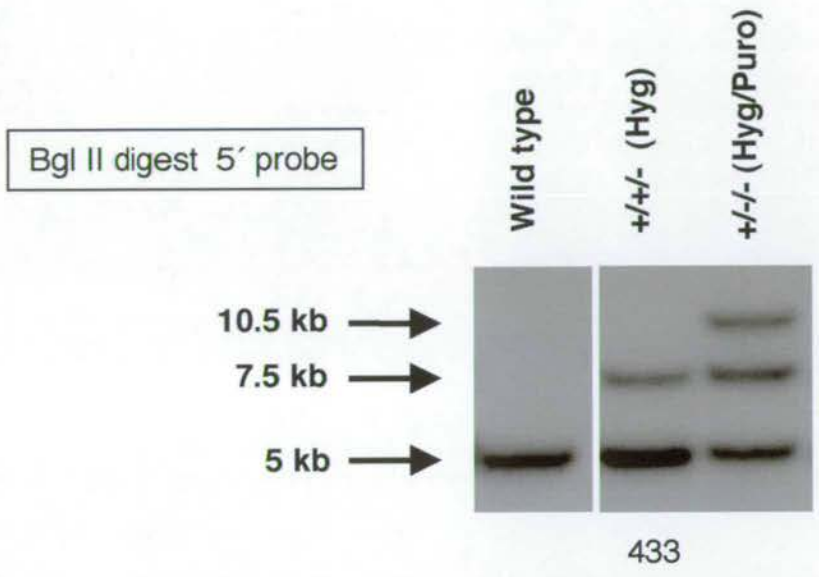

Figure 4.8 Continued. **D**,Southern blot showing that heterozygote cell line 433 was targeted with KOV2 Puro and a further allele was apparently generated as shown.

Since it now appeared that clone 433 was not the ideal cell line to work with, in order to target the second allele, the aim was to generate other heterozygote lines expressing the rescue construct.

The targeting frequency of these vectors varies quite considerably, from 1/20 for Puro to 2/63 for HisD and 1/85 for Hyg, but it is difficult to state conclusively how efficient these vectors are. In the case of the Puro vector, 1/20 clones screened were positive, however, since only 20 colonies were screened and only 1 detected this is not statistically significant. Therefore, the Puro vector was used subsequently in the attempts to target clone 433. In this case, out of 45 colonies screened, one Hyg targeted allele was replaced by Puro, and in two cases a second allele appears to have been targeted. It therefore seems that the most efficient vector, with the frequency of targeting being around 1/15 (6%), is Puro. It could therefore be estimated that the frequency of targeting for the second allele using this vector would be around 1/30 (3%).

In order to test the prediction that BubR1 is an essential gene I attempted second allele targeting in two of the heterozygote cell lines in the absence of a rescue construct. Transfections were carried out in the cell lines 511, which was targeted with the HisD marker and 812, which was targeted with the Puro marker. No targeted clones were identified, thereby supporting the conclusion that BubR1 is essential in these cells.

4.2.4 Analysis of heterozygous (+/-) cells

Initial phenotypic analysis of the heterozygous cells 511, 812 and 821 showed that they grew normally in culture and appeared normal in morphology. In order to investigate the cells more carefully, their growth rate was calculated and compared to that of wild type DT40 cells (Figure 4.9A). This experiment was carried out in triplicate, however, all three experiments gave similar results and the results of just one are plotted here. The results show that the cell line 511 grows more slowly than the other heterozygote lines 812, 821 or wild type cells. Clone 18 (wild-type DT40) had a doubling time of 6.9 hours, clone 511 had a doubling time of 9.5 hours, clone 812 had a doubling time of 7.25 hours and clone 821 had a doubling time of 7.2 hours.

Immunofluorescence microscopy re-affirmed initial observations that the cells appeared normal in morphology and divided normally. In addition it was shown that BubR1 staining is normal in these +/- cells (Figure 4.9B). Since it has been reported that the spindle assembly checkpoint component Mad2 is haploinsufficient in mouse (Michel *et al.*, 2001) it was interesting to determine if this was also the case for BubR1 in DT40 cells. To test if the spindle assembly checkpoint was intact, +/- cells were treated with the microtubule drugs colcemid and taxol (paclitaxel). Colcemid is a microtubule depolymerising agent, whereas taxol suppresses microtubule dynamics. According to current hypotheses, BubR1 senses tension at the kinetochore (Skoufias *et al.*, 2001) and so should respond to treatment with both colcemid and taxol. In order to determine if the checkpoint was intact in the +/- cells, the mitotic index was counted after treatment with these drugs and compared to wild type cells. In addition, the cells were stained with the antibody to BubR1 to determine if the protein was at the kinetochore. As shown in Figure 4.9C the cells did respond to spindle damage induced by both colcemid and taxol, resulting in a mitotic block with BubR1 present on unattached kinetochores. In order to quantify this response the number of cells in mitosis was counted before and after treatment with the microtubule drugs and compared to wild type cells. The results of this analysis are shown graphically in Figure 4.9D. It can be seen from this analysis that the spindle assembly checkpoint appears to be active in these +/- cells, as they block in mitosis. In order to further confirm this result the samples were also prepared for immunoblotting. After treatment with the microtubule drugs the cells were subjected to SDS-PAGE, transferred to membrane and then blotted for BubR1. The results of this experiment (Figure 4.9E), reveal that the +/- cells do indeed respond to the checkpoint, as judged by the presence of the upper putative phosphorylated band of BubR1 after treatment with these drugs (as discussed in chapter 3). This experiment also allowed me to determine the level of BubR1 in the +/- cells.

Although the protein loading was not absolutely equal for the untreated samples, as judged by the α-tubulin loading control, it appears that the level of BubR1 protein is reduced in the heterozygote cells as compared to wild type DT40 cells. In conclusion, the heterozygotes appear to grow normally with no obvious kinetochore or mitotic defects and to have an active spindle assembly checkpoint although the protein level is reduced.

Figure 4.9

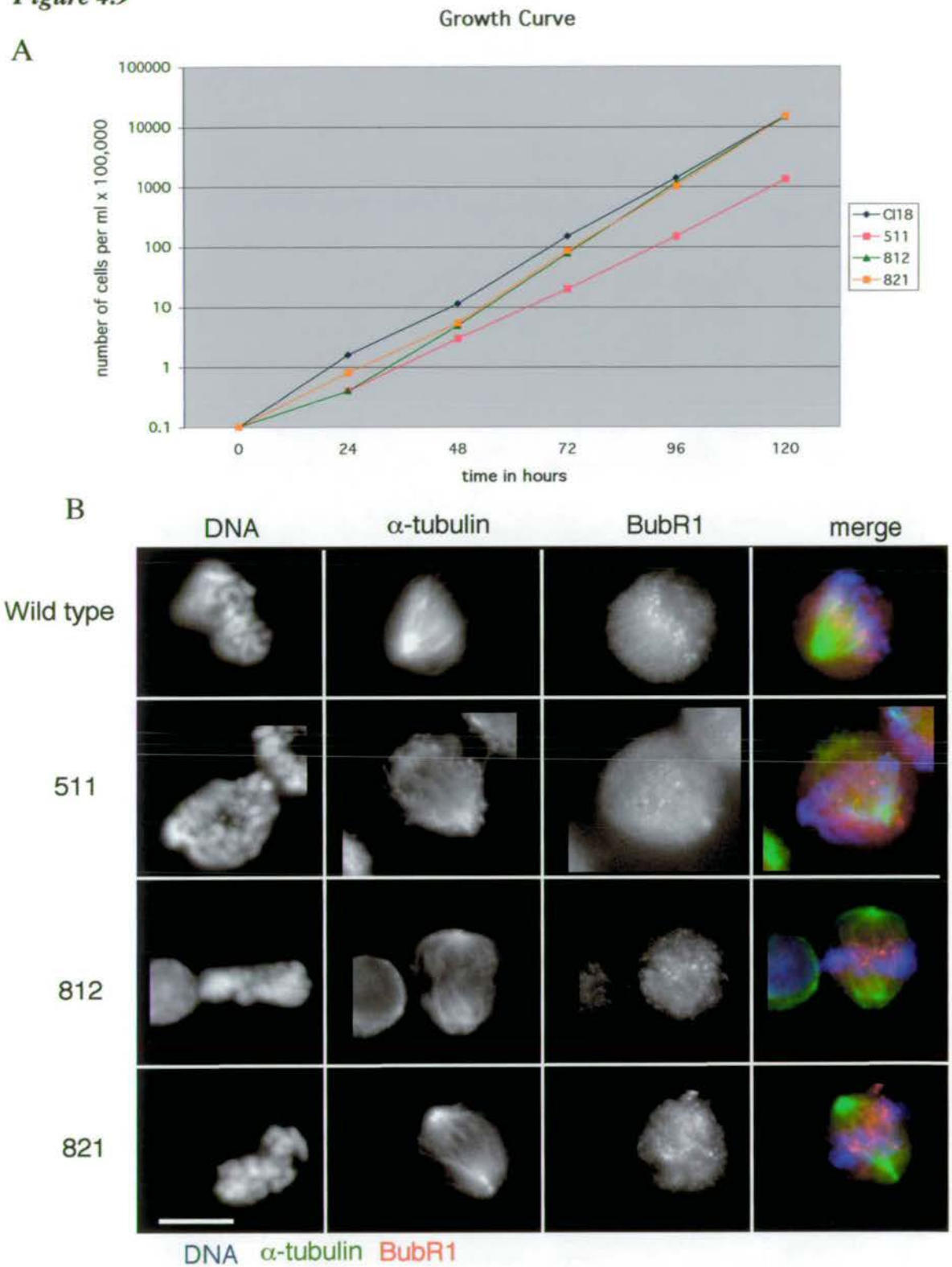

Figure 4.9 Analysis of BubR1 +/- DT40 cells. **A,** Growth curve of heterozygotes as compared to wild type (Cl18) DT40 cells. The cells were seeded at a density of 1 x 10^4 per ml and counted every 24 hours for 5 days. When the cells reached a density of 1 x 10^6 per ml they were split 1:10 into fresh medium. This experiment was carried out in triplicate. The results of all three experiments were very similar and one is plotted here. **B,** Immunofluorescence of heterozygote cells stained for BubR1 (red), alpha tubulin (green) and DNA with DAPI (blue), scale bar is 10 μm.

Figure 4.9 Continued

C

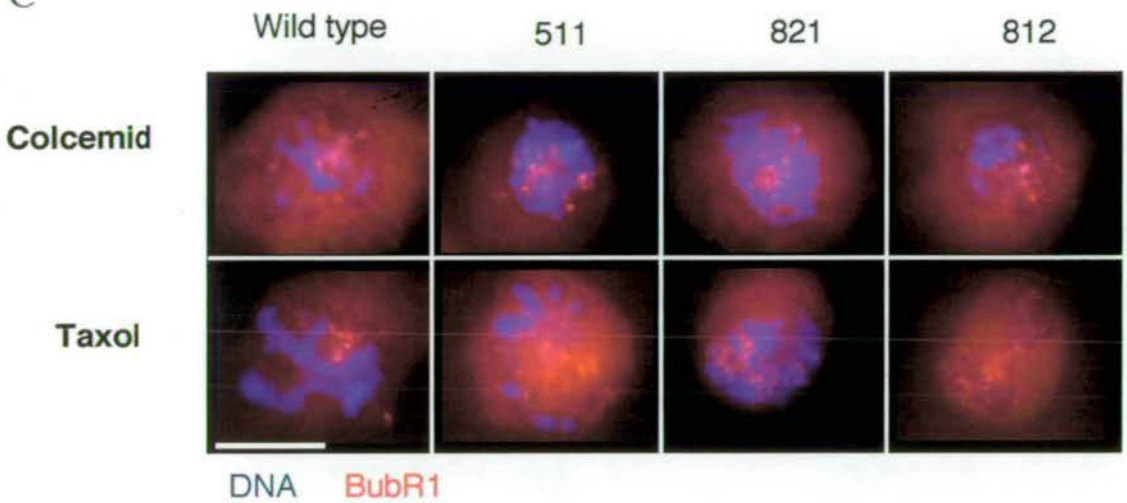

D

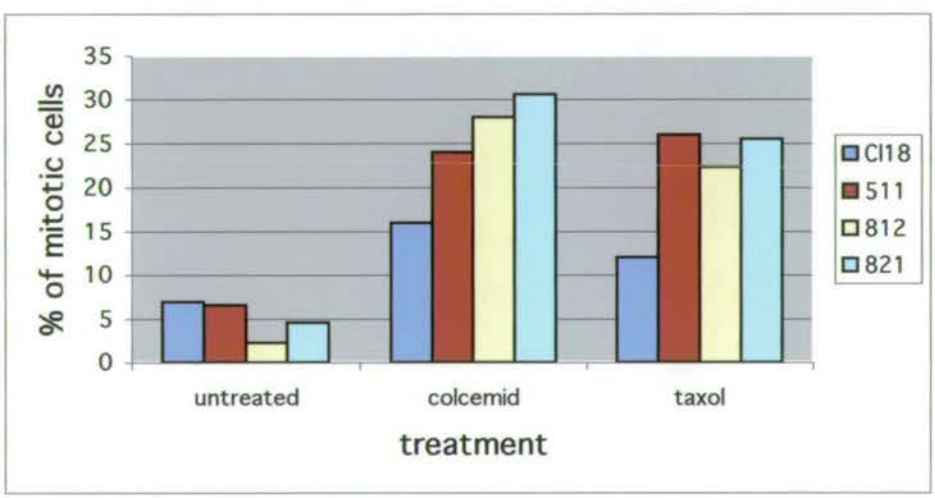

***Figure 4.9 Continued*. C**, BubR1 responds to spindle damage in +/- cells. BubR1 +/- DT40 cells and wild type cells (Cl18) were treated with either colcemid (0.1 μg/ml) or taxol (10 μM) for 3 hours and then stained for BubR1. Scale bar is 10 μm. **D**, +/- cells block in mitosis in response to spindle damage. The mitotic index was determined after treatment with either colcemid or taxol as described above.

Figure 4.9 Continued

E

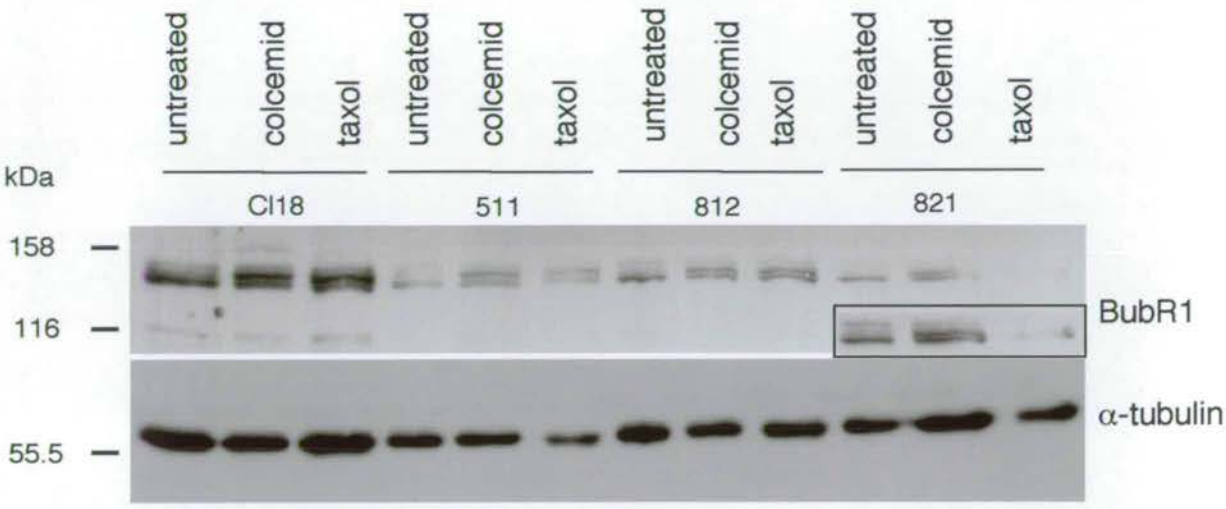

Figure 4.9 Continued **. E**, BubR1 protein levels are reduced in +/- cells but BubR1 is phosphorylated in response to spindle damage. BubR1 +/- DT40 cells were treated with colcemid or taxol as described in C, and the cell lysates were then subjected to 10% SDS-PAGE, transferred to membrane and immunoblotted for BubR1. The signal was detected using ECL. Inset shows longer exposure time. Alpha tubulin was used as a loading control. Cl18 are wild type DT40 cells.

Since the evidence led to the conclusion that BubR1 is essential in these cells, attention was focussed on the generation of heterozygote cell lones expressing stable levels of the BubR1 cDNA, which could be repressed by the addition of doxycycline.

4.2.5 Generation of +/- cells expressing rescue construct

As discussed in the Introduction, different levels of rescue expression could be produced by co-transfection with different transactivator vectors, tTa2, tTa3 and tTa4. Lines were generated with all three transactivators in the HisD resistant cell lines 812 and 821, so that the more efficient KOV2 Puro vector could be used for targeting the second allele. Initially the strategy was to check that these lines could express and repress the transgene by either immunoblot or RT-PCR. The cells expressing the rescue construct were also analysed by immunofluorescence (IF). The results of this analysis were quite surprising, because although by RT-PCR and western blot it seemed that these cell lines were expressing fairly high levels of the transgene, the IF indicated that this expression was very heterogeneous within the population (see Figure 4.10B). It was observed that only a low percentage of the cells appeared to be actually expressing the rescue construct, as judged by BubR1 antibody staining. This was quantified for some cell lines, and was never higher than 10%. Since the rescue construct was untagged, then it was very difficult to determine on a cell by cell basis if the transgene was expressed, unless this was at a high enough level to detect it with an antibody. The best way to determine this would be by using a rescue construct with a tag, however previous experience led me to worry that this might disrupt the function of the protein. A series of targeting experiments were carried out, the results of which are detailed in Table 4.5. In brief the targeting experiments were unsuccessful. The most likely reason for this was that the transgene was not being expressed at all, or expressed at the correct levels in a large enough population of cells, thus making the chances of targeting fadingly slim. An example of the RT-PCR results for two of the cell lines is shown in Figure 4.10A, indicating that they did express the transgene and that it could be repressed by doxycycline. Some examples of the IF images of +/- cells transfected with the rescue construct are shown in Figure 4.10B. It was very difficult to determine if these cells were actually progressing through mitosis or if the expression of the rescue construct was having a toxic effect leading to the cell shutting off expression. In the top panels (i) several normal looking cells

expressing various levels of the transgene are shown in various stages of normal progression through mitosis. In the middle panels (ii), overexpressing cells, which appear apoptotic, are shown. In the bottom panels (iii), some cells with abnormal multipolar spindles are shown. Thus, although some expressing different levels of the transgene appeared normal and progressed through mitosis, many cells highly overexpressing BubR1 appeared to be apoptotic(Figure 4.10B(ii). This led to the hypothesis that overexpression of BubR1 may lead to apoptosis.

Table 4.5 Attempts at targeting in cell lines expressing the rescue construct.

+/- Background	*tTa*	*Cell line*	*Number screened*	*-/-*
812	2	2/16	40	0
812	3	3/1	55	0
821	3	A/11	50	0
812	4	4/34	61	0
812	4	4/36	60	0
812	4	4/41	35	0
812	4	A12	69	0
821	4	B13	77	0

In order to overcome the problem of heterogenous expression levels of the rescue construct, a number of possible approaches were considered. Firstly, in order to try and generate a more stable population of cells, transfections with the rescue construct were carried out in the presence of doxycycline (10 ng/ml). Cells were cultured in doxycycline for 2-3 days before the transfection and then plated out into selective medium with doxycycline present. When the colonies were visible, they were split evenly between medium with and without doxycycline. The hope was that this would prevent the potentially toxic expression of the protein and allow for the generation of a more stable population. Unfortunately, this protocol also resulted in cell lines with very heterogeneous levels of expression. Two of these cell lines, which repressed in the presence of doxycycline, namely A12 and B13 were transfected with the KOV2 Puro. However, as shown in Table 4.5 this targeting was unsuccessful.

Figure 4.10

Figure 4.10 BubR1 heterozygote DT40 cells expressing rescue construct. **A,** Example of expression of rescue lines A12 and B13 as shown in A as judged b RT-PCR. The expression of the transgene is repressed after treatment with doxycycline (10 ng/ml) for 48 hours. All lines in Table 4.5 were tested for expression or repression by either immunoblot or RT-PCR.

Figure 4.10 Continued

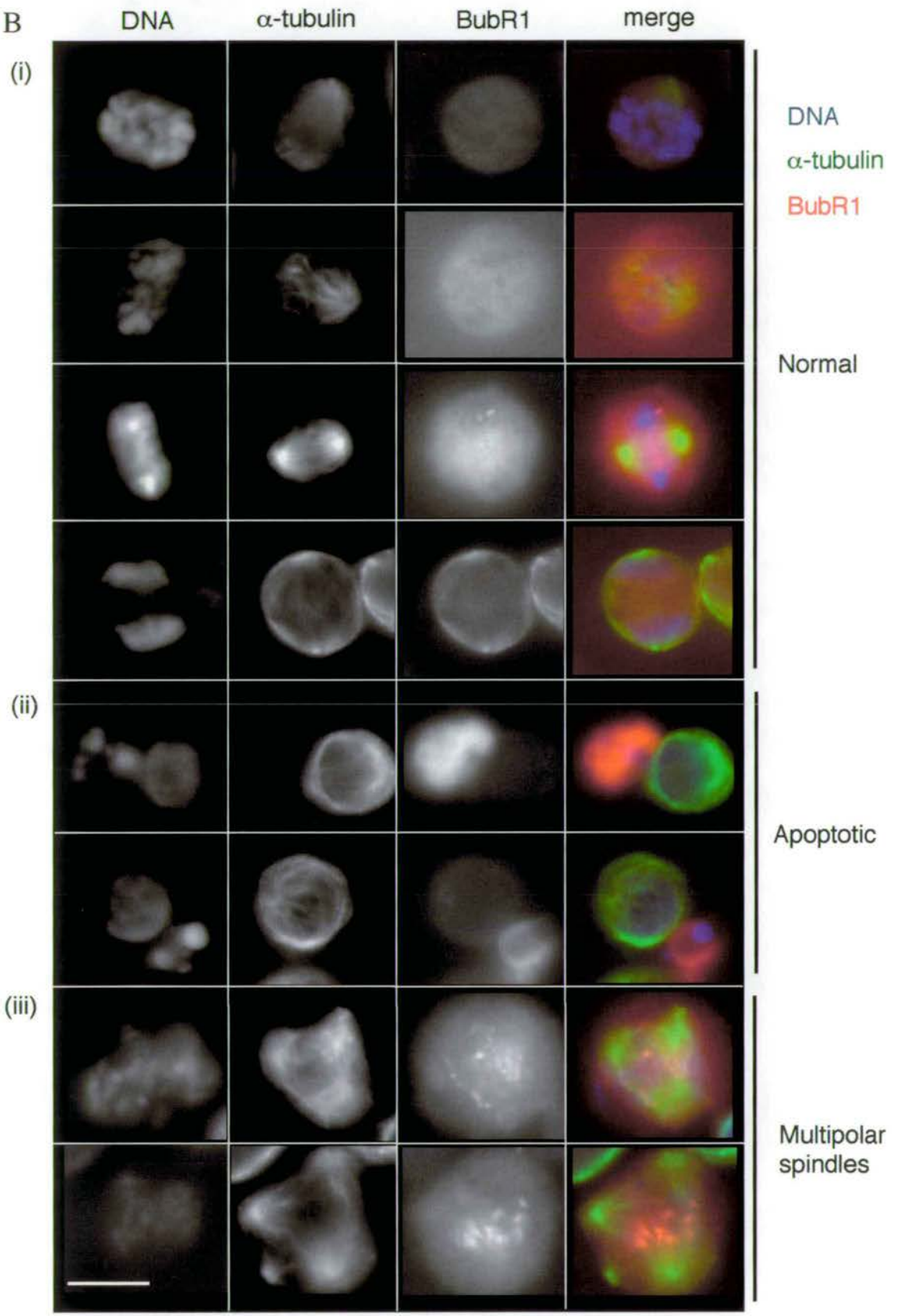

Figure 4.10 continued. **B**, Heterozygotes expressing the rescue construct were fixed with paraformaldehyde and stained for BubR1 (red), alpha tubulin (green), DNA with DAPI (blue), scale bar is 10 μm.

One further experiment was attempted, in which both the rescue construct and the second allele targeting vector were transfected at the same time, in the hope that targeting and introduction of the rescue construct would occur simultaneously, thereby placing the rescue construct under positive selection pressure. In this case, however, it would be impossible to assess whether the rescue could be repressed until after a targeted cell line had been generated. This experiment was carried out in two independent +/- cell lines. However, no colonies were obtained.

4.2.6 BubR1 is cleaved in DT40 cells when apoptosis is induced

Upon further investigation of the apoptotic cells apparently expressing high levels of BubR1 it was noticed that wild type DT40 cells in some stages of apoptosis also appear to stain brightly with this antibody, as shown in Figure 4.11A. There are several possible explanations for this. For example, the secondary antibody used might stain apoptotic cells. However, use of the secondary antibody anti-rabbit Texas Red in the absence of primary antibody did not give this result. Another potential explanation is that the rabbit polyclonal serum might recognise a protein that is overexpressed in apoptotic cells. Alternatively, BubR1 might be upregulated in apoptotic cells. This could cast doubt on the hypothesis that overexpression of BubR1 causes apoptosis, since the apoptotic cells in a wild type culture also appeared to overexpress BubR1. In order to investigate this further, apoptosis was induced in DT40 cells using 10 μM etoposide for 1, 2, 3 or 4 hours. Cell extracts were then subjected to SDS-PAGE and immunoblotted with anti-BubR1. The results of this experiment, as shown in Figure 4.11B, reveal that BubR1 is apparently cleaved as DT40 cells undergo apoptosis. The cleavage product detected is approximately 80-90 kDa. It is worth noting that this cleavage occurs fairly early in the apoptotic progression, being complete by 3 hours after induction of apoptosis. It is unclear what happens to the protein at around 2 hours since neither the full-length protein nor the cleavage product was visible by immunoblot. It is possible that there are two cleavages: one, which is earlier and unstable; and another, which produces a stable product of around 80-90 kDa. It also appears that the levels of the protein increase as judged relative to the loading control. The loading control used in this experiment was alpha tubulin, however it can be seen from the blot in Figure 4.11B that the amount of this protein was not constant. This experiment was set up by splitting a population of cells into different wells of a six well plate and

then adding the etoposide at the appropriate time, and collecting all samples and preparing them for SDS-PAGE at the same time. Since the starting culture was spilt between different wells, it is unlikely that this much variation would occur. However, it must also be taken into account that the control population was growing over the course of the experiment whilst in other cells apoptosis was being induced. Also, when apoptosis is induced, a large number of cellular proteins are cleaved and degraded (Earnshaw *et al.*, 1999). It is possible to see from the immunofluorescence of apoptotic cells, that alpha tubulin is degraded or destabilised, Figure 4.10. This protein therefore may not be the ideal loading control for an experiment such as this. However, it was evident from this experiment that there is more BubR1 cleavage product present at the end of the experiment than there was intact BubR1 at the beginning.

A further question was whether BubR1 is cleaved in this manner once the checkpoint has been satisfied and cells progress into anaphase. In order to investigate this, DT40 cells were blocked using nocodazole (0.5 μg/ml) for 3 hours. Nocodazole is a microtubule depolymerising drug and was used rather than colcemid because it is more readily reversible by washing it out of the cells. The drug was then removed from the cells by washing twice in warm medium, and cells were allowed to release into anaphase. Time points were collected as indicated in Figure 4.12 and samples prepared for SDS-PAGE. In addition, at the 1 and 2 hour time points, cells were fixed and stained with DAPI to check for mitotic progression after release. At the 1 hour time point, 16% of cells were in mitosis, and 22% of these were in anaphase. At the 2 hour time point only 1% of cells were mitotic, but 100% of these were in anaphase. This indicates that the cells were released from the block and progressed through anaphase. The results of this experiment showed that BubR1 was not cleaved as DT40 cells were released from a nocodazole block. In a manner similar to treatment with colcemid and taxol, an upper phosphorylated form of BubR1 was detected when cells were treated with this drug, presumably because the spindle assembly checkpoint was activated. The membrane was then blotted with alpha-tubulin as a loading control and it can be seen that at later time point, when less BubR1 was present, the level of tubulin remained constant. This indicates that the amount of BubR1 was decreasing in the cells as they released from nocodazole arrest and exited mitosis.

Figure 4.11

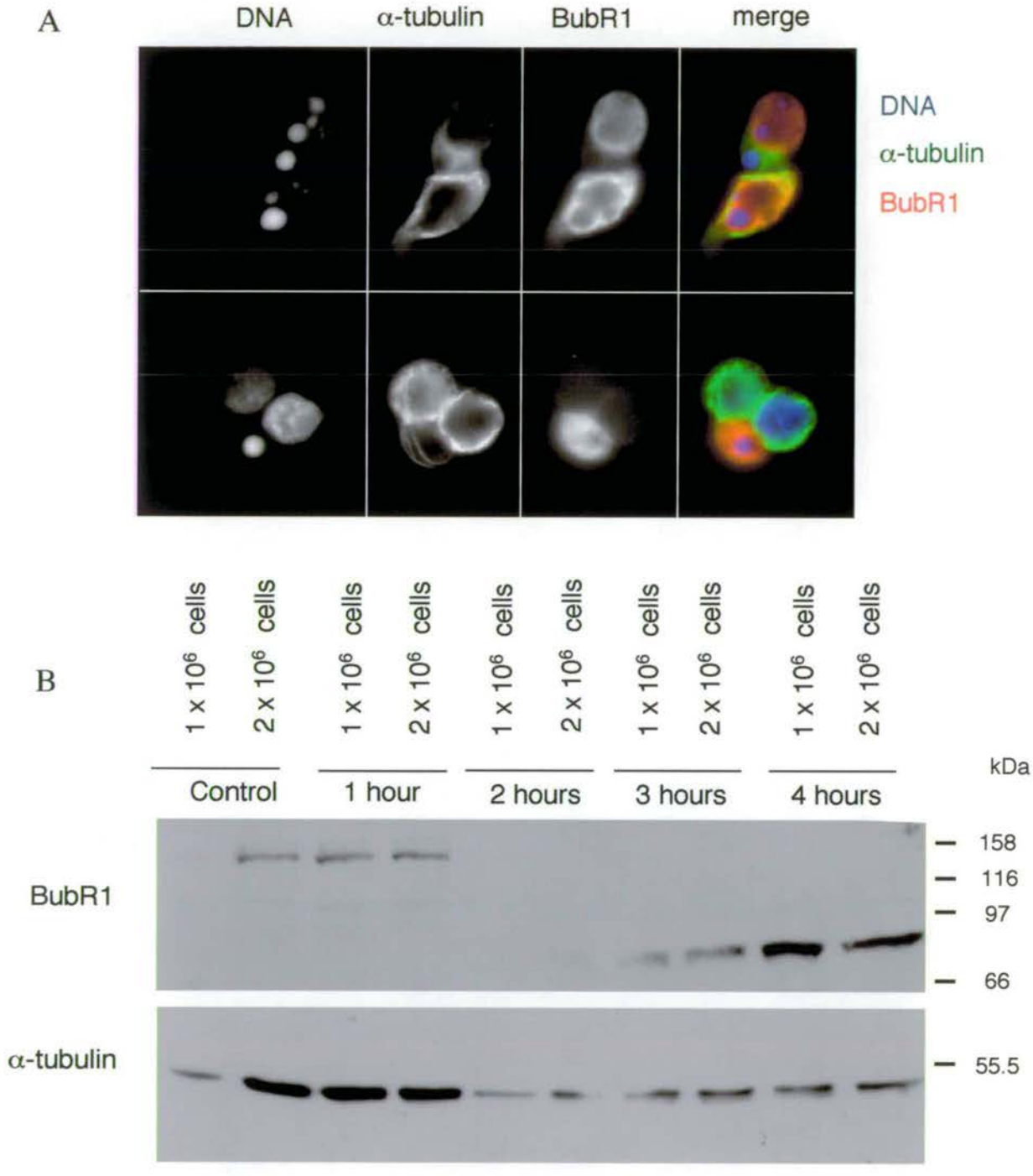

Figure 4.11 BubR1 is cleaved in DT40 cells after treatment with etoposide. **A,** Immunofluorescence of wild type DT40 cells stained with anti-BubR1 (red), alpha-tubulin (green) and DNA with DAPI (blue), scale bar is 10 μm. It can be clearly seen that apoptotic cells stain brightly for BubR1. **B,** DT40 cells were treated with 10 μM etoposide for the number of hours shown and then extracts from the number of cells indicated were subjected to 10% SDS-PAGE and transferred to nitrocellulose membrane. The membrane was blotted for BubR1 (above) and alpha-tubulin (below) as a loading control.

Figure 4.12

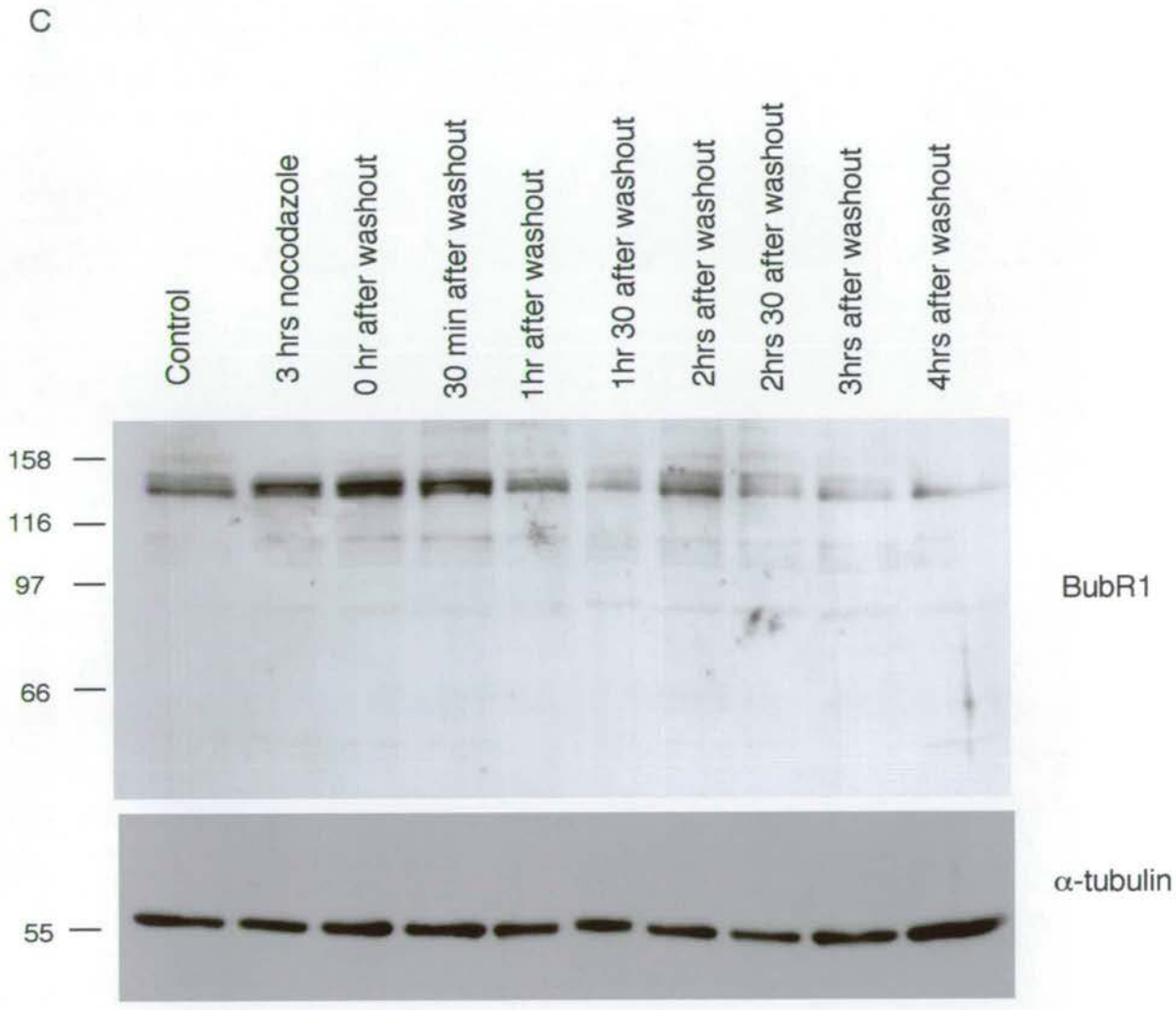

Figure 4.12 BubR1 is not cleaved after nocodazole block and release into anaphase. DT40 cells were treated with nocodazole for 3 hours (0.5 μg/ml), this was then washed out and cells released for the time shown. Cell extrracts were subjected to 10% SDS-PAGE and immunoblotted with anti-BubR1(above), and the loading control alpha tubulin (below). Signal was detected using ECL.

4.3 Discussion

4.3.1 Screening genomic library for BubR1 phage.

Screening of the λ Fix II DT40 genomic library resulted in the identification of phage 3B3, which contains a 5′ portion of the *BubR1* locus. Unfortunately this did not contain the entire genomic region and only contained a small portion upstream of the ATG. This limited the possibility of knocking out the entire ORF, or of deleting the ATG. The final targeting vector constructed, KOV2 will leave 375 bp of cDNA, which could potentially produce a small fragment of 125 amino acids of the very N-terminus of the protein. However, it is suspected that this product will not be made, since a small, unpolyadenylated mRNA will be generated and it is likely that this will be unstable and degraded. There is also the possibility that this fragment could be generated and have a dominant effect. In order to assess this, an antibody could be generated to this portion of the protein. Attempts were made to do this and although the fragment was cloned with a N-terminal 6xHis tag the fragment did not express well and I was unable to purify it over nickel agarose beads.

Another way to avoid this problem would be to find a phage with more sequence in the 5′ region of the gene and generate targeting vectors that would remove the ATG. For this reason, the library was screened a second time, this time using a probe derived from the most 5′ 400 bp of phage 3B3. In this case, two positive phage were identified, however restriction analysis showed that these were identical to phage 3B3. It was therefore concluded that no other phage exist in the library with a more 5′ region of BubR1. To solve this problem a new library would have to be generated and due to time limitations this was not possible.

4.3.2 Construction of Targeting Vectors

The main problem encountered in the construction of targeting vectors was that the majority of the phage sequence was unknown. The 3′ arm was fairly straightforward to clone since a convenient 5 kb portion of the 3′ end of the phage was subcloned into pBluescript. In order to orientate this fragment, partial sequencing of the ends was carried out. Fortunately this identified exons, allowing the 5′ and 3′ ends of this fragment to be defined. This subcloned fragment was then used as the basis of the 3′ targeting arm and 3′ external probe. Cloning a suitable 5′ arm was more problematic, and in this case a PCR

approach was undertaken. However, the problem was that the genomic sequence, and in particular the size of the introns was unknown. Several primers were designed to positions likely to be the start of exons based on the known rule that introns begin with GU and end in AG, and PCR fragments were generated. In the first instance, a fragment of 1.6 kb was cloned and used to construct a 5′ targeting arm. However, it was subsequently found that this was too short a length of homology to target a genomic region of around 10 kb. A longer 3 kb 5′ arm was generated by PCR and this was the basis of the KOV2 vector, which was able to target the locus. A potential way to overcome these cloning problems would be to have the phage entirely sequenced. In fact this strategy has been adopted within the Laboratory, for a number of genes, which have been successfully disrupted ((Samejima *et al.*, 2001) N. Korfali, personal communication). The approach allows the 5′ and 3′ arms to either be cloned by restriction digest directly from the phage, or PCR fragments to be generated with restriction sites on the end for even more convenient cloning. This approach can save time in the construction of the vectors. In addition, because the screening strategy must be determined by mapping the locus, this is much easier if the sequence of the phage is available.

4.3.3 Generation of BubR1 +/- DT40 cells

The main problem encountered in the generation of +/- cells was the total length of homology used. When this was increased from 4.6 kb to 6 kb, targeting events occurred. As mentioned above, cloning of longer arms can be made easier if the sequence of the entire phage is available. The efficiency of targeting may be increased even further if this length is increased. For example, it is known that the ovalbumin locus can be targeted at an efficiency of 80% using a vector with a total of 8 kb, although this is a disruption rather than a replacement (Buerstedde & Takeda, 1991). The targeting efficiencies with the vectors were zero for Bsr, 3% for HisD, 1% for Hyg and 6% for Puro. These are relatively low compared to what is usually expected for DT40 cells, which may be explained by the size of the region being removed. In order to increase the targeting efficiency the size of the region to be deleted could be decreased. Simply by the generation of a construct which disrupts a gene with a resistance marker, targeting efficiencies can be increased (P. Vagnarelli, personal communication). If the targeting of this locus was to be started again it would certainly be worth considering an approach

which either disrupted the open reading frame or removed only a small portion of the 5' end.

Three heterozygous cell lines were analysed, 511, 812 and 821. These were investigated by immunofluorescence and found to divide normally and have normal BubR1 kinetochore localisation. In addition the growth rate of these cells was calculated and although this varied from 6.9 hours in wild type cells to 9.5 hours for +/- 511 cells this was within the normal range for DT40 cells. To address the question as to whether BubR1 is haploinsufficient in the +/- cells, the checkpoint activity was assessed following exposure of the cells to the drugs taxol or colcemid. In both cases, the cells arrested in mitosis with BubR1 at the kinetochores. In addition, an upper, presumably phosphorylated, band was detected by immunoblot after treatment with these drugs. In conclusion, the spindle assembly checkpoint appears to be active in the +/- cells although the BubR1 protein levels are reduced.

4.3.4 Generation of +/- cells expressing rescue construct

One of the biggest problems faced in this project was the expression of BubR1 in DT40 cells. It is possible that the overexpression of BubR1 was toxic to the cells, which in turn selected against cells expressing it. Problems with heterogeneous levels of expression, low numbers of cells actually expressing, and changes in expression levels with time in culture were all experienced. It was difficult to determine whether a cell overexpressing BubR1 was actually able to progress through the cell cycle, or whether the overexpression meant that the cell was unable to turn off the spindle checkpoint in order to allow the APC to become inactivated and anaphase to progress. I was also unable to determine if the overexpressed protein was actually localising to the kinetochore. It was obvious from the immunoflourescence that the protein was being mis-expressed throughout the entire cell but this could have been due to the fact that the kinetochores were saturated and no more could bind. Other experiments with overexpression of full length BubR1 in chicken cells were also carried out. These include BubR1 with an HA-His tag at the C-terminus transfected into MSB1 cells and DT40 cells and EGFP-BubR1 transfected into DT40 cells. In the case of the MSB1 cells, as discussed in Chapter 3, this construct did not localise appropriately to the kinetochores as judged by immunostaining using the anti-HA antibody 12CA5. However, when this same construct was transfected into

DT40 cells it was possible to detect the recombinant protein at the kinetochores of prometaphase cells, although heterogeneous levels of expression and low percentages of cells expressing were again observed. In the case of the expression of EGFP-BubR1 this was not seen to localise to the kinetochores and similar problems with heterogeneous expression were encountered. One reason for this may be due to the tag, and in order to overcome this problem it may be necessary to tag the protein at the C-terminus. The advantage to using a tagged rescue construct is that expression levels can be determined on a cell by cell basis. However, the main and outstanding disadvantage is that the tag may interfere in some way with the function of the protein, which must be able to act normally to rescue the cells. In this study, it was decided that an untagged version of the protein was best and since the rescue construct was based on the same cDNA as the HA-His tagged version there is no reason to suspect that the rescue construct cannot localise properly.

There are several reports of human BubR1 being expressed in cells either as GFP (Chan *et al.*, 1998) or GST (Sudakin *et al.*, 2001; Taylor *et al.*, 2001) fusions, however these were transient transfections. Since it does not appear that any stable cell lines expressing human BubR1 have been reported, this may indicate that problems of expression have been encountered in this system also.

In order to try and overcome some of these problems with expression two experiments were carried out. The first of which was to keep the cells in the presence of doxycycline until a stable line had been generated, which had the potential to express and repress the rescue construct. Several such cell lines were generated, two of which were tested for targeting of the second allele, namely A12 and B13. As shown in Table 4.5, no targeted clones were generated, and the results of immunofluorescence showed that the population still expressed BubR1 at heterogeneous levels. In addition, the rescue construct, tTa and targeting vector was transfected into heterozygote cells at the same time in order to try and overcome the problems of expression. Unfortunately, no colonies were obtained from these transfections, which were carried out on two independent cell lines. One reason for this might be that random and homologous recombination may not be able to occur at the same time in the same cell. Another possibility is that the ratio of DNAs used was incorrect.

An ideal way to overcome difficulties encountered would be to express the protein from its endogenous promoter. This would mean that it is expressed at the correct levels and regulated correctly during the cell cycle. In order to achieve this the Tet operator would have to be knocked into the locus after the first allele had been targeted and a stable cell line generated. A cell line could then be generated which expressed BubR1 at appropriate levels throughout the cell cycle and could be repressed by the addition of doxycycline. This cell line would then be the basis of the attempts to target the second allele. The generation of such a cell line would require some knowledge of the promoter sequence and also the question would arise as to which transactivator should be used. Yet again, this approach relies on sequence of the 5´ region, which is not currently available. Unfortunately time constraints prevented this approach being adopted with this project.

In addition to the Tet system, an IRES approach could be adopted to improve the expression levels of chicken BubR1 in DT40 cells. The IRES or internal ribosome entry site allows the expression of a dicistronic transcript: the translation of two open reading frames from one mRNA. In this case the BubR1 cDNA and the hygromycin B resistance marker would hopefully force the cell to express the BubR1 cDNA in order for the cell to survive in medium containing the drug hygromycin B. The IRES is a 500 bp element derived from the picinovirus family, which allows the virus to express dicistronic transcripts in mammalian cells (Mountford *et al.*, 1994). Unfortunately, the cloning of the BubR1 cDNA and the IRES-Hyg construct into the pUHG 10.3 plasmid so that it would be under the control of the tet operator proved not to be possible in the time allowed. As with the previous rescue strategy, the 3' UTR of chicken BubR1 was modified in order that a difference in size could be detected by RT-PCR. In this case the polyadenylation signal was removed. Once this construct is cloned it could be used to generate a heterozygote cell line which can maintain a stable level of BubR1 expression.

A further method of generating a conditionally null cell line would be to utilise the Cre recombination system (Kuhn & Torres, 2002). This is a bacterial recombinase which very specifically recombines sequences at target sites called *loxP* sites. These are 32 bp long and can be inserted artificially into a desired sequence. In a cell line expressing *loxP* a particular DNA sequence can be removed by recombination. The way to use this system for DT40 would be to

first target *loxP* sites into an intron at the 5′ end of the gene, screen by Southern blotting to confirm this, then add Cre recombinase which would result in one *loxP* site remaining. Then, an intron further downstream would be targeted in a similar manner, recombination would be induced by Cre, and the resulting locus would have *loxP* sites in two introns. In this way, the locus could be disrupted by the addition of Cre to this cell line without the need for expression of a rescue construct. The second allele could be removed or disrupted in a more conventional manner. The disadvantages of this system are that Cre is not 100% efficient, and perhaps only 90% at best (Zheng *et al.*, 2000). The outcome would therefore be that in some cells the locus might not be removed, allowing for some expression of the gene. This may be acceptable if the phenotype is analysed on a cell by cell basis by immunofluorescence, however would cause problems for biochemical experiments where a whole population of cells is used.

4.3.5 BubR1 is cleaved in DT40 cells after the induction of apoptosis

Although targeted disruption of BubR1 has not been possible thus far, work on the expression of the protein has led to some interesting observations. The most striking of these being that BubR1 appears to be upregulated or stabilised in DT40 cells undergoing apoptosis as judged by immunofluorescence with the BubR1 antibody. In order to determine that this was not just an artefact of staining, the secondary antibody was used alone and no staining of apoptotic cells was observed. In order to further investigate this observation, apoptosis was induced in DT40 cells using etoposide. The cell extracts were then immunoblotted with BubR1, which revealed that the protein is cleaved to an 80-90 kDa species after 3 hours of etoposide treatment. It also appears that this product is stabilised, as there is more present at the end of the experiment than at the beginning. It could be speculated that this stabilisation is due to the fact that the cleaved product is lacking one or both of the putative degradation signals, the destruction box or KEN box.

One major family of proteins involved in the progression of apoptosis and protein cleavage is the caspases, which are cysteine/aspartase proteases. There are 14 known mammalian caspases, 7 of which have been implicated to have a role in apoptosis, and the consensus cleavage sites for these is known. The sequence of BubR1 has therefore been investigated to see if there are any

obvious caspase cleavage sites within it. This was carried out using the computer programme, (http://ca.expasy.org/tools/peptidecutter_enzymes.html) ExPASy Peptide-Cutter tool and by eye. Two sequences, which were close to the consensus, were identified. These are KEED at amino acid 357, and FEKD at position 785. The molecular weights of the fragments generated by cleavage at these sites has been calculated and found to be 41 kDa and 81 kDa for KEED and 88 kDa and 34 kDa for FEKD. Since the observed cleavage product is around 80 – 90 kDa, either of these sites may be theoretically possible. Also it must be noted that the antibody is generated to amino acids 653 – 778 so would recognise the larger fragment if it were to be generated by cleavage at either of these sites. However, it has been noted that neither of these sites is completely conserved in human BubR1, which may make them unlikely candidates.

Once a strong candidate site is identified this could be mutated by site directed mutagenesis in order to determine if this is a real cleavage site. In addition specific caspases could be tested in an *in vitro* assay. This would require the transcription and translation of BubR1 in order that it could be labelled with S^{35} methionine, then the addition of purified caspases in order to determine if they have the ability to cleave BubR1 *in vitro*. In addition, an immunoprecipitation experiment could be carried out using anti-BubR1 antibodies after the induction of apoptosis. Sequencing of the cleavage fragment would reveal whether the N and C-terminus of the protein is stabilised and may lead to the identification of the cleavage site.

It is known that caspases cleave a wide variety of substrates during apoptotic execution. These substrates include structural proteins, DNA repair proteins and kinases (for review see (Earnshaw *et al.*, 1999)). It is therefore interesting to speculate if the cleavage of BubR1 in apoptosis is important for apoptotic progression and whether or not the cleavage product may have any additional roles.

It is not clearly understood how the spindle assembly checkpoint is turned off after all microtubules are aligned in order to allow the cell to proceeds into anaphase. Proteins such as BubR1 may be regulated by phosphorylation or dephosphorylation or may be degraded. As discussed previously, BubR1 has both a putative destruction box and a putative KEN box. However, to date it has not been shown whether BubR1 is targeted for destruction by the APC.

I therefore investigated if BubR1 is cleaved in this manner after the spindle assembly checkpoint is inactivated and cells are released into anaphase. DT40 cells were blocked with nocodazole, which stimulated the checkpoint as judged by the presence of phosphorylated BubR1, and then released into anaphase. In this experiment the 80-90 kDa cleavage product was not observed, although the levels of the protein were quite dramatically reduced towards the end of the experiment as compared to the loading control. In order to further investigate this, cells could be blocked at different stages of the cell cycle. For example a double thymidine block can be used to arrest cell in S phase, mimosine to block in G1 or serum starvation to block at G_0/G1. This would therefore address the question as to if this cleavage occurs at other points during the cell cycle. It will also be interesting to determine the levels of expression at these different stages. In addition it will be interesting to try and determine how BubR1 is inactivated after the checkpoint is satisfied, if it is targeted for degradation by the APC/C or some other means. This could perhaps be done by mutation of the putative KEN and destruction box identified in chicken BubR1. In addition it will be interesting to determine if overexpression of BubR1 causes cells to go into apoptosis, and if this is related to a potential role of the BubR1 cleavage product in progression of the apoptotic cascade.

Chapter 5

A Screen to Identify Kinetochore Associated Proteins in *Xenopus laevis*

5.1 Introduction

The aim of the work described in this chapter was to identify and clone kinetochore components from the organism *Xenopus laevis*. The reason for choosing this organism is that an extract made from the unfertilised eggs is an ideal tool for the biochemist. These eggs are very large, 1 mm in diameter, and contain stockpiles of proteins required by the egg, once fertilised, in order that it can undergo rapid, synchronous cell divisions as the embryo starts to develop. Manipulation of this system has led to the identification of a number of complexes required for mitotic progression. These include, identification of the 8S (XCAP-C and XCAP-E) (Hirano & Mitchison, 1994) and 13S (XCAP-C and XCAP-E and XCAP-H (Barren)) condensin complexes (Hirano *et al.*, 1997). In addition, the cohesin complex was also identified in *Xenopus*, as a 9S complex composed of XSMC1 and XSMC3 and a 14S complex (Losada *et al.*, 1998). In this Laboratory the passenger complex of INCENP and Aurora-B was identified in *Xenopus* egg extracts (Adams *et al.*, 2000).

It was therefore decided that *Xenopus* might be an ideal system in which to attempt to identify both known and novel kinetochore components. The hypothesis that a pre-kinetochore complex may exist in the eggs, enabling identification of the components of the kinetochore was drawn up. In addition to the identification of novel complexes, the *Xenopus* system also lends itself to functional studies by both depletion and 'add back' experiments. For example, proteins can be specifically immunodepleted, and the effect on progression of the cell cycle assayed in this *in vitro* system. In addition, components can then be added back to ensure that the effect is specific and also other proteins can be added in excess to determine the order of components in a pathway.

Initial experiments focussed on the constitutive centromere protein CENP-C with efforts being made to clone the *Xenopus* orthologue. CENP-C is a DNA binding protein, which is localised to the centromere throughout the cell cycle. It is

specifically localised to the inner kinetochore plate and is generally believed to have a structural role within the kinetochore. Cloning of this gene was attempted in a number of ways including screening *Xenopus* extract using antibodies raised to CENP-C from different organisms, using degenerate PCR primers to try to amplify a fragment of the gene from a *Xenopus* cDNA library and screening the library using CENP-C probes from different organisms.

Attempts were also made to clone two other kinetochore associated proteins namely, CENP-H and Zwint. The *Xenopus* cDNA library was screened for these genes using human probes.

The focus of attention then changed to the identification of the spindle assembly checkpoint components Zw10 and Rod, which are localised to the kinetochore in *Drosophila* and vertebrate cells (Basto *et al.*, 2000) (Chan *et al.*, 2000). As discussed in Chapter 1, these proteins form a complex in *Drosophila* which is involved in the spindle checkpoint. These proteins have not been identified in yeast and their interactions, if any, with the Mad and Bub components of the checkpoint are presently unknown. For this reason it was interesting to investigate if these proteins are present in a complex in *Xenopus* and if so which other proteins they are associated with. No known functional domains have been identified in either Zw10 or Rod, so any information regarding these proteins in another organism will be potentially interesting.

5.2 Results

This work was carried out in collaboration with Ciaran Morrison, in particular the degenerate PCR for CENP-C and the library screen for CENP-C, CENP-H and hZwint. The cloning, expression and analysis of Zw10 and Rod was entirely my own work.

5.2.1 Screening Xenopus egg extracts with antibodies to centromere proteins

Since a large number of antibodies to centromere proteins from various organisms were available in the Laboratory, these were used in order to try to identify orthologues in *Xenopus*. The aim was to screen *Xenopus* egg extracts for these

proteins by immunoblotting. If any antibodies were found to cross-react, the plan was to immunoprecipitate the antigen from extract and analyse the proteins 'pulled down', and any other potentially interesting interactors, by mass spectrometry. Once a specific sequence was obtained this would allow for the generation of primers in order to amplify the sequence by PCR or RT-PCR and allow screening of a library. The cloned genes could then be expressed and purified to enable the generation of *Xenopus*-specific antibodies.

The antibodies used were, anti-human CENP-C, human broad spectrum Anti-Centromere Antibodies (ACA), anti-chicken CENP-C, anti-chicken BubR1 and anti-human Rod (Table 5.1). All antibodies were used at 1:500 dilution for the immunoblot, which was carried out as described in section 2.2.26. The results of this screen (Table 5.1), show that the majority of antibodies do not cross-react with *Xenopus* extract proteins to give bands of the appropriate size based on the predicted or apparent molecular weight, as shown in Table 5.2. However, a band was observed with the anti-chicken BubR1 antibody of around 100 kDa in *Xenopus* extract. Since this antibody recognises a protein of 140 kDa in chicken cells (as discussed in Chapter 3), it was decided that this might be a spurious band and no further investigation was carried out. It should be noted that the predicted molecular weight of *Xenopus* BubR1 is 117 kDa. Furthermore, one antibody to human CENP-C, designated 558, did show a band at approximately 90 kDa in *Xenopus* egg extracts (Figure 5.1). It should be noted that the predicted molecular weight of CENP-C is 100 kDa, but human, mouse and chicken CENP-C migrate at 140 kDa. Further experiments using this antibody included immunoprecipitation from extracts, immunoblotting of sucrose gradients and attempts at staining *Xenopus* tissue culture cells.

Table 5.1 Results of antibody screen

Antibody	Results
Human CENP-C- 350	No cross reactivity
Human CENP-C- 418	No cross reactivity
Human CENP-C- 420	No cross reactivity
Human CENP-C- 422	No cross reactivity
Human CENP-C- 554	No cross reactivity
Human CENP-C- 556	No cross reactivity
Human CENP-C- 558	Band of approximately 90 kDa
Chicken BubR1	Potential band of approximately 100 kDa
Chicken CENP-C	No cross reactivity
ACA - 1	No cross reactivity
ACA - 2	No cross reactivity
ACA - 3	No cross reactivity
Human Rod	No cross reactivity

Human Rod antibody was kindly given to me by F. Scaerou.

Table 5.2 Predicted and apparent molecular weight of proteins used in this study

Protein	Species	Predicted molecular weight (Daltons)	Apparent molecular weight (kDa)
BubR1	human	119,469	120
	chicken	122,226	140
	Xenopus	117,337	145
CENP-A	human	15,980	17
CENP-B	human	65,131	85
CENP-C	human	106,860	140
	chicken	97,177	140
CENP-H	human	28,462	34
	chicken	26,783	34
Rod	human	250,588	205
	Drosophila	240,581	200
Zw10	human	88,772	85
	chicken	85,598	Not published
	Drosophila	82,210	85
Zwint	human	31,175	43

Figure 5.1

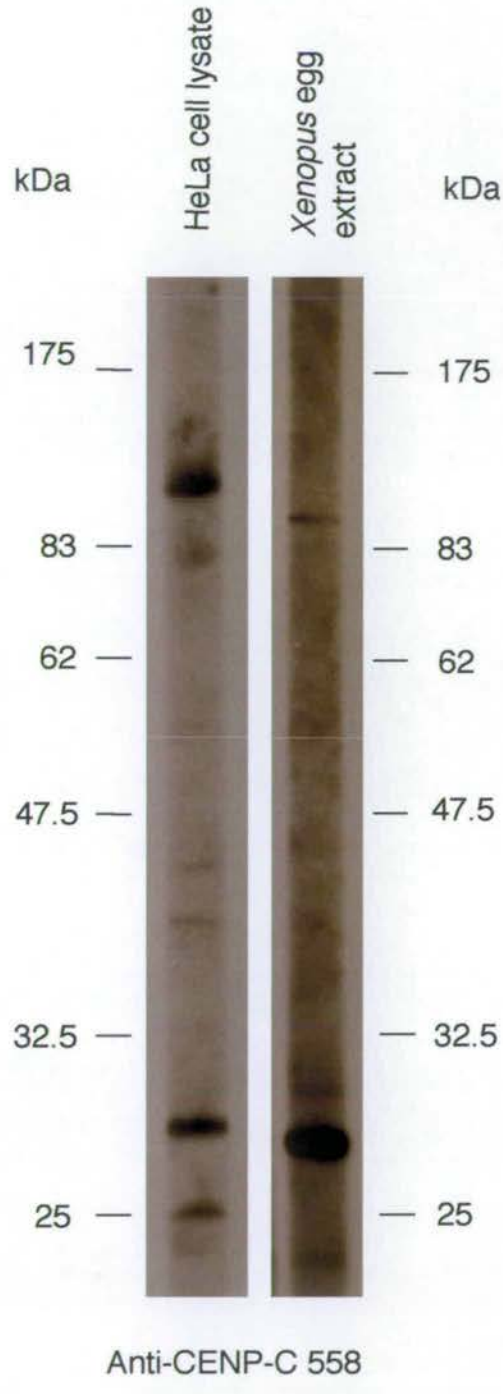

Figure 5.1 Anti-human CENP-C 558 recognises a protein of approximately 90 kDa in Xenopus egg extracts. Immunoblot of HeLa lysate and *Xenopus* egg extracts using anti-human CENP-C 558 and detected using protein-A I^{125}.

Immunoprecipitation experiments showed that a protein of around 90 kDa could be 'pulled down', from *Xenopus* extracts, by the human CENP-C antibody 558, as detected by immunoblot (Figure 5.2A). Silver staining of the immunoprecipitated proteins revealed a species at around 90 kDa. However, in addition to this there were many contaminating proteins of lower molecular weight also in this lane. A sucrose gradient of *Xenopus* egg extracts was immunoblotted with this antibody in order to investigate if the protein being recognised was indeed part of a complex, and if so of what size. Unfortunately the results of this experiment were somewhat ambiguous since the antibody recognised two proteins; one of around 80 kDa, and one of around 140 kDa (Figure 5.2B). The sucrose gradient showed that the 140 kDa protein was present in fractions 7-9, whereas the smaller 80 kDa protein was present in fractions 5-9. In order to give a rough estimation of the size of this complex, the gradient was also immunoblotted with anti-INCENP. INCENP is known to be present in an 11S complex with aurora-B in *Xenopus* egg extracts (Adams *et al.*, 2000). Both proteins recognised by anti-human 558 were present in a complex smaller than 11S. The protein of around 80 kDa was likely to be the species initially identified in *Xenopus* egg extracts as shown in Figure 5.1 and the potential immunoprecipitated protein as shown in Figure 5.2A. However, this protein was of lower molecular weight than the apparent molecular weight of human and chicken CENP-C. The sucrose gradient showed that anti-human 558 recognises two proteins that are partly present in the same size complex. The larger of these proteins, which is around 140 kDa, was similar in size to the apparent molecular weight of chicken and human CENP-C. It could therefore be hypothesised that this is indeed *Xenopus* CENP-C and that the smaller protein might be either a degradation product or an unrelated protein.

Figure 5.2

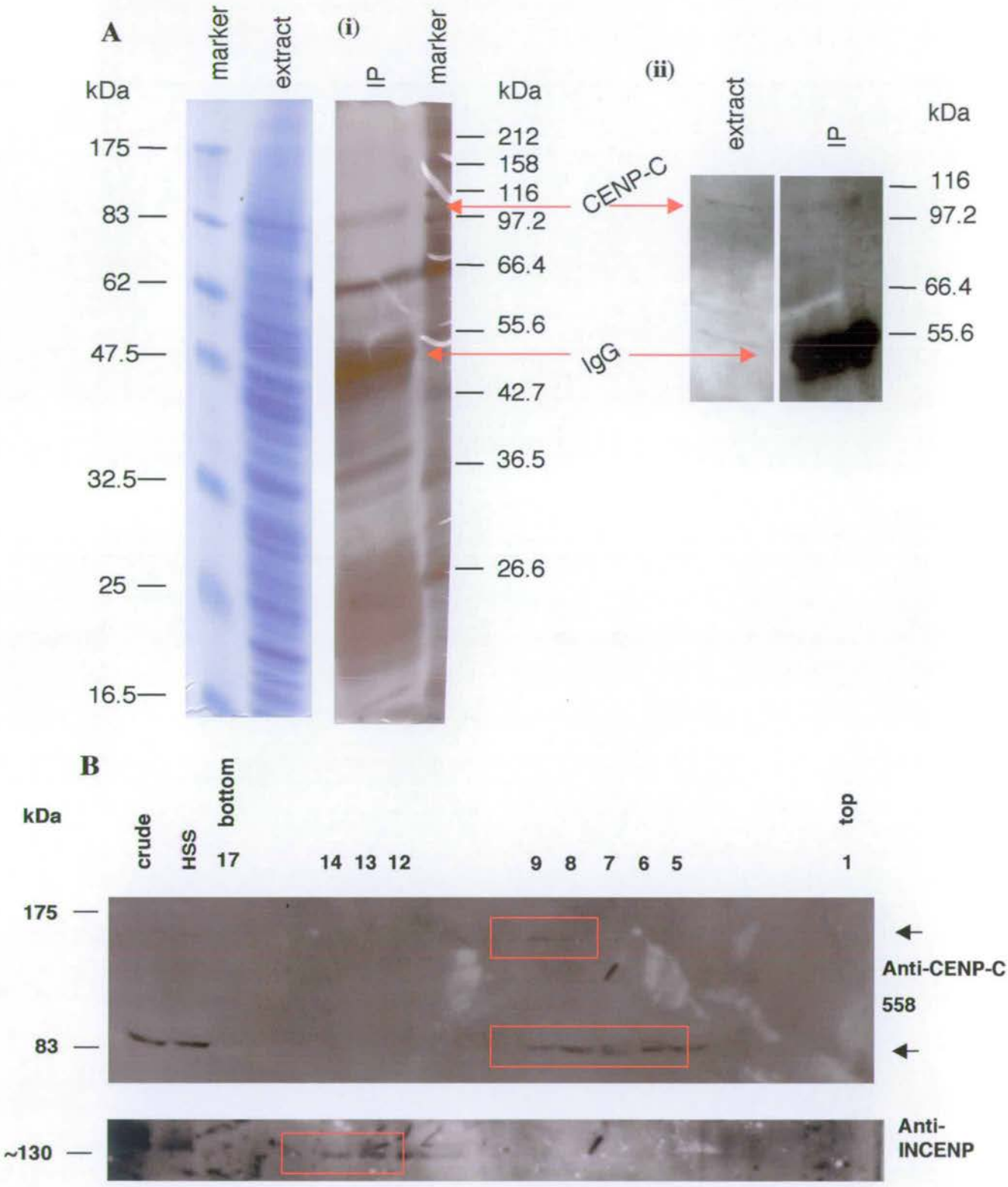

Figure 5.2, Immunoprecipitation from Xenopus egg extracts using anti-CENP-C 558. A, anti-CENP-C 558 was used in immunoprecipitation from *Xenopus* egg extracts, i) silver stained gel and ii) western blot, detected by ECL. **B,** 5-20% sucrose gradient of *Xenopus* high speed supernatant (HSS) run at 53,000 rpm for 5h30. The gradient was fractionated into 17 samples, run on a 7.5% SDS-Polyacrylamide gel and blotted with anti-CENP-C 558 (above) and anti-INCENP (below). Anti-CENP-C 558 recognises two proteins as indicated by the arrows, one of approximately 80-90 kDa and the other 130-140 kDa.

Since immunoblot experiments had resulted in confusion over the size of the potential CENP-C protein it was decided that immunofluorescence might be the best technique to use to address the question as to whether anti-CENP-C 558 did indeed cross react with *Xenopus* CENP-C. Several attempts were made to stain *Xenopus* A6 tissue culture cells using various different staining conditions, described in section 2.24.1and 2.24.2. The antibody 558 recognised the kinetochores of HeLa cells as shown in Figure 5.3A. However, although the A6 cells had an excellent morphology for immunofluorescence, as shown (Figure 5.3B), no specific staining was observed (not shown). Since I was unable to determine conclusively by immunofluorescence, immunoblot or immunoprecipitation whether 558 actually recognised *Xenopus* CENP-C, it was decided to adopt a different approach towards the identification of *Xenopus* CENP-C.

5.2.2 Using degenerate PCR to clone *Xenopus* CENP-C

It is known that vertebrate CENP-C shares at least two regions of homology with the *S. cerevisiae* protein Mif-2 (Brown, 1995). These homology blocks are in the C-terminal region of the protein. CENP-C has been identified in diverse species including, human, sheep, mouse, chicken, maize, *Arabidopsis*, tomato, *C. elegans, S. cerevisiae, S. pombe and Neurospora crassa.* However, surprisingly CENP-C has not been identified in *Drosophila.*

As shown in Table 5.3 a number of different primers were designed to the C-terminal homology regions (Figure 5.4, *Xenopus* sequence added since it has been recently identified and placed in the database). Initially, primers 1-6 were designed to the sequences 1, 2 and 3 as indicated. Unfortunately, no PCR products were generated. Some of these primers were then replaced with primers containing the base inosine rather than the degenerate base N (7, 8 and 9). This modified nucleotide can bind to all four bases with varying affinities. In addition, primers 10 and 11, the published primers used by Fukagawa in cloning chicken CENP-C (Fukagawa & Brown, 1997), were obtained.

Figure 5.3

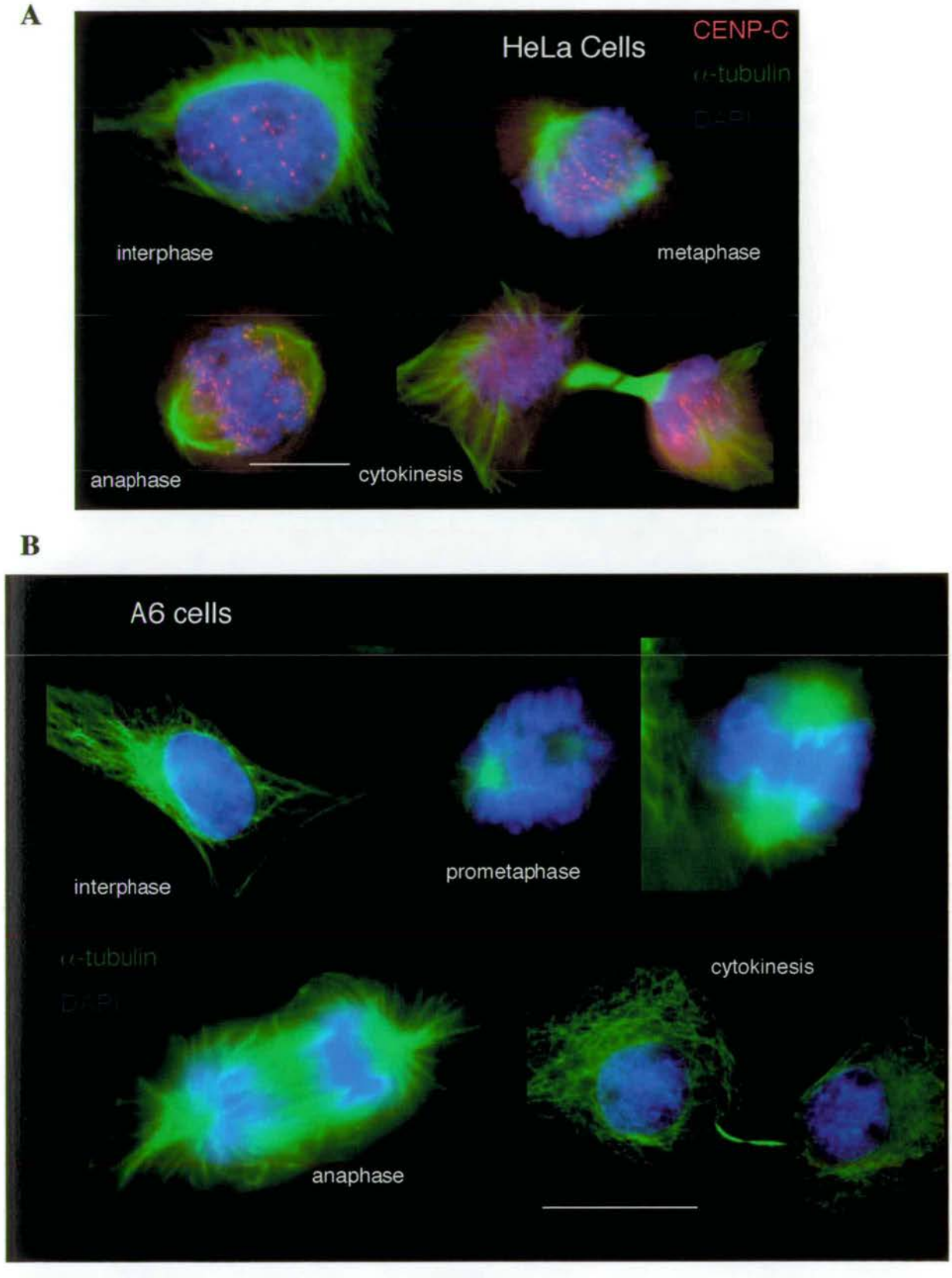

Figure 5.3 Immunofluorescence using anti-CENP-C 558 A, HeLa JW cells stained with anti-CENP-C 558 (red), alpha-tubulin (green) and DNA with DAPI (blue). **B,** *Xenopus* A6 cells stained for alpha tubulin (green) and DNA with DAPI (blue), scale bar is 10 μm.

Table 5.3 Degenerate primers used in attempts to clone Xenopus CENP-C

Primer	Sequence
1	CCNYTNMARTAYTGGMGNNNNGAR
2	YTCNNNNCKCCARTAYTKNARNGG
3	TTYTATGTNNNNMRNGGN
4	NCCNYKNNNNACATARAA
5	CCNGCNGGNAAYNNNTAYAAYATHNNNAAY
6	RTTNNNDATRTTRTANNNRTTNCCNGCNGG
7	CCHYTISARTAYTGGMG
8	CCIMRIIIIACRTRRAA
9	DATRTTRTAIIIRTTICCIGCDGG
10	CCRYTGGARTAYTGGMG
11	TTMCYBGAVGGVACRTAGAA

Nucleotide Code

B	C or G or T
D	A or G or T
H	A or C or T
K	G or T
M	A or C
N	A or C or G or T
R	A or G
S	C or G
V	A or C or G
Y	C or T
W	A or T
I	Inosine

The template used for this PCR screen was DNA prepared from the *Xenopus* oocyte cDNA library (Rebagliati *et al.*, 1985). Also RT-PCR was attempted using RNA prepared from *Xenopus* A6 cells. Various combinations of degenerate primers were used, as indicated in Figure 5.4, and many different conditions were attempted, including various temperatures ranging from 44°C – 54°C for the annealing reaction. In addition, the primer concentration was varied from 0.2 to 0.5 μM and the polymerases Roche Taq and TaKaRa Taq were both used. Additional controls to assess the PCR were used. For the library PCR, Zw10 specific primers were used as described in section 5.2.4. For the RT-PCR, both *Xenopus* specific primers were used to assess the PCR, and chicken RNA was prepared and used with chicken specific primers in order to asses the reverse transcription reaction. Unfortunately no specific bands were generated using any of these primers.

5.2.3 Screening a *Xenopus* cDNA library for CENP-C

As described in sections 5.2.1 and 5.2.2, attempts to identify *Xenopus* CENP-C using human antibodies and degenerate PCR both failed. It was therefore decided to adopt another approach to this problem, namely screening a *Xenopus* cDNA library. As discussed in the previous section, a number of sequences are available for CENP-C proteins and regions of homology have been identified between the *S. cerevisae* protein Mif2 and vertebrate CENP-C. As with the degenerate PCR, the screen was based on these similarity regions, block 2 and block 3.

Figure 5.4

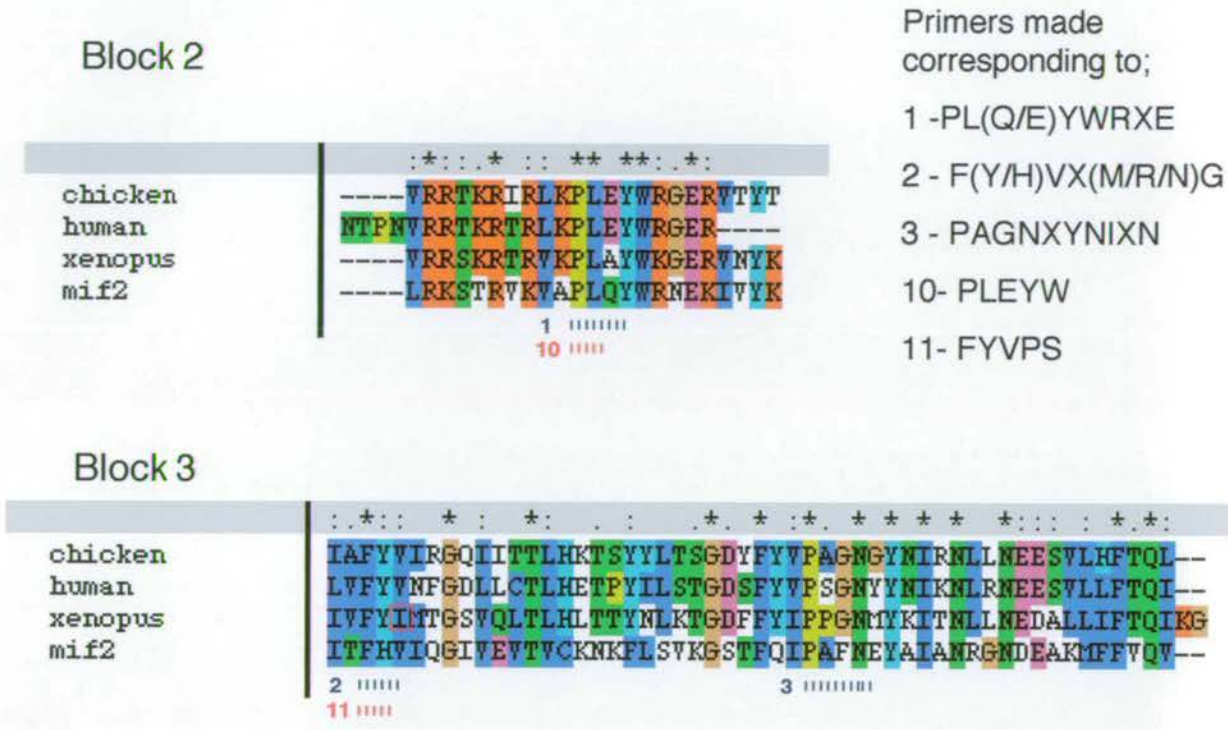

Figure 5.4 CENP-C and Mif2 homology domains. Clustal alignment of homology domains, block 2 and 3, identified between *S. cerevisae mif2* and vertebrate CENP-C (Brown, 1995). Sequences used to design primers for degenerate PCR are indicated. See Figure 3.2 for Clustal alignment symbol and colour explanation.

Since all the probes used were from species other than *Xenopus*, the library membranes were hybridised at the low stringency temperature of 42°C. The cDNA library used was generated from *X. laevis* oocytes and cloned into λgt10. It contains around 2 x 10^6 independent clones with an average insert size of 2.5 kb (Rebagliati *et al.*, 1985). Three different CENP-C probes were used to screen the library as detailed in Table 5.4.

Table 5.4 CENP-C probes used.

Probe	Details	Tertiary Screen	Clone identification
human CENP-C	nt 778-943 contains block 3	2 clones identified	syndecan-2
chicken CENP-C	nt 667-872 contains part of block 2 and block 3	3 clones identified	metavinculin
mif-2	full length	6 clones identified	Ran-GAP 1

Human and chicken CENP-C clones used were obtained from Ciaran Morrison, Mif-2 cDNA was a kind gift from Kevin Hardwick.

Plaques were purified through a tertiary screen and then inserts were amplified by PCR and cloned so they could be sequenced, thereby avoiding time-consuming DNA preparations from each phage. The method used to generate the template DNA is described in section 2.10.5. The λgt10 forward and reverse primers were used and the insert amplified and cloned into pGEM-T so that it could be sequenced. Again this approach failed to identify the *Xenopus* cDNA for CENP- C (Table 5.4). It is unknown why the genes shown in Table 5.4 were identified in the screen since no sequence homology could be found between these genes and CENP-C from any organism.

Since this screen also failed to identify *Xenopus* CENP-C, it was decided to focus attention on cloning other centromere-associated proteins, as described in the following sections. However, during the period of writing this Thesis, an EST from *Xenopus* (Sirulana) *tropicalis,* became available in the database. The sequence was deposited on 16/09/02, with the accession number AL894189, as shown in Appendix 2. Presently, there is an initiative to clone *Xenopus tropicalis* genes and sequence the genome, since this organism is being developed in order to make transgenic animals. *X. tropicalis* has advantages over *X. laevis* in that it is diploid and has a shorter generation time of 5 months as compared to 1-2 years. It has

slightly smaller eggs than *X. laevis* but these are still amenable to manipulation. Figure 5.4 shows the alignment between the C-termini of CENP-C from various species, including the *X. tropicalis* sequence, indicating the block 2 and block 3 homology regions. It should be noted that the published sequence appeared to be wrong in the most 3′ region. This was noticed because the level of homology deceased in this region. It seems that the published sequence is missing one base pair, and the sequence shown here has been adjusted accordingly, with the reading frame simply changing from +2 to +3 for the last 28 amino acids. Analysis of the *X. tropicalis* protein reveals that it is very highly conserved in block 2 and 3 relative to the vertebrate sequences and Mif2. This EST has been obtained by the Laboratory and in the future could be used to generate a *Xenopus*-specific antibody such that some of the questions and ideas postulated in the introduction to this chapter may be addressed.

5.2.4 Screening a *Xenopus* cDNA library for the centromere associated proteins CENP-H and Zwint

The *Xenopus* cDNA library was screened for the constitutive centromere protein CENP-H. CENP-H is known to be required for cell cycle progression. It is localised to the inner kinetochore plate, and is required for the targeting of CENP-C, but not CENP-A, to the kinetochore (Fukagawa *et al.*, 2001). To date this protein has only been identified in human, mouse and chicken. At the time of this work, the chicken sequence was not published, so the full length human cDNA was used as a probe. The probe was generated from the full length EST and again this was radiolabelled and hybridised with the membranes at the low stringency temperature of 42°C. The results of this screen identified 6 putative clones to the tertiary screen. The sequences contained within these phage were then amplified by PCR using the λgt10 primers. These PCR products were then cloned into pGEM-T and sequenced. Unfortunately, the sequences identified had no homology to vertebrate CENP-H.

As with CENP-C, the *Xenopus* database was recently searched for CENP-H. Again a clone had been newly deposited, with the accession number BF047824, as shown in Appendix 2. In this case, the sequence was from *Xenopus laevis*. CENP-H is highly conserved between human, chicken and *Xenopus,* with 42% similarity to human. As

with CENP-C, this EST has been obtained by the Laboratory to enable the generation of an antibody to *Xenopus* CENP-H.

The human centromere-associated protein hZwint was identified in a yeast two hybrid screen based on an interaction with Zw10 (Starr *et al.*, 2000). As discussed in Section 1.9, Zw10 is a checkpoint protein, which along with its binding partner, Rod, participates in the spindle assembly checkpoint in metazoans. In an approach similar to that used for CENP-C, the cDNA library was screened using the human full length sequence. This sequence was generated by RT-PCR, using primers HD19 and HD20, as shown in Table 2.5. The cDNA was radiolabelled and hybridised to the library at the low stringency temperature of 42°C. Unfortunately, although clones were obtained through to the level of the tertiary screen, upon sequencing, these were found not to be homologous to hZwint. As in the case of CENP-C and CENP-H, the *Xenopus* database was recently searched for potential Zwint sequences, and as with the other two genes, a putative *X. laevis* EST sequence was identified. This was deposited on 10/12/01 with the accession number BJ061344, as shown in Appendix 2.

5.2.5 Cloning and characterisation of *Xenopus* Zw10

Since attempts to clone *Xenopus* genes by degenerate PCR and low stringency library screening had failed, an alternative, more direct approach of using *Xenopus* specific sequences in order to clone kinetochore associated genes and raise antibodies was adopted. Short EST sequences were identified in the *Xenopus* database for the kinetochore associated proteins Zw10 and Rod. These proteins have been shown to be components of the spindle assembly checkpoint in both *Drosophila* (Basto *et al.*, 2000) and human cells, (Chan *et al.*, 2000).

An EST was identified in the database with homology to Zw10 with the accession number BE680749, (see Appendix 2). This was 460 bp in length and corresponded to the 3´ end of the cDNA. Primers were designed to this sequence and a PCR product was generated using the DNA prepared from the cDNA library. The PCR successfully generated a fragment of 177 bp when using one specific primer (HD12, Table 2.8) and one λgt10 primer. This fragment was cloned into pGEM-T and then excised in order to generate a probe for library screening. In this case, the

temperature used for hybridisation to the library was 65°C. Five positive phage were identified at the tertiary screen and these sequences were amplified using the λgt10 primers as described previously. Sequences were obtained from these phage with the longest clone being 1.3 kb, encoding 325 amino acids of *Xenopus* Zw10. The sequencing of these clones revealed that the database sequence was wrong, as it had an extra base A, which resulted in a frameshift of the last 23 amino acids. In order to clone the full length Zw10 cDNA, 5′ RACE was attempted. The full length human and *Drosophila* sequences are known and are 2337 bp and 2163 bp respectively, it was therefore predicted that the *Xenopus* sequence was missing around 1 kb of sequence. Unfortunately, attempts at cloning the remainder of the gene failed. This may be because the distance was too far for the 5′ RACE reaction to work. Another possibility would be to screen the library again with the most 5′ sequence now available. Since the project was focussed on generating antibodies rather than using the full length construct, it was decided not to proceed with this. The sequence of the longest clone, as compared to human and chicken sequence, is shown in Figure 5.5. It has been calculated that the *Xenopus* sequence is 77% identical to that of the human over this C-terminal portion of the protein. Figure 5.6 shows the comparison between the partial sequence of *Xenopus* Zw10 and the other known Zw10 proteins, human, chicken and *Drosophila*.

The initial Zw10 sequence generated by PCR was cloned into pGEM-T. This was then used as a template for PCR in order to create a GST fusion for antibody production. This PCR product was cloned into pGEX-4T-1. This construct encoded the final 50 amino acids of *Xenopus* Zw10 (as indicated in Figure 5.5), with an N-terminal GST tag. The construct was cloned and expressed, as described in section 2.2.27, resulting in a polypeptide of approximately 30 kDa (5 kDa for Zw10 peptide plus 25 kDa for GST), as shown in Figure 5.7A. This polypeptide was used as an antigen and injected into rabbits in order to generate polyclonal antibodies. The bleeds were tested on *Xenopus* extract to see if they recognised a protein of the size expected for Zw10. The human and *Drosophila* proteins migrate at 85 kDa. The second bleed from rabbit 1107 recognises a band of approximately 80 kDa in *Xenopus* extracts as shown in Figure 5.7B, which is not seen with the pre-immune serum. From now on, this serum will be referred to as anti-Zw10.

Figure 5.5

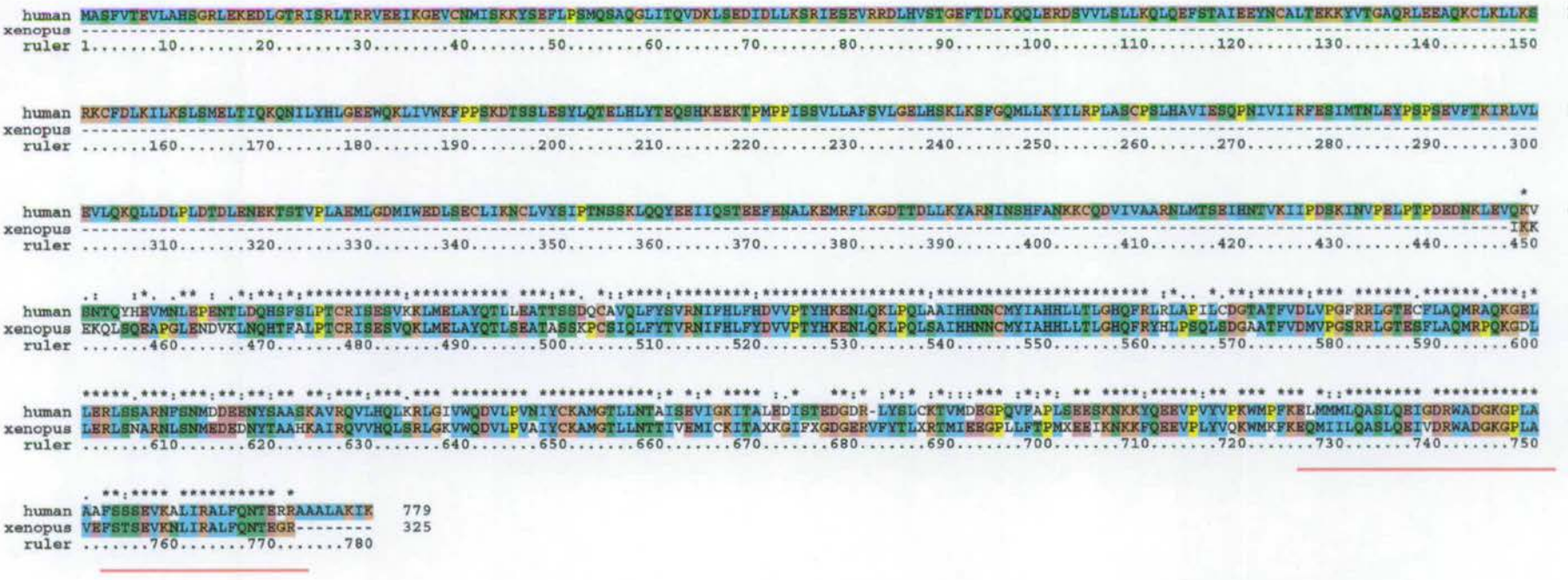

Figure 5.5 Human Zw10 versus Xenopus partial sequence. Clustal alignment of full length human Zw10 compared to the partial cloned sequence of *Xenopus* Zw10. This sequence is 90% similar and 73% identical over its length. The red bar indicates the region used as an antigen. Key to Clustal symbols, * - amino acid fully conserved, : strong group fully conserved, STA, NEQK, NHQK, NDEQ, QHRK, MILV, MIL, HY, FYW, . Weaker group fully conserved CSA, ATV, SAG, STNK, STAP, SGND, SNDEQK, NDEQHK, NEQHRK, FVLIM, HFY. Colouring of Clustal alignment Blue: AFILMVW, Purple: ED, Green: NQST, Yellow: P, Orange: G, Red:KR, Turquoise: YH, Salmon: C.

Figure 5.6

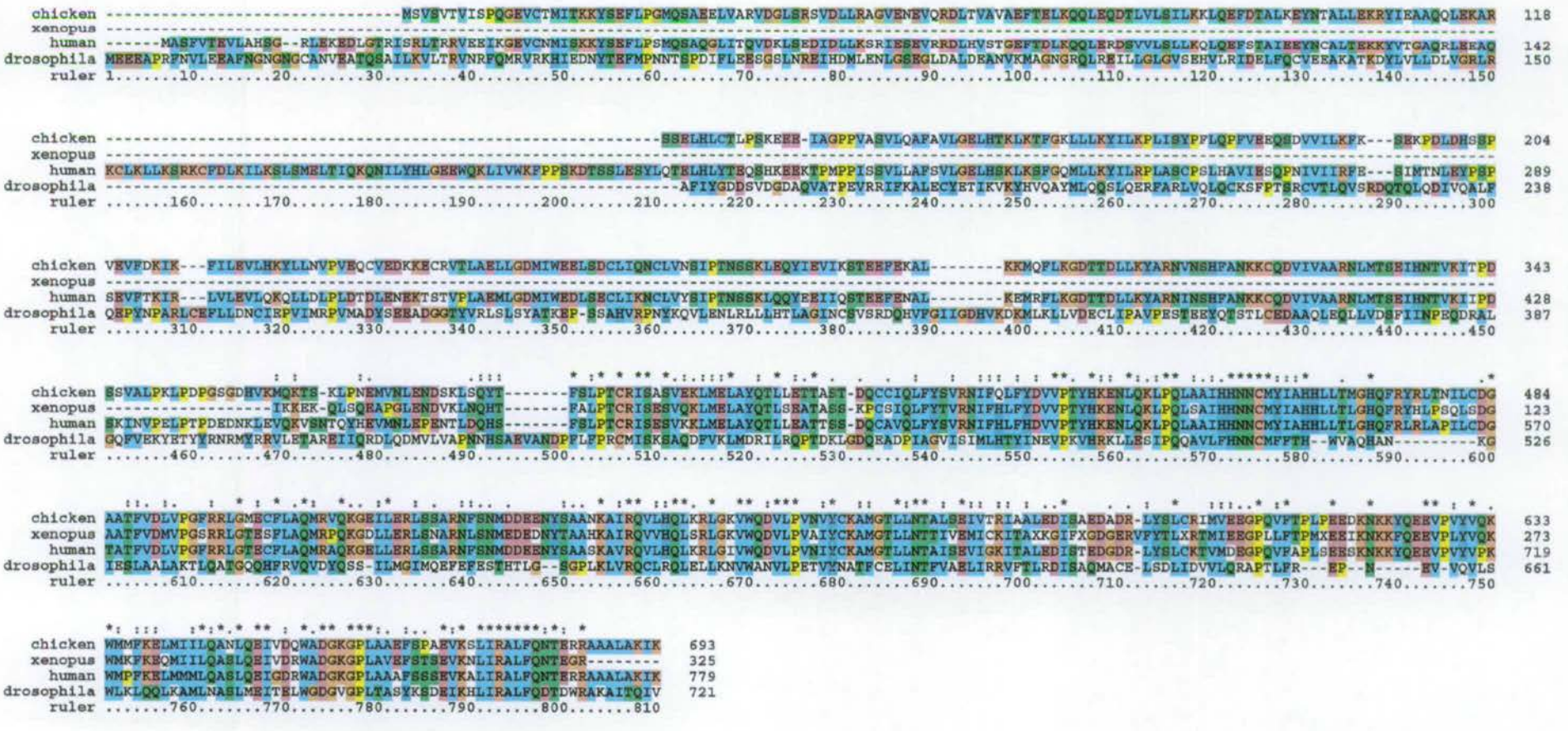

Figure 5.6 Zw10 sequences compared to Xenopus partial sequence. Clustal alignment of full length human, chicken and *Drosophila* Zw10 compared to the partial cloned sequence of *Xenopus* Zw10. Key to Clustal symbols, * - amino acid fully conserved, : strong group fully conserved, STA, NEQK, NHQK, NDEQ, QHRK, MILV, MIL, HY, FYW, . Weaker group fully conserved CSA, ATV, SAG, STNK, STAP, SGND, SNDEQK, NDEQHK, NEQHRK, FVLIM, HFY. Colouring of Clustal alignment Blue: AFILMVW, Purple: ED, Green: NQST, Yellow: P, Orange: G, Red:KR, Turquoise: YH, Salmon: C.

To further verify that this antibody was specific and recognised Zw10, it was used to stain the kinetochores of *Xenopus* A6 tissue culture cells. Cells were fixed using a number of different conditions. These included paraformaldehyde fixation and methanol fixation on whole cells treated with and without colcemid synchronisation (see Section 2.2.23.1 and 2.2.23.4). In addition, methods recommended to me (R.Adams and L. Campbell, Personal Communication) for fixation of *Xenopus* cells were attempted as described in Section 2.2.23.2. Unfortunately, no signal was seen with either the serum or affinity purified antibody under any of these conditions. Two control antibodies were used, 1186 which although raised against chicken INCENP recognises the *Xenopus* protein and *Xenopus* Bub3. Since staining whole cells was proving difficult attempts were also made at staining metaphase spreads. Two protocols were used, as described in section 2.2.23.3 and 2.2.23.6, with the later protocol giving better results. This method involves staining the cells before fixation. In this case the antibody clearly stained the kinetochores of the metaphase chromosomes, as shown in Figure 5.7C, and it was concluded that the serum did specifically recognise *Xenopus* Zw10. Unfortunately, it was not possible to determine the localisation of the protein throughout mitosis since only spreads could be stained.

Figure 5.7

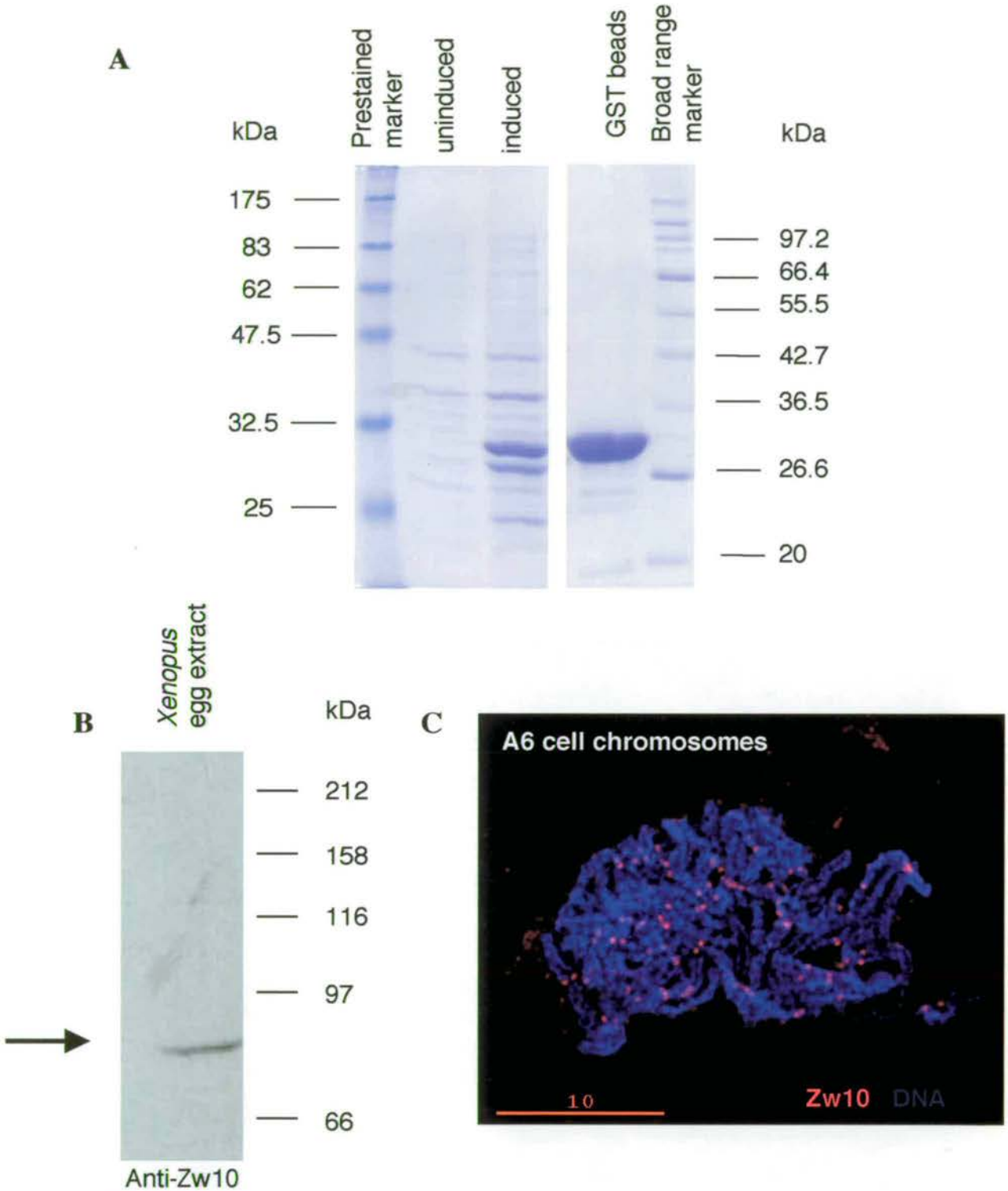

Figure 5.7. Anti-Xenopus Zw10 recognises a protein of approximately 80 kDa in egg extracts and stains the kinetochores of A6 cells. ***A,*** 12.5% SDS-Polyacrylamide gel showing induction of Zw10 peptide with 0.5 mM IPTG for 4 hours at 30°C and purification from glutathione agarose beads. This peptide was used as an antigen for antibody production. **B,** Western blot of *Xenopus* egg extracts showing that anti-*Xenopus* Zw10 recognises a band of approximately 80 kDa in egg extracts as indicated. **C,** *Xenopus* A6 chromosomes stained with anti-*Xenopus* Zw10 antibody (red) and DNA with DAPI (blue), scale bar is 10 μm.This image was captured using the DeltaVision deconvolution microscope with the help of Paola Vagnarelli.

In order to address the initial aims of this project, immunoprecipitation experiments were carried out using anti-Zw10 antibodies (see Section 2.32). In an attempt to precipitate entire complexes from the extract, conditions were kept non-denaturing to preserve the complexes in the native state. The results of two such immunoprecipitation experiments are shown in Figure 5.8. The antibody recognised Zw10 in the starting extract and this protein appeared to be immunoprecipitated as shown in lanes 4, 5, 6 and 7 of Figure 5.8A. The precipitated protein, however, may be slightly larger than that in the starting lane. This experiment was repeated using various bleeds from the two rabbits injected with antigen (1107 and 1109), in addition to the pre-immune serum. The results of this experiment (Figure 5.8B) again showed that the antibody recognised a protein, presumably Zw10 in the starting extract. However, in the lanes containing the immunoprecipitate a large band of around 80-90 kDa was recognised by the antibody in addition to the heavy chain IgG band at 55 kDa. Since this protein was also pulled down by the pre-immune sera (lanes 2 and 6) it is most likely that this was a non-specific contaminant, rather than a protein specifically bound by the anti-Zw10 antibody. It was therefore concluded that these experiments were unsuccessful, with the one possible explanation for the result shown in Figure 5.8 being due to the heavy chain IgG potentially generating a dimer. The protocol used did not involve the crosslinking of the antibody to the beads, so when they were boiled in sample buffer the antibody could fall off. In addition, the sample buffer, although containing β-mercaptethanol did not contain DTT, and therefore a possibility of antibody dimer formation remains. In conclusion, I was unable to immunoprecipitate Zw10 or any interacting proteins from *Xenopus* egg extracts using the antibodies generated, either serum or affinity purified.

Figure 5.8

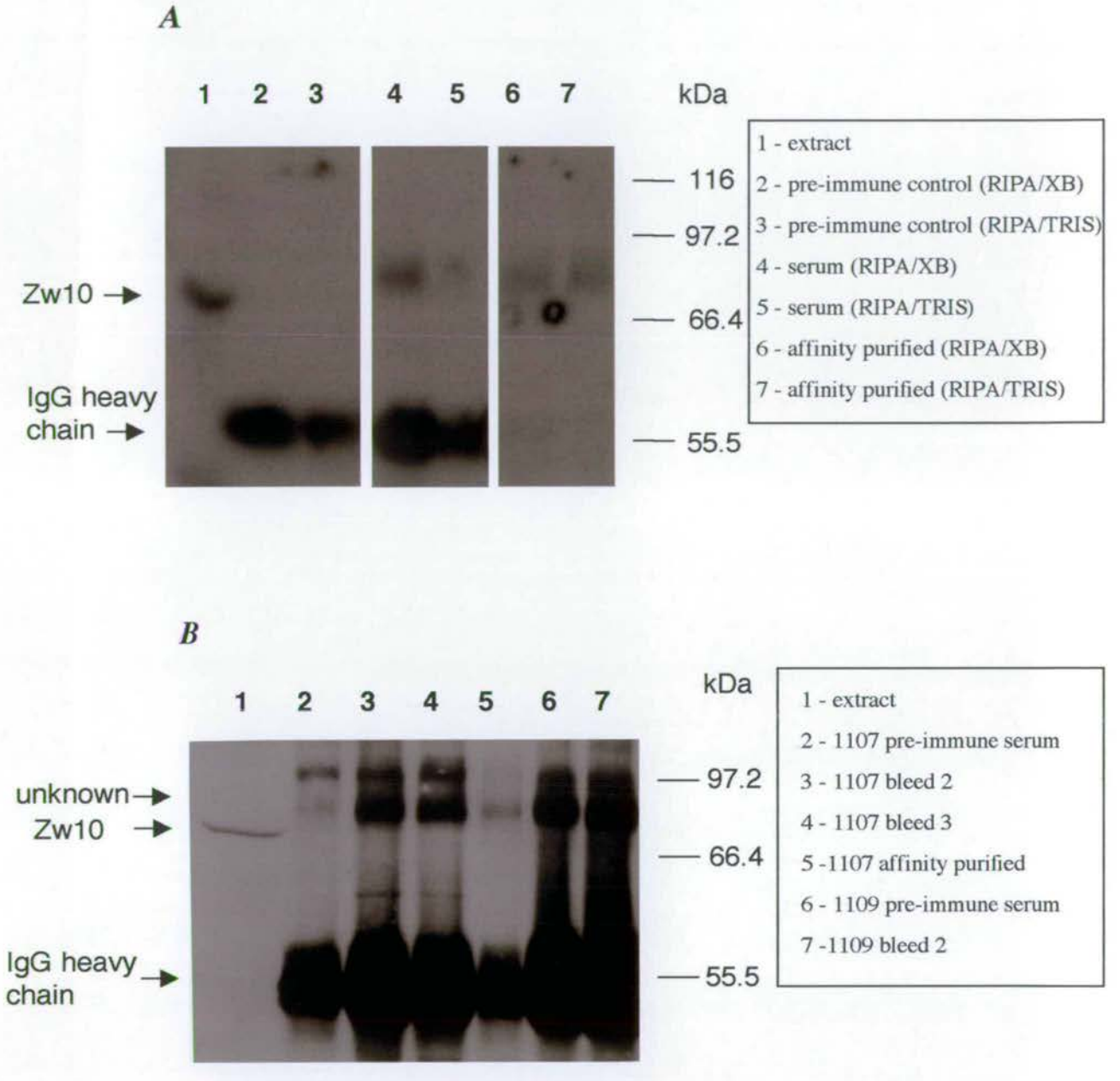

Figure 5.8. Immunoprecipitation from Xenopus egg extracts using anti-Zw10. **A,** The antibody (1107) was bound to beads then washed in RIPA buffer, the beads were then incubated with extract and then washed in either XB or TRIS buffer, as shown in table. The samples were subjected to SDS-PAGE, transferred to membrane, blotted with anti-Zw10 and the signal detection using Protein-A-I^{125}. **B,** Subsequent immunoprecipitation from *Xenopus* egg extracts using anti-Zw10 serum from two rabbits (1107 and 1109) in addition to the pre-immune serum. The conditions used were as in lane 4 above. Detection using ECL.

5.2.6 Cloning and characterisation of *Xenopus* Rod

In a manner very similar to that described above for Zw10, a short database sequence was available for the kinetochore-associated protein, Rod. This sequence allowed generation of antibodies to the protein for further analysis in *Xenopus*.

Two short EST sequences were present in the database with homology to the C-terminal region of human and *Drosophila* Rod, with the accession numbers BG233529 (1) and BG159891 (2) as shown in Appendix 2. Primers for PCR were designed to these regions and products generated (Figure 5.9A) using the DNA from the cDNA library as a template. These two products were cloned into pGEM-T. Unfortunately, one PCR product stretching from the most 5′ of EST 1 to the most 3′ of EST 2 could not be generated. However, since the two products were generated using the forward and reverse version of the same primer, the sequence could be pieced together. In an attempt to clone the full length cDNA the most 5′ available sequence, which was cloned into pGEM-T-XlRod5′, was isolated by restriction digest, radiolabelled and used as a probe to screen the cDNA library. Nine positive phage were identified to the tertiary screen, the DNA was then amplified by PCR and cloned into pGEM-T as described previously. These plasmids were sequenced revealing that 2.5 kb of *Xenopus* Rod cDNA had been cloned. This encoded the C-terminal 759 amino acids of the protein.

The full length cDNA of *Drosophila* and human Rod is 6627 bp and 6294 bp respectively. Since the longest clone identified was 2607 bp, this was still around 4 kb from full length, out with the range for 5′ RACE reactions. One possible way to clone this would be to screen the library again with the now most 5′ available sequence. However, since the aim of the project was to raise antibodies, it was decided not to screen again. The sequence alignment of the C-terminal third of the protein is compared with human Rod in Figure 5.9B. Over this region of the protein, *Xenopus* Rod is 54% identical to the human sequence.

Figure 5.9

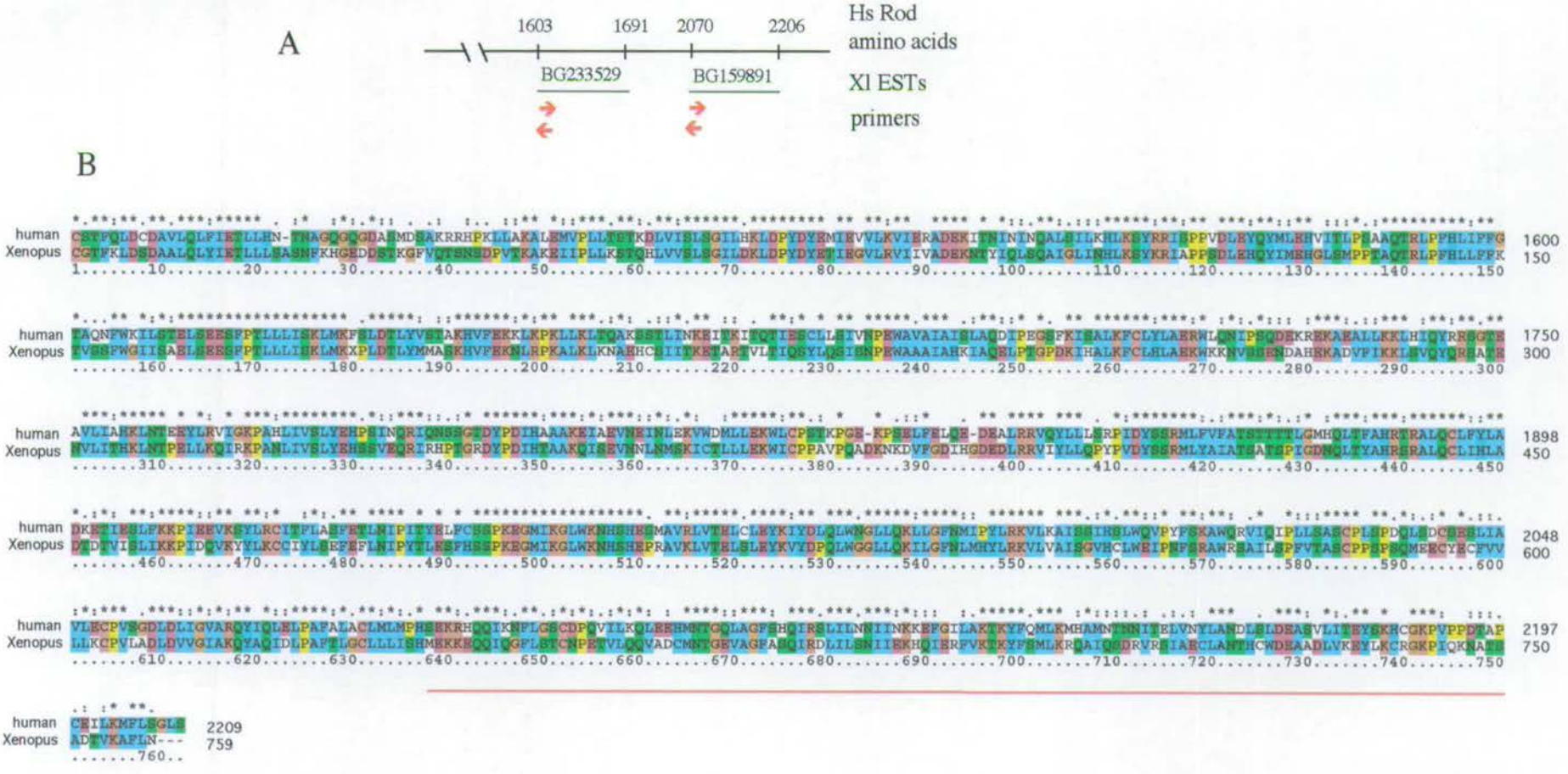

Figure 5.9 Rod sequences compared to Xenopus partial sequence. A, Diagram representing the *Xenopus* Rod EST sequences in the database and the primers used to amplify these sequences. **B,** Clustal alignment of partial sequence of human Rod compared to the partial cloned sequence of *Xenopus* Rod. The human sequence begins at amino acid 1451. The red bar indicates the region used as an antigen. Key to Clustal symbols, * - amino acid fully conserved, : strong group fully conserved, STA, NEQK, NHQK, NDEQ, QHRK, MILV, MIL, HY, FYW, . Weaker group fully conserved CSA, ATV, SAG, STNK, STAP, SGND, SNDEQK, NDEQHK, NEQHRK, FVLIM, HFY. Colouring of Clustal alignment Blue: AFILMVW, Purple: ED, Green: NQST, Yellow: P, Orange: G, Red:KR, Turquoise: YH, Salmon: C.

To generate antibodies to *Xenopus* Rod, PCR primers were designed to enable cloning of the last 126 amino acids of the protein with an N-terminal GST fusion. The PCR product was generated using pGEM-T XlRod3′ (see Table 2.7) as a template and cloned into pGEX-4T-1, using primers HD17 and HD18 as detailed in Table 2.8. This construct was expressed, and a polypeptide of approximately 40 kDa purified using glutathione agarose (as shown in Figure 5.10B). This corresponded to 14.3 kDa for the Rod peptide and 25 kDa for GST. This polypeptide was purified and used as an antigen to generate rabbit polyclonal antibodies. Rabbit serum was obtained and tested for activity on *Xenopus* egg extracts. After affinity purification the serum from rabbit UED6 recognised a protein of approximately 200 kDa (as shown in Figure 5.10C), which is not seen with the pre-immune serum. The size of human and *Drosophila* Rod is around 200-205 kDa. As in the case of Zw10, it was necessary to determine whether this serum was specific for *Xenopus* Rod. Immunofluorescence on *Xenopus* A6 cells was attempted using a number of different fixation and staining conditions as described for Zw10 in section 5.2.5, however these attempts failed to show any specific staining. The bleeds and affinity-purified antibodies were also tested, but none gave a positive signal. Finally in a manner similar to the experiments described for Zw10, immunoprecipitation was attempted using serum and affinity purified antibodies. However, this also proved to be unsuccessful.

Figure 5.10

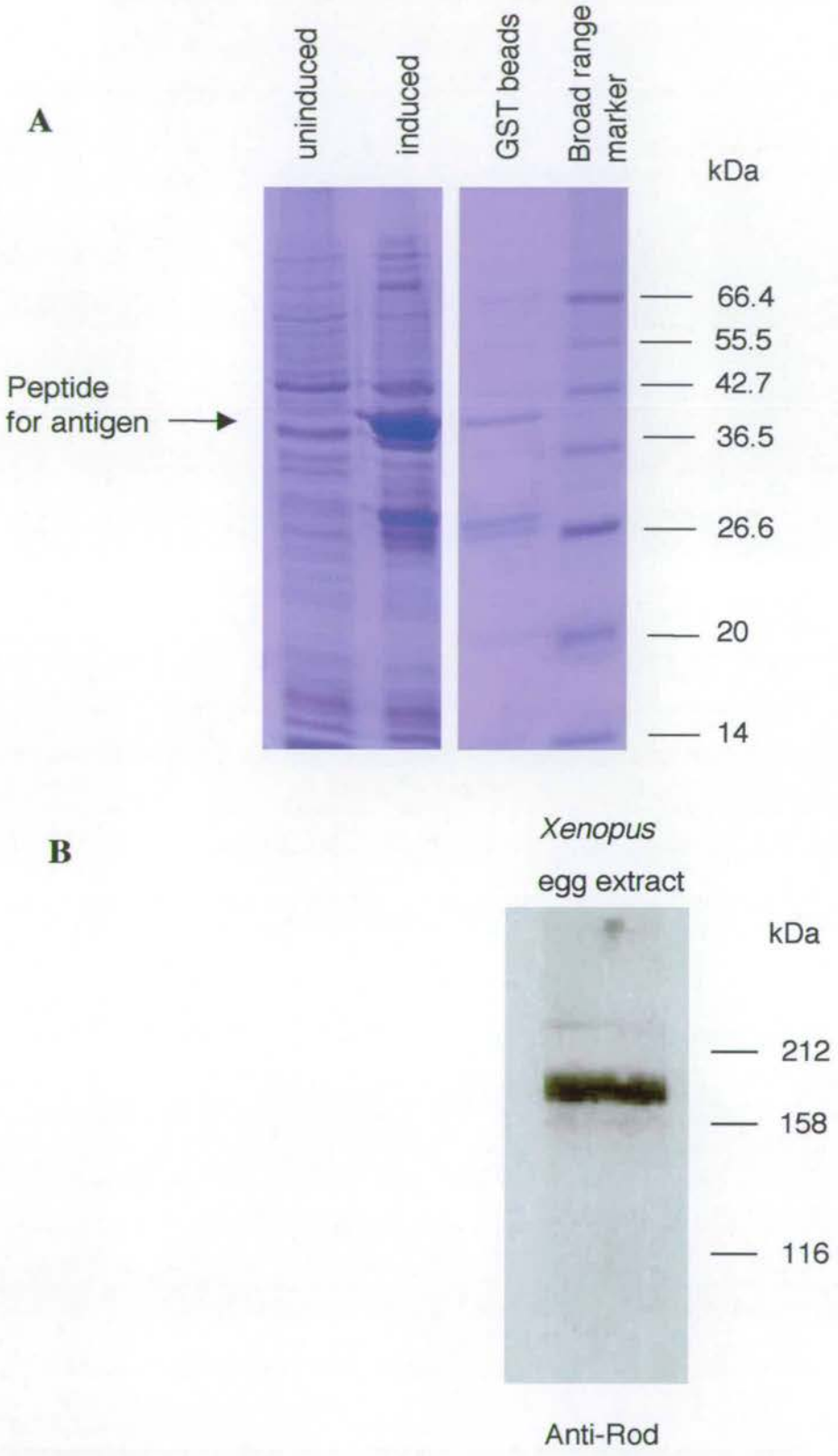

Figure 5.10 Generation of an antibody to Xenopus Rod. **A,** Rod peptide expression was induced with 0.1 mM IPTG for 3hrs 30mins at 30°C and purified over glutathione agarose, before being subjected to 12.5% SDS-PAGE. This purified peptide, as indicated, was used as an antigen for antibody production. **B,** *Xenopus* egg extracts blotted with anti-Rod antibody, detected using ECL.

5.2.7 Preliminary Investigation of the Zw10/Rod complex in *Xenopus* egg extracts

Since Zw10 and Rod have been reported in a complex in both *Drosophila* and human cells, it was of interest to determine whether this complex could be identified in *Xenopus* egg extracts. In *Drosophila,* this complex is approximately 19S, as judged by Superose 6 gel exclusion column (Scaerou *et al.*, 2001). To address this question in *Xenopus,* sucrose gradients were used to separate high speed supernatant (HSS) from egg extracts. As described in section 2.2.23, HSS was run on either 5-20% or 10-40% sucrose gradients. The fractions from each gradient were then run on a gel, transferred to membrane, and blotted with the antibody of interest. Initial experiments with the 5-20% gradient showed Zw10 at the bottom of the gradient, in a large complex (Figure 5.11A). Zw10 in this experiment is present in both the crude extract and HSS, which is the starting material of the experiment. The Zw10 antibody recognises a protein present in fractions 15, 16 and 17. This gradient was also blotted with an anti-INCENP antibody. As discussed earlier, INCENP is present in a complex of approximately 11S in *Xenopus* egg extracts (Adams *et al.*, 2000), so this was used as a control for the size of the complex. INCENP is present in fractions 12, 13 and 14, indicating that the Zw10 complex is larger than this. To determine more accurately the size of this complex, a 10-40% gradient was run for 4 hours. Zw10 is present in fractions 6, 7, 8, 9 and 10 (Figure 5.11B). This gradient was then probed with anti-Rod, which recognised a protein in fractions 7, 8, 9 and 10. As in 5.11A, this gradient was also blotted with a component of the INCENP complex, Aurora-B, which was found to be present in a number of fractions but with the greatest intensity at 6 and 7. The membrane was also blotted with anti-INCENP and it was possible to determine that the complex was in fractions 6 and 7 (not shown). In order to determine the size of this complex, standards were run on a parallel gradient as shown. These standards confirmed the size of the INCENP/aurora B complex as 11S and showed that the Zw10/Rod complex is larger than this. In conclusion, Zw10 and Rod are present in a complex of larger than 11S in *Xenopus* egg extracts and this complex is distinct from the INCENP/AuroraB complex.

Figure 5.11

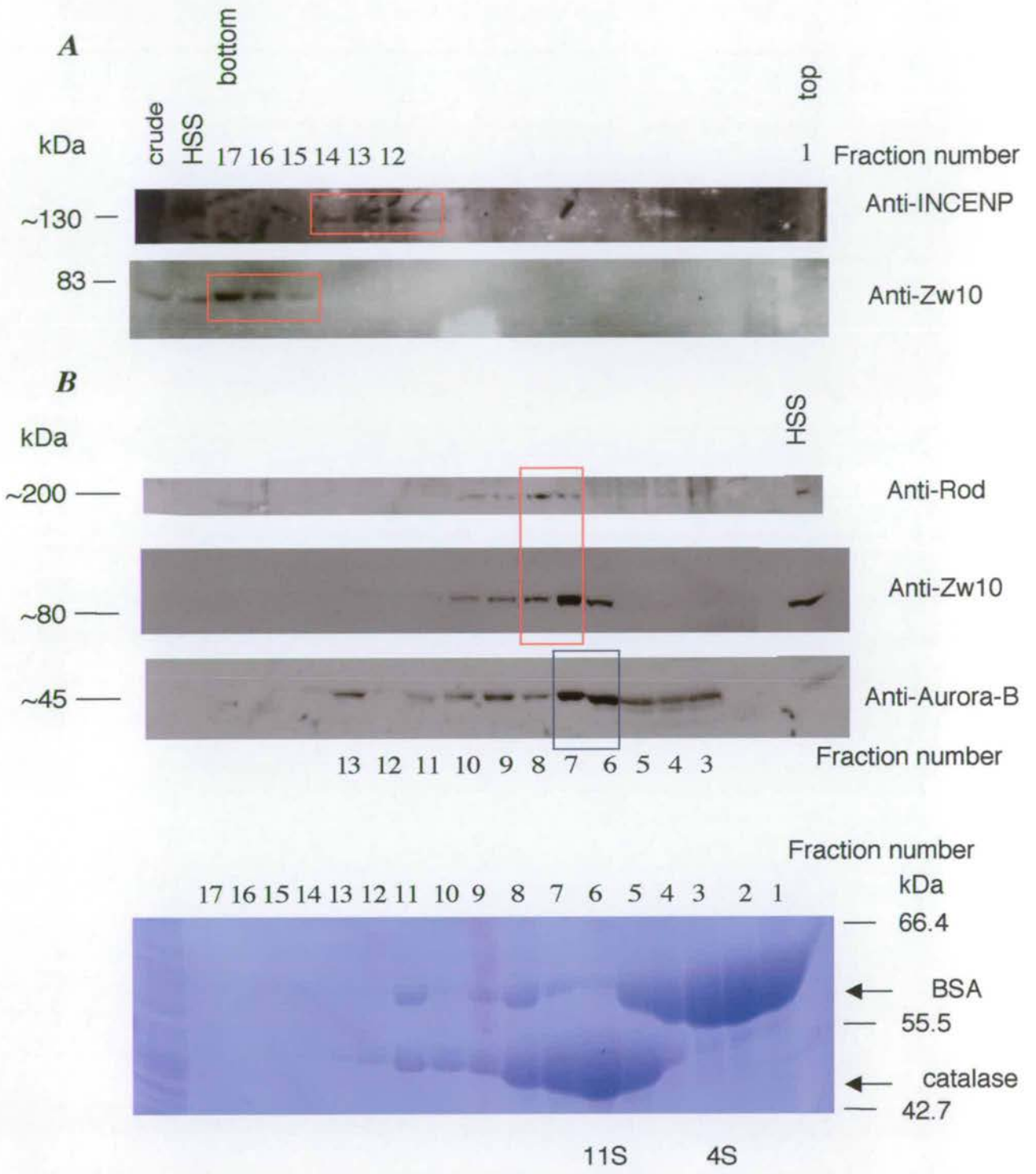

Figure 5.11 Zw10 and Rod are present in a complex of larger than 11S in Xenopus egg extracts. **A,** 5-20% sucrose gradient of *Xenopus* high speed supernatant (HSS) run at 53,000 rpm for 5h 30mins. The gradient was fractionated into 17 samples, run on a 7.5% SDS-PAGE and blotted with anti-Zw10 (below) and anti-INCENP (above). **B,** 10-40% sucrose gradient of *Xenopus* high speed supernatant (HSS) run at 53,000 rpm for 4 hours. The gradient was fractionated into 17 samples, run on a 7.5% SDS-Polyacrylamide and blotted with anti-Rod (top), anti-Zw10 (middle) and anti-Aurora-B (bottom). BSA and catalase standards were run on a parallel gradient and the fractions were stained with Coomassie blue.

5.3 Discussion

5.3.1 Attempts at cloning the *Xenopus* orthologue of CENP-C

A number of different approaches were attempted in order to clone *Xenopus* CENP-C, including antibody screening, degenerate PCR and low stringency library screening using cross species probes. Unfortunately, none of these attempts were successful. The screening of antibodies identified one human CENP-C antibody, which potentially cross-reacted with *Xenopus*. However, immunoprecipitation experiments were difficult to interpret and sucrose gradients revealed two different sized proteins being recognised by the antibody. These proteins were of approximately 80 kDa and 140 kDa. Although the predicted molecular weight of human CENP-C is just over 100 kDa it runs at 140 kDa on protein gels. It may, therefore be possible that the antibody did indeed recognise *Xenopus* CENP-C, which is around 140 kDa, as shown in the sucrose gradient, (Figure 5.2B). However, another protein or degradation product of around 90-100 kDa was also recognised by this antibody. Another possible experiment would be to immunoprecipitate from the fractions of the sucrose gradient. In order to determine conclusively if anti-human 558 did indeed recognise *Xenopus* CENP-C, this would have had to be shown either by immunofluorescence on *Xenopus* cells or immunoprecipitation, and sequencing by mass spectrometry. Unfortunately, neither immunoprecipitation experiments nor immunofluorescence were successful.

Since the CENP-C sequence was available from a number of diverse species, degenerate PCR primers were designed. The primers were based mainly on the amino acids conserved between the *S. cerevisae* protein Mif2, and the human and chicken sequences. The degenerate primers were designed to the blocks of homology as identified by Brown, (1995) and were based on the degenerate primers used by Fukagawa et al., 1997 to clone chicken CENP-C. Unfortunately attempts to generate PCR products using either the cDNA library as a template, or RT-PCR using *Xenopus* A6 cell RNA as a template, failed. In the case of both the RT-PCR and PCR from the library, primers to *Xenopus* Zw10 were used as a positive control. An additional control for the RT-PCR used RNA from chicken cells as a positive control and chicken specific primers. The final approach adopted was to screen the *Xenopus* cDNA library with cross species probes by low stringency Southern

hybridisation at 42°C. The probes used were human and chicken sequences containing the homology domains or, alternatively, the full length Mif2 sequence. Although some positive clones were identified to the stage of a tertiary screen, upon sequencing, these were found not to be CENP-C. Why in particular these genes were cloned is unknown, since no sequence homology was identified. One explanation is that the temperature used was too low, and therefore allowed the probes to hybridise to non-specific library sequences. If these experiments were to be repeated, the temperature could be increased slightly. In addition, the washing conditions could be varied in order to prevent false positives. The conditions used for washing were 40 mM NaPi and 1% SDS at 42°C. The stringency of this wash could be increased, by decreasing the salt and SDS concentrations.

Since a partial sequence for the CENP-C gene in a related *Xenopus* species, *Xenopus (Sirulana) tropicalis,* has recently been made available, it is now possible to assess the similarity between the sequences and speculate why the adopted approaches failed. The regions of homology designated block 2 and block 3 are highly conserved (Figure 5.4), although it should be noted that the database sequence is most likely wrong for the translation of the last 28 amino acids, presumably due to one missing nucleotide and a frame change from +2 to +3. This new sequence is highly conserved as compared to the vertebrate CENP-C sequences and Mif2. By looking at the partial sequence now available, the reasons why the library screen was unsuccessful are not at all clear.

Reasons for the failure of the degenerate PCR may be because of several key differences between the *Xenopus* sequence and that of yeast Mif2 and the other vertebrate species. The degenerate primers were based on the regions indicated in Figure 5.4. In some cases it seemed clear that an amino acid would be conserved. In others any amino acid was expected, and in the third scenario, a guess was made based on the Mif2, chicken or human sequence. The result is that all three primers designed had two errors compared to the actual sequence. In the light of this knowledge, it is unsurprising that the experiment failed. What is surprising, however, is that the sequence of the *Xenopus* protein varies in these conserved regions as compared to the other sequences. In the case of primer 1, the mistake at amino acid 3 was due to the fact that the human and chicken have a glutamic acid at

this position and Mif2 a glutamine. It was therefore reasoned that one of these would be conserved in *Xenopus*. In actual fact the amino acid is alanine in *Xenopus*. The second mistake in primer 1 is at amino acid position 6. In Mif2, human and chicken this is an arginine. However, in *Xenopus* it is lysine. Primer 2 also has two mistakes, the first at position 3. This residue is valine in Mif2, human and chicken. However, in *Xenopus* it is isoleucine. The second mistake in primer 2 is at position 5. This is a different amino acid in all three organisms, therefore a primer with high degeneracy was designed. This could have encoded for asparagine, lysine, serine, arginine, histidine, or glutamine. Unluckily the *Xenopus* amino acid is threonine. In primer 3, again there are two mistakes, the first at position 2, which is alanine in Mif2, human and chicken, but proline in *Xenopus*. The second mistake is at position 7 which is asparagine in both chicken and human. However the amino acid in *Xenopus* is lysine. Therefore since all three primers had two mistakes, it is unlikely that they could have annealed specifically in order to generate a product.

5.3.2 Screening a Xenopus cDNA library for CENP-H and ZWINT

Library screening, using cross species probes for the centromere associated proteins, CENP-H and Zwint, also failed, presumably due to the fact that the temperature used was incorrect or the washing conditions were incorrect as discussed previously. In the case of CENP-H a partial *Xenopus laevis* EST is now available in the database and when compared to the human sequence is 43% identical over this region.

As with CENP-C and CENP-H, a partial *Xenopus laevis* EST is now also available for Zwint and when compared to the human sequence is 26% identical. To date, the only information concerning Zwint is that it interacts with human Zw10. Identification of the *Xenopus* protein in the database revealed that it is conserved and hopefully further investigation will determine if it is in a complex with Zw10 and Rod in *Xenopus* egg extracts.

5.3.3 Cloning and Characterisation of Xenopus ZW10

After identification of a short EST sequence for *Xenopus* Zw10 in the database, amplification by PCR from the library DNA was relatively simple. This sequence was then used as a probe to screen the cDNA library. The longest clone obtained

contained 1.3 kb of the C-terminal portion of Zw10 cDNA. Sequencing of this clone revealed that the C-terminal half of *Xenopus* Zw10 is 77% identical to the human sequence. Unfortunately, attempts to clone the full length cDNA by 5′ RACE failed. The reason for this could be that the distance between the specific primers and the 5′ end was beyond the range of this reaction. To clone this sequence, the best solution may be to screen the library again with the most 5′ sequence now available to see of there is a longer clone which was missed on the initial screen. The library is generated from polyA primed sequences so many clones will not be full length in the 5′ region.

To generate an antibody to Zw10, the most C-terminal 50 amino acids were cloned into a pGEX vector, resulting in an N-terminal GST fusion. This fusion protein was expressed, purified and injected into rabbits. The serum from two rabbits was tested and rabbit 1107 recognised a band of approximately 80 kDa, potentially Zw10. To verify that this was indeed an antibody specific for Zw10, immunofluorescence experiments on *Xenopus* tissue culture cells were carried out. On metaphase chromosome spreads it was possible to show that the antibody recognised the kinetochores of *Xenopus* cells. Unfortunately, attempts to determine the localisation of this protein throughout mitosis were unsuccessful. The reason why this immunofluorescence failed may be that the antigen is somehow masked at the kinetochore, making it difficult for the antibody to interact. Kinetochores did stain in chromosome spreads. However, it was noted that the chromosomes with the worst morphology, which had been harshly treated with the hypotonic solution, had the strongest staining with the antibody, an indication that the antigen may be masked somehow. The antibody either as serum or affinity purified was used in immunoprecipitation experiments in order to 'pull down' a potential complex from *Xenopus* egg extracts. Unfortunately, the immunoprecipitation experiments failed to 'pull down' Zw10 or any interacting proteins. Initial confusion over whether the experiment had been successful arose because an unknown band, recognised by the Zw10 antibody was present in the IP lane. Upon further investigation, this band was also identified in the control lanes and is most likely due to the antibody. One way to resolve this problem would be to crosslink the antibody to the protein A beads, using 20 mM dimethyl pimeliminidate in 0.2 M sodium borate pH 9.0, preventing it coming off when the beads are boiled in sample buffer. The identity of this species

is still unknown since the heavy and light chain IgG molecules are easily identifiable on the gels. The sample buffer, although containing β-mercaptoethanol, which is a reducing agent that breaks disulphide bonds between protein molecules, does not contain DTT. The presence of DTT may be advantageous in preventing any complexes from remaining in the gel. However, since the gel is denaturing, this may be an unlikely explanation. The conditions used to do these immunoprecipitation experiments were non-denaturing so that whole complexes could be pulled down. However, in order to determine if this antibody works, it may be necessary to change the conditions to denaturing ones and see if Zw10 alone can be pulled down. If Zw10 is present in a very large complex this may have prevented the interaction between antibody and antigen. A scenario could be imagined where the epitope recognised by this antibody is buried in a complex and not accessible. Since only a small fragment was used to generate the antibody, this may be a possibility. In addition, it may have been a limiting factor that relatively small volumes of extract were used for the immunoprecipitation experiments compared to the large scale experiments, using up to 100 times more extract, which lead to the identification of the INCENP/Aurora B complex in egg extracts (Adams *et al.*, 2000).

5.3.4 Cloning and characterisation of Xenopus ROD

In a manner very similar to that described for Zw10, database identification of ESTs allowed a portion of the C-terminus of *Xenopus* Rod to be cloned. cDNA encoding the last 759 amino acids of *Xenopus* Rod was cloned. Sequencing revealed that the identity to human is 54% over the C-terminal third of this protein. A rabbit polyclonal antibody was raised to the C-terminal 126 amino acids. This antibody recognised a band of approximately 200 kDa on immunoblot of *Xenopus* egg extracts.

As with Zw10, immunoprecipitation experiments were attempted, but failed to pull down Rod or any interacting proteins. As discussed above for Zw10, if these experiments were to be repeated, it might be best to use denaturing conditions in case a complex was preventing the association between epitope and antibody. In addition, the attempts at immunofluorescence using anti-Rod on *Xenopus* cells did not yield positive results, even though a number of protocols were used.

Recently, the cloning and generation of antibodies to *Xenopus* Zw10 and Rod has been reported by another group and used in the study of the Ndc80 kinetochore complex in *Xenopus* (McCleland *et al.*, 2003). The authors state that the antibodies raised to *Xenopus* Zw10 and Rod recognises bands of 80 and around 250 kDa respectively on western blot, which is consistent with the results described here.

By sucrose gradient fractionation of *Xenopus* HSS it was possible to show that Zw10 and Rod are present in a complex. The complex size was determined to be larger than 11S by using protein standards and blotting with the antibodies to INCENP and Aurora-B. These passenger proteins have been identified in an 11S complex in egg extracts (Adams *et al.*, 2000). The results of this blot (Figure 5.11A), showed that the passenger complex is distinct from that containing Zw10 and Rod in a 5-20% gradient. However, in a 10-40% gradient, as shown in 5.11B, the complexes were closer together. This may be due to the fact that this gradient was run for a shorter time. In order to further separate these complexes it might be necessary to run a 10-40% gradient for 5-6 hours. In addition, a larger protein standard could be run in order to determine more accurately the size of this complex. An additional approach to the identification of the components of this complex might be to immunoprecipitate from the sucrose gradient fractions. In this case there would be less contaminating proteins, and this might favour a positive result. In addition, the presence of any other proteins in the complex could be investigated. Zw10 and Rod have been reported to interact with the dynein/dynactin complex and if antibodies were available to these, the gradient fractions could be probed by immunoblotting. The size of this complex is somewhat different from that identified in *Drosophila* (Scaerou *et al.*, 2001), where it was found to be 700-900 kDa by a Superose-6 sizing column and was said to sediment at 19S. It may be that the complex identified in *Drosophila* has additional components not present in the *Xenopus* complex.

Both Zw10 and Rod have no known domains or motifs in common with other proteins. Their role in cell cycle progression and in particular the spindle assembly checkpoint is unclear, and any further information regarding these proteins may be of potential interest. Although this study was unable to draw any significant conclusions regarding this complex or the kinetochore in general in *Xenopus*, other

than confirmation that a complex does exist, it is hoped that the reagents generated will be useful in addressing the initial aims. If the antibodies generated to *Xenopus* Zw10 and Rod are not useful for immunoprecipitation experiments, then others could be generated based on the sequences now cloned. In addition, identification of *Xenopus* CENP-C, CENP-H and Zwint in the database will allow them to be cloned and antibodies raised in order that they can be further studied in the Laboratory.

Chapter 6

Discussion and Future Work

6.1 Discussion

Chicken *BubR1* cDNA was cloned from a library and sequencing revealed that it is 52% identical to human BubR1. Clustal alignments revealed that it is highly conserved as compared to BubR1 from other species and to S. *cerevisae* Mad3 in the conserved domains (Figure 3.3 and 3.4). An antibody was raised against this protein by the expression of a fragment (653-778) as a GST fusion. In order that an antibody specific for BubR1, and not Bub1 would be generated this portion of the protein was out with the kinase domain or any other identified motifs. Immunofluorescence with this antibody revealed that BubR1 is localised in chicken cells in a manner similar to that reported for BubR1 and other spindle assembly checkpoint components in various species. BubR1 becomes localised to the kinetochores during prometaphase and then the signal is decreased as kinetochores become attached to microtubules and are under tension. The signal is most intense as the cell proceeds from metaphase to anaphase, and no specific staining is seen during later stages of the cell cycle. In addition, the antibody brightly stains the kinetochores of cells treated with the microtubule depolymerising drug colcemid and the microtubule stabilising drug taxol, both of which activate the spindle assembly checkpoint. The antibody was also used for immunoblots of chicken cell extracts. This revealed that BubR1 migrates at approximately 140 kDa although the predicted molecular weight is 122 kDa. After treating cells with colcemid and taxol, to activate the checkpoint, cell lysates were immunoblotted with the antibody. This revealed that a higher molecular weight form, presumably phosphorylated BubR1 is detectable after activation of the checkpoint. This form of the protein is present in untreated cells, but appears to be more abundant after treatment with these drugs. As discussed in Chapter 3, this antibody has been useful in a number of studies in DT40 cells in order to assess the checkpoint and also the kinetochore. Hopefully, it will be of

further use in the future in the study of DT40 knockouts, or other studies in chicken cells.

Attempts at generation of a stable MSB1 cell line with which to investigate the structure of the kinetochore were unsuccessful. The aim was to generate a cell line with a tagged version of BubR1 expressed at the kinetochore. Since it is known that BubR1 is localised to the outer kinetochore plate, this was intended to be used as a handle with which to identify novel kinetochore components and BubR1 interactors. Unfortunately, although some MSB1 cell lines were generated none showed kinetochore localisation of BubR1. Subsequently, investigation of the expression of exogenous BubR1 in a different chicken cell line, DT40, revealed that stable expression is very difficult to maintain. This led to the hypothesis that exogenous BubR1 may be toxic. Whilst investigating BubR1 expression in DT40 cells with the aim of generating a rescued cell line, the tagged construct was expressed. In this case a cell line was observed with tagged BubR1 at the kinetochores. This may, therefore, be a useful tool with which to investigate the kinetochore in chicken cells. Alternatively, it may be better to use a constitutive centromere protein such as CENP-C or CENP-H as the 'handle'. In addition, it may be easier to do these experiments in human cells. Although there is a chicken database and an ever-increasing number of chicken sequences are deposited, this is far from the comprehensive human genome data now available. For this reason, the identification of proteins by mass spectrometry would be much easier if they were human.

In order to investigate the roles of BubR1 in mitosis, the aim was to generate a conditionally null DT40 cell line. Initially, this required cloning of the *BubR1* genomic locus for use as the basis of targeting vectors. A phage, 3B3, was identified which contained the ATG and around half of the predicted exons of chicken BubR1. Unfortunately, this phage had little sequence upstream of the ATG, and re-screening the library proved unsuccessful in the identification of subsequent phage with more sequence in the 5′ region of the gene. Targeting vectors were generated with a number of resistance cassettes, and it was determined that the total length of homology of 4.6 kb was insufficient to target the genomic region of approximately 10 kb. When the total homology was increased to 6 kb targeting occurred, however,

at a low frequency for DT40 cells (Table 4.4). The resulting cell lines, heterozygous for BubR1, were investigated in a number of ways. Since it is known that Mad2 is haploinsufficient in mouse (Michel *et al.*, 2001), it was interesting to determine if this was the case for BubR1 in chicken cells. Initially, the +/- cells were visualised by immunofluorescence microscopy and it could be seen that they progressed through mitosis apparently normally with BubR1 localised to the kinetochores during prometaphase. The cells grew normally in culture and their growth rate was compared to wild type cells. As shown in Figure 4.9, the heterozygote cell 812 and 821 grow at a very similar rate to wild type DT40, Cl18. However, the heterozygote cell line 511 appears to grow a little more slowly, although within the normal range for DT40 cells. Although it has been shown that BubR1 is present at the kinetochores of heterozygote cells, it was interesting to ask if the checkpoint was still active. In order to do this, the cells were treated with colcemid and taxol, both of which activate the checkpoint. The mitotic index was calculated, and the cells were prepared for immunofluorescence and immuoblotting. The results of this experiment show that the heterozygote cells respond normally to spindle damage, as judged by an increase in the mitotic index, the presence of BubR1 at the kinetochores of arrested cells, and the increase in the phosphorylated form of BubR1 as judged by immunoblot. Finally, the amount of BubR1 protein was quantified in these cells by immunoblot, and it can be seen that it is reduced as compared to wild type cells. These results therefore demonstrated that BubR1 does not appear to be haploinsufficient in DT40 cells and that the heterozygote cells have an active spindle assembly checkpoint, although the levels of BubR1 are reduced.

Unfortunately, generation of null cells was unsuccessful. Targeting experiments in the absence of a rescue cDNA showed that the gene was essential. A strategy with the rescue construct (cDNA) under the control of the Tet operator was therefore adopted. However, it proved difficult to express the cDNA even though different tTa plasmids were used. Although the expression was detected by RT-PCR and immunoblot it was very difficult to determine the expression levels on a cell by cell basis. One way to overcome this problem may be to express a tagged rescue construct. Both a GFP-BubR1 construct and a BubR1-HA-His construct were made and tested in DT40 cells. The GFP construct did not localise appropriately. As

discussed previously a cell line was generated with the BubR1-HA-His localised to the kinetochore, however this construct was not cloned under the control of the Tet promoter, so therefore could not be used as a rescue. In the future, however, this is a possibility. An additional possibility would be to use the cDNA from a different species in order to rescue the knockout. In this case an antibody specific for the exogenous BubR1 would be used in order to determine the expression levels in a particular cell or cell line. Several attempts were made at controlling the expression levels by using different tTa plasmids. However, even with the weakest tTa 4 which should give an expression level of 10%, as compared to the original plasmid, some cells were seen with very high levels of the protein as judged by immunofluorescence. To try and avoid some of the detrimental effects of exogenous BubR1 expression, transfections were carried out in the presence of doxycycline. In this case, the transgene would not be expressed until the drug was removed. However, in targeting experiments carried out in these cell lines, no homozygous clones were identified. In conclusion, expression of the transgene proved very difficult. Cell lines generated showed extremely heterogenous expression levels as judged by immunofluorescence with the BubR1 antibody. It is predicted that this would make targeting experiments very difficult as there might be few or no cells, expressing BubR1 at the correct levels, which could be targeted. Obviously, if the targeting was more efficient, this might be overcome by screening more colonies. However, with the reagents currently available, this may be an impossible task.

A few other possibilities exist in order to overcome this problem. As discussed in Chapter 4, an IRES construct may be a potential approach. In this case, the expression of the transgene would have to be maintained by the cell in order that it was drug resistant. Unfortunately, plans to attempt this approach were not completed since the construct proved extremely problematic to clone. This still remains a possibility for the future. In addition, approaches using Cre technology may be the answer, as this would allow the rescue to be expressed from the endogenous promoter, hopefully bypassing any toxicity issues.

If a BubR1 null cell line were generated in the future there are many questions which could be addressed. Firstly, an assessment of the checkpoint function would

be very interesting. It is known that the checkpoint has a number of components, and recent experiments have drawn the conclusion that BubR1 and Mad2 sense distinct tension and attachment checkpoints. This would be an ideal system with which to address this hypothesis, since the function of only one of the proteins would be removed. In addition, the function of various domains of the protein could be dissected. It would be possible to put back structural mutants into the cell line and ask if they can rescue the function. In particular the function of the kinase domain could be addressed in this manner. Site directed mutagenesis was carried out on chicken BubR1 to generate the kinase dead form (K830R). This construct could be used firstly to address whether the kinase domain is required for the checkpoint to function, and if not, an alternative role could be investigated. Also, it would be interesting to address the affect on other checkpoint components such as Zw10 and Rod if BubR1 were missing and the checkpoint therefore potentially inactive. The structure of the kinetochore could also be studied by electron microscopy.

Surprisingly, BubR1 appears to be overexpressed or stabilised in apoptotic cells. Initially, this was seen by immunofluorescence on apoptotic cells using the BubR1 antibody. Subsequent investigation has shown that BubR1 is apparently cleaved after DT40 cells are induced to go into apoptosis by treatment with etoposide. This data is preliminary, but intriguing, especially since it is known that caspases cleave other kinases during apoptosis. These kinases often then have a role to play in the apoptotic process (reviewed by (Earnshaw *et al.*, 1999; Utz & Anderson, 2000)). To investigate this further BubR1, could be *in vitro* translated and tested for cleavage with a number of purified caspases. In addition the fragment could be immunoprecipitated and then sequenced. This would identify the end of the protein which is stabilised.

The method of BubR1 destruction or inactivation after the checkpoint is satisfied is unclear. It has a putative destruction box and also a putative KEN box, which could both indicate that it is targeted for destruction by the APC. To address the question as to if this cleavage seen during apoptosis also occurs once the checkpoint is satisfied in a normal cell cycle, cells were treated with nocodazole and then released into anaphase. This cleavage is not observed after the cells are released from a

nocodazole block (fig 4.12), which may indicate another mechanism is active, since the protein levels do decrease.

An alternative approach to study the kinetochore and spindle checkpoint in vertebrates was attempted in the *Xenopus* egg extract system. Initially, attempts were made at cloning the constitutive centromere proteins CENP-C and CENP-H. A number of approaches were employed in order to clone *Xenopus* CENP-C, including screening extract with antibodies, degenerate PCR and screening a cDNA library. Unfortunately these attempts were unsuccessful. As discussed in Chapter 5, the *Xenopus* homologue has recently been deposited in the database. This information shows that the C-terminal of *Xenopus* CENP-C is conserved and that it contains the domains conserved in the *S. cerevevisae* protein Mif2. Perhaps the temperature used for the library screen was inappropriate, resulting in the identification of false positives. The reasons for failure of the degenerate PCR appear to be due to bad luck with the choice of primers. Now that the sequence is available, the EST has been obtained by the Laboratory and antibodies may be generated to this protein. Hopefully, these will be useful in immunoprecipitation experiments leading to the investigation of the kinetochore in *Xenopus*. The cloning of *Xenopus* CENP-H also proved to be unsuccessful. However, as with CENP-C a *Xenopus* homologue of CENP-H is now available in the database and this could also be used to generate antibodies and investigate the kinetochore.

Since library screening with cross species probes proved unsuccessful, a more direct approach was adopted. Short EST sequences were identified for the checkpoint proteins Zw10 and Rod. These sequences were used to generate GST fusions for antibody production and as probes for cDNA library screens. Around one half of the *Xenopus* Zw10 cDNA was cloned and this is highly conserved compared to human Zw10. In addition, antibodies were raised that recognise a protein of approximately 80 kDa by immunoblot and stain the kinetochores of *Xenopus* A6 cell. In a similar manner, around one third of the *Xenopus* Rod cDNA was cloned. Sequencing revealed that it is homologous to the human Rod. An antibody was generated which recognises a protein of approximately 200 kDa by immunoblot. Unfortunately this antibody was not useful in immunofluorescence studies. Although

immunoprecipitation experiments failed, it was possible to determine that Zw10 and Rod were present in a complex in *Xenopus* egg extracts. The size of this complex was estimated to be larger than 11S. The size of this complex could, perhaps, be determined more accurately by running gradients for different lengths of time. In addition more protein standards could be used. This complex differs in size from that identified in *Drosophila* which is estimated to be 19S (Scaerou *et al.*, 2001). One possible explanation for this could be that this complex identified in *Xenopus* contains less components, or that there are multiple complexes which contain Zw10 and Rod. Hopefully, the generation of these *Xenopus* reagents will be useful in future studies into the spindle checkpoint and Zw10 and Rod interactors.

References

Abrieu, A., Kahana, J. A., Wood, K. W. and Cleveland, D. W. (2000). "CENP-E as an essential component of the mitotic checkpoint in vitro." Cell **102**(6): 817-26.

Abrieu, A., Magnaghi-Jaulin, L., Kahana, J. A., Peter, M., Castro, A., Vigneron, S., Lorca, T., Cleveland, D. W. and Labbe, J. C. (2001). "Mps1 is a kinetochore-associated kinase essential for the vertebrate mitotic checkpoint." Cell **106**(1): 83-93.

Adams, R. R., Wheatley, S. P., Gouldsworthy, A. M., Kandels-Lewis, S. E., Carmena, M., Smythe, C., Gerloff, D. L. and Earnshaw, W. C. (2000). "INCENP binds the Aurora-related kinase AIRK2 and is required to target it to chromosomes, the central spindle and cleavage furrow." Curr Biol **10**(17): 1075-8.

Alexandru, G., Uhlmann, F., Mechtler, K., Poupart, M. A. and Nasmyth, K. (2001). "Phosphorylation of the cohesin subunit Scc1 by Polo/Cdc5 kinase regulates sister chromatid separation in yeast." Cell **105**(4): 459-72.

Alexandru, G., Zachariae, W., Schleiffer, A. and Nasmyth, K. (1999). "Sister chromatid separation and chromosome re-duplication are regulated by different mechanisms in response to spindle damage." Embo J **18**(10): 2707-21.

Allshire, R. C., Nimmo, E. R., Ekwall, K., Javerzat, J. P. and Cranston, G. (1995). "Mutations derepressing silent centromeric domains in fission yeast disrupt chromosome segregation." Genes Dev **9**(2): 218-33.

Arakawa, H., Hauschild, J. and Buerstedde, J. M. (2002). "Requirement of the Activation-Induced Deaminase (*AID*) Gene for Immunoglobulin Gene Conversion." Science **295**: 1301-6.

Aravin, A. A., Naumova, N. M., Tulin, A. V., Vagin, V. V., Rozovsky, Y. M. and Gvozdev, V. A. (2001). "Double-stranded RNA-mediated silencing of genomic tandem repeats and transposable elements in the D. melanogaster germline." Curr Biol **11**(13): 1017-27.

Baba, T. W., Giroir, B. P. and Humphries, E. H. (1985). "Cell lines derived from avian lymphomas exhibit two distinct phenotypes." Virology **144**(1): 139-51.

Baba, T. W. and Humphries, E. H. (1984). "Avian leukosis virus infection: analysis of viremia and DNA integration in susceptible and resistant chicken lines." J Virol **51**(1): 123-30.

Banks, J. D. and Heald, R. (2001). "Chromosome movement: dynein-out at the kinetochore." Curr Biol **11**(4): R128-31.

Baron, U., Gossen, M. and Bujard, H. (1997). "Tetracycline-controlled transcription in eukaryotes: novel transactivators with graded transactivation potential." Nucleic Acids Res **25**(14): 2723-9.

Basto, R., Gomes, R. and Karess, R. E. (2000). "Rough deal and Zw10 are required for the metaphase checkpoint in Drosophila." Nat Cell Biol **2**(12): 939-43.

Basu, J., Bousbaa, H., Logarinho, E., Li, Z., Williams, B. C., Lopes, C., Sunkel, C. E. and Goldberg, M. L. (1999). "Mutations in the essential spindle checkpoint gene bub1 cause chromosome missegregation and fail to block apoptosis in Drosophila." J Cell Biol **146**(1): 13-28.

Basu, J., Logarinho, E., Herrmann, S., Bousbaa, H., Li, Z., Chan, G. K., Yen, T. J., Sunkel, C. E. and Goldberg, M. L. (1998). "Localization of the Drosophila

checkpoint control protein Bub3 to the kinetochore requires Bub1 but not Zw10 or Rod." Chromosoma **107**(6-7): 376-85.
Baumann, P., Benson, F. E., Hajibagheri, N. and West, S. C. (1997). "Purification of human Rad51 protein by selective spermidine precipitation." Mutat Res **384**(2): 65-72.
Bazett-Jones, D. P., Kimura, K. and Hirano, T. (2002). "Efficient supercoiling of DNA by a single condensin complex as revealed by electron spectroscopic imaging." Mol Cell **9**(6): 1183-90.
Bernard, P., Hardwick, K. and Javerzat, J. P. (1998). "Fission yeast bub1 is a mitotic centromere protein essential for the spindle checkpoint and the preservation of correct ploidy through mitosis." J Cell Biol **143**(7): 1775-87.
Bloecher, A., Venturi, G. M. and Tatchell, K. (2000). "Anaphase spindle position is monitored by the BUB2 checkpoint." Nat Cell Biol **2**(8): 556-8.
Bobinnec, Y., Khodjakov, A., Mir, L. M., Rieder, C. L., Edde, B. and Bornens, M. (1998). "Centriole disassembly in vivo and its effect on centrosome structure and function in vertebrate cells." J Cell Biol **143**(6): 1575-89.
Bolton, M. A., Lan, W., Powers, S. E., McCleland, M. L., Kuang, J. and Stukenberg, P. T. (2002). "Aurora B Kinase Exists in a Complex with Survivin and INCENP and Its Kinase Activity Is Stimulated by Survivin Binding and Phosphorylation." Mol Biol Cell **13**(9): 3064-77.
Brady, D. M. and Hardwick, K. G. (2000). "Complex formation between Mad1p, Bub1p and Bub3p is crucial for spindle checkpoint function." Curr Biol **10**(11): 675-8.
Brinkley, B. R. and Stubblefield, E. (1966). "The fine structure of the kinetochore of a mammalian cell in vitro." Chromosoma **19**(1): 28-43.
Brown, M. T. (1995). "Sequence similarities between the yeast chromosome segregation protein Mif2 and the mammalian centromere protein CENP-C." Gene **160**(1): 111-6.
Buerstedde, J. M. and Takeda, S. (1991). "Increased ratio of targeted to random integration after transfection of chicken B cell lines." Cell **67**(1): 179-88.
Cahill, D. P., Lengauer, C., Yu, J., Riggins, G. J., Willson, J. K., Markowitz, S. D., Kinzler, K. W. and Vogelstein, B. (1998). "Mutations of mitotic checkpoint genes in human cancers." Nature **392**(6673): 300-3.
Campbell, M. S., Chan, G. K. and Yen, T. J. (2001). "Mitotic checkpoint proteins HsMAD1 and HsMAD2 are associated with nuclear pore complexes in interphase." J Cell Sci **114**(Pt 5): 953-63.
Campbell, M. S. and Gorbsky, G. J. (1995). "Microinjection of mitotic cells with the 3F3/2 anti-phosphoepitope antibody delays the onset of anaphase." J Cell Biol **129**: 1195-204.
Canman, J. C., Salmon, E. D. and Fang, G. (2002). "Inducing precocious anaphase in cultured mammalian cells." Cell Motil Cytoskeleton **52**(2): 61-5.
Canman, J. C., Sharma, N., Straight, A., Shannon, K. B., Fang, G. and Salmon, E. D. (2002). "Anaphase onset does not require the microtubule-dependent depletion of kinetochore and centromere-binding proteins." J Cell Sci **115**(Pt 19): 3787-95.
Chan, C. S. and Botstein, D. (1993). "Isolation and characterization of chromosome-gain and increase-in-ploidy mutants in yeast." Genetics **135**: 677-91.
Chan, G. K., Jablonski, S. A., Starr, D. A., Goldberg, M. L. and Yen, T. J. (2000). "Human Zw10 and ROD are mitotic checkpoint proteins that bind to kinetochores." Nat Cell Biol **2**(12): 944-7.

Chan, G. K., Jablonski, S. A., Sudakin, V., Hittle, J. C. and Yen, T. J. (1999). "Human BUBR1 is a mitotic checkpoint kinase that monitors CENP-E functions at kinetochores and binds the cyclosome/APC." J Cell Biol **146**(5): 941-54.

Chan, G. K., Schaar, B. T. and Yen, T. J. (1998). "Characterization of the kinetochore binding domain of CENP-E reveals interactions with the kinetochore proteins CENP-F and hBUBR1." J Cell Biol **143**(1): 49-63.

Chan, T. A., Hermeking, H., Lengauer, C., Kinzler, K. W. and Vogelstein, B. (1999). "14-3-3Sigma is required to prevent mitotic catastrophe after DNA damage." Nature **401**(6753): 616-20.

Cheeseman, I. M., Anderson, S., Jwa, M., Green, E. M., Kang, J., Yates, J. R. r., Chan, C. S., G., D. D. and Barnes, G. (2002). "Phospho-regulation of kinetochore-microtubule attachments by the Aurora kinase Ipl1p." Cell **111**: 163-72.

Chen, R. H. (2002). "BubR1 is essential for kinetochore localization of other spindle checkpoint proteins and its phosphorylation requires Mad1." J Cell Biol **158**(3): 487-96.

Chen, R. H., Brady, D. M., Smith, D., Murray, A. W. and Hardwick, K. G. (1999). "The spindle checkpoint of budding yeast depends on a tight complex between the Mad1 and Mad2 proteins." Mol Biol Cell **10**(8): 2607-18.

Chen, R. H., Shevchenko, A., Mann, M. and Murray, A. W. (1998). "Spindle checkpoint protein Xmad1 recruits Xmad2 to unattached kinetochores." J Cell Biol **143**(2): 283-95.

Chen, Y., Riley, D. J., Chen, P. L. and Lee, W. H. (1997). "HEC, a novel nuclear protein rich in leucine heptad repeats specifically involved in mitosis." Mol Cell Biol **17**.

Ciosk, R., Zachariae, W., Michaelis, C., Shevchenko, A., Mann, M. and Nasmyth, K. (1998). "An ESP1/PDS1 complex regulates loss of sister chromatid cohesion at the metaphase to anaphase transition in yeast." Cell **93**(6): 1067-76.

Cohen-Fix, O., Peters, J. M., Kirschner, M. W. and Koshland, D. (1996). "Anaphase initiation in Saccharomyces cerevisiae is controlled by the APC-dependent degradation of the anaphase inhibitor Pds1p." Genes Dev **10**(24): 3081-93.

Collins, N., McManus, R., Wooster, R., Mangion, J., Seal, S., Lakhani, S. R., Ormiston, W., Daly, P. A., Ford, D., Easton, D. F. and et al. (1995). "Consistent loss of the wild type allele in breast cancers from a family linked to the BRCA2 gene on chromosome 13q12-13." Oncogene **10**(8): 1673-5.

Cross, S. M., Sanchez, C. A., Morgan, C. A., Schimke, M. K., Ramel, S., Idzerda, R. L., Raskind, W. H. and Reid, B. J. (1995). "A p53-dependent mouse spindle checkpoint." Science **267**(5202): 1353-6.

Cutts, S. M., Fowler, K. J., Kile, B. T., Hii, L. L., O'Dowd, R. A., Hudson, D. F., Saffery, R., Kalitsis, P., Earle, E. and Choo, K. H. (1999). "Defective chromosome segregation, microtubule bundling and nuclear bridging in inner centromere protein gene (Incenp)-disrupted mice." Hum Mol Genet **8**(7): 1145-55.

D'Assoro, A. B., Lingle, W. L. and Salisbury, J. L. (2002). "Centrosome amplification and the development of cancer." Oncogene **21**(40): 6146-53.

Darwiche, N., Freeman, L. A. and Strunnikov, A. (1999). "Characterization of the components of the putative mammalian sister chromatid cohesion complex." Gene **233**(1-2): 39-47.

Davenport, J. W., Fernandes, E. R., Harris, L. D., Neale, G. A. and Goorha, R. (1999). "The mouse mitotic checkpoint gene bub1b, a novel bub1 family member, is expressed in a cell cycle-dependent manner." Genomics **55**(1): 113-7.

Deng, C. and Capecchi, M. R. (1992). "Reexamination of gene targeting frequency as a function of the extent of homology between the targeting vector and the target locus." Mol Cell Biol **12**(8): 3365-71.

Dobles, M., Liberal, V., Scott, M. L., Benezra, R. and Sorger, P. K. (2000). "Chromosome missegregation and apoptosis in mice lacking the mitotic checkpoint protein Mad2." Cell **101**(6): 635-45.

Doolittle, R. F., Feng, D. F., Tsang, S., Cho, G. and Little, E. (1996). "Determining divergence times of the major kingdoms of living organisms with a protein clock." Science **271**(5248): 470-7.

du Sart, D., Cancilla, M. R., Earle, E., Mao, J. I., Saffery, R., Tainton, K. M., Kalitsis, P., Martyn, J., Barry, A. E. and Choo, K. H. (1997). "A functional neo-centromere formed through activation of a latent human centromere and consisting of non-alpha-satellite DNA." Nat Genet **16**(2): 144-53.

Dutcher, S. K. (2001). "Motile organelles: the importance of specific tubulin isoforms." Curr Biol **11**(11): R419-22.

Earnshaw, W. C., Martins, L. M. and Kaufmann, S. H. (1999). "Mammalian caspases: Structure, activation, substrates and functions during apoptosis." Ann. Rev. Biochem.: in press.

Earnshaw, W. C., Ratrie, H., 3rd and Stetten, G. (1989). "Visualization of centromere proteins CENP-B and CENP-C on a stable dicentric chromosome in cytological spreads." Chromosoma **98**(1): 1-12.

Efimov, V. P. and Morris, N. R. (1998). "A screen for dynein synthetic lethals in Aspergillus nidulans identifies spindle assembly checkpoint genes and other genes involved in mitosis." Genetics **149**(1): 101-16.

Fang, G. (2002). "Checkpoint Protein BubR1 Acts Synergistically with Mad2 to Inhibit Anaphase-promoting Complex." Mol Biol Cell **13**(3): 755-66.

Fang, G., Yu, H. and Kirschner, M. W. (1998). "The checkpoint protein MAD2 and the mitotic regulator CDC20 form a ternary complex with the anaphase-promoting complex to control anaphase initiation." Genes Dev **12**(12): 1871-83.

Fesquet, D., Fitzpatrick, P. J., Johnson, A. L., Kramer, K. M., Toyn, J. H. and Johnston, L. H. (1999). "A Bub2p-dependent spindle checkpoint pathway regulates the Dbf2p kinase in budding yeast." Embo J **18**(9): 2424-34.

Fisk, H. A. and Winey, M. (2001). "The mouse Mps1p-like kinase regulates centrosome duplication." Cell **106**(1): 95-104.

Fraschini, R., Formenti, E., Lucchini, G. and Piatti, S. (1999). "Budding yeast Bub2 is localized at spindle pole bodies and activates the mitotic checkpoint via a different pathway from Mad2." J Cell Biol **145**(5): 979-91.

Freeman, L., Aragon-Alcaide, L. and Strunnikov, A. (2000). "The condensin complex governs chromosome condensation and mitotic transmission of rDNA." J Cell Biol **149**(4): 811-24.

Fukagawa, T. and Brown, W. R. (1997). "Efficient conditional mutation of the vertebrate CENP-C gene." Hum Mol Genet **6**(13): 2301-8.

Fukagawa, T., Hayward, N., Yang, J., Azzalin, C., Griffin, D., Stewart, A. F. and Brown, W. (1999). "The chicken HPRT gene: a counter selectable marker for the DT40 cell line." Nucleic Acids Res **27**(9): 1966-9.

Fukagawa, T., Mikami, Y., Nishihashi, A., Regnier, V., Haraguchi, T., Hiraoka, Y., Sugata, N., Todokoro, K., Brown, W. and Ikemura, T. (2001). "CENP-H, a constitutive centromere component, is required for centromere targeting of CENP-C in vertebrate cells." Embo J **20**(16): 4603-17.

Fukagawa, T., Regnier, V. and Ikemura, T. (2001). "Creation and characterization of temperature-sensitive CENP-C mutants in vertebrate cells." Nucleic Acids Res **29**(18): 3796-803.

Futamura, M., Arakawa, H., Matsuda, K., Katagiri, T., Saji, S., Miki, Y. and Nakamura, Y. (2000). "Potential role of BRCA2 in a mitotic checkpoint after phosphorylation by hBUBR1." Cancer Res **60**(6): 1531-5.

Gatti, M. and Goldberg, M. L. (1991). "Mutations affecting cell division in Drosophila." Methods Cell Biol **35**: 543-86.

Gimelli, G., Zuffardi, O., Giglio, S., Zeng, C. and He, D. (2000). "CENP-G in neocentromeres and inactive centromeres." Chromosoma **109**(5): 328-33.

Glotzer, M., Murray, A. W. and Kirschner, M. W. (1991). "Cyclin is degraded by the ubiquitin pathway." Nature **349**(6305): 132-8.

Glover, D. M., Leibowitz, M. H., McLean, D. A. and Parry, H. (1995). "Mutations in aurora prevent centrosome separation leading to the formation of monopolar spindles." Cell **81**(1): 95-105.

Goldberg, I. G., Sawhney, H., Pluta, A. F., Warburton, P. E. and Earnshaw, W. C. (1996). "Surprising deficiency of CENP-B binding sites in African green monkey alpha-satellite DNA: implications for CENP-B function at centromeres." Mol Cell Biol **16**(9): 5156-68.

Gorbsky, G. J. and Ricketts, W. A. (1993). "Differential expression of a phosphoepitope at the kinetochores of moving chromosomes." J Cell Biol **122**(6): 1311-21.

Goshima, G., Kiyomitsu, T., Yoda, K. and Yanagida, M. (2003). " Human centromere chromatin protein hMis12, essential for equal segregation, is independent of CENP-A loading pathway." J Cell Biol **160**: 25-39.

Gossen, M. and Bujard, H. (1992). "Tight control of gene expression in mammalian cells by tetracycline- responsive promoters." Proc Natl Acad Sci U S A **89**(12): 5547-51.

Gualberto, A., Aldape, K., Kozakiewicz, K. and Tlsty, T. D. (1998). "An oncogenic form of p53 confers a dominant, gain-of-function phenotype that disrupts spindle checkpoint control." Proc Natl Acad Sci U S A **95**(9): 5166-71.

Haaf, T. and Schmid, M. (1989). "Centromeric association and non-random distribution of centromeres in human tumour cells." Hum Genet **81**(2): 137-43.

Haering, C. H., Lowe, J., Hochwagen, A. and Nasmyth, K. (2002). "Molecular architecture of SMC proteins and the yeast cohesin complex." Mol Cell **9**(4): 773-88.

Hagstrom, K. A., Holmes, V. F., Cozzarelli, N. R. and Meyer, B. J. (2002). "C. elegans condensin promotes mitotic chromosome architecture, centromere organization, and sister chromatid segregation during mitosis and meiosis." Genes Dev **16**(6): 729-42.

Hammond, S. M., Caudy, A. A. and Hannon, G. J. (2001). "Post-transcriptional gene silencing by double-stranded RNA." Nature Rev. Genet. **2**: 110-19.

Hardwick, K. G., Johnston, R. C., Smith, D. L. and Murray, A. W. (2000). "MAD3 encodes a novel component of the spindle checkpoint which interacts with Bub3p, Cdc20p, and Mad2p." J Cell Biol **148**(5): 871-82.

Hardwick, K. G. and Murray, A. W. (1995). "Mad1p, a phosphoprotein component of the spindle assembly checkpoint in budding yeast." J Cell Biol **131**(3): 709-20.

Hardwick, K. G., Weiss, E., Luca, F. C., Winey, M. and Murray, A. W. (1996). "Activation of the budding yeast spindle assembly checkpoint without mitotic spindle disruption." Science **273**(5277): 953-6.

Haruki, N., Saito, H., Harano, T., Nomoto, S., Takahashi, T., Osada, H. and Fujii, Y. (2001). "Molecular analysis of the mitotic checkpoint genes BUB1, BUBR1 and BUB3 in human lung cancers." Cancer Lett **162**(2): 201-5.

Hasty, P., Rivera-Perez, J. and Bradley, A. (1991). "The length of homology required for gene targeting in embryonic stem cells." Mol Cell Biol **11**(11): 5586-91.

He, D., Zeng, C., Woods, K., Zhong, L., Turner, D., Busch, R. K., Brinkley, B. R. and Busch, H. (1998). "CENP-G: a new centromeric protein that is associated with the alpha-1 satellite DNA subfamily." Chromosoma **107**(3): 189-97.

He, X., Jones, M. H., Winey, M. and Sazer, S. (1998). "Mph1, a member of the Mps1-like family of dual specificity protein kinases, is required for the spindle checkpoint in S. pombe." J Cell Sci **111**(Pt 12): 1635-47.

Hinchcliffe, E. H., Miller, F. J., Cham, M., Khodjakov, A. and Sluder, G. (2001). "Requirement of a centrosomal activity for cell cycle progression through G1 into S phase." Science **291**(5508): 1547-50.

Hinchcliffe, E. H. and Sluder, G. (2002). "Two for two: Cdk2 and its role in centrosome doubling." Oncogene **21**(40): 6154-60.

Hirano, M. and Hirano, T. (2002). "Hinge-mediated dimerization of SMC protein is essential for its dynamic interaction with DNA." Embo J **21**(21): 5733-44.

Hirano, T., Kobayashi, R. and Hirano, M. (1997). "Condensins, chromosome condensation protein complexes containing XCAP- C, XCAP-E and a Xenopus homolog of the Drosophila Barren protein." Cell **89**(4): 511-21.

Hirano, T. and Mitchison, T. J. (1994). "A heterodimeric coiled-coil protein required for mitotic chromosome condensation in vitro." Cell **79**(3): 449-58.

Hogg, D., Guidos, C., Bailey, D., Amendola, A., Groves, T., Davidson, J., Schmandt, R. and Mills, G. (1994). "Cell cycle dependent regulation of the protein kinase TTK." Oncogene **9**(1): 89-96.

Howell, B. J., Hoffman, D. B., Fang, G., Murray, A. W. and Salmon, E. D. (2000). "Visualization of Mad2 dynamics at kinetochores, along spindle fibers, and at spindle poles in living cells." J Cell Biol **150**(6): 1233-50.

Howell, B. J., McEwen, B. F., Canman, J. C., Hoffman, D. B., Farrar, E. M., Rieder, C. L. and Salmon, E. D. (2001). "Cytoplasmic dynein/dynactin drives kinetochore protein transport to the spindle poles and has a role in mitotic spindle checkpoint inactivation." J Cell Biol **155**(7): 1159-72.

Howman, E. V., Fowler, K. J., Newson, A. J., Redward, S., MacDonald, A. C., Kalitsis, P. and Choo, K. H. (2000). "Early disruption of centromeric chromatin organization in centromere protein A (Cenpa) null mice." Proc Natl Acad Sci U S A **97**(3): 1148-53.

Hoyt, M. A., Totis, L. and Roberts, B. T. (1991). "S. cerevisiae genes required for cell cycle arrest in response to loss of microtubule function." Cell **66**(3): 507-17.

Hudson, D. F., Fowler, K. J., Earle, E., Saffery, R., Kalitsis, P., Trowell, H., Hill, J., Wreford, N. G., de Kretser, D. M., Cancilla, M. R., Howman, E., Hii, L.,

Cutts, S. M., Irvine, D. V. and Choo, K. H. (1998). "Centromere protein B null mice are mitotically and meiotically normal but have lower body and testis weights." J Cell Biol **141**(2): 309-19.
Hudson, D. F., Morrison, C., Ruchaud, S. and Earnshaw, W. C. (2002). "Reverse genetics of essential genes in tissue-culture cells: 'dead cells talking'." Trends Cell Biol **12**(6): 281-7.
Hussein, D. and Taylor, S. S. (2002). "Farnesylation of Cenp-F is required for G2/M progression and degradation after mitosis." J Cell Sci **115**(Pt 17): 3403-14.
Ikui, A. E., Furuya, K., Yanagida, M. and Matsumoto, T. (2002). "Control of localization of a spindle checkpoint protein, Mad2, in fission yeast." J Cell Sci **115**(Pt 8): 1603-10.
Itzhaki, J. E., Gilbert, C. S. and Porter, A. C. (1997). "Construction by gene targeting in human cells of a "conditional' CDC2 mutant that rereplicates its DNA." Nat Genet **15**(3): 258-65.
Jablonski, S. A., Chan, G. K., Cooke, C. A., Earnshaw, W. C. and Yen, T. J. (1998). "The hBUB1 and hBUBR1 kinases sequentially assemble onto kinetochores during prophase with hBUBR1 concentrating at the kinetochore plates in mitosis." Chromosoma **107**(6-7): 386-96.
Jokelainen, P. T. (1967). "The ultrastructure and spatial organization of the metaphase kinetochore in mitotic rat cells." J Ultrastruct Res **19**(1): 19-44.
Kaitna, S., Mendoza, M., Jantsch-Plunger, V. and Glotzer, M. (2000). "Incenp and an aurora-like kinase form a complex essential for chromosome segregation and efficient completion of cytokinesis." Curr Biol **10**(19): 1172-81.
Kalitsis, P., Earle, E., Fowler, K. J. and Choo, K. H. (2000). "Bub3 gene disruption in mice reveals essential mitotic spindle checkpoint function during early embryogenesis." Genes Dev **14**(18): 2277-82.
Kalitsis, P., Fowler, K. J., Earle, E., Hill, J. and Choo, K. H. (1998). "Targeted disruption of mouse centromere protein C gene leads to mitotic disarray and early embryo death." Proc Natl Acad Sci U S A **95**(3): 1136-41.
Kallio, M., Weinstein, J., Daum, J. R., Burke, D. J. and Gorbsky, G. J. (1998). "Mammalian p55CDC mediates association of the spindle checkpoint protein Mad2 with the cyclosome/anaphase-promoting complex, and is involved in regulating anaphase onset and late mitotic events." J Cell Biol **141**(6): 1393-406.
Kaplan, K. B., Burds, A. A., Swedlow, J. R., Bekir, S. S., Sorger, P. K. and Nathke, I. S. (2001). "A role for the Adenomatous Polyposis Coli protein in chromosome segregation." Nat Cell Biol **3**(4): 429-32.
Kapoor, M., Montes de Oca Luna, R., Liu, G., Lozano, G., Cummings, C., Mancini, M., Ouspenski, I., Brinkley, B. R. and May, G. S. (1998). "The cenpB gene is not essential in mice." Chromosoma **107**(8): 570-6.
Karess, R. E. and Glover, D. M. (1989). "rough deal: a gene required for proper mitotic segregation in Drosophila." J Cell Biol **109**(6 Pt 1): 2951-61.
Ketting, R. F., Haverkamp, T. H., van Luenen, H. G. and Plasterk, R. H. (1999). "Mut-7 of C. elegans, required for transposon silencing and RNA interference, is a homolog of Werner syndrome helicase and RNaseD." Cell **99**(2): 133-41.
Khodjakov, A., Cole, R. W., Oakley, B. R. and Rieder, C. L. (2000). "Centrosome-independent mitotic spindle formation in vertebrates." Curr Biol **10**(2): 59-67.

Khodjakov, A. and Rieder, C. L. (2001). "Centrosomes enhance the fidelity of cytokinesis in vertebrates and are required for cell cycle progression." J Cell Biol **153**(1): 237-42.

Kim, J. H., Kang, J. S. and Chan, C. S. (1999). "Sli15 associates with the ipl1 protein kinase to promote proper chromosome segregation in Saccharomyces cerevisiae." J Cell Biol **145**(7): 1381-94.

Kimura, K., Cuvier, O. and Hirano, T. (2001). "Chromosome condensation by a human condensin complex in Xenopus egg extracts." J Biol Chem **276**(8): 5417-20.

Kimura, K. and Hirano, T. (1997). "ATP-dependent positive supercoiling of DNA by 13S condensin: a biochemical implication for chromosome condensation." Cell **90**(4): 625-34.

Kimura, K. and Hirano, T. (2000). "Dual roles of the 11S regulatory subcomplex in condensin functions." Proc Natl Acad Sci U S A **97**(22): 11972-7.

Kimura, K., Rybenkov, V. V., Crisona, N. J., Hirano, T. and Cozzarelli, N. R. (1999). "13S condensin actively reconfigures DNA by introducing global positive writhe: implications for chromosome condensation." Cell **98**(2): 239-48.

Kinzler, K. W. and Vogelstein, B. (1996). "Lessons from hereditary colorectal cancer." Cell **87**(2): 159-70.

Kipling, D. and Warburton, P. E. (1997). "Centromeres, CENP-B and Tigger too." Trends Genet **13**(4): 141-5.

Kornberg, R. D. (1974). "Chromatin structure: a repeating unit of histones and DNA." Science **184**(139): 868-71.

Kozak, M. (1987). "An analysis of 5'-noncoding sequences from 699 vertebrate messenger RNAs." Nucleic Acids Res **15**(20): 8125-48.

Kuhn, R. and Torres, R. M. (2002). "Cre/loxP recombination system and gene targeting." Methods Mol Biol **180**: 175-204.

Lacey, K. R., Jackson, P. K. and Stearns, T. (1999). "Cyclin-dependent kinase control of centrosome duplication." Proc Natl Acad Sci U S A **96**(6): 2817-22.

Lahti, J. M. (1999). "Use of gene knockouts in cultured cells to study apoptosis." Methods **17**(4): 305-12.

Lahti, J. M., Li, H. and Kidd, V. J. (1997). "Elimination of cyclin D1 in vertebrate cells leads to an altered cell cycle phenotype, which is rescued by overexpression of murine cyclins D1, D2, or D3 but not by a mutant cyclin D1." J Biol Chem **272**(16): 10859-69.

Lee, H., Trainer, A. H., Friedman, L. S., Thistlethwaite, F. C., Evans, M. J., Ponder, B. A. and Venkitaraman, A. R. (1999). "Mitotic checkpoint inactivation fosters transformation in cells lacking the breast cancer susceptibility gene, Brca2." Mol Cell **4**(1): 1-10.

Lengauer, C., Kinzler, K. W. and Vogelstein, B. (1997). "Genetic instability in colorectal cancers." Nature **386**(6625): 623-7.

Li, R. (1999). "Bifurcation of the mitotic checkpoint pathway in budding yeast." Proc Natl Acad Sci U S A **96**(9): 4989-94.

Li, R. and Murray, A. W. (1991). "Feedback control of mitosis in budding yeast." Cell **66**(3): 519-31.

Li, X. and Nicklas, R. B. (1995). "Mitotic forces control a cell-cycle checkpoint." Nature **373**(6515): 630-2.

Li, Y. and Benezra, R. (1996). "Identification of a human mitotic checkpoint gene: hsMAD2." Science **274**(5285): 246-8.

Li, Y. and Dodgson, J. B. (1995). "The chicken HMG-17 gene is dispensable for cell growth in vitro." Mol Cell Biol **15**(10): 5516-23.

Liao, H., Winkfein, R. J., Mack, G., Rattner, J. B. and Yen, T. J. (1995). "CENP-F is a protein of the nuclear matrix that assembles onto kinetochores at late G2 and is rapidly degraded after mitosis." J Cell Biol **130**(3): 507-18.

Liu, Y. C., Pan, J., Zhang, C., Fan, W., Collinge, M., Bender, J. R. and Weissman, S. M. (1999). "A MHC-encoded ubiquitin-like protein (FAT10) binds noncovalently to the spindle assembly checkpoint protein MAD2." Proc Natl Acad Sci U S A **96**(8): 4313-8.

Lo, A. W., Craig, J. M., Saffery, R., Kalitsis, P., Irvine, D. V., Earle, E., Magliano, D. J. and Choo, K. H. (2001). "A 330 kb CENP-A binding domain and altered replication timing at a human neocentromere." Embo J **20**: 2087-96.

Losada, A., Hirano, M. and Hirano, T. (1998). "Identification of Xenopus SMC protein complexes required for sister chromatid cohesion." Genes Dev **12**(13): 1986-97.

Luo, X., Fang, G., Coldiron, M., Lin, Y., Yu, H., Kirschner, M. W. and Wagner, G. (2000). "Structure of the Mad2 spindle assembly checkpoint protein and its interaction with Cdc20." Nat Struct Biol **7**(3): 224-9.

Luo, X., Tang, Z., Rizo, J. and Yu, H. (2002). "The Mad2 spindle checkpoint protein undergoes similar major conformational changes upon binding to either Mad1 or Cdc20." Mol Cell **9**(1): 59-71.

Mackay, A. M., Ainsztein, A. M., Eckley, D. M. and Earnshaw, W. C. (1998). "A dominant mutant of inner centromere protein (INCENP), a chromosomal protein, disrupts prometaphase congression and cytokinesis." J Cell Biol **140**(5): 991-1002.

Marsden, M. P. and Laemmli, U. K. (1979). "Metaphase chromosome structure: evidence for a radial loop model." Cell **17**(4): 849-58.

Martin-Lluesma, S., Stucke, V. M. and Nigg, E. A. (2002). " Role of Hec1 in spindle checkpoint signaling and kinetochore recruitment of Mad1/Mad2." Science **297**: 2267-70.

Martinez-Exposito, M. J., Kaplan, K. B., Copeland, J. and Sorger, P. K. (1999). "Retention of the BUB3 checkpoint protein on lagging chromosomes." Proc Natl Acad Sci U S A **96**(15): 8493-8.

Masumoto, H., Masukata, H., Muro, Y., Nozaki, N. and Okazaki, T. (1989). "A human centromere antigen (CENP-B) interacts with a short specific sequence in alphoid DNA, a human centromeric satellite." J Cell Biol **109**(5): 1963-73.

McCartney, B. M., Dierick, H. A., Kirkpatrick, C., Moline, M. M., Baas, A., Peifer, M. and Bejsovec, A. (1999). "Drosophila APC2 is a cytoskeletally-associated protein that regulates wingless signaling in the embryonic epidermis." J Cell Biol **146**(6): 1303-18.

McCartney, B. M. and Peifer, M. (2000). "Teaching tumour suppressors new tricks." Nat Cell Biol **2**(4): E58-60.

McCleland, M. L., Gardner, R. D., Kallio, M. J., Daum, J. R., Gorbsky, G. J., Burke, D. J. and Stukenberg, P. T. (2003). "The highly conserved Ndc80 complex is required for kinetochore assembly, chromosome congression, and spindle checkpoint activity." Genes Dev **17**: 101-14.

McEwen, B. F., Hsieh, C. E., Mattheyses, A. L. and Rieder, C. L. (1998). "A new look at kinetochore structure in vertebrate somatic cells using high-pressure freezing and freeze substitution." Chromosoma **107**(6-7): 366-75.

Meeks-Wagner, D., Wood, J. S., Garvik, B. and Hartwell, L. H. (1986). " Isolation of two genes that affect mitotic chromosome transmission in S. cerevisiae." Cell **44**: 53-63.

Meluh, P. B. and Koshland, D. (1995). " Evidence that the MIF2 gene of Saccharomyces cerevisiae encodes a centromere protein with homology to the mammalian centromere protein CENP-C." Mol Biol Cell **6**: 793-807.

Meluh, P. B., Yang, P., Glowczewski, L., Koshland, D. and Smith, M. M. (1998). "Cse4p is a component of the core centromere of Saccharomyces cerevisiae." Cell **94**(5): 607-13.

Michel, L. S., Liberal, V., Chatterjee, A., Kirchwegger, R., Pasche, B., Gerald, W., Dobles, M., Sorger, P. K., Murty, V. V. and Benezra, R. (2001). "MAD2 haplo-insufficiency causes premature anaphase and chromosome instability in mammalian cells." Nature **409**(6818): 355-9.

Millband, D. N. and Hardwick, K. G. (2002). "Fission yeast Mad3p is required for Mad2p to inhibit the anaphase- promoting complex and localizes to kinetochores in a Bub1p-, Bub3p-, and Mph1p-dependent manner." Mol Cell Biol **22**(8): 2728-42.

Mills, G. B., Schmandt, R., McGill, M., Amendola, A., Hill, M., Jacobs, K., May, C., Rodricks, A. M., Campbell, S. and Hogg, D. (1992). "Expression of TTK, a novel human protein kinase, is associated with cell proliferation." J Biol Chem **267**(22): 16000-6.

Mimori-Kiyosue, Y., Shiina, N. and Tsukita, S. (2000). "Adenomatous polyposis coli (APC) protein moves along microtubules and concentrates at their growing ends in epithelial cells." J Cell Biol **148**(3): 505-18.

Minshull, J., Sun, H., Tonks, N. K. and Murray, A. W. (1994). "A MAP kinase-dependent spindle assembly checkpoint in Xenopus egg extracts." Cell **79**(3): 475-86.

Moroi, Y., Hartman, A. L., Nakane, P. K. and Tan, E. M. (1981). "Distribution of kinetochore (centromere) antigen in mammalian cell nuclei." J Cell Biol **90**(1): 254-9.

Morrison, C. and Takeda, S. (2000). "Genetic analysis of homologous DNA recombination in vertebrate somatic cells." Int J Biochem Cell Biol **32**(8): 817-31.

Mountford, P., Zevnik, B., Duwel, A., Nichols, J., Li, M., Dani, C., Robertson, M., Chambers, I. and Smith, A. (1994). "Dicistronic targeting constructs: reporters and modifiers of mammalian gene expression." Proc Natl Acad Sci U S A **91**(10): 4303-7.

Murphy, T. D. and Karpen, G. H. (1995). "Localization of centromere function in a Drosophila minichromosome." Cell **82**(4): 599-609.

Murray, A. (1991). Cell Cycle Extracts. *Xenopus laevis*: Practical Uses in Cell and Molecular Biology. B. K. K. a. H. B. Peng. London, Academic Press, Inc. **36:** 581-605.

Nathke, I. S., Adams, C. L., Polakis, P., Sellin, J. H. and Nelson, W. J. (1996). "The adenomatous polyposis coli tumor suppressor protein localizes to plasma membrane sites involved in active cell migration." J Cell Biol **134**(1): 165-79.

Nicklas, R. B., Ward, S. C. and Gorbsky, G. J. (1995). "Kinetochore chemistry is sensitive to tension and may link mitotic forces to a cell cycle checkpoint." J Cell Biol **130**: 929-39.

Nishihashi, A., Haraguchi, T., Hiraoka, Y., Ikemura, T., Regnier, V., Dodson, H., Earnshaw, W. C. and Fukagawa, T. (2002). "CENP-I is essential for centromere function in vertebrate cells." Dev Cell **2**(4): 463-76.

O'Neill, T. J., Zhu, Y. and Gustafson, T. A. (1997). "Interaction of MAD2 with the carboxyl terminus of the insulin receptor but not with the IGFIR. Evidence for release from the insulin receptor after activation." J Biol Chem **272**(15): 10035-40.

Ochs, R. L. and Press, R. I. (1992). "Centromere autoantigens are associated with the nucleolus." Exp Cell Res **200**(2): 339-50.

Ohshima, K., Haraoka, S., Yoshioka, S., Hamasaki, M., Fujiki, T., Suzumiya, J., Kawasaki, C., Kanda, M. and Kikuchi, M. (2000). "Mutation analysis of mitotic checkpoint genes (hBUB1 and hBUBR1) and microsatellite instability in adult T-cell leukemia/lymphoma." Cancer Lett **158**(2): 141-50.

Ohzeki, J., Nakano, M., Okada, T. and Masumoto, H. (2002). "CENP-B box is required for de novo centromere chromatin assembly on human alphoid DNA." J Cell Biol **159**(5): 765-75.

Ouyang, B., Knauf, J. A., Ain, K., Nacev, B. and Fagin, J. A. (2002). "Mechanisms of aneuploidy in thyroid cancer cell lines and tissues: evidence for mitotic checkpoint dysfunction without mutations in BUB1 and BUBR1." Clin Endocrinol (Oxf) **56**(3): 341-50.

Pangilinan, F., Li, Q., Weaver, T., Lewis, B. C., Dang, C. V. and Spencer, F. (1997). "Mammalian BUB1 protein kinases: map positions and in vivo expression." Genomics **46**(3): 379-88.

Peifer, M. and Polakis, P. (2000). "Wnt signaling in oncogenesis and embryogenesis--a look outside the nucleus." Science **287**(5458): 1606-9.

Perez-Castro, A. V., Shamanski, F. L., Meneses, J. J., Lovato, T. L., Vogel, K. G., Moyzis, R. K. and Pedersen, R. (1998). "Centromeric protein B null mice are viable with no apparent abnormalities." Dev Biol **201**(2): 135-43.

Pfleger, C. M. and Kirschner, M. W. (2000). "The KEN box: an APC recognition signal distinct from the D box targeted by Cdh1." Genes Dev **14**(6): 655-65.

Piel, M. and Bornens, M. (2001). "Centrosome reproduction in vitro: mammalian centrosomes in Xenopus lysates." Methods Cell Biol **67**: 289-304.

Planas-Silva, M. D. and Weinberg, R. A. (1997). "The restriction point and control of cell proliferation." Curr Opin Cell Biol **9**(6): 768-72.

Poelzl, G., Kasai, Y., Mochizuki, N., Shaul, P. W., Brown, M. and Mendelsohn, M. E. (2000). "Specific association of estrogen receptor beta with the cell cycle spindle assembly checkpoint protein, MAD2." Proc Natl Acad Sci U S A **97**(6): 2836-9.

Porter, A. (1998). "Controlling your losses: conditional gene silencing in mammals." Trends Genet **14**(2): 73-9.

Putkey, F. R., Cramer, T., Morphew, M. K., Silk, A. D., Johnson, R. S., McIntosh, J. R. and Cleveland, D. W. (2002). "Unstable kinetochore-microtubule capture and chromosomal instability following deletion of CENP-E." Dev Cell **3**(3): 351-65.

Rao, H., Uhlmann, F., Nasmyth, K. and Varshavsky, A. (2001). "Degradation of a cohesin subunit by the N-end rule pathway is essential for chromosome stability." Nature **410**(6831): 955-9.

Rattner, J. B., Rao, A., Fritzler, M. J., Valencia, D. W. and Yen, T. J. (1993). "CENP-F is a .ca 400 kDa kinetochore protein that exhibits a cell-cycle dependent localization." Cell Motil Cytoskeleton **26**(3): 214-26.

Rebagliati, M. R., Weeks, D. L., Harvey, R. P. and Melton, D. A. (1985). "Identification and cloning of localized maternal RNAs from Xenopus eggs." Cell **42**(3): 769-77.

Reis, R. M., Nakamura, M., Masuoka, J., Watanabe, T., Colella, S., Yonekawa, Y., Kleihues, P. and Ohgaki, H. (2001). "Mutation analysis of hBUB1, hBUBR1 and hBUB3 genes in glioblastomas." Acta Neuropathol (Berl) **101**(4): 297-304.

Rieder, C. L., Cole, R. W., Khodjakov, A. and Sluder, G. (1995). "The checkpoint delaying anaphase in response to chromosome monoorientation is mediated by an inhibitory signal produced by unattached kinetochores." J Cell Biol **130**(4): 941-8.

Rieder, C. L. and Salmon, E. D. (1998). "The vertebrate cell kinetochore and its roles during mitosis." Trends Cell Biol **8**(8): 310-8.

Rieder, C. L., Schultz, A., Cole, R. and Sluder, G. (1994). "Anaphase onset in vertebrate somatic cells is controlled by a checkpoint that monitors sister kinetochore attachment to the spindle." J Cell Biol **127**(5): 1301-10.

Roberts, B. T., Farr, K. A. and Hoyt, M. A. (1994). "The Saccharomyces cerevisiae checkpoint gene BUB1 encodes a novel protein kinase." Mol Cell Biol **14**(12): 8282-91.

Russel, S. a. (2001). Molecular Cloning: A Laboratory Manual. Cold Spring Harbour, New York, Cold Spring Harbour Laboratory Press.

Saeki, A., Tamura, S., Ito, N., Kiso, S., Matsuda, Y., Yabuuchi, I., Kawata, S. and Matsuzawa, Y. (2002). "Frequent impairment of the spindle assembly checkpoint in hepatocellular carcinoma." Cancer **94**(7): 2047-54.

Saka, Y., Sutani, T., Yamashita, Y., Saitoh, S., Takeuchi, M., Nakaseko, Y. and Yanagida, M. (1994). "Fission yeast cut3 and cut14, members of a ubiquitous protein family, are required for chromosome condensation and segregation in mitosis." Embo J **13**(20): 4938-52.

Samejima, K., Tone, S. and Earnshaw, W. C. (2001). "CAD/DFF40 nuclease is dispensable for high molecular weight DNA cleavage and stage I chromatin condensation in apoptosis." J Biol Chem **276**(48): 45427-32.

Sato, M., Sekido, Y., Horio, Y., Takahashi, M., Saito, H., Minna, J. D., Shimokata, K. and Hasegawa, Y. (2000). "Infrequent mutation of the hBUB1 and hBUBR1 genes in human lung cancer." Jpn J Cancer Res **91**(5): 504-9.

Savoian, M. S., Goldberg, M. L. and Rieder, C. L. (2000). "The rate of poleward chromosome motion is attenuated in Drosophila zw10 and rod mutants." Nat Cell Biol **2**(12): 948-52.

Scaerou, F., Aguilera, I., Saunders, R., Kane, N., Blottiere, L. and Karess, R. (1999). "The rough deal protein is a new kinetochore component required for accurate chromosome segregation in Drosophila." J Cell Sci **112**(Pt 21): 3757-68.

Scaerou, F., Starr, D. A., Piano, F., Papoulas, O., Karess, R. E. and Goldberg, M. L. (2001). "The ZW10 and Rough Deal checkpoint proteins function together in a large, evolutionarily conserved complex targeted to the kinetochore." J Cell Sci **114**(Pt 17): 3103-14.

Seeley, T. W., Wang, L. and Zhen, J. Y. (1999). "Phosphorylation of human MAD1 by the BUB1 kinase in vitro." Biochem Biophys Res Commun **257**(2): 589-95.

Shannon, K. B., Canman, J. C. and Salmon, E. D. (2002). "Mad2 and BubR1 Function in a Single Checkpoint Pathway that Responds to a Loss of Tension." Mol Biol Cell **13**(10): 3706-19.

Shapiro, L., Heidenreich, K. A., Meintzer, M. K. and Dinarello, C. A. (1998). "Role of p38 mitogen-activated protein kinase in HIV type 1 production in vitro." Proc Natl Acad Sci U S A **95**(13): 7422-6.

Sharp-Baker, H. and Chen, R. H. (2001). "Spindle checkpoint protein Bub1 is required for kinetochore localization of Mad1, Mad2, Bub3, and CENP-E, independently of its kinase activity." J Cell Biol **153**(6): 1239-50.

Shelby, R. D., Vafa, O. and Sullivan, K. F. (1997). "Assembly of CENP-A into centromeric chromatin requires a cooperative array of nucleosomal DNA contact sites." J Cell Biol **136**(3): 501-13.

Shichiri, M., Yoshinaga, K., Hisatomi, H., Sugihara, K. and Hirata, Y. (2002). "Genetic and epigenetic inactivation of mitotic checkpoint genes hBUB1 and hBUBR1 and their relationship to survival." Cancer Res **62**(1): 13-7.

Shinohara, A., Ogawa, H. and Ogawa, T. (1992). "Rad51 protein involved in repair and recombination in S. cerevisiae is a RecA-like protein." Cell **69**(3): 457-70.

Sironi, L., Mapelli, M., Knapp, S., De Antoni, A., Jeang, K. T. and Musacchio, A. (2002). "Crystal structure of the tetrameric Mad1-Mad2 core complex: implications of a 'safety belt' binding mechanism for the spindle checkpoint." Embo J **21**(10): 2496-506.

Sironi, L., Melixetian, M., Faretta, M., Prosperini, E., Helin, K. and Musacchio, A. (2001). "Mad2 binding to Mad1 and Cdc20, rather than oligomerization, is required for the spindle checkpoint." Embo J **20**(22): 6371-82.

Skoufias, D. A., Andreassen, P. R., Lacroix, F. B., Wilson, L. and Margolis, R. L. (2001). "Mammalian mad2 and bub1/bubR1 recognize distinct spindle-attachment and kinetochore-tension checkpoints." Proc Natl Acad Sci U S A **98**(8): 4492-7.

Smith, J. and Burt, D. W. (1998). "Parameters of the chicken genome (Gallus gallus)." Anim Genet **29**(4): 290-4.

Sonoda, E., Matsusaka, T., Morrison, C., Vagnarelli, P., Hoshi, O., Ushiki, T., Nojima, K., Fukagawa, T., Waizenegger, I. C., Peters, J. M., Earnshaw, W. C. and Takeda, S. (2001). "Scc1/Rad21/Mcd1 is required for sister chromatid cohesion and kinetochore function in vertebrate cells." Dev Cell **1**(6): 759-70.

Sonoda, E., Morrison, C., Yamashita, Y. M., Takata, M. and Takeda, S. (2001). "Reverse genetic studies of homologous DNA recombination using the chicken B-lymphocyte line, DT40." Philos Trans R Soc Lond B Biol Sci **356**(1405): 111-7.

Sonoda, E., Sasaki, M. S., Buerstedde, J. M., Bezzubova, O., Shinohara, A., Ogawa, H., Takata, M., Yamaguchi-Iwai, Y. and Takeda, S. (1998). "Rad51-deficient vertebrate cells accumulate chromosomal breaks prior to cell death." Embo J **17**(2): 598-608.

Speliotes, E. K., Uren, A., Vaux, D. and Horvitz, H. R. (2000). "The survivin-like C. elegans BIR-1 protein acts with the Aurora-like kinase AIR-2 to affect chromosomes and the spindle midzone." Mol Cell **6**(2): 211-23.

Starr, D. A., Saffery, R., Li, Z., Simpson, A. E., Choo, K. H., Yen, T. J. and Goldberg, M. L. (2000). "HZwint-1, a novel human kinetochore component that interacts with HZW10." J Cell Sci **113**(Pt 11): 1939-50.

Starr, D. A., Williams, B. C., Hays, T. S. and Goldberg, M. L. (1998). "ZW10 helps recruit dynactin and dynein to the kinetochore." J Cell Biol **142**(3): 763-74.

Starr, D. A., Williams, B. C., Li, Z., Etemad-Moghadam, B., Dawe, R. K. and Goldberg, M. L. (1997). "Conservation of the centromere/kinetochore protein ZW10." J Cell Biol **138**(6): 1289-301.

Steffensen, S., Coelho, P. A., Cobbe, N., Vass, S., Costa, M., Hassan, B., Prokopenko, S. N., Bellen, H., Heck, M. M. and Sunkel, C. E. (2001). "A role for Drosophila SMC4 in the resolution of sister chromatids in mitosis." Curr Biol **11**(5): 295-307.

Strunnikov, A. V., Hogan, E. and Koshland, D. (1995). "SMC2, a Saccharomyces cerevisiae gene essential for chromosome segregation and condensation, defines a subgroup within the SMC family." Genes Dev **9**(5): 587-99.

Stucke, V. M., Sillje, H. H., Arnaud, L. and Nigg, E. A. (2002). "Human Mps1 kinase is required for the spindle assembly checkpoint but not for centrosome duplication." Embo J **21**(7): 1723-32.

Sudakin, V., Chan, G. K. and Yen, T. J. (2001). "Checkpoint inhibition of the APC/C in HeLa cells is mediated by a complex of BUBR1, BUB3, CDC20, and MAD2." J Cell Biol **154**(5): 925-36.

Sugata, N., Li, S., Earnshaw, W. C., Yen, T. J., Yoda, K., Masumoto, H., Munekata, E., Warburton, P. E. and Todokoro, K. (2000). "Human CENP-H multimers colocalize with CENP-A and CENP-C at active centromere--kinetochore complexes." Hum Mol Genet **9**(19): 2919-26.

Sugata, N., Munekata, E. and Todokoro, K. (1999). "Characterization of a novel kinetochore protein, CENP-H." J Biol Chem **274**(39): 27343-6.

Sullivan, B. A. and Schwartz, S. (1995). "Identification of centromeric antigens in dicentric Robertsonian translocations: CENP-C and CENP-E are necessary components of functional centromeres." Hum Mol Genet **4**(12): 2189-97.

Sumara, I., Vorlaufer, E., Gieffers, C., Peters, B. H. and Peters, J. M. (2000). "Characterization of vertebrate cohesin complexes and their regulation in prophase." J Cell Biol **151**(4): 749-62.

Sumara, I., Vorlaufer, E., Stukenberg, P. T., Kelm, O., Redemann, N., Nigg, E. A. and Peters, J. M. (2002). "The dissociation of cohesin from chromosomes in prophase is regulated by Polo-like kinase." Mol Cell **9**(3): 515-25.

Sutani, T., Yuasa, T., Tomonaga, T., Dohmae, N., Takio, K. and Yanagida, M. (1999). "Fission yeast condensin complex: essential roles of non-SMC subunits for condensation and Cdc2 phosphorylation of Cut3/SMC4." Genes Dev **13**(17): 2271-83.

Takahashi, K., Chen, E. S. and Yanagida, M. (2000). "Requirement of Mis6 centromere connector for localizing a CENP-A-like protein in fission yeast." Science **288**(5474): 2215-9.

Takahashi, T., Haruki, N., Nomoto, S., Masuda, A., Saji, S. and Osada, H. (1999). "Identification of frequent impairment of the mitotic checkpoint and molecular analysis of the mitotic checkpoint genes, hsMAD2 and p55CDC, in human lung cancers." Oncogene **18**(30): 4295-300.

Takata, M., Sabe, H., Hata, A., Inazu, T., Homma, Y., Nukada, T., Yamamura, H. and Kurosaki, T. (1994). "Tyrosine kinases Lyn and Syk regulate B cell

receptor-coupled Ca2+ mobilization through distinct pathways." Embo J **13**(6): 1341-9.
Takeda, S., Masteller, E. L., Thompson, C. B. and Buerstedde, J. M. (1992). "RAG-2 expression is not essential for chicken immunoglobulin gene conversion." Proc Natl Acad Sci U S A **89**(9): 4023-7.
Takenaka, K., Moriguchi, T. and Nishida, E. (1998). "Activation of the protein kinase p38 in the spindle assembly checkpoint and mitotic arrest." Science **280**(5363): 599-602.
Tang, Z., Bharadwaj, R., Li, B. and Yu, H. (2001). "Mad2-Independent inhibition of APCCdc20 by the mitotic checkpoint protein BubR1." Dev Cell **1**(2): 227-37.
Tavtigian, S. V., Simard, J., Rommens, J., Couch, F., Shattuck-Eidens, D., Neuhausen, S., Merajver, S., Thorlacius, S., Offit, K., Stoppa-Lyonnet, D., Belanger, C., Bell, R., Berry, S., Bogden, R., Chen, Q., Davis, T., Dumont, M., Frye, C., Hattier, T., Jammulapati, S., Janecki, T., Jiang, P., Kehrer, R., Leblanc, J. F., Goldgar, D. E. and et al. (1996). "The complete BRCA2 gene and mutations in chromosome 13q-linked kindreds." Nat Genet **12**(3): 333-7.
Taylor, S. S., Ha, E. and McKeon, F. (1998). "The human homologue of Bub3 is required for kinetochore localization of Bub1 and a Mad3/Bub1-related protein kinase." J Cell Biol **142**(1): 1-11.
Taylor, S. S., Hussein, D., Wang, Y., Elderkin, S. and Morrow, C. J. (2001). "Kinetochore localisation and phosphorylation of the mitotic checkpoint components Bub1 and BubR1 are differentially regulated by spindle events in human cells." J Cell Sci **114**(Pt 24): 4385-95.
Taylor, S. S. and McKeon, F. (1997). "Kinetochore localization of murine Bub1 is required for normal mitotic timing and checkpoint response to spindle damage." Cell **89**(5): 727-35.
Tighe, A., Johnson, V. L., Albertella, M. and Taylor, S. S. (2001). "Aneuploid colon cancer cells have a robust spindle checkpoint." EMBO Rep **2**: 609-614.
Tomkiel, J., Cooke, C. A., Saitoh, H., Bernat, R. L. and Earnshaw, W. C. (1994). "CENP-C is required for maintaining proper kinetochore size and for a timely transition to anaphase." J Cell Biol **125**(3): 531-45.
Uhlmann, F., Lottspeich, F. and Nasmyth, K. (1999). "Sister-chromatid separation at anaphase onset is promoted by cleavage of the cohesin subunit Scc1." Nature **400**(6739): 37-42.
Uren, A. G., Wong, L., Pakusch, M., Fowler, K. J., Burrows, F. J., Vaux, D. L. and Choo, K. H. (2000). "Survivin and the inner centromere protein INCENP show similar cell- cycle localization and gene knockout phenotype." Curr Biol **10**(21): 1319-28.
Utz, P. J. and Anderson, P. (2000). "Life and death decisions: regulation of apoptosis by proteolysis of signaling molecules." Cell Death Differ **7**(7): 589-602.
Vafa, O. and Sullivan, K. F. (1997). "Chromatin containing CENP-A and alpha-satellite DNA is a major component of the inner kinetochore plate." Curr Biol **7**(11): 897-900.
Volpe, T. A., Kidner, C., Hall, I. M., Teng, G., Grewal, S. I. and Martienssen, R. A. (2002). "Regulation of heterochromatic silencing and histone H3 lysine-9 methylation by RNAi." Science **297**(5588): 1833-7.
Voullaire, L. E., Slater, H. R., Petrovic, V. and Choo, K. H. (1993). "A functional marker centromere with no detectable alpha-satellite, satellite III, or CENP-

B protein: activation of a latent centromere?" Am J Hum Genet **52**(6): 1153-63.
Waizenegger, I. C., Hauf, S., Meinke, A. and Peters, J. M. (2000). "Two distinct pathways remove mammalian cohesin from chromosome arms in prophase and from centromeres in anaphase." Cell **103**(3): 399-410.
Wang, J., Takagaki, Y. and Manley, J. L. (1996). "Targeted disruption of an essential vertebrate gene: ASF/SF2 is required for cell viability." Genes Dev **10**(20): 2588-99.
Wang, X., Babu, J. R., Harden, J. M., Jablonski, S. A., Gazi, M. H., Lingle, W. L., de Groen, P. C., Yen, T. J. and van Deursen, J. M. (2001). "The mitotic checkpoint protein hBUB3 and the mRNA export factor hRAE1 interact with GLE2p-binding sequence (GLEBS)-containing proteins." J Biol Chem **276**(28): 26559-67.
Wang, X., Jin, D. Y., Wong, Y. C., Cheung, A. L., Chun, A. C., Lo, A. K., Liu, Y. and Tsao, S. W. (2000). "Correlation of defective mitotic checkpoint with aberrantly reduced expression of MAD2 protein in nasopharyngeal carcinoma cells." Carcinogenesis **21**(12): 2293-7.
Wang, X. M., Zhai, Y. and Ferrell, J. E., Jr. (1997). "A role for mitogen-activated protein kinase in the spindle assembly checkpoint in XTC cells." J Cell Biol **137**(2): 433-43.
Warburton, P. E., Cooke, C. A., Bourassa, S., Vafa, O., Sullivan, B. A., Stetten, G., Gimelli, G., Warburton, D., Tyler-Smith, C., Sullivan, K. F., Poirier, G. G. and Earnshaw, W. C. (1997). "Immunolocalization of CENP-A suggests a distinct nucleosome structure at the inner kinetochore plate of active centromeres." Current Biology **7**(11): 901-4.
Wassmann, K. and Benezra, R. (1998). "Mad2 transiently associates with an APC/p55Cdc complex during mitosis." Proc Natl Acad Sci U S A **95**(19): 11193-8.
Waters, J. C., Chen, R. H., Murray, A. W. and Salmon, E. D. (1998). "Localization of Mad2 to kinetochores depends on microtubule attachment, not tension." J Cell Biol **141**(5): 1181-91.
Weiss, E. and Winey, M. (1996). "The Saccharomyces cerevisiae spindle pole body duplication gene MPS1 is part of a mitotic checkpoint." J Cell Biol **132**(1-2): 111-23.
Wheatley, S. P., Carvalho, A., Vagnarelli, P. and Earnshaw, W. C. (2001). "INCENP is required for proper targeting of Survivin to the centromeres and the anaphase spindle during mitosis." Curr Biol **11**(11): 886-90.
Wheatley, S. P. and Wang, Y. L. (1998). "Indirect immunofluorescence microscopy in cultured cells." Methods Cell Biol **57**: 313-32.
Williams, B. C. and Goldberg, M. L. (1994). "Determinants of Drosophila zw10 protein localization and function." J Cell Sci **107**(Pt 4): 785-98.
Winey, M., Goetsch, L., Baum, P. and Byers, B. (1991). "MPS1 and MPS2: novel yeast genes defining distinct steps of spindle pole body duplication." J Cell Biol **114**(4): 745-54.
Wojcik, E., Basto, R., Serr, M., Scaerou, F., Karess, R. and Hays, T. (2001). "Kinetochore dynein: its dynamics and role in the transport of the Rough deal checkpoint protein." Nat Cell Biol **3**(11): 1001-7.
Wood, K. W., Sakowicz, R., Goldstein, L. S. and Cleveland, D. W. (1997). "CENP-E is a plus end-directed kinetochore motor required for metaphase chromosome alignment." Cell **91**(3): 357-66.

Wooster, R., Bignell, G., Lancaster, J., Swift, S., Seal, S., Mangion, J., Collins, N., Gregory, S., Gumbs, C. and Micklem, G. (1995). "Identification of the breast cancer susceptibility gene BRCA2." Nature **378**(6559): 789-92.

Wu, H., Lan, Z., Li, W., Wu, S., Weinstein, J., Sakamoto, K. M. and Dai, W. (2000). "p55CDC/hCDC20 is associated with BUBR1 and may be a downstream target of the spindle checkpoint kinase." Oncogene **19**(40): 4557-62.

Yao, X., Abrieu, A., Zheng, Y., Sullivan, K. F. and Cleveland, D. W. (2000). "CENP-E forms a link between attachment of spindle microtubules to kinetochores and the mitotic checkpoint." Nat Cell Biol **2**(8): 484-91.

Yasuda, T., Maeda, A., Kurosaki, M., Tezuka, T., Hironaka, K., Yamamoto, T. and Kurosaki, T. (2000). "Cbl suppresses B cell receptor-mediated phospholipase C (PLC)-gamma2 activation by regulating B cell linker protein-PLC-gamma2 binding." J Exp Med **191**(4): 641-50.

Yen, T. J., Compton, D. A., Wise, D., Zinkowski, R. P., Brinkley, B. R., Earnshaw, W. C. and Cleveland, D. W. (1991). "CENP-E, a novel human centromere-associated protein required for progression from metaphase to anaphase." Embo J **10**(5): 1245-54.

Yen, T. J., Li, G., Schaar, B. T., Szilak, I. and Cleveland, D. W. (1992). "CENP-E is a putative kinetochore motor that accumulates just before mitosis." Nature **359**(6395): 536-9.

Yu, H. G., Hiatt, E. N. and Dawe, R. K. (2000). "The plant kinetochore." Trends Plant Sci **5**(12): 543-7.

Yucel, J. K., Marszalek, J. D., McIntosh, J. R., Goldstein, L. S., Cleveland, D. W. and Philp, A. V. (2000). "CENP-meta, an essential kinetochore kinesin required for the maintenance of metaphase chromosome alignment in Drosophila." J Cell Biol **150**(1): 1-11.

Zecevic, M., Catling, A. D., Eblen, S. T., Renzi, L., Hittle, J. C., Yen, T. J., Gorbsky, G. J. and Weber, M. J. (1998). "Active MAP kinase in mitosis: localization at kinetochores and association with the motor protein CENP-E." J Cell Biol **142**(6): 1547-58.

Zetterberg, A., Larsson, O. and Wiman, K. G. (1995). "What is the restriction point?" Curr Opin Cell Biol **7**(6): 835-42.

Zheng, B., Sage, M., Sheppeard, E. A., Jurecic, V. and Bradley, A. (2000). "Engineering mouse chromosomes with Cre-loxP: range, efficiency, and somatic applications." Mol Cell Biol **20**(2): 648-55.

Zhou, J., Panda, D., Landen, J. W., Wilson, L. and Joshi, H. C. (2002). "Minor alteration of microtubule dynamics causes loss of tension across kinetochore pairs and activates the spindle checkpoint." J Biol Chem **277**(19): 17200-8.

Appendix 1

Full length chicken BubR1 cDNA sequence with the ATG and STOP codon indicated in red.

TTCGCGCGGTCGCCTCAGAGCTGGGGCTGCGGCGCTCAGAGCTTGAAGATGTCACGGGACGGTGACG
ATGAGTGGGAGCTGAGCAAGGAGAACGTGCAGCCGCTGCGGCAGGGCCGGGTCATGGCCACACTGCA
GGAGGCCCTGGCTCAGCAGGACACCTCCAGCCACACTGCCGCTCAGCTGAGAAAACAAGAATTCGAA
TCAGAAATCAGATTTTATTCTGGAGATGATCCACTGGATGTCTGGGACAGGTACATCAAGTGGACCG
AGCAAACCTTCCCCCAGGGTGGAAAGGAGAGTAATCTCTCTGCAGTATTGGAAAGGGCAGTGAAAGC
ACTCAACAAGCAGCAGAGATACTACCAAGATCCCCGCTATCTTAGTCTCTGGCTCAAATTTGGAAAT
TGCTGTAATGAACCCTTGGATCTGTACAGTTATCTGCATAGTCAGGAAATTGGTACAACGCTGGCAC
AACTCTATATTACATGGGCAGAAGAACTTGAGGCTAGAGGAAGTTTTAAGAAAGCAGATATAATCTT
CCAGGAAGGCCTTAATCGCAAGGCAGAGCCTTTGGACAAACTCCAGTCTCATCACAGGCAGTTTCAG
ACCCGTGTTTCTCGGCAAACACTACTGGGACTTGAGGAAGCTGCTGATGAAGATACGGGTCTTCTGG
AAACTGAAGAACCTCAGAGGAGCACATTGGCAGATCTAAAAGGCGGGGGAAAGAAAAAAGTGAGAGG
CTCAATTAGTCGTGTAGGAGATGCACTTAAAGCCACAAACCAAAACAGAAACTTCCAGACTCCTCAG
CAGTTTTCAAACAATCTGGGTTTTGCTGTGTTTGATGAAAATTCCGCTTCAGCTTCTGGACCTGAGA
TTCCCATACTTACTCCACAGCACTGGACAGAACCTCCAGCTCCAAGGGGCAAGGAGAATGAACTAAG
CGCAGGACCTTGGAACTCTGGGAGGCGTCCTCGCAACAGTGCAAATTCTGGTGTAGAAGTGCCCTGT
CCAATGCCCAGTTTCACCCCCTACGTGGAAGAGTCAGCTCAGCAGCAAGTCATGACTCCCTGCAAGA
TTGAACCCAGCATAAACCACGTTTTAAGCGCTCGCAAGCCTGAGAAGGAGGAGGATCCTCTACGACG
GGTCCAGAATCACCATCAGGATACCCAGGAGAAGAAAGAGGTGGTGAGTACTGTAAAGACAAAGTTT
ATGCTGGAGTGGAGGAATTCTCTTTCGAAGAGATTCGAGCTGAAGTCTACAGAAAGAAAGCAAAAAA
GAAAGCTGAAGAGGAGATACAGACCATAGCACAGAAAAAGGAAGAAATACAAAAGAAAATTGAGGAA
CTGGAGAAGAAATTAAAGGAGAAAGAAAACCACAAGCAACAACAATTACATGAGCAGCCAACAGAGG
TAACAAAGCCTTCACCACCTTTGGGACTAAAAGAACGTACTTTATCCAGTGCAACAGAACTTGGGAT
GAAACAGCCTCACTTGCAAAGTGAATGCTGCCTCTCAGAAGATATTCAACTGCATAAACTGTCTTGT
TCTGAGGATACGGAAGGAGGAAGTGTATTTTCTGACTCTGAGGATGAACAGGCAGATCAGAGAAATA
AAGCCAACCTTGGGAAAAAAAGATGCAGTATTCCTTCCCCCACCAGATCTGCTACATCTTTCTCCAT
ATTTGATGAATCATCTACTTCAGCAAACCAAAATACAAGTCGTTCTACAGATCGTGGCCAGAAAACT
GCTCGGCGCCCTCTTGCTGTTCGCAAACCTTCAGAGTCTATCACTGCGAAAGAAAACTTACAACCAG
AGGCCTGTGATGAGCTGCATGGAATTGAACCTTTGACTGAAGATGCCATTGTGACAGGCTCCTACAA
GCACAAAAGCCTTTGTGCCAACCCAGAAGACACGTGTGATTTTGTTAGGGCTGCCCATCTGGCCTCA
ACTCCCTTTCATGGGGTGGTAGCTCAGAGAATCCCAGCTCCTGCTTATTCACAGAGTGTTCTAAAGG
AAGACTGTGCAGAATCTAAGAGTGCACCTCTGGATGAGAAAACACCAGTTTGCGAGGGAACATACAG
TGAAGCTCTCTGTGTAAATAAATTGAGCCCGATCATGGAAGCAAGCCTGGAGGATACTCATTTGTCA
GGTTCTTCTGTCTCTTCAGGATCTTCTCTTTCTTCTGTTACACAAACATCCACAATTAAATACCTGC
ACATCCCTGAGAAACTGGAACTTGCTCAGAGCTTGCCTGCTGAACCAATTACTGATCCTGGAGGTGA
TGATGCAACTGAGTTCTTGTGGACTGCTGAACAGCGTAAAAAGCTTCTAGATCCCATGCCAGAGTCA
TTGACTGCTTCTCCACATTTTCATTTGGAGGCTGGTTTCCTGCCTGTCATTGAGTTTGAGAAAGACA
TTGAGCTAGGAAATGAGACTTATTGTATCAAACGGGAATATTGGACCAATGAAGAATACAAAATGCT
TTTTGCCATTCCTGTTAACTTTCTTCAGTTGGATGCAAAGGGATTTGCAATAAAGGTGTATTCTCAG
CCTGTGCCTTGGGATTTTTATATCATGCTTCAACTGCAGGAGCGTTTGAATGCTGACTTTGACCAAA
GCTTCAGTGGGAACTGTAGCTGTTTCTTGTACCAAGACGGCTGTGCTATCCTGCACAAGAATATAAA
TCGCTTCACGCTTGGGGATGTTATTTGTGGCTGCAAGTCCATTGAAGAGGAAGTTATTCTACTAGTT
GTTTATAATCTTCTGGGTGTGGTAGAGAAGCTCCACAAAGCAGAGATTGTCCATGGAGATCTGAGGC
CAGAAATATTCTTTCTGGGAGACAGGATCTGTGATCCATTTGCTAATAATGGGATGACAAGAGCTCT
GAAGATAGTGGATTTCTCTCACAGTCTGGATTTAAGGTTGCAGTCTCGAGTAAGCTTGCCCAACAGC
TTTCCAATATCTCAGACTCCTCATGGACAGCAGCTTCTGGCAAAAAGTTGCCTTCCTTATCAGGCAG
ACTTGGTTGGTATAGCAGATATAGCCCATTTGATGCTGTTTGGTGAGCATGTCCAGGTCTATCAGGA
GAACTCCGTTTGGAAAATCAGCCAAAATGTATCCAAGACTGTTGGCTCTGATTTCTGGGGTAAATTT
TTCCGGCAAATTCTGAATGCAGATGGTAAGTCCACAGTGCTTCTGCTGAGGGAGTTGAGAGAGGAAA
TGAGTGACATGTTTGACAGCTGTTTCCAAGAACGTCTTTGTGAATCCTTAGTAGCGCTGGGTGATGT
TTTCTTCTTGGAGAAGTTCTGATTTCACAGAGGACAAATCTGTTTTGTATTATAGAAGGAAATTTGT
TGTTAACATCTTATTTTATTCAAATGTAAGCATGAGCAGTGATTGTAGCCATTTCCACAGTACTTCA
CACAGGACTCACCAAAGCACATCACATCAGTGCCTAAATATCCGAAAACTGTTACGTGAACTAGTCT

GTGTCCAAGCAGTTTGCCACAGAAAATAGGTTGTCCTAACTGTCCCCCTACCCTTTTTGTATAGCTC
CTTAAAAATGTTTAGTGCCTTGTTCATGCTGCATTCTCAAAAGTGTCTTGGTCCTCCATTTATATTG
TCTAGTGTACTGTTTTTAATCATTGCTTCTTTAATAAAGTTGTATCTTGATAGTAAAAAAAAAAAAA
AAAA

Appendix 2

AL894189 *Xenopus tropicalis* CENP-C EST

AATTCCCCGGGGAGAAATTATTCAACCTTCCAAAACACCAAATGTTCGTCGTTCCAAAAGAACAAGA
GTCAAGCCTTTGGCATACTGGAAAGGAGAACGTGTAAATTACAAGATCAGACCATCAGGAGGCTTTT
TGGTTGAAGGGGTTGTACCTCCAGCAGAGGTGGAACCACCAAGGAAAGCTTTGGCAAAAAGACGAGT
GTACAGAAAACAAAAAGGGGATATACCTACATGTGTAGAACCTCCAAAAGATGATTACCTAGAGCCT
GCCAATGTTATTGATGTGGCTACAGGAACAATAACAAGTATTGAATGTGTCTGTACCAGTGAAGACT
GCTTTTACCATTGGCCAGATAAACCAGTATCCATTTGCAAGAGTATTAGCACCTCAGATTTTTCAAC
AGGAAAAGTAAAAATTGGCCCTCTCCAAGAGAAGGGTTTGCAATATGTATGTTTGCATACAATTGTA
TTCTACATAATGACGGGTTCTGTGCAGTTAACACTTCATTTGACTACTTACAATCTGAAAACAGGGG
ACTTTTTTTTACATACCACCTGGCAATATGTACAAGATAACGAATCTGCTAAACGAAGATGCACTTC
TTATTTTTACTCAAATTAAAGGTTGATAGTAGCATAACCTGAACAACAATGT

BF047824 *Xenopus laevis* CENP-H EST

GAAGACCTTAAAGTTTCCTACCAAAATAAAACAATGGTGCTGCAGAGAATGCAGTTTGTGAATGCTC
TTCTCAATAAGATACAAGATAACAACAATGAATCAAGGTTAATCCAAGAGAAATTCACTCACATTTT
GACACTCTCCTCTGCAGTAATTAACTCACAGCAGGAGACACGAGAATTGGAGGACAGATTGTATGAC
ATCAGAAAGAAGAGATTAGTGCTAAAGGAACTTGGCTCTGCTAAAATGTTAGAAATTCAAACCCTGA
AAAGCAACTGGAAAGCCAATAGAGAAGAAACGCAAAATGAGAAAATAAAGAGACTGAATAAAATCCT
TAAAGATGAAATAGACAGCACAACAGTATTACAGAATGTGTTTCAGAACATCATTCTTGCCAGTCAC
GTTGATTGGGCAAAGGATCCACAACTAACAGATATTGGTCTAAAGTTAGAAACAAAC

BJ061344 *Xenopus laevis* Zwint EST

CAGCTGGTCGGCTGCTGGNANCTTTGCCACGTGTCCTGTGTGTGGATGGGCGGCACAGNANAGGACA
GCGATGGAGAAGCTAAAGTGTTGCTGGATTATTCTATGGAGAGACGGAGGAAGCAGAAAATGCTCTG
TGGGCAACTCCAGGTTTTACGTTTCCTCTTGGAATTCCTGCAGCAAGCCGACACTGCCAATTGGGAA
GAGACCAGCGCCAAAAGTGCCAGCCAGGAAGTGGAGGAGATGAAAGGCAAGTGGAAGAGGCTGAAGG
CTGAGTATGAGGAGAAGGTGAAAGAGGTGGAGGAGATGCTCCCTATGCTGCTTCAGAGGCTGGAGCT
CCTGCATGGGAAGAGAGAGGCCATAGAGGAGATTGTGCGGCGCTATGAACAGAAGAAGGCAGCTGTG
GAGGCTCTGCAAGAAAGCCAGATGAAAGAGAAGGTGCAGAAGCTACAGGGGGCAGTGCAGAACCAGC
AAGTGAATGTACAGAAGGGCCATGTTCATATCCAGCAGTTACAGGGCACATTAGAGAAGCTGGAGCA
GTCTCTGGATGGTTGGATACAGACCGTGAGCCGAGACTCACAGCTCTGCCAT

BE680749 *Xenopus laevis* Zw10 EST

GGAATTCCCTATGCCAGAAGAAACAAAAAACAAAAAATATCAGGAAGAAGTAACTCTCTATGTTCAA
AAGTGGATGAAGTTTAAAGAACAAATGATTATATTGCAGGCCAGCTTGCAGGAGATAGTGGATCGGT
GGGCAGATGGAAAAGGACCCCTTGCTGTGGAGTTTTCCCCTAGTGAAAGTGAAGAACCTAATAAGAG
CACTGTTTCAGAATACAGAGAGAAGGGCAGCCGCCCTGGCAAAGATCAAATAACTTGTATAGCAATT
TCACCATAATGCCTGTAAATTTTTGTACATAAAGTATGCTTCAGTGAACTCCAGTAAACAAGTTCTT
AAGAAGCCCTTTTCTTCTGTACATTTTAATTCTAGGGACAGTAGAATGTAAATTCTGGGACAGTTTC
AGTTCAATCTGAACAGTGTCTAGTAACCATTGTAAATATGACTTGTAATGGGGAGGG

BG233529 *Xenopus laevis* Rod EST

GTATCAAGTTTTTGGGGAATTATATCTGCAGAACTTAGTGAGGAGTCTTTTCCAACGCTGCTACTTA
TTTCAAAATTAATGAAGGTTTCTCTAGATACCTTATATATGATGGCGTCCAAGCATGTTTTTGAAAA
GAACTTGCGTCCTAAAGCACTGAAACTTAAAAATGCAGAACACTGCTCTATCATTACTAAAGAAACT
GCTAGGACTGTTTTAACTATCCAGTCTTACCTGCAGTCCATCAGTAATCCTGAGTGGGCTGCAGCTA
TTGCT

BG159891 *Xenopus laevis* Rod EST

TCATTTCATATAGACATTTTATTAGCACAAACATTTCAATTTATTTTATACGTATTTTTATGTATAT
ACAGGAAATAGTTGGGACAAAAGAAGAAAAACATTAAAAAGACAAACACTTAAATAAATGCAATATA
TAATGTCCGTTCAAAAGTGTTGTTTTTGGACCATCTTGTCACAGGATGACTAACCAACATATACTCC
CATTTATATATCTGAATGATCATTTAAAAAGGCCTTTACAGTGTCAGCTGAAGTTGCATTCTTTTGG
ATAGGTTTTCCACGGCACTTAAGATATTCTTTCACAAGGTCGGCAGCCTCATCCCAGCAATGTGTGT
TTGCAAGGCATTCTGCAATAGATCTCACTCTGTCGGATTGGATGGCTTGCCGTTTCAACATACTAAA
GTACTTAGTCTTCACAAACCTTTCAATCTGATGTTTCTCAATTATGTTGCTTAATATCAGGTCTCTT
ATCTGAGAAGCAAAGCCAGCCACTTCACCAGTGTTCATGCAGTCAGCCACTTGTTGAAAACAAGTTC
TGGATACATGTAGACAGGAAACCCTGAATTTGTTGCTCCTTTTTTTTCATGTGGGGATTAACCAAAGG
CCCCCAAAGTAAAGCCGGAAGATC

Developmental Cell, Vol. 2, 463–476, April, 2002, Copyright ©2002 by Cell Press

CENP-I Is Essential for Centromere Function in Vertebrate Cells

Ai Nishihashi,[1] Tokuko Haraguchi,[2] Yasushi Hiraoka,[2] Toshimichi Ikemura,[1] Vinciane Regnier,[3] Helen Dodson,[4] William C. Earnshaw,[4] and Tatsuo Fukagawa[1,5]

[1]PRESTO
The Japan Science and Technology Corporation (JST)
National Institute of Genetics and
The Graduate University for Advanced Studies
Mishima
Shizuoka 411-8540
[2]CREST Research Project
The Japan Science and Technology Corporation
Kansai Advanced Research Center
Communications Research Laboratory
588-2 Iwaoka
Nishi-ku
Kobe 651-2492
Japan
[3]Department of Biochemistry
University of Oxford
South Parks Road
Oxford OX1 3QU
[4]Wellcome Trust Center for Cell Biology
Institute of Cell and Molecular Biology
King's Buildings
University of Edinburgh
Mayfield Road
Edinburgh EH9 3JR
United Kingdom

Summary

We identified a novel essential centromere protein, CENP-I, which shows sequence similarity with fission yeast Mis6 protein, and we showed that CENP-I is a constitutive component of the centromere that colocalizes with CENP-A, -C, and -H throughout the cell cycle in vertebrate cells. To determine the precise function of CENP-I, we examined its role in centromere function by generating a conditional loss-of-function mutant in the chicken DT40 cell line. In the absence of CENP-I, cells arrested at prometaphase with misaligned chromosomes for long periods of time. Eventually, cells exited mitosis without undergoing cytokinesis. Immunocytochemical analysis of CENP-I-deficient cells demonstrated that both CENP-I and CENP-H are necessary for localization of CENP-C but not CENP-A to the centromere.

Introduction

The centromere is an essential component of the chromosome that is required for accurate segregation of chromosomes during mitosis and meiosis in eukaryotes. Its functions include sister chromatid cohesion and separation, microtubule attachment, chromosome movement, and mitotic checkpoint control (Choo, 1997). Although problems in chromosome segregation can lead to aneuploidy, cancer, and cell death, the mechanism by which centromeres interact with microtubules of the spindle apparatus during cell division is not fully understood in any organism.

The centromere of the budding yeast *Saccharomyces cerevisiae* has been characterized extensively. A combination of biochemical and genetic studies has led to identification of a 125 bp *cis*-acting CEN DNA and many associated proteins (Lechner and Carbon, 1991; Doheny et al., 1993). In comparison to centromere DNAs of *S. cerevisiae*, centromere DNAs of the fission yeast *Schizosaccharomyces pombe* are significantly larger. These DNAs range in size from 35 to 110 kb and contain repetitive DNAs flanking a central region (Pidoux and Allshire, 2000). Screening of fission yeast mutants that lose a minichromosome at the nonpermissive temperature has led to identification of proteins such as Mis6 and Mis12 that bind specifically to the central regions of *S. pombe* centromere DNAs (Takahashi et al., 1994; Saitoh et al., 1997; Goshima et al., 1999). Evolutionarily conserved centromere-specific proteins such as CENP-A and CENP-C are also present in fission yeast centromeres (Pidoux and Allshire, 2000).

Centromere proteins in vertebrate cells have been identified primarily by immunological methods. Antibodies against centromere proteins have been isolated from patients with autoimmune diseases and from immunized animals, and this has led to the identification of several centromere-associated proteins known as CENPs (Moroi et al., 1980; Earnshaw and Rothfield, 1985; Pluta et al., 1995; Craig et al., 1999; Dobie et al., 1999; Choo, 2000; Tyler-Smith and Floridia, 2000; Sullivan, 2001; Sullivan et al., 2001). CENP-A, a variant of histone H3, is present in both yeasts (Stoler et al., 1995; Meluh et al., 1998; Takahashi et al., 2000), *C. elegans* (Buchwitz et al., 1999), *D. melanogaster* (Henikoff et al., 2000; Blower and Karpen, 2001), and vertebrate cells (Palmer and Margolis, 1987). Immunolocalization of CENP-A suggests a distinct nucleosome structure at the inner kinetochore plate of active centromeres (Warburton et al., 1997; C.A. Cooke and W.C.E., unpublished data). Nucleosomes can be assembled in vitro from purified CENP-A and from histones H2A, H2B, and H4 (Yoda et al., 2000). Data from analyses of CENP-A knockout mice suggest that CENP-A plays a role in early organization of the centromeric chromatin during interphase (Howman et al., 2000). Therefore, it seems likely that a centromeric nucleosome containing a specific variant of H3 is a fundamental feature of eukaryotic kinetochore organization (Palmer and Margolis, 1987). To establish kinetochore assembly and function, other centromere components including CENP-C (Saitoh et al., 1992), which is an evolutionarily conserved protein, interact with the CENP-A-containing nucleosome structure (Howman et al., 2000; Moore and Roth, 2001;

[5]Correspondence: tfukagaw@lab.nig.ac.jp

Oegema et al., 2001). CENP-C is also an important component in kinetochore function, because inactivation of CENP-C results in cell death due to kinetochore disruption, chromosome missegregation, and metaphase arrest (Tomkiel et al., 1994; Fukagawa and Brown, 1997; Kalitsis et al., 1998; Fukagawa et al., 1999a). We recently found that CENP-H, a newly identified centromere component, is required for centromere targeting of CENP-C in vertebrate cells (Fukagawa et al., 2001).

CENP-A, -C, and -H are known to play important roles in the establishment of centromere identity in cells of higher vertebrates, and we hypothesized that there are other components involved in the centromere function. Therefore, one of the current goals of our research is to identify and characterize potential centromere components so as to develop an assembly pathway for the vertebrate kinetochore. In this paper, we report identification of a novel component of vertebrate centromeres, CENP-I. CENP-I shows sequence similarity with Mis6, which is necessary for recruitment of CENP-A to form proper centromeres in fission yeast (Takahashi et al., 2000). We show that CENP-I, like CENP-A, -C, and -H, is associated with centromeres throughout the cell cycle. Furthermore, we report the generation of a conditional mutant of CENP-I in the hyperrecombinogenic chicken B lymphocyte cell line DT40 to evaluate the in vivo function of CENP-I in higher vertebrate cells. Phenotypic analysis of these mutants revealed that CENP-I plays an essential role in the formation of functional centromeres and in mitosis. Immunofluorescence analysis of interphase ΔCENP-I cells revealed that CENP-I is necessary for recruitment of CENP-C and CENP-H to form functional centromeres in higher vertebrate cells.

Results

Isolation of a Chicken Gene Homologous to Fission Yeast *Mis6* Gene

Mis6 was previously identified as a centromere-associated protein in fission yeast (Saitoh et al., 1997). After searching DNA databases, Saitoh et al. (1997) reported a potential vertebrate homolog of Mis6, LRPR1, which is regulated by follicle-stimulating hormone. However, the function of this early response protein and its relation to the centromere are unknown. Therefore, we attempted to isolate a chicken homolog of Mis6 to characterize the gene product in chicken DT40 cells. We cloned and sequenced several cDNAs that contained the entire coding sequence. The full-length sequence encodes a 753 amino acid polypeptide with a predicted molecular mass of 86.9 kDa. The deduced chicken Mis6 protein has 56% amino acid sequence identity with human LRPR1, 52% amino acid identity with rat LRPR1, and 25% amino acid identity with *S. pombe* Mis6 (data not shown). Like fission yeast Mis6, the chicken Mis6 is basic (pI, 7.90) and relatively rich (45%) in hydrophobic amino acids.

Chicken Mis6 Homolog Associates with Chicken Inner Centromeres and Is Designated CENP-I

To determine the subcellular localization of the chicken Mis6 homolog, green fluorescent protein (GFP) was tagged to the C terminus, and the fused gene was expressed in DT40 cells. The fusion protein was functional and able to fully suppress the phenotype of chicken Mis6 knockout cells (described below). Subcellular localization of chicken Mis6-GFP was observed by fluorescence microscopy in combination with immunostaining with anti-CENP-C antibody. CENP-C was used as a centromeric marker because it localizes to centromeres throughout the cell cycle. Chicken Mis6-GFP signals and anti-CENP-C signals throughout the cell cycle are shown in Figure 1A. During interphase, Mis6-GFP was colocalized with CENP-C as discrete signals in the nucleus (Figure 1A, panel 1). Colocalization of Mis6-GFP with CENP-C was also observed during prophase (Figure 1A, panel 2), metaphase (Figure 1A, panel 3), and anaphase (Figure 1A, panel 4) of mitosis. We also generated a polyclonal antibody against the central region of chicken Mis6 and examined the distribution of this protein in a cell line in which the *CENP-H* gene had been replaced with a gene encoding CENP-H-GFP (Fukagawa et al., 2001). CENP-H-GFP signals colocalized with anti-Mis6 signals throughout the cell cycle (Figure 1B). Our results indicate that chicken Mis6 is localized to the centromere throughout the cell cycle in vertebrate cells. Therefore, we have designated the chicken homolog of Mis6 as centromere protein I (CENP-I).

CENP-I-GFP signals on metaphase chromosomes of DT40 cells showed a typical paired-dot pattern at every centromere. To determine the precise localization of CENP-I on metaphase chromosomes, we stained CENP-I-GFP-marked chromosomes with anti-BubR1 and anti-ZW10 antibodies. BubR1 was shown by immunoelectron microscopy to be localized in the outer kinetochore plate (Jablonski et al., 1998), and ZW10 is thought to be localized in the fibrous corona (Starr et al., 1998). Our results indicate that CENP-I is located internal to BubR1 and ZW10 (Figures 1C and 1D). These data, together with the finding that CENP-C and CENP-I-GFP colocalize (Figure 1E), suggest that CENP-I is localized in or near the inner kinetochore plate.

Generation of Conditional Mutants of CENP-I in DT40 Cells

To investigate the role of CENP-I in higher vertebrate cells, we generated conditional mutants of CENP-I in which cells with disruptions of the *CENP-I* gene were sustained by expression of the *CENP-I* cDNA under control of a tetracycline (tet)-repressible promoter. A CENP-I deletion construct was generated such that the 2.5 kb genomic fragment encoding amino acids 221–402 was replaced with one of several selection cassettes (Figure 2A). Three CENP-I alleles were found to be present in the chicken DT40 genome by fluorescence in situ hybridization (FISH; data not shown). We sequentially transfected *CENP-I* disruption constructs containing either the histidinol or puromycin resistance cassettes into DT40 cells (Figure 2A) and isolated *CENP-I*$^{+/-/-}$ clones (Figure 2B). One *CENP-I*$^{+/-/-}$ clone was cotransfected with a chicken *CENP-I* transgene under the control of a tet-repressible promoter and a tet-repressible transactivator containing a zeocin (zeo) resistance cassette. We selected zeo-resistant colonies and identified several clones carrying these constructs integrated at random sites in the genome (*CENP-I*$^{+/-/-/CENP\text{-}I\ transgene}$). Four clones with *CENP-I*$^{+/-/-/CENP\text{-}I\ transgene}$ genotype were transfected with the neomycin *CENP-I* disruption construct to disrupt the remaining CENP-I allele (Figure 2B). We

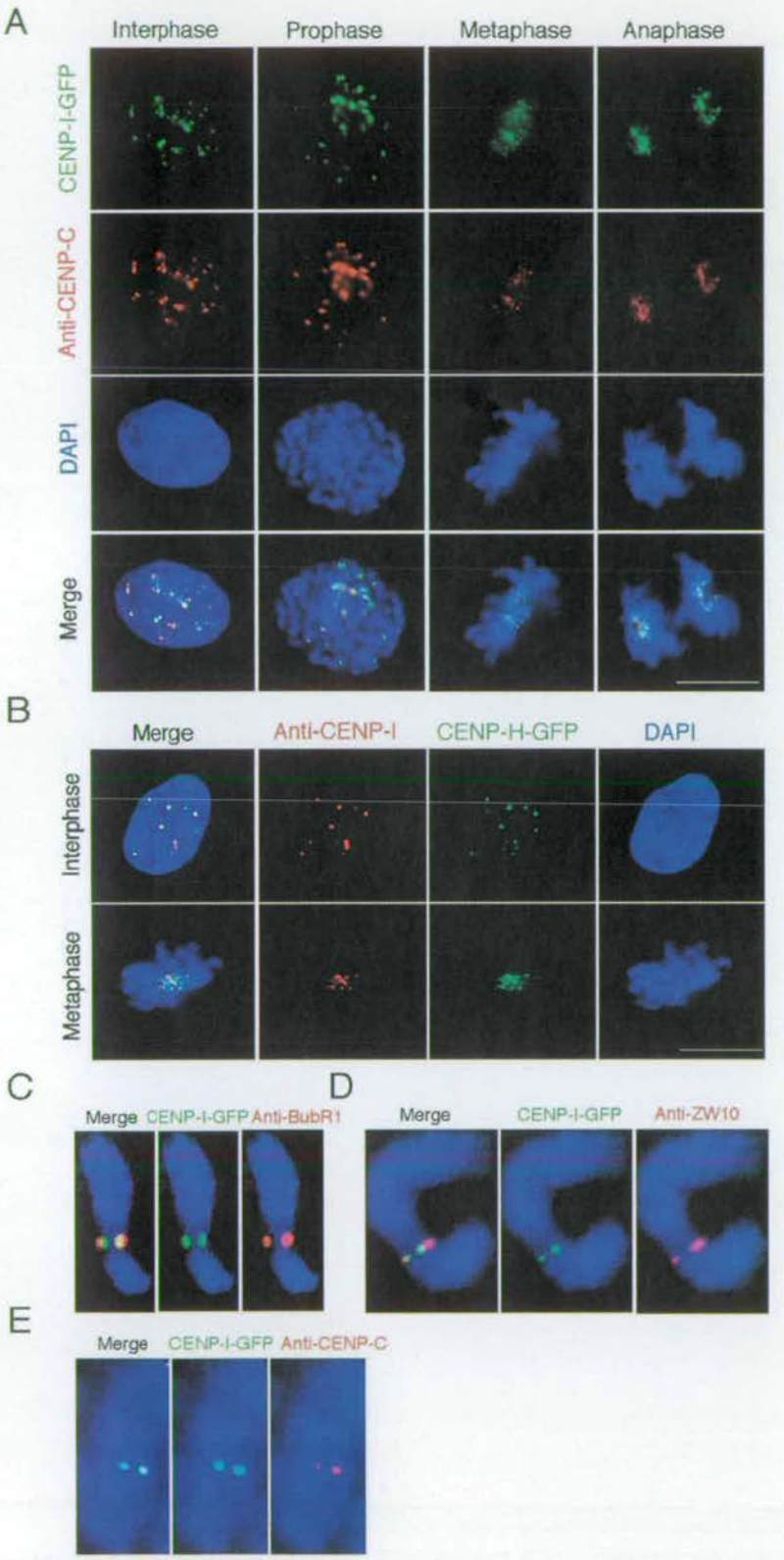

Figure 1. Chicken CENP-I Localizes to Centromeres throughout the Cell Cycle and Is Located in or near the Inner Kinetochore

(A) Localization of CENP-I-GFP at progressive stages of the cell cycle in DT40 cells. Cells were stained with anti-CENP-C antibody (red), and green signals are specific for CENP-I-GFP. Nuclei and chromosomes were visualized by counterstaining with DAPI (blue). The scale bars correspond to 10 μm.

(B) Cells with expression of CENP-H-GFP (green) were fixed and stained with anti-CENP-I antibody (red). As shown in the merged images, CENP-H-GFP signals are colocalized with CENP-I signals throughout the cell cycle.

(C) CENP-I localizes in or near the inner kinetochore. CENP-I-GFP signals (green) are internal to signals of anti-BubR1 (red) on the metaphase chromosome (blue).

(D) ZW10 signals (red) are external to CENP-I-GFP-signals (green).

(E) CENP-C signals (red) are colocalized with CENP-I-GFP signals (green).

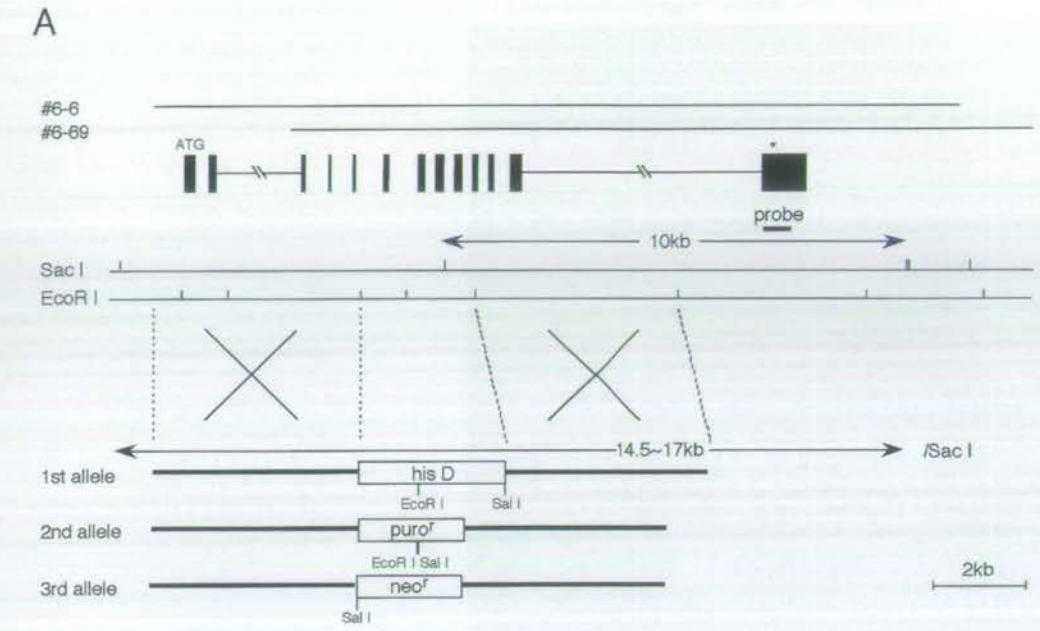

Figure 2. Generation of a *CENP-I*$^{-/-}$ Clone Carrying a Chicken *CENP-I* Transgene under the Control of a Tet-Repressible Promoter

(A) Restriction maps of the *CENP-I* locus, the gene disruption constructs, and the targeted loci. Black boxes indicate the positions of exons, and the targeted constructs are expected to disrupt four exons. EcoRI and SacI restriction sites are shown. The position of the probe used for Southern hybridization is indicated. Novel 14.5–17 kb SacI fragments hybridize to the probe if targeted integrations of the constructs occur.

(B) Restriction analysis of the targeted integration of the *CENP-I* disruption constructs. Genomic DNAs from wild-type DT40 cells (Wt), a clone after first round targeting (+/+/−, 1st), a clone after second round targeting (+/−/−, 2nd), a clone after second round targeting and random integration of the *CENP-I* transgene (+/−/− CENP-I+, 2nd + cDNA), and a clone after third round targeting (−/−/− CENP-I+, 3rd + cDNA) were analyzed by Southern hybridization with the probe indicated in (A).

(C) Western blot analysis of M90 whole-cell extracts with anti-CENP-I antibody at the indicated times following addition of tet. Protein contents of extracts were measured with the DC protein assay (Bio-Rad). Equal amounts of extracts were separated by SDS-PAGE and analyzed by Western blot with anti-tubulin antibody.

A

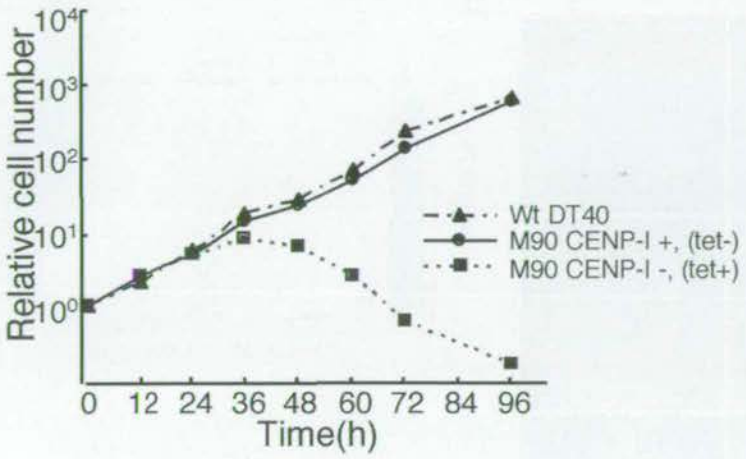

B

	0 h	12 h	24 h	36 h	48 h	60 h	72 h	96 h
+tet	$3.6x10^5$	$8.8x10^5$	$1.7x10^6$	$2.7x10^6$	$2.2x10^6$	$6.8x10^6$	$2.2x10^6$	$5.6x10^6$
-tet	$3.6x10^5$	$8.7x10^5$	$1.7x10^6$	$4.7x10^6$	$7.6x10^6$	$1.7x10^7$	$4.3x10^7$	$1.8x10^8$
Wild	$2.6x10^5$	$7.4x10^5$	$1.9x10^6$	$6.1x10^6$	$9.3x10^6$	$2.2x10^7$	$7.5x10^7$	$2.1x10^8$

C

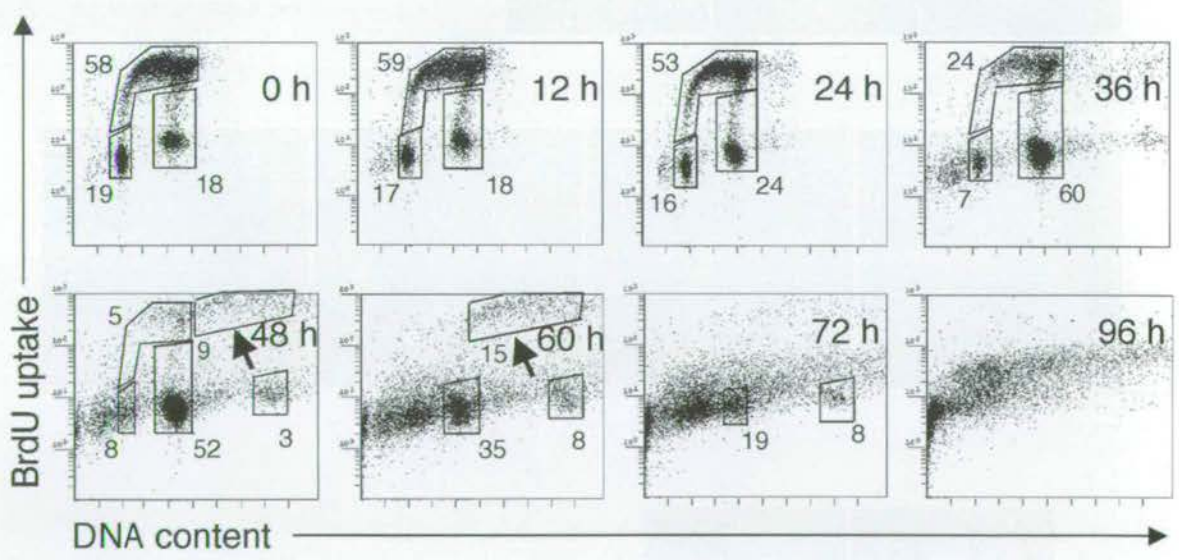

Figure 3. CENP-I Is Essential for Normal Progression of the Cell Cycle

(A) Representative growth curves for the indicated cell cultures. Tet was added at time 0 to the M90 CENP-I-deficient cell +tet culture, and the number of cells not stained with trypan blue was counted. Each experiment was performed twice, and each time point was examined in duplicate.

(B) Total cell number plotted in (A).

(C) Cell cycle distribution of M90 cells following inhibition of *CENP-I* transgene expression due to addition of tet at time 0. Cells were stained with FITC-anti-BrdU (*y* axis, log scale) to detect BrdU incorporation (DNA replication) and with propidium iodide to detect total DNA (*x* axis, linear scale). The lower left box represents G1 phase cells, the upper box represents S phase cells, and the lower right box represents G2/M phase cells. The numbers given in the boxes indicate the percentage of gated events. Arrows at 48 and 60 hr indicate further BrdU uptake by cells with 4N DNA content. Cells with 8N DNA content were observed at 48, 60, and 72 hr.

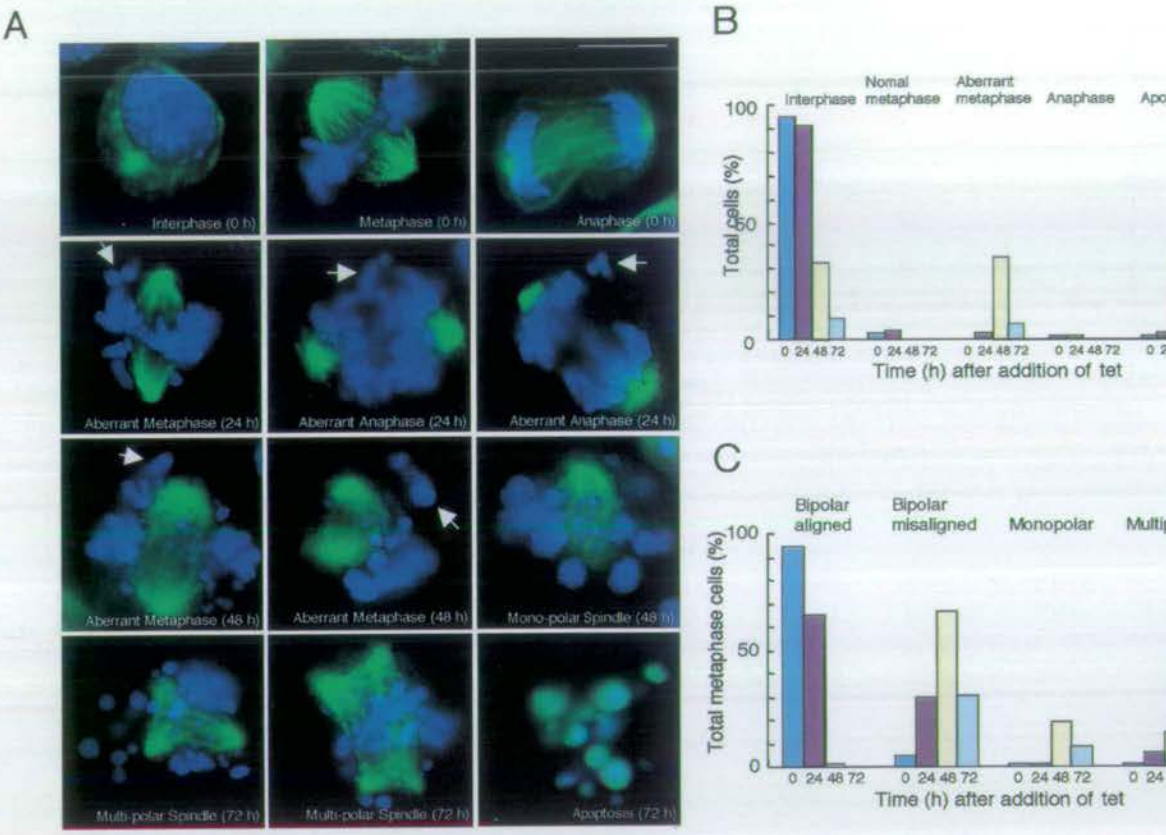
A
Interphase (0 h)
Metaphase (0 h)
Anaphase (0 h)
Aberrant Metaphase (24 h)
Aberrant Anaphase (24 h)
Aberrant Anaphase (24 h)
Aberrant Metaphase (48 h)
Aberrant Metaphase (48 h)
Mono-polar Spindle (48 h)
Multi-polar Spindle (72 h)
Multi-polar Spindle (72 h)
Apoptosis (72 h)
B
Interphase
Nomal metaphase
Aberrant metaphase
Anaphase
Apoptosis
Total cells (%)
100
50
0
0 24 48 72
Time (h) after addition of tet
C
Bipolar aligned
Bipolar misaligned
Monopolar
Multipolar
Total metaphase cells (%)
100
50
0
0 24 48 72
Time (h) after addition of tet

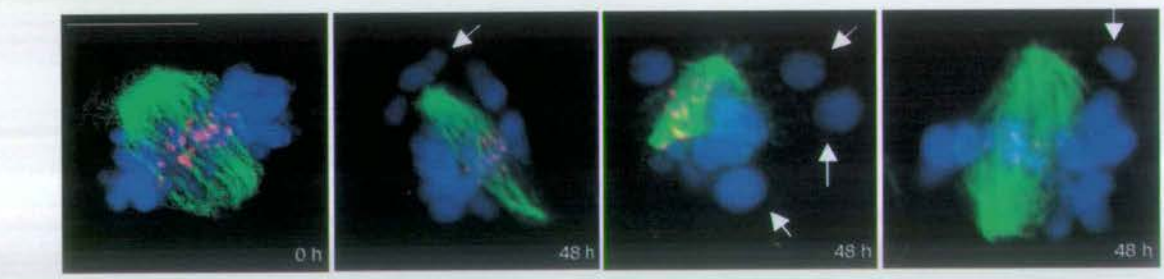
D
0 h
48 h
48 h
48 h

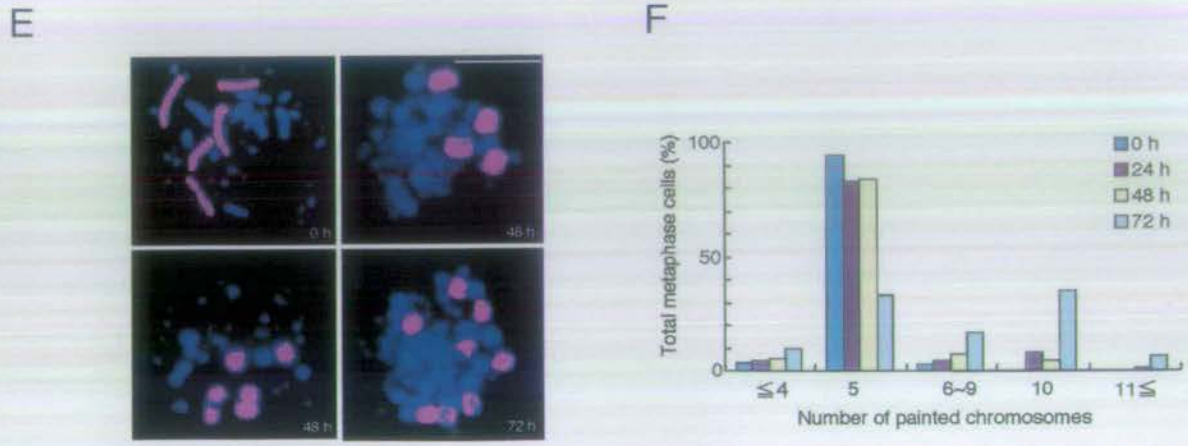
E
0 h
48 h
48 h
72 h
F
Total metaphase cells (%)
100
50
0
0 h
24 h
48 h
72 h
≦4
5
6~9
10
11≦
Number of painted chromosomes

obtained two clones with the *CENP-I*$^{-/-/-/CENP\text{-}I\ transgene}$ genotype, and one clone, M90, was chosen for further analysis. CENP-I protein in M90 cells was not detected by Western blot analysis at 48 hr after addition of tet (Figure 2C), indicating that CENP-I is actively turned over.

Deletion of CENP-I Results in Accumulation of Cells in Prometaphase and Subsequent Cell Death

The growth curve of M90 cells (CENP-I+, −tet) was indistinguishable from that of wild-type DT40 cells (Figures 3A and 3B). M90 cells (−tet) and wild-type DT40 cells divided approximately nine times during the 96 hr culture, which indicates that the doubling time of these cells is approximately 10.6 hr (Figures 3A and 3B). We then examined cell proliferation and viability following the addition of tet to the medium. M90 cells (CENP-I−, +tet) stopped proliferating approximately 2.5 cell cycles after the addition of tet (Figures 3A and 3B), and most cells had died by 96 hr, indicating that depletion of CENP-I results in growth arrest and subsequent cell death.

For cell cycle analysis following CENP-I depletion in M90 cells, we measured both cellular DNA content and DNA synthesis by fluorescence-activated cell sorting (FACS) after pulse labeling with BrdU (Figure 3C). CENP-I − M90 cells (+tet) started to accumulate in G2/M phase 24 hr after addition of tet, reaching a maximum by 36 hr (Figure 3C). After a prolonged delay in G2/M, further uptake of BrdU occurred between 48 and 60 hr (Figure 3C) as cells progressed to the next cycle without undergoing cytokinesis (see below). Degradation of chromosomal DNA due to massive cell death was observed between 72 and 96 hr (Figures 3C and 4B).

To determine the exact nature of the mitotic delay, we used DNA staining and immunocytochemical staining of microtubules to examine the time course of events following the depletion of CENP-I (Figures 4A and 4B). The mitotic index began to increase at 24 hr and reached 36% at 48 hr after the addition of tet. We did not observe any anaphase cells at 48 hr (Figure 4B). By considering FACS data with data from cytological analysis, we estimated that 16% (52% − 36%) of cells are in G2 phase at 48 hr (Figures 3C and 4B). In control cultures (0 hr), 3%–4% of cells are in mitosis (Figure 4B) and 18% of cells are in G2/M as determined by FACS (Figure 3C), and 14%–15% of cells are in G2 phase. These data indicate that CENP-I-deficient cells accumulate in M phase rather than G2 phase and that they arrest prior to anaphase.

Deletion of CENP-I Causes Chromosome Aberrations and Leads to Chromosome Missegregation

In the course of cytological analysis of CENP-I-deficient cells, we observed many abnormal mitotic cells with hypercondensed chromosomes that failed to congress normally to a metaphase plate (Figure 4A; 24, 48, and 72 hr). Eventually, the cells underwent apoptotic death (Figure 4A; 72 hr). In controls, chromosomes appeared ordered and aligned on the metaphase plate (Figure 4A; 0 hr, metaphase).

Control cells cultured in the absence of tet showed well-ordered bipolar spindles during both metaphase and anaphase (Figure 4A; 0 hr). At 48 hr, most cells cultured in the presence of tet appeared to have normal bipolar spindles, but some contained multi- or monopolar spindles (Figures 4A and 4C). This might in part account for the abnormal chromosome alignments described above; however, even in the 70% (48 hr after addition of tet) and 30% (72 hr after addition of tet) of mutant cells that had proper bipolar spindle poles, some chromosomes failed to achieve a proper alignment (Figures 4A and 4C). In other cells, chromosome alignment was completely disordered. Double staining of M90 cells with anti-tubulin and anti-CENP-A antibodies at 48 hr after addition of tet revealed that congressed chromosomes appeared to attach to microtubules, whereas misaligned chromosomes appeared not to be attached (Figure 4D). These results indicate that CENP-I, like CENP-H (Fukagawa et al., 2001), is required either directly or indirectly for congression and/or maintenance

Figure 4. CENP-I-Deficient Cells Show Prometaphase Delay Associated with Aberrant Chromosomes and Spindles that Lead to Chromosome Missegregation

(A) Chromosome morphology and α-tubulin staining (green) in the absence or presence of tet. DNA was counterstained with DAPI (blue). In the absence of tet, cells show the normal staining pattern for α-tubulin (upper three panels). In the presence of tet, cells in which chromosomes were not aligned at the metaphase plate were observed. Arrows indicate misaligned chromosomes at the metaphase plate or lagging chromosomes in anaphase at 24 or 48 hr after addition of tet. Apoptotic cells were observed at 72 hr after addition of tet. An apoptotic cell was detected by TUNEL assay (green). We also detected cells with monopolar and multipolar spindles. The scale bars correspond to 10 μm.

(B) Quantitation of aberrant M90 cells following inhibition of *CENP-I* transgene expression after addition of tet at time 0. We scored the number of interphase cells, normal metaphase cells, aberrant metaphase cells described in (A), anaphase cells, and apoptotic cells. Apoptotic cells were detected by TUNEL assay.

(C) Quantitation of cells with misaligned chromosomes after addition of tet at time 0. Misaligned chromosomes were classified as bipolar spindle with misaligned chromosomes, monopolar spindle, or multispindle.

(D) Double staining of M90 cells at 0 hr (−tet) or 48 hr (+tet) after addition of tet with anti-α-tubulin (green) and anti-CENP-A (red) antibodies. Arrows indicate misaligned chromosomes that do not appear to attach to microtubules, although many other chromosomes appear to have formed microtubule attachments.

(E) To examine chromosome loss, we used FISH analysis with chromosome-specific painting probes. We used painting probes for chicken chromosomes 1 and 2. Because DT40 cells have three copies of chromosome 2, we detected five painted chromosomes in normal cells (upper left panel). M90 cells with loss of chromosomes (upper right panel) and increase in chromosomes (lower panels) were detected after addition of tet.

(F) Distribution of the number of painted chromosomes per cell. M90 cells were cultured after addition of tet. At the indicated time, cells were treated with colcemid for 3 hr.

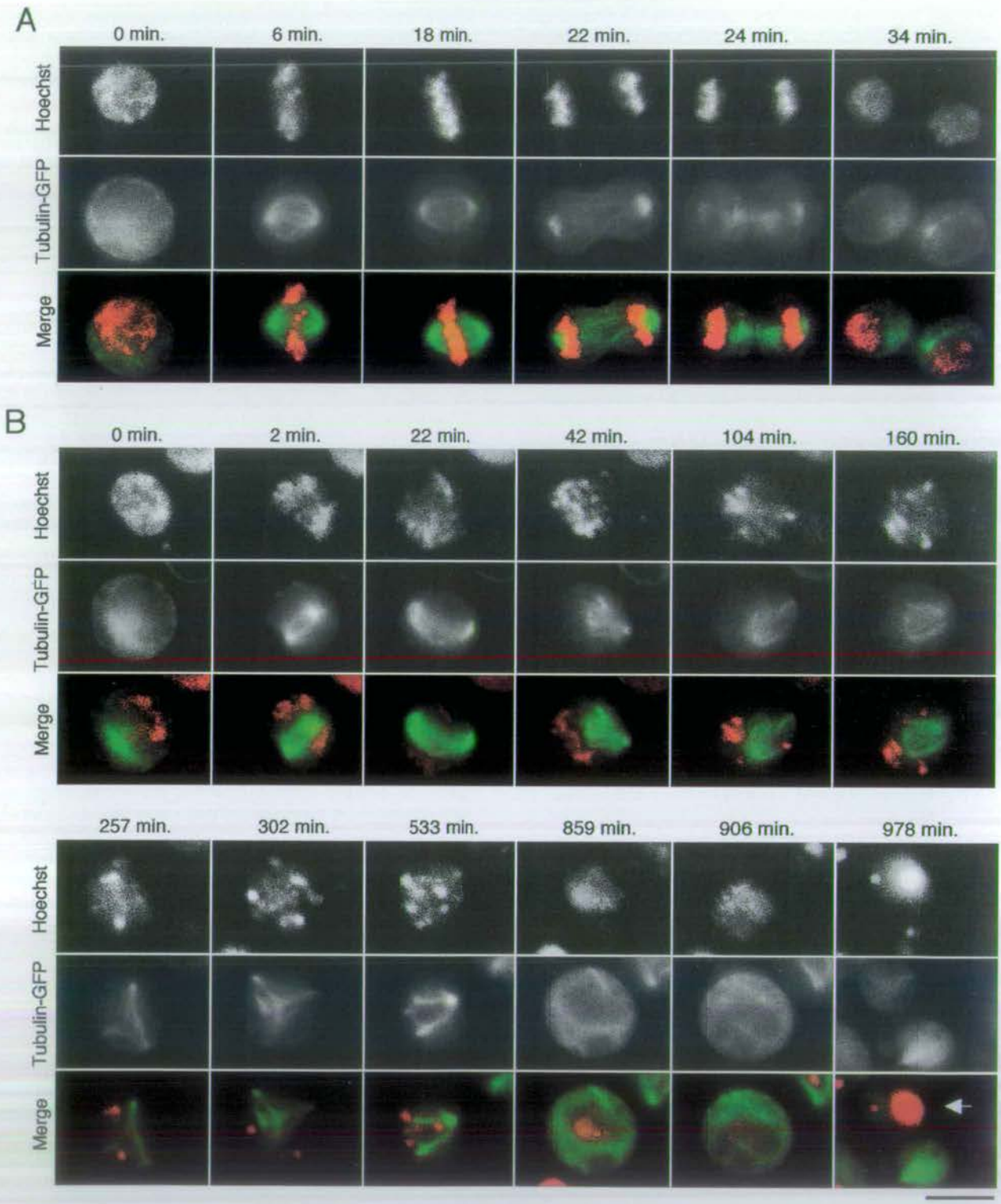

Figure 5. Dynamics of Chromosomes and Microtubules in CENP-I-Deficient Cells by Time-Lapse Observation

(A) Selected images of chromosomes (upper) and microtubules (middle) from prophase to telophase in M90 cells (−tet). In the superimposed images (lower), chromosomes and microtubules are displayed in red and green, respectively. The numbers at the top of each image represent the time from telophase in minutes. The scale bar corresponds to 10 μm.

(B) From 40 hr after addition of tet, one prophase cell was followed for time-lapse observations. Selected frames are shown. Once the cell entered mitosis, it was arrested at prometaphase for more than 800 min. At 859 min, the cell proceeded to the next cell cycle without normal cell division. We observed interphase-type microtubules between 859 and 906 min.

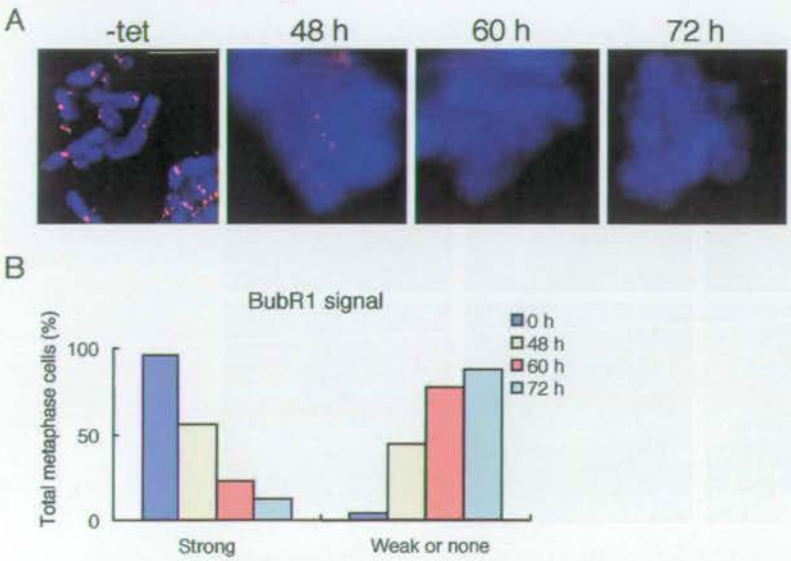

Figure 6. CENP-I-Deficient Cells Proceed through the Cell Cycle without Undergoing Cytokinesis

(A) Immunofluorescence analysis of (pro)-metaphase M90 cells at 0, 48, 60, and 72 hr after addition of tet with antibody against BubR1 checkpoint protein (red). In the control experiment (−tet), cells were treated with colcemid for 3 hr before staining of BubR1. DNA was counterstained with DAPI (blue). The scale bar corresponds to 10 μm.

(B) Quantitation of (pro)metaphase chromosomes with strong, weak, or no BubR1 signals. The numbers of (pro)metaphase chromosomes with strong BubR1 signals decreased following addition of tet to M90 cells.

of stable chromosome alignment and, ultimately, for progression from metaphase to anaphase.

We next examined whether mitotic defects caused by CENP-I depletion were associated with the induction of aneuploidy. We performed FISH analysis of metaphase spreads with chromosome painting probes specific for chicken chromosomes 1 and 2. Because DT40 cells contain three copies of chromosome 2, five fluorescent chromosomes can be observed for each wild-type cell (Figure 4E, upper left panel). As shown in Figure 4E, we observed abnormal numbers of painted chromosomes in CENP-I-deficient M90 cells in the presence of tet. The proportion of these aneuploid cells gradually increased after 24 hr (Figure 4F), suggesting that CENP-I deficiency induces chromosome missegregation.

Dynamic Behavior of Chromosomes and Microtubules in CENP-I-Deficient Cells

To determine the consequences of CENP-I deficiency in greater detail, we observed the dynamic behavior of individual living cells after suppression of CENP-I expression (Figure 5; see Supplemental Movies S1 and S2 [corresponding to Figures 5A and 5B, respectively] at http://www.developmentalcell.com/cgi/content/full/2/4/463/DC1). To visualize microtubules in living cells, human α-*tubulin* gene fused with GFP was integrated into the genome of M90 cells. We then stained the chromosomes of living M90 cells expressing GFP-tubulin with Hoechst 33342 and observed the cells microscopically at 37°C. An example of the time-lapse data for M90 cells in the absence of tet (control) is shown in Figure 5A. We were able to observe a well-ordered metaphase plate and bipolar spindle in control cells (6–18 min). Chromosomes began segregating as the central spindle elongated (22 min). Cells then underwent cytokinesis, the mitotic spindle disassembled (24 min), and the chromosomes decondensed (34 min). Phototoxicity induced by UV light irradiation is known to cause mitotic arrest. To avoid this, we used an ND filter and did not observe cells arrested at mitosis in control experiments. Control cells (n = 10) required approximately 34 min to progress from prophase to telophase. After addition of tet to M90 cells, we observed abnormal mitotic behavior (Figure 5B). Time point 0 in Figure 5B corresponds to 40 hr after addition of tet to cultures of M90 cells. The cell shown in Figure 5B entered mitosis (2 min) as condensed individual chromosomes appeared and the mitotic spindle formed. However, chromosome congression to the metaphase plate and subsequent anaphase were not observed. Instead, the cell remained arrested in prometaphase for 800 min with hypercondensed chromosomes. During this prolonged mitotic delay, the spindle structure underwent a series of abnormal changes. Early after mitotic entry (Figure 5B, 2–22 min) a normal-looking bipolar mitotic spindle formed. We subsequently observed fragmentation of the spindle poles (Figure 5B, 42 min) and formation of a multipolar spindle (Figure 5B, 25 and 257 min). After prolonged mitotic arrest, the chromosomes decondensed, and the mitotic spindle disassembled without chromosome segregation (859–906 min). Ultimately, this cell underwent apoptosis (Figure 5B, 978 min).

CENP-I-Deficient Cells Exit Mitosis without Normal Cytokinesis

FACS and cytological analysis showed that after a lengthy prometaphase delay, M90 cells exited mitosis without cytokinesis and underwent a further round of DNA replication between 48 and 72 hr after the addition of tet (Figures 3C and 4B). These findings suggest that the mitotic checkpoint is inactivated by 72 hr after the addition of tet. Accordingly, we stained the prometaphase-arrested cells with antibody against the BubR1 checkpoint protein (Jablonski et al., 1998; Chan et al., 1999). In controls, we stained the metaphase chromosomes of M90 cells (−tet, CENP-I+) arrested with colcemid and observed strong centromere staining of BubR1 (Figure 6A, −tet). We then stained chromosomes of M90 cells with anti-BubR1 after addition of tet. We detected BubR1 signals on some metaphase cells at 48 hr after addition of tet (Figures 6A and 6B). However, the signal intensity became weak at 60 hr, and weak or

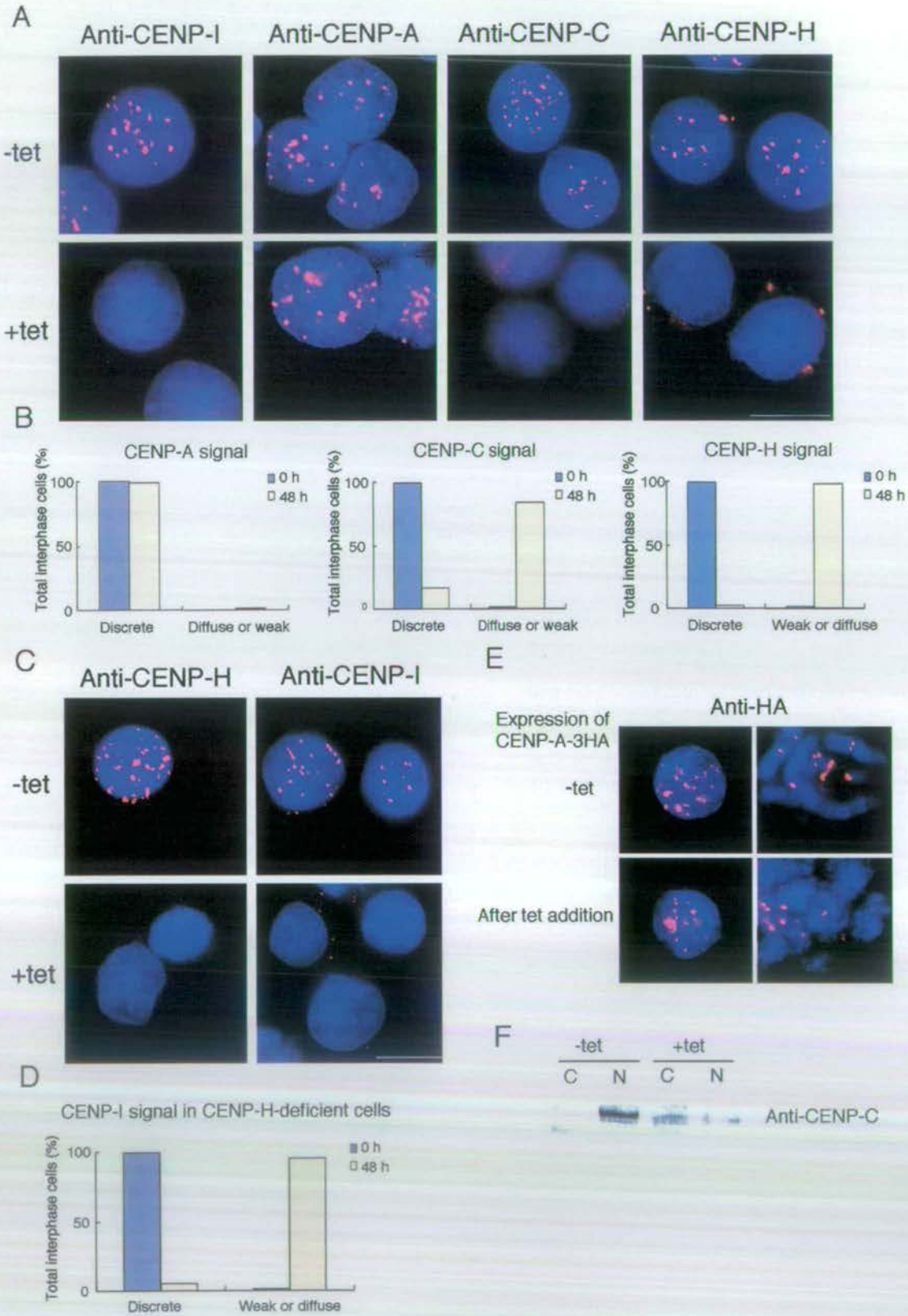

Figure 7. Localization of Other Centromere Proteins in CENP-I-Deficient Cells

(A) Immunofluorescence analysis of M90 cells at 0 hr (−tet) or 48 hr (+tet) after addition of tet. Interphase cells were stained with anti-CENP-I, anti-CENP-A, anti-CENP-C, and anti-CENP-H antibodies. Antibody signals were detected with Cy3-conjugated secondary antibodies (red). DNA was counterstained with DAPI (blue). The scale bars correspond to 10 μm.

no signals were detected at 72 hr after addition of tet (Figures 6A and 6B), suggesting that the association of the checkpoint signaling proteins with the kinetochore structure is lost by 72 hr. In control experiments, if wild-type cells were arrested with nocodazole for 60 hr, the majority of cells died, although 5%–6% of cells progressed to the next cell cycle.

Localization of Other Centromere Proteins in CENP-I-Deficient Cells

CENP-A, -C, and -H are thought to form a "prekinetochore structure" that exists throughout the cell cycle and marks the location of the centromere on the chromosome in vertebrate cells. To understand the role of CENP-I in formation of the prekinetochore structure, we asked whether CENP-I was required to target CENP-A, -C, and -H to the kinetochore. Interphase nuclei of M90 cells were analyzed with antibodies against chicken CENP-A, -C, -H, and -I in the presence or absence of tet. Typical results are shown in Figure 7A. In the absence of tet, all four antibodies gave strong, discrete signals on interphase nuclei of M90 cells (Figure 7A, upper panel). At 48 hr after the addition of tet, we could not detect CENP-I signals in interphase nuclei of M90 cells, consistent with the complete depletion of CENP-I (Figure 7A, lower left panel). CENP-A antibody gave positive signals on interphase nuclei of CENP-I-deficient cells (Figure 7A, lower panel, lane 2); however, the normal prominent, discrete CENP-C (Figure 7A, upper panel, lane 3) and CENP-H (Figure 7A, upper panel, lane 4) signals were absent. Instead, diffuse or weak signals for CENP-C and CENP-H were observed (Figure 7A, lower right panel). We counted interphase cells that showed diffuse or weak signals (Figure 7B) and found that approximately 83% and 98% of interphase cells displayed diffuse CENP-C and CENP-H signals, respectively, after addition of tet (Figure 7B).

Immunocytochemical analysis of CENP-I-deficient cells showed that CENP-I is necessary for localization of CENP-H to the centromere. It was, therefore, of interest to determine whether CENP-H was necessary for CENP-I localization to the centromere. To address this question, we performed immunofluorescence analysis of the #5-5 cell line, which is a conditional loss-of-function mutant of CENP-H (Fukagawa et al., 2001). We previously showed that CENP-H signals were lost and that CENP-C signals were diffuse in #5-5 cells 48 hr after addition of tet (Fukagawa et al., 2001). We then analyzed localization of CENP-I and found that CENP-I signals were also lost (Figures 7C and 7D) in CENP-H-deficient cells. These results suggest that CENP-I and CENP-H are mutually interdependent for targeting to the prekinetochore structure and that both are necessary for CENP-C localization to centromeres.

Although our data showed that CENP-A localization did not change in CENP-I-deficient cells (Figure 7A), it is possible that we observed only CENP-A that was previously targeted to the centromere and that newly synthesized CENP-A is not targeted to centromeres. To address this question, we expressed CENP-A-3HA in M90 cells and detected it with anti-HA after addition of tet (Figure 7E). We found that newly synthesized CENP-A-3HA was targeted to the centromere in CENP-I-deficient cells.

We showed that CENP-C staining was diffuse in CENP-I-deficient cells by immunocytochemistry (Figure 7A). To confirm the mislocalization of CENP-C biochemically, we extracted the CENP-C-enriched nuclear fraction with 1 M NaCl. The majority of CENP-C in M90 cells was detected in this fraction when cells were cultured without tet. However, little CENP-C was detected in this fraction after addition of tet (Figure 7F).

Discussion

CENP-I Is Required for Centromere Function during Mitosis

This study describes CENP-I, a novel essential component of vertebrate centromeres, which has sequence similarity with the *S. pombe* Mis6 protein. CENP-I localizes to the centromere throughout the cell cycle in chicken DT40 cells. Simultaneous colocalization experiments with CENP-I-GFP and antibodies against several centromere proteins suggest that CENP-I, like CENP-A, -C, and -H (Saitoh et al., 1992; Warburton et al., 1997; Fukagawa et al., 2001), localizes in or near the inner kinetochore plate. Phenotypic analysis of a conditional loss-of-function mutant of CENP-I in the hyperrecombinogenic chicken DT40 cell line reveals that CENP-I is required for mitosis in vertebrate cells.

CENP-I-deficient cells underwent a lengthy delay in prometaphase, characterized by the presence of hypercondensed chromosomes and abnormal spindle structures. The cells eventually exited mitosis following loss of spindle checkpoint components from kinetochores, rereplicated their DNA, and ultimately underwent apoptosis. Lengthy delays in prometaphase had previously been observed with targeted disruptions of the kinetochore proteins CENP-C and CENP-H (Fukagawa and Brown, 1997; Fukagawa et al., 2001), suggesting that this phenotype is characteristic of the loss of inner kinetochore plate function in vertebrate cells.

(B) Quantitation of M90 interphase cells with diffuse CENP-A, CENP-C, and CENP-H signals. The graphs provide a quantitative representation of the data. We scored approximately 2000 interphase cells.

(C) Immunofluorescence analysis of #5-5 (*ΔCENP-H*, *CENP-H* transgene) cells grown in the absence (−tet) or presence (+tet, restrictive conditions) of tet for 48 hr. Rabbit antibodies to CENP-H or CENP-I were applied to interphase cells and detected with Cy3-conjugated second antibodies (red). DNA was counterstained with DAPI (blue).

(D) Quantitation of #5-5 interphase cells with diffuse or weak CENP-I signals. We scored approximately 2000 interphase cells.

(E) Immunofluorescence analysis of M90 cells transiently expressing CENP-A-3HA. M90 cells were cultured for 24 hr with tet and transfected with a CENP-A-3HA construct. At 48 hr after addition of tet, cells were stained with anti-HA (red).

(F) Western blot analysis of the nuclear fraction of M90 cells extracted with 1 M NaCl with anti-CENP-C. C, cytoplasm fraction; N, 1 M NaCl fraction. The CENP-C band is weak in the 1 M NaCl fraction after addition of tet.

Role of CENP-I in Assembly of the Inner Kinetochore

Recent data suggest that centromere-specific nucleosome structures including CENP-A may determine centromere identity (Karpen and Allshire, 1997; Ahmad and Henikoff, 2001; Choo, 2001; Lo et al., 2001). However, the mechanism of CENP-A loading into centromeric nucleosomes and which proteins are involved with the CENP-A-containing structure in vertebrate cells are not understood. Mitotic defects caused by CENP-I deficiency occur after passage through G1 phase (Figure 3), suggesting that a functional "centromere chromatin" structure is formed during interphase. This was also the conclusion of prior experiments in which the cell cycle effects of microinjection of anti-centromere antibodies were examined (Bernat et al., 1990, 1991).

In fission yeast, CENP-A localization is altered in Mis6 mutants, suggesting that Mis6 may be involved in CENP-A localization to the centromere (Takahashi et al., 2000). The situation in vertebrate cells appears to be different. We found that depletion of CENP-I does not alter the discrete, typical centromeric signals of CENP-A, whereas discrete centromeric CENP-C and CENP-H signals are lost in CENP-I-deficient cells (Figure 7). Furthermore, the normally discrete CENP-I signals are diffuse in CENP-H-deficient cells, indicating that CENP-H and CENP-I are mutually interdependent for targeting to centromeres. A preliminary *E. coli* two-hybrid analysis using CENP-H and CENP-I revealed that the N-terminal region of CENP-H interacts with the N terminus of CENP-I (see Supplemental Figure S1; details will be published elsewhere). Our present data, together with our previous results showing that CENP-H is necessary for recruitment of CENP-C to form a functional centromere (Fukagawa et al., 2001), suggest that formation of CENP-A-containing nucleosomes, which is mediated by unknown factors, occurs first, and that CENP-H and CENP-I are then targeted to these structures, possibly as a macromolecular complex. CENP-C then interacts with CENP-A/CENP-H/CENP-I chromatin to form the kinetochore plate structure.

Vertebrate CENP-I, unlike *S. pombe* Mis6, is not required for centromere targeting of CENP-A in our model. A similar conclusion has recently been reached using microinjection with anti-Mis6 antibody (T. Yen, personal communication). Also, Measday et al. (2002) reported that Ctf3p, the Mis6 budding yeast homolog, is not required for loading of CENP-A homolog Cse4p onto CEN DNA. As will be seen below, our results suggest that vertebrate kinetochores may not be assembled in a simple linear pathway.

CENP-I Is Required for Normal Mitotic Progression

Individual CENP-I-deficient cells observed in real time by live-cell analysis after addition of tet were delayed in prometaphase for more than 10 hr and underwent an aberrant mitosis. This phenotype resembled that of CENP-H-deficient cells (Fukagawa et al., 2001) or cells injected with anti-CENP-C antibody (Tomkiel et al., 1994). Inactivation of CENP-C has previously been shown to alter or disrupt kinetochore structure in affected cells (Tomkiel et al., 1994). In that and other studies, we showed that cells with disrupted kinetochores (confirmed by electron microscopy) could bind to microtubules, and in some cases congress normally to a metaphase plate (Tomkiel et al., 1994; Bernat et al., 1991). The affected cells eventually executed a highly aberrant exit from mitosis following an extensive delay in prometaphase. We concluded from those studies that assembly of an ordered trilaminar kinetochore structure is not required for microtubule binding, but may be required for the mitotic checkpoint to be inactivated following chromosome attachment to the spindle (Bernat et al., 1991).

Our cytological and live-cell analyses of CENP-I-deficient cells showed that many chromosomes attached to microtubules and congressed normally, although in each cell several chromosomes failed to align at the metaphase plate. The similarity of this phenotype to our previous antibody injection experiments and studies of CENP-H-disrupted cells suggests that kinetochores assembled in the absence of CENP-I can bind microtubules but not inactivate the mitotic checkpoint. In support of this hypothesis, we observed that many of the bioriented chromosomes in M90 cells arrested in prometaphase 48 hr after the addition of tet showed positive labeling with the BubR1 checkpoint protein (Figure 4D). This suggests that the prolonged mitotic delay observed in CENP-I-deficient cells is due to synergistic effects arising from defects in the kinetochore structure and activation of the checkpoint.

The lengthy delay in mitosis observed in CENP-I-deficient cells eventually ends, and the cells exit mitosis without undergoing cytokinesis. This appears to reflect the eventual adaptation of the checkpoint pathway, leading to loss of checkpoint proteins such as BubR1 from the kinetochore (Figure 6). This may indicate that as previously seen with antibody-injected HeLa cells, the mitotic checkpoint is only able to delay the exit from mitosis for a limited time if a mitotic spindle is present. Whatever the explanation, the cells eventually exit from mitosis, reform a nuclear membrane around the near-tetraploid genome, and ultimately undergo apoptosis.

The fact that microtubule binding and mitotic checkpoint signaling can proceed even though a number of essential components of the inner kinetochore plate are absent reveals that kinetochore assembly does not follow a simple linear ordered assembly pathway in vertebrates. Partial outer kinetochore function can be observed even when assembly of the inner kinetochore structure is disrupted. Furthermore, these results suggest that one function of the inner kinetochore plate may be to create a foundation that enables the checkpoint proteins in the outer kinetochore to detect when the chromosome is properly attached to the spindle.

Experimental Procedures

Molecular Biology

The chicken *Mis6/LRPR1/CENP-I* gene was isolated by degenerate RT-PCR of mRNA extracted from DT40 cells. The sequences of the degenerate primers were 5′-TC(ACG) A(AG)(AG) CA(AG) TG(AGT) AT(AG) TT-3′ and 5′-TA(CT) AA(AG) TT(CT) TT(CT) GC(ACT) CC-3′. We screened a chicken testis cDNA library (Stratagene) with the RT-PCR product as a probe. We used the chicken *CENP-I* cDNA as a probe to isolate genomic clones specific for CENP-I from a DT40 genomic DNA library.

Full-length *CENP-I* cDNA was cloned into the EcoRI site of

pUHD10-3 (Fukagawa et al., 2001) to yield a tetracycline-sensitive expression plasmid, pUHD-CENP-I. The left (4.5 kb) and right (4.5 kb) arms of the *CENP-I* disruption constructs were cloned sequentially into pBluescript. For the disruption constructs, the histidinol (hisD), puromycin (puro), or neomycin (neo) resistance cassette under control of the β-actin promoter was inserted between the two arms.

To generate the expression construct for the CENP-I-GFP fusion gene, a full-length chicken *CENP-I* cDNA was inserted into pEGFP-N1 plasmid (Clontech). An expression construct for GFP-tubulin (pEGFP-Tub) was purchased from Clontech.

Cell Culture and Cell Cycle Analysis

DT40 cells were cultured and transfected as described previously (Fukagawa and Brown, 1997). G418 (Sigma) was used at a final concentration of 2 mg/ml, puromycin (Clontech) at a final concentration of 0.5 μg/ml, hygromycin (Wako) at a final concentration of 2.5 mg/ml, histidinol (Sigma) at a final concentration of 1 mg/ml, and zeocin (Invitrogen) at a final concentration of 1 mg/ml to select for stable transfectants. To suppress expression of the tetracycline-responsive *CENP-I* transgene, tetracycline (Sigma) was added to the culture medium to a final concentration of 2 μg/ml.

Cell cycle analysis was carried out as described previously (Fukagawa et al., 2001). Flow cytometry was performed with an Epics Altra cytometer (Beckman-Coulter).

Antibody Production

A chicken CENP-I expression construct (amino acids 307–525) was created in vector pET28a (Novagen). The histidine-tagged recombinant protein was expressed in *E. coli* BL21 (DE3) cells after 4 hr induction with 0.5 mM IPTG and purified by nickel column chromatography. Purified recombinant CENP-I was used to immunize a rabbit. Serum was affinity purified against recombinant CENP-I protein on a CNBr-activated Sepharose 4B column.

Immunocytochemistry and FISH Analysis

Immunofluorescent staining of whole cells was performed as described previously (Fukagawa et al., 1999a). Anti-α-tubulin monoclonal antibody (1:50; Sigma), rabbit anti-chicken CENP-A antibody (1:50; Fukagawa et al., 2001), rabbit anti-chicken CENP-C antibody (1:1000; Fukagawa et al., 1999a), rabbit anti-chicken CENP-H antibody (1:2000; Fukagawa et al., 2001), or rabbit anti-chicken CENP-I antibody (1:2000) were used. Binding of primary antibodies was then detected with either FITC-conjugated rabbit anti-mouse IgG diluted 1:200 (Jackson ImmunoResearch Laboratories) or Cy3-conjugated goat anti-rabbit IgG diluted 1:1000 (Amersham) in PBS/0.5% BSA. Aberrant metaphase cells or mitotic spindles were observed and scored at the indicated time points. Approximately 3000 cells were scored for each time point. TUNEL assay was performed with an apoptosis detection system (Promega).

Metaphase chromosome spreads for immunofluorescence staining were prepared by a method modified from Earnshaw et al. (1989). Chromosome spreads were stained with rabbit anti-chicken ZW10 antibody (1:200; Fukagawa et al., 1999a) or rabbit anti-chicken BubR1 (1:500).

FISH was performed as described previously (Fukagawa et al., 1999b). For chromosome stability assay, the number of chromosomes 1 and 2 (five in normal cells) were scored in approximately 1000 metaphase cells at the indicated time points.

All immunofluorescence and FISH images were collected with a cooled CCD camera (Photometrics Image Point) mounted on a Zeiss Axioscope microscope with a 63× objective (Zeiss) together with a filter wheel. Images were manipulated with Iplab software (Signal Analytics).

Fluorescence Microscopy in Living Cells

Cells were stained with Hoechst 33342 for 10–15 min at a final concentration of 100 ng/ml and washed three times with culture medium. For microscopic observation, HEPES buffer (pH 7.4) was added to a final concentration of 20 mM to avoid the need for CO_2 gas. Fluorescently stained living cells were observed with an Olympus inverted microscope IX70 with an oil immersion objective lens (PlanApo 60×, NA = 1.40). The DeltaVision microscope system used in this study was purchased from Applied Precision. For temperature control during microscopic observations, the system was assembled in a custom-made, temperature-controlled room (Haraguchi et al., 1997, 1999). Time-lapse images were recorded at 2 min intervals with an exposure time of 0.2–0.3 s.

Acknowledgments

The authors are very grateful to Y. Miyauchi, K. Suzuki, K. Kita, and Y. Fukagawa for technical assistance. This work was supported by the PRESTO of JST and by a Grant-in-Aid for Scientific Research on Priority Areas (C) "Genome Biology" from the Ministry of Education, Science, Sports, and Culture of Japan. Work in the W.C.E. lab is supported by The Welcome Trust of which W.C.E. is a Principal Research Fellow.

Received: November 6, 2001
Revised: February 27, 2002

References

Ahmad, K., and Henikoff, S. (2001). Centromeres are specialized replication domains in heterochromatin. J. Cell Biol. *153*, 101–109.

Bernat, R.L., Borisy, G.G., Rothfield, N.F., and Earnshaw, W.C. (1990). Injection of anticentromere antibodies in interphase disrupts events required for chromosome movement at mitosis. J. Cell Biol. *111*, 1519–1533.

Bernat, R.L., Delannoy, M.R., Rothfield, N.F., and Earnshaw, W.C. (1991). Disruption of centromere assembly during interphase inhibits kinetochore morphogenesis and function in mitosis. Cell *66*, 1229–1238.

Blower, M.D., and Karpen, G.H. (2001). The role of *Drosophila* CID in kinetochore formation, cell-cycle progression and heterochromatin interactions. Nat. Cell Biol. *3*, 730–739.

Buchwitz, B.J., Ahmad, K., Moore, L.L., Roth, M.B., and Henikoff, S. (1999). A histone-H3-like protein in *C. elegans*. Nature *401*, 547–548.

Chan, G.K.T., Jablonski, S.A., Sudakin, V., Hittle, J.C., and Yen, T.J. (1999). Human BubR1 is a mitotic checkpoint kinase that monitors CENP-E functions at kinetochores and binds the cyclome/APC. J. Cell Biol. *146*, 941–954.

Choo, K.H.A. (1997). The Centromere (Oxford UK: Oxford University Press).

Choo, K.H.A. (2000). Centromerization. Trends Cell Biol. *10*, 182–188.

Choo, K.H.A. (2001). Domain organization at the centromere and neocentromere. Dev. Cell *1*, 165–177.

Craig, J.M., Earnshaw, W.C., and Vagnarelli, P. (1999). Mammalian centromeres: DNA sequence, protein composition, and role in cell cycle progression. Exp. Cell Res. *246*, 249–262.

Dobie, K.W., Hari, K.L., Maggert, K.A., and Karpen, G.H. (1999). Centromere proteins and chromosome inheritance: a complex affair. Curr. Opin. Genet. Dev. *9*, 206–217.

Doheny, K.F., Soger, P.K., Hyman, A.A., Tugendreich, S., Spencer, F., and Hieter, P. (1993). Identification of essential components of the *S. cerevisiae* kinetochore. Cell *73*, 761–774.

Earnshaw, W.C., and Rothfield, N. (1985). Identification of a family of human centromere proteins using autoimmune sera from patients with scleroderma. Chromosoma *91*, 313–321.

Earnshaw, W.C., Ratrie, H., and Stetten, A.C.G. (1989). Visualization of centromere proteins CENP-B and CENP-C on a stable dicentric chromosome in cytological spreads. Chromosoma *98*, 1–12.

Fukagawa, T., and Brown, W.R.A. (1997). Efficient conditional mutation of the vertebrate CENP-C gene. Hum. Mol. Genet. *6*, 2301–2308.

Fukagawa, T., Pendon, C., Morris, J., and Brown, W. (1999a). CENP-C is necessary but not sufficient to induce formation of a functional centromere. EMBO J. *18*, 4196–4209.

Fukagawa, T., Hayward, N., Yang, J., Azzalin, C., Griffin, D., Stwart, A.F., and Brown, W. (1999b). The chicken HPRT gene: a counter selectable marker for the DT40 cell line. Nucleic Acids Res. *27*, 1966–1969.

Fukagawa, T., Mikami, Y., Nishihashi, A., Regnier, V., Haraguchi, T., Hiraoka, Y., Sugata, N., Todokoro, K., Brown, W., and Ikemura, T. (2001). CENP-H, a constitutive centromere component, is required for centromere targeting of CENP-C in vertebrate cells. EMBO J. *20*, 4603–4617.

Goshima, G., Saitoh, S., and Yanagida, M. (1999). Proper metaphase spindle length is determined by centromere proteins Mis12 and Mis6 required for faithful chromosome segregation. Genes Dev. *13*, 1664–1677.

Haraguchi, T., Kaneda, T., and Hiraoka, Y. (1997). Dynamics of chromosomes and microtubules visualized by multiple-wavelength fluorescence imaging in living mammalian cells: effects of mitotic inhibitors on cell cycle progression. Genes Cells *2*, 369–380.

Haraguchi, T., Ding, D.-Q., Yamamoto, A., Kaneda, T., Koujin, T., and Hiraoka, Y. (1999). Multiple-color fluorescence imaging of chromosomes and microtubules in living cells. Cell Struct. Funct. *24*, 291–298.

Henikoff, S., Ahmad, K., Platero, J.S., and van Steensel, B. (2000). Heterochromatic deposition of centromeric histone H3-like proteins. Proc. Natl. Acad. Sci. USA *97*, 716–721.

Howman, E.V., Fowler, K.J., Newson, A.J., Redward, S., MacDonald, A.C., Kalitsis, P., and Choo, K.H.A. (2000). Early disruption of centromeric chromatin organization in centromere protein A (*Cenpa*) null mice. Proc. Natl. Acad. Sci. USA *97*, 1148–1153.

Jablonski, S.A., Chan, G.K.T., Cooke, C.A., Earnshaw, W.C., and Yen, T.J. (1998). The hBUB1 and BUBR1 kinases sequentially assemble onto kinetochores during prophase with hBUBR1 concentrating at the kinetochore plates in mitosis. Chromosoma *107*, 386–396.

Kalitsis, P., Fowler, K.J., Earle, E., Hill, J., and Choo, K.H.A. (1998). Targeted disruption of mouse centromere protein C gene leads to mitotic disarray and early embryo death. Proc. Natl. Acad. Sci. USA *95*, 576–582.

Karpen, G.H., and Allshire, R.C. (1997). The case for epigenetic effects on centromere identity and function. Trends Genet. *13*, 489–496.

Lechner, J., and Carbon, J. (1991). A 240 kDa multisubunit protein complex, CBF3, is a major component of the budding yeast centromere. Cell *64*, 717–725.

Lo, A.W., Craig, J.M., Saffery, R., Kalitsis, P., Irvine, D.V., Earle, E., Magliano, D.J., and Choo, K.H. (2001). A 330 kb CENP-A binding domain and altered replication timing at a human neocentromere. EMBO J. *20*, 2087–2096.

Measday, V., Hailey, D.W., Pot, I., Givan, S.A., Hyland, K.M., Cagney, G., Fields, S., Davis, T.N., and Hieter, P. (2002). Ctf3, the Mis6 budding yeast homolog, interacts with Mcm22p and Mcm16p at the yeast outer kinetochore. Genes Dev. *16*, 101–113.

Meluh, P.B., Yang, P., Glowczewski, L., Koshland, D., and Smith, M. (1998). Cse4p is a component of the core centromere of *Saccharomyces cerevisiae*. Cell *94*, 607–613.

Moore, L.L., and Roth, M.B. (2001). HCP-4, a CENP-C-like protein in *Caenorhabditis elegans*, is required for resolution of sister centromeres. J. Cell Biol. *153*, 1199–1207.

Moroi, Y., Peebles, C., Fritzler, M.J., Steigerwald, J., and Tan, E.M. (1980). Autoantibody to centromere (kinetochore) in scleroderma sera. Proc. Natl. Acad. Sci. USA *77*, 1627–1631.

Oegema, K., Desai, A., Rybina, S., Kirkham, M., and Hyman, A.A. (2001). Functional analysis of kinetochore assembly in *Caenorhabditis elegans*. J. Cell Biol. *153*, 1209–1225.

Palmer, D.K., and Margolis, R.L. (1987). A 17-kD centromere protein (CENP-A) copurifies with nucleosome core particles and with histones. J. Cell Biol. *104*, 805–815.

Pidoux, A.L., and Allshire, R.C. (2000). Centromeres: getting a grip of chromosomes. Curr. Opin. Cell Biol. *12*, 308–319.

Pluta, A.F., Mackay, A.M., Ainsztein, A.M., Goldberg, I.G., and Earnshaw, W.C. (1995). The centromere: hub of chromosomal activities. Science *270*, 1591–1594.

Saitoh, H., Tomkiel, J., Cooke, C.A., Ratrie, H., Maurer, M., Rothfield, N.F., and Earnshaw, W.C. (1992). CENP-C, an autoantigen in scleroderma, is a component of the human inner kinetochore plate. Cell *70*, 115–125.

Saitoh, S., Takahashi, K., and Yanagida, M. (1997). Mis6, a fission yeast inner centromere protein, acts during G1/S and forms specialized chromatin required for equal segregation. Cell *90*, 131–143.

Starr, D.A., Williams, B., Hays, T.S., and Goldberg, M.L. (1998). ZW10 helps recruit dynactin and dynein to the kinetochore. J. Cell Biol. *142*, 763–774.

Stoler, S., Keith, K.C., Curnick, K.E., and Fitzgerald-Hayes, M. (1995). A mutation in *CSE4*, an essential gene encoding a novel chromatin-associated protein in yeast, cause chromosomes nondisjunction and cell cycle arrest at mitosis. Genes Dev. *9*, 573–586.

Sullivan, K.F. (2001). A solid foundation: functional specialization of centromeric chromatin. Curr. Opin. Genet. Dev. *11*, 182–188.

Sullivan, B.A., Blower, M.D., and Karpen, G.H. (2001). Determining centromere identity: cyclical stories and forking paths. Nat. Rev. Genet. *2*, 584–596.

Takahashi, K., Yamada, H., and Yanagida, M. (1994). Fission yeast minichromosome loss mutants mis cause lethal aneuploidy and replication abnormality. Mol. Biol. Cell *5*, 1145–1158.

Takahashi, K., Chen, E.S., and Yanagida, M. (2000). Requirement of Mis6 centromere connector for localizing a CENP-A-like protein in fission yeast. Science *288*, 2215–2219.

Tomkiel, J., Cooke, C.A., Saitoh, H., Bernat, R.L., and Earnshaw, W.C. (1994). CENP-C is required for maintaining proper kinetochore size and for a timely transition to anaphase. J. Cell Biol. *125*, 531–545.

Tyler-Smith, C., and Floridia, G. (2000). Many paths to the top of the mountain: diverse evolutionary solutions to centromere structure. Cell *102*, 5–8.

Warburton, P.E., Cooke, C.A., Bourassa, S., Vafa, O., Sullivan, B.A., Stetten, G., Gimelli, G., Warburton, D., Tyler-Smith, C., Sullivan, K.F., et al. (1997). Immunolocalization of CENP-A suggests a distinct nucleosome structure at the inner kinetochore plate of active centromeres. Curr. Biol. *7*, 901–904.

Yoda, K., Ando, S., Morishita, S., Houmura, K., Hashimoto, K., Takeyasu, K., and Okazaki, T. (2000). Human centromere protein A (CENP-A) can replace histone H3 in nucleosome reconstitution in vitro. Proc. Natl. Acad. Sci. USA *97*, 7266–7271.

Accession Numbers

The DDBJ/EMBL/NCBI accession number for chicken CENP-I/Mis6 gene is AB073426.

5318–5327 Nucleic Acids Research, 2002, Vol. 30, No. 23

Proteomic analysis of human metaphase chromosomes reveals topoisomerase II alpha as an Aurora B substrate

Ciaran Morrison*, Alexander J. Henzing, Ole Nørregaard Jensen[1], Neil Osheroff[2], Helen Dodson, Stefanie E. Kandels-Lewis, Richard R. Adams and William C. Earnshaw

Wellcome Trust Centre for Cell Biology, Institute of Cell and Molecular Biology, Swann Building, King's Buildings, University of Edinburgh, Mayfield Road, Edinburgh EH9 3JR, UK, [1]Protein Research Group, Department of Biochemistry and Molecular Biology, University of Southern Denmark, Odense University, DK-5230 Odense M, Denmark and [2]Department of Biochemistry, Vanderbilt University School of Medicine, Nashville, TN 37232-0146, USA

Received June 10, 2002; Revised August 27, 2002; Accepted October 12, 2002

ABSTRACT

The essential Aurora B kinase is a chromosomal passenger protein that is required for mitotic chromosome alignment and segregation. Aurora B function is dependent on the chromosome passenger, INCENP. INCENP, in turn, requires sister chromatid cohesion for its appropriate behaviour. Relatively few substrates have been identified for Aurora B, so that the precise role it plays in controlling mitosis remains to be elucidated. To identify potential novel mitotic substrates of Aurora B, extracted chromosomes were prepared from mitotically-arrested HeLa S3 cells and incubated with recombinant human Aurora B in the presence of radioactive ATP. Immunoblot analysis confirmed the HeLa scaffold fraction to be enriched for known chromosomal proteins including CENP-A, CENP-B, CENP-C, ScII and INCENP. Mass spectrometry of bands excised from one-dimensional polyacrylamide gels further defined the protein composition of the extracted chromosome fraction. Cloning, fluorescent tagging and expression in HeLa cells of the putative GTP-binding protein NGB/CRFG demonstrated it to be a novel mitotic chromosome protein, with a perichromosomal localisation. Identification of the protein bands corresponding to those phosphorylated by Aurora B revealed topoisomerase II alpha (topo IIα) as a potential Aurora B substrate. Purified recombinant human topo IIα was phosphorylated by Aurora B *in vitro*, confirming this proteomic approach as a valid method for the initial definition of candidate substrates of key mitotic kinases.

INTRODUCTION

Progression through mitosis is regulated by a number of protein kinases (1). One of these is Aurora B, an essential kinase that is required for chromosome alignment at the metaphase plate and for completion of cytokinesis in metazoan cells (2–7; reviewed in 8). Aurora B may also be involved in mitotic chromosome condensation, but the extent of this involvement is unclear (3,6,9,10). Aurora B is a chromosomal passenger protein. Chromosomal passengers are a class of proteins that show a complex and defined localisation during mitosis; associating along the chromosome during prophase, concentrating at the centromere at metaphase and moving from the centromere to the central region of the mitotic spindle at anaphase (11). Other chromosome passengers include INCENP and survivin, both of which physically interact with Aurora B. INCENP or survivin deficiency causes Aurora B mislocalisation and cellular defects indistinguishable from those occasioned by Aurora B deficiency, while the loss of Aurora B prevents both INCENP and survivin from behaving normally (2,4,6,12–15). The appropriate localisation of INCENP and survivin also requires the cohesin subunit, Scc1 [(16) and C.Morrison, P.Vagnarelli and W.C.Earnshaw, unpublished data], implying that the activities of the chromosome passengers are closely linked to the other key processes occurring during mitosis.

Histone H3 is serine-phosphorylated by Aurora B (2,3,6,14,17), as are CENP-A (18) and myosin II regulatory light chain (19), although the effects of these modifications are not yet clear. The *in vitro* activity of the *Caenorhabditis elegans* Aurora B kinase, AIR-2, is enhanced by the presence of ICP-1, the *C.elegans* INCENP, which is a target for serine phosphorylation by the kinase (20). The budding yeast homologue of Aurora B, Ipl-1p, which is necessary for symmetric chromosome segregation, phosphorylates the kinetochore component Ndc10p (21,22), and a recent model for Ipl-1p function has suggested that an unknown kinetochore

*To whom correspondence should be addressed at present address: Department of Biochemistry, National University of Ireland, Galway, Ireland. Tel: +353 91 512 334; Fax: +353 91 512 504; Email: ciaran.morrison@nuigalway.ie

Ipl-1p target may be the mediator of Ipl-1p control of the attachments between the spindle pole bodies and the kinetochores that result in bipolar kinetochore attachment (23). Clearly, the identification of further substrates of Aurora B kinase is an important issue in defining the mechanism by which the passengers control mitotic events.

Recent advances in the ability to identify peptides present in mixed protein samples using mass spectrometry have provided an invaluable tool for the analysis of cellular subfractions (24–26). One such fraction is the metaphase chromosome, which can be prepared from mitotically-blocked tissue culture cells (27). The chromosome scaffold fraction comprises the residual insoluble, non-histone proteins that remain after extraction of nuclease-digested, isolated metaphase chromosomes by high salt, low ionic strength or chaotropic buffers (27). Proteins that have been identified in this fraction include CENP-E, DNA topoisomerase II and the condensin subunit, ScII (28–31) and kinetochores are also components of the scaffold (32). Candidate Aurora B substrates might be anticipated in metaphase chromosomes, or in the chromosome scaffold fraction. Here we describe experiments in which we characterise the components of partially-extracted metaphase chromosomes using mass spectrometry in order to identify potential Aurora B substrates.

MATERIALS AND METHODS

Cloning, protein overexpression and purification and antibody preparation

An EST containing a cDNA for human Aurora B was obtained from the UK HGMP Resource Centre (Babraham, UK) and subcloned into pGEX4T (Amersham Biosciences UK, Little Chalfont, UK). For site-directed mutagenesis of the pGEX4T-Aurora B construct, the QuikChange kit (Stratagene, La Jolla, CA) was used, following the manufacturer's instructions, with the primer 5′-CAT TTC ATC GTG GCG CTC CGA GTC CTC TTC AAG TCC-3′. Bacterial overexpression and chromatography over glutathione-sepharose was performed as previously described (2). For polyclonal antibody generation, rabbits were immunised with gel-purified GST-Aurora B: this yielded anti-Aurora B antiserum R902. Human topoisomerase II alpha (topo IIα) was expressed and purified from *Saccharomyces cerevisiae* as described previously (33,34).

Total RNA was extracted from HeLa S3 cells using Trizol (Invitrogen, Carlsbad, CA) and reverse transcription using oligo(dT) primers performed using the Superscript system (Invitrogen). Amplification of the CRFG sequence was performed with LA-Taq (Takara Bio, Shiga, Japan) and the product cloned into pEGFP-N1 and pEGFP-C1 (BD Clontech UK, Cowley, UK) using the *Xho*I and *Hin*dIII sites contained in the primers 5′-ACT CGA GAA ATG GCA CAT TAC AAC TTC AAG-3′ and 5′-AAA GCT TTC TCC TGT CCT TTT TAC CAG C-3′, respectively.

Cell culture, transfection and microscopy

HeLa JW cells were grown in RPMI 1640 medium (Invitrogen) supplemented with 10% foetal bovine serum (FBS) and antibiotics, while HeLa S3 cells were grown in the same medium supplemented with only 5% FBS and antibiotics. HeLa S3 cells were treated with colcemid (0.1 μg/ml) for 2 h before harvest and were then hyptotonically swollen in 75 mM KCl for 10 min before being dropped on to polylysine coated slides. Transfection of HeLa JW cells was performed using Fugene 6 reagent (Roche, Basel, Switzerland). For microscopy, cells were fixed with 4% paraformaldehyde and permeabilised with 0.15% Triton in cytoskeleton buffer (137 mM NaCl, 5 mM KCl, 1.1 mM Na_2HPO_4, 0.4 mM KH_2PO_4, 2 mM $MgCl_2$, 2 mM EGTA, 5 mM PIPES, 5.5 mM glucose). Monoclonal anti-α-tubulin B512 was from Sigma (St Louis, MO) and was used in immunofluorescence applications at 1:2000 dilution. The monoclonal AIM-1, which recognises Aurora B, was used at 1:200 dilution and was obtained from BD Transduction Laboratories (Lexington, KY). Rabbit polyclonal anti-topoisomerase II (29) was used at 1:50. Fluorescently labelled secondary antibodies were from Jackson Immunoresearch Laboratories (West Grove, PA) and were used at 1:200 dilution. Micrographs consist of single plane projections of deconvolved, three-dimensional data sets taken with a DeltaVision microscope (Applied Precision, Issaquah, WA) or of images captured with a CCD camera (Princeton Instruments, Trenton, NJ) from an Axioplan 2 microscope (Zeiss, Jena, Germany).

Chromosome preparation and immunoblotting

Chromosomes were prepared by sequential sucrose and Percoll gradients from colcemid-treated HeLa S3 cells according to Lewis and Laemmli (27). Unless otherwise stated, chromosomes were resuspended in 5 mM Tris–Cl pH 7.4, 2 mM KCl, 375 μM spermidine (Sigma, St Louis MO), 0.01% Ammonyx Lo, 1 mM $CaCl_2$ plus protease inhibitors (aprotinin, PMSF and chymostatin, leupeptin, antipain and pepstatin) and digested for 1 h at 4°C with 30 μg/ml micrococcal nuclease (Sigma). For partial extraction (27,35,36), chromosome suspensions were diluted 1:1 with 2× dextran sulphate/heparin lysis buffer [20 mM Tris–Cl pH 8.8, 20 mM Na-EDTA, 0.2% Ammonyx Lo, 0.4 mg/ml dextran sulphate (Amersham), 0.04 mg/ml heparin (Sigma)], incubated for 5 min on ice and spun for 10 min at 10 000 *g*. More extensive extractions were performed as previously described (27,36). Pellets were resuspended in SDS–polyacrylamide gel electrophoresis (SDS–PAGE) sample loading buffer and chromosome protein samples were resolved on SDS–PAGE gels and transferred to nitrocellulose membranes by standard means. Membrane strips were incubated with antibodies to ScII (37) at 1:2500, human anti-centromere antiserum GS (38) at 1:2500, anti-CENP-C (39) at 1:2500, anti-INCENP ra2 (40) at 1:1000 and anti-Aurora B (R902), prepared as described above, at 1:500. Antibody binding was visualised by incubation with ^{125}I-Protein A (Amersham). Immunblotting with the monoclonal MPM-2 (Upstate Biotechnology, Lake Placid, NY) was performed at 1:1000 dilution and signal was visualised by enhanced chemiluminesence (Amersham).

Kinase assays

Chromosomes were resuspended in kinase buffer 1 (10 mM HEPES pH 7.5, 100 mM KCl), kinase buffer 2 (10 mM HEPES pH 7.5, 20 mM KCl), kinase buffer 3 (50 mM Tris–Cl pH 7.5, 100 mM KCl) or kinase buffer 4 (50 mM Tris–Cl pH 7.5, 20 mM KCl), containing 10 mM $MgCl_2$ and 1 mM $CaCl_2$, plus a protease inhibitor cocktail. Following

micrococcal nuclease digestion as described above, heat treatment, if indicated, consisted of 10 min incubation at 65°C followed by at least 5 min incubation on ice. Topo IIα was heat-treated prior to its being incubated with or without Aurora B kinase in kinase buffer. Kinase assays were carried out in the presence of 1 mM ATP, 1 mM dithiothreitol, 20 mM EGTA and 2.5–5 μCi [γ-^{32}P]ATP per 100 μl, along with fresh protease inhibitors, at 37°C for 20 min, at which point reactions were extracted as described above and prepared for SDS–PAGE.

Matrix-assisted laser desorption/ionization time-of-flight mass spectrometry (MALDI-TOF MS)

Protein identification was accomplished by peptide mass fingerprinting and sequence database searching (41). Proteins were separated by SDS–PAGE and relevant protein bands were cut from the gel by using a scalpel. In-gel digestion of protein by trypsin was performed as previously described (42), followed by sample preparation using miniaturised sample concentration/desalting techniques (43). Two separate mass spectrometry research laboratories were involved in these experiments. However, several proteins were identified in both sets of experiments, thereby confirming both protocols. For one preparation of proteins, the mass spectrometry system was Reflex IV (Bruker-Daltonics, Bremen, Germany), for another we used a PerSeptive Biosystems Voyager DE™STR MALDI-TOF mass spectrometer (Applied Biosystems, Foster City, CA). Peptide ion signals were assigned with a mass error <50 p.p.m. Lists of tryptic peptide masses were used to search protein sequence databases using the ProFound internet-based protein identification tool (44) available at http://prowl.rockefeller.edu/cgi-bin/ProFound or the MS-Fit tool (http://prospector.ucsf.edu/ucsfhtml4.0/msfit.htm). For positive identification, a MOWSE (45) score of 10^4 and at least 20% coverage of the protein by the peptide fragments was required for 'small' proteins (<100 kDa), but 5–10% coverage was allowed for high molecular weight proteins (>100 kDa). Where indicated, we used an 'Exp value', which is a probability based expectation value which in all cases provided a significant score for a positive protein identification.

RESULTS

A metaphase chromosome fraction can be prepared from colcemid-treated tissue culture cells by Dounce homogenisation and sequential density gradients (27). The metaphase chromosome scaffold generated by stringent extraction of histones from this fraction includes the kinetochore and contains several prominent protein bands upon SDS–PAGE resolution, notably topoisomerase II and ScII (27,29,32, 35,36). A less stringent procedure was followed here, to retain more chromosome-associated material in the search for candidate Aurora B substrates. To confirm that the resultant fraction, shown in Figure 1A and B, indeed contained the chromosome scaffold proteins, we performed immunoblot analysis with antibodies specific for various proteins expected to be in the scaffold. As shown in Figure 1C, this partially-extracted scaffold contained CENP-A, CENP-B, CENP-C, INCENP, Aurora B and ScII. The monoclonal antibody MPM-2, which recognises a mitotic phosphoepitope, also detected a number of bands. To confirm the reproducibility of this extraction protocol, 11 separate chromosome preparations were run on the same one-dimensional gel. Visual inspection of the band patterns of these different preparations revealed them to have essentially the same composition (data not shown). To examine how this extraction procedure compared with the more stringent protocols previously published, we performed gel electrophoresis on equivalent amounts of chromosomal protein extracted by differing methods. As shown in Figure 1D, there exist clear differences between the protein scaffold fractions prepared by the different extraction methods, but further analysis will be necessary to determine to what extent the content of minor, possibly unknown, components of the scaffolds is increased under the different conditions.

To define the components of this chromosome subfraction, we subjected the preparations to one-dimensional SDS–PAGE (Fig. 1A and B) and excised individual bands from Coomassie-stained gels. MALDI-TOF analysis of the peptide composition of these bands was performed and proteins in the fraction identified by database comparison. Table 1 lists the proteins identified in this initial analysis of the extracted chromosome fraction and Figure 2 summarises these results graphically. Of the 62 proteins identified in the fraction, 29% are nuclear or chromosome-associated. Some 34% are primarily associated with membranes or the cytoskeleton, 18% are mitochondrial, 3% centrosomal and the remainder are from the cytoplasm, act as chaperones or have unknown properties. Since the extent to which the cytoskeletal proteins interact with the chromosomes in forming a scaffold is not clear, some of the cytoskeletal proteins may actually represent chromosome-associated material, rather than artefactual or contaminant protein. We hypothesise that the mitochondria may be co-fractionating with the chromosomes in the Percoll density gradients, which would explain the relatively high proportion of mitochondrial proteins identified.

To test whether the identification of proteins by this method can define new chromosomal proteins, we examined the localisation of the putative GTP-binding protein NGB/CRFG during mitosis. Green fluorescent protein (GFP)-tagging in pEGFP-C1 and transfection of the gene encoding this protein into HeLa JW cells revealed that it forms subnuclear assemblies in interphase, as has been noted previously (46), but that it is associated with chromosomes throughout mitosis (Fig. 3). Transfection with pEGFP-N1-CRFG did not result in any detectable GFP signal and use of the vector alone gave rise to the typical diffuse staining of GFP throughout the cell cycle (data not shown). The perichromosomal localisation, seen clearly in metaphase (Fig. 3B), has been observed for a number of nucleolar proteins, but does not exclude a role for this protein in mitotic chromosomes, nuclear function or in cell cycle control (47,48). These findings confirm that the analysis of scaffolds in this manner is a useful means to discover new proteins associated with mitotic chromosomes.

Since Aurora B itself was shown to be in the chromosome fraction, we tested whether there was a kinase activity associated with the preparation. A number of different buffer conditions were assayed and a reproducible pattern of phosphorylated bands was found to result upon incubation of the chromosomes with [γ-^{32}P]ATP (Fig. 4A), irrespective of the buffer used. This activity was lost upon heat treatment

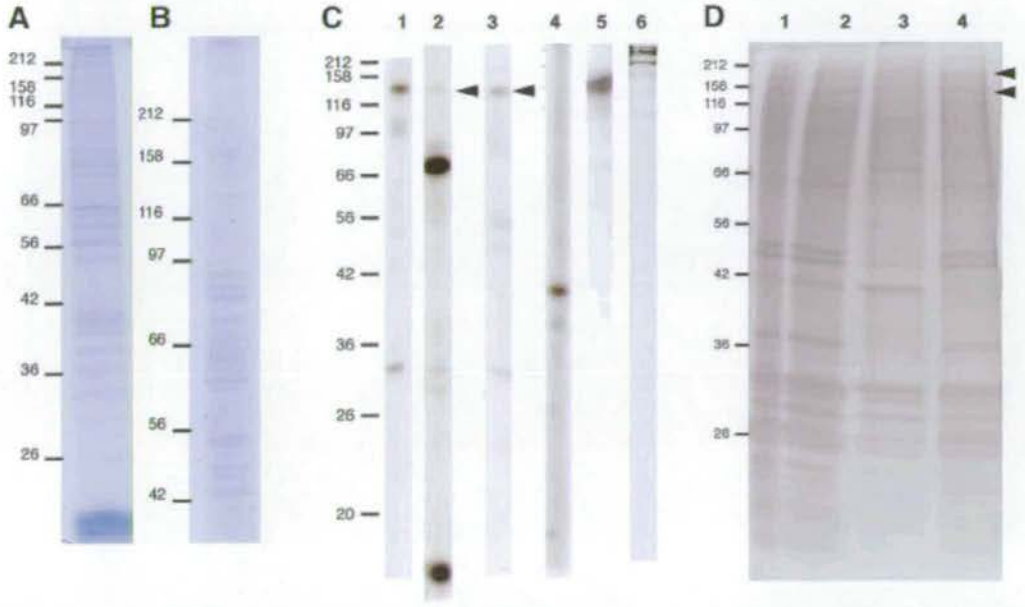

Figure 1. Preparation of chromosome scaffold fractions from colcemid-treated HeLa S3 cells. Proteins were separated by 12.5% (**A**) and 7.5% (**B**) SDS–PAGE and gels stained with Coomassie Blue. Apparent molecular masses are shown in kDa on the left. (**C**) Immunoblot characterisation of the partially-extracted chromosome scaffold fraction. After SDS–PAGE, proteins were transferred to a nitrocellulose membrane and strips of the same membrane were hybridised with antibodies as follows: lane 1, anti-INCENP; lane 2, anti-centromere antibodies (ACA); lane 3, anti-CENP-C; lane 4, anti-Aurora B; lane 5, anti-ScII; lane 6, MPM-2 monoclonal. Arrowheads indicate the CENP-C polypeptide recognised by the ACA and the CENP-C-specific antibody. Apparent molecular masses are shown in kDa on the left. (**D**) Comparison of scaffold fractions resulting from extraction under different conditions. A 12.5% polyacrylamide gel was silver stained after separation of proteins by electrophoresis. To control for protein loading, different cell equivalents were used as follows: lane 1, total chromosomes from 10^6 cells; lane 2, partially-extracted chromosome scaffold prepared as described in this paper from 5×10^6 cells; lane 3, chromosome scaffolds extracted by dextran sulphate-heparin as described (36) from 12.5×10^6 cells; lane 4, chromosome scaffolds extracted by NaCl as described (36) from 12.5×10^6 cells. Arrowheads indicate the two abundant protein bands typically found in chromosome scaffolds, ScI and ScII. Apparent molecular masses are shown in kDa on the left.

(Fig. 4B). At present, the identities of the endogenous kinases that carry out this phosphorylation are unknown.

To identify new potential substrates of Aurora B, we next incubated the heat-inactivated, extracted chromosomes with recombinant human Aurora B kinase. As shown in Figure 4B, incubation of the chromosomes with the recombinant enzyme resulted in the phosphorylation of a number of proteins, notably giving rise to a strong band at the approximate size of the histones. Distinct bands were observed that indicated substrates with apparent molecular masses of approximately 16, 20, 22, 32, 39, 52, 56, 62, 76, 105 and 170 kDa (Fig. 4B). That these were not the same as those found following the incubation of the chromosomes with radiolabel but without recombinant enzyme indicates that Aurora B is not the only kinase in the fraction and that the recombinant enzyme we prepared has a restricted specificity for its activity. Next, to identify candidate substrates for Aurora B, we performed one-dimensional SDS–PAGE and excised bands that corresponded in size to those phosphorylated in parallel experiments (Fig. 4B). MALDI-TOF analysis of these bands identified the proteins listed in Table 2. MALDI-TOF analysis of a negative control region, which contained no distinct bands, gave a complex mixture of peptides and no protein was identified. This list includes a number of potentially relevant Aurora B substrates, based on intracellular distribution. It should be noted that the most common investigator-derived, artefactual keratin contaminants are keratins 1, 2 and 10, so that the keratins 8 and 17 found here are likely real components of the HeLa preparation. Three nuclear proteins—the GTP-binding protein NGB, topo IIα and CAP-C—were identified as candidate Aurora B substrates in this screen, with the DEAD/H box polypeptide 30 representing a possible fourth. It should be noted that the experiment performed to identify potential Aurora B substrates (using ProFound) was carried out at the beginning of our study, separately to the work used to generate the bulk of the data in Table 1 (using MS-Fit, generating MOWSE scores), so that the peptides identified in the screen in Table 2 are clearly not the only components of the bands we examined.

Since it is known that topo IIα is a phosphoprotein (49–54), we then tested whether it could serve as an *in vitro* substrate for Aurora B. Recombinant topo IIα and recombinant Aurora B were co-incubated in the presence of [γ-^{32}P]ATP and we found that Aurora B did indeed phosphorylate the topo-isomerase, as well as itself (Fig. 5). As a control for the specificity of this phosphorylation, we incubated topo IIα with a recombinant kinase-inactive Aurora B in which a key active site residue was mutated from lysine to arginine (7). This protein failed to phosphorylate topo IIα (Fig. 5), confirming that this is an activity derived only from functional Aurora B. It is noteworthy here that the Aurora B activity was very dependent on buffer choice, even though the kinase was active on chromosomes to essentially the same extent in either Tris- or HEPES-containing buffers (data not shown). This may

Table 1. Classification of proteins identified from partially-extracted metaphase chromosomes by intracellular localisation

Apparent mass (kDa)	Protein	MOWSE	Calculated mass	Coverage (%)	GenBank accession no.	Classification
>212	A kinase anchor protein 9 (PRKA9, AKAP450, AKAP350)	1.78E + 09	453671.0	8	Q99996	C
43	Actin	1.76E + 08	40220.4	51	BC012854	S
>212	Actin cross-linking family protein 7	2.80E + 05	620365.6	9	Q9UPN3	S
29	Adenine nucleotide translocator-2	1.94E + 04	32895.4	42	M57424	M
>212	Ankyrin	1.34E + 04	206278.5	8	P16157	S
50	APC2 protein	5.80E + 04	80877.7	16	AJ012652	N
>212	Apolipoprotein D-100	1.54E + 15	515566.9	11	P04114	Y
50	ATP synthase α subunit	2.35E + 11, 8.3E − 5[a]	59750.9	46, 31[b]	D14710	M
49	ATP synthase β subunit	1.54E + 11, 4.2E − 3[a]	56560.2	44, 20[b]	BC010111	M
50	β tubulin	5.24E + 04	49907.3	17	X79535	S
66	BiP	9.25E + 13, 0.039[a]	72333.3	50, 17[b]	AJ271729	S
>212	Breast cancer type 2 susceptibility protein	5.51E + 06	384228.5	6	P51587	N
>212	Bullous pemphigoid antigen 1	8.43E + 07	313090.5	12	Q03001	S
>212	Cadherin 23 precursor (Otocadherin)	7.54E + 10	369527.8	9	Q9H251	S
80	Carnithine palmitoyltransferase I	1.22E + 09	86239.6	30	BC000185	M
<20	Cdc23	1.95E + 04	68285.9	17	AB011472	N
>212	CENP-E	3.77E + 07	312092.9	12	Q02224	N
⩾158	Chromosome-associated polypeptide C	0.016[a]	147090	14[b]	NP_005487	N
>212	Chromodomain helicase-DNA-binding protein 4	7.89E + 05	217992.4	8	Q14839	N
>212	Ciliary dynein	1.14E + 07	511935.6	8	Q9NYC9	Y
>212	Collagen α 3 (VI) chain precursor	1.44E + 04	343555.2	4	P12111	S
90	Cullin 3	4.16E + 08	88930.7	29	AF064087	N
62	DEAD/H box polypeptide 30	2.1E − 3[a]	124173	14[b]	XM_084133	N
>212	Desmoplakin	3.36E + 10	331778.6	15	P15924	S
170	DNA topo II α	1.95E + 04, 0.014[a]	174386.6	10, 6[b]	P11388	N
170	DNA topo II β	3.17E + 04	183298.7	7	Q02880	N
>212	DNA-dependent protein kinase	9.94E + 17	469145.2	16	P78527	N
>212	Dystrophin	2.33E + 08	426680.1	9	P11532	S
82	Glutaminyl-tRNA synthetase	3.43E + 05	87799.2	21	X76013	Y
<20	Glycerol-3-phosphate dehydrogenase	8.20E + 03	44734.8	23	U79250	M
76	GTP-binding protein NGB/CRFG	0.020[a]	73786	12[b]	AF120334	N
66	Heat shock protein, 71 kDa	2.27E + 09	70898.4	40	Y00371	H
62	Hypothetical protein FLJ10709	0.026[a]	66177	15[b]	NP_060658	U
150	Isoleucyl-tRNA synthetase	1.58E + 07	144959.9	12	P41252	Y
>212	Kendrin	7.66E + 10	376355	12	O95613	C
90	Keratin 1	8.93E + 09	66018.0	35	M98776	S
52	Keratin 8	4.8E − 3[a]	53671	25[b]	NP_002264	S
50	Keratin 17	9.3E − 3[a]	48076	34[b]	NP_000413	S
46	KIAA1692 protein	3.51E + 04	97050.6	20	AB051479	U
95	Ksam/FGFR2	1.15E + 07	92832.7	23	AB030075	S
66	Lamin A/C	4.08E + 08	65135.1	21	BC000511	N
95	MAD1	8.16E + 07	83067.3	40	BC009964	N
33	Mitochondrial carrier homologue 2	1.29E + 04	33331.1	37	BC000875	M
82	Mitofilin, inner membrane protein mitochondrion	2.24E + 10	83668.3	35	D21092	M
>212	Monocytic leukemia zinc finger protein	7.14E + 05	225057.8	10	Q92794	N
>212	Myosin	1.02E + 08	224037.7	15	P11055	S
>212	Myosin XV	7.92E + 10	395177.8	9	Q9UKN7	S
66	NADH dehydrogenase precursor, 75kDa subunit	2.41E + 08, 9.8E − 3[a]	79574.1	20, 20[b]	X61100	M
>212	Plectin1	6.83E + 17	531741.0	17	Q15149	Y
29	Prohibitin	1.87E + 04	29804.2	34	S85655	M
>212	Protein-tyrosine phosphatase delta precursor	8.33E + 06	214761.7	13	P23468	N
>212	Ryanodine receptor 2	9.68E + 09	564503.5	8	Q92736	N
>212	Sacsin	1.80E + 07	436980.0	6	Q9NZJ4	H
>212	Spectrin α chain, fodrin	6.61E + 15	284284.3	20	Q13813	S
>212	Spectrin β chain	1.64E + 05	288987.7	7	Q9H254	S
>212	Talin	4.99E + 07	269720.3	9	Q9Y490	S
62	TOB3 AAA ATPase	3.96E + 09	66218.6	38	AK001571	M
40	Tubulin, β	7.23E + 05	50433.0	25	BC000748	S
95	Un-named protein product	7.56E + 06	69753.6	19	AK023035	U
>212	Utrophin	5.07E + 08	394497.6	11	P46936	S
33	VDAC (porin1)	6.52E + 06	30722.7	50	AJ250032	M
>212	Zinc finger protein HRX	1.56E + 06	431895.2	6	Q03164	N

Each protein identified was given only a single classification. Abbreviated classifications were: C, centrosomal; H, chaperone; M, mitochondrial; N, nuclear/chromosomal; S, cytoskeletal/membrane component; U, unknown; Y, cytoplasmic. Apparent masses were derived from the preparative gels from which MALDI-TOF identification was performed. Degradation and/or proteolytic cleavage is assumed to account for sizes significantly smaller than the published molecular weight. MOWSE scores were derived using the MS-Fit tool and 'Exp values'[a] using the ProFound programme.

[a]'Exp values' obtained with ProFound analysis.

[b]Coverage in the experiments generating the Exp value.

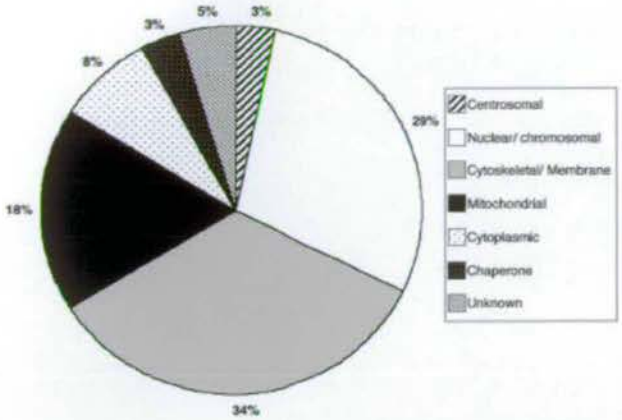

Figure 2. Putative subcellular distribution of 62 proteins identified by MALDI-TOF in the extracted chromosome fraction. Only one localisation was given for any one protein. Table 1 lists these proteins and their individual assignations to a subcellular localisation.

reflect the likely presence of co-factors necessary for optimal activity of the enzyme, e.g. INCENP, in the chromosome preparation, which are not available to the reaction with recombinant protein. Attempts to localise phosphorylation sites using Fe(III)-IMAC and electrospray tandem mass spectrometry (55) revealed one endogenously phosphorylated residue in the recombinant topoisomerase II. No Aurora B phosphorylation sites in topo IIα were identified, due perhaps to the low efficiency of the phosphorylation activity and to the large size and complexity of the topoisomerase molecule (i.e., there are approximately 200 serines and threonines in the peptide sequence). Since there is, as yet, no clear consensus site for the Aurora B kinase, it has been difficult to further explore this observation.

In order for the *in vitro* data to have any significance *in vivo*, topoisomerase II and Aurora B must be able to interact during mitosis. Both are known to be nuclear proteins during mitosis and to examine the relationship between them we performed immunofluorescence localisation experiments. As shown in Figure 6, topo IIα is located along the axis of the chromosomes, while Aurora B is centromeric, as expected. These findings show that at least a subfraction of the topo IIα population is available for phosphorylation by Aurora B and, given recent evidence for the mobility of the topoisomerase (56,57), suggests that Aurora B may be able to phosphorylate a significant amount of this substrate during mitosis.

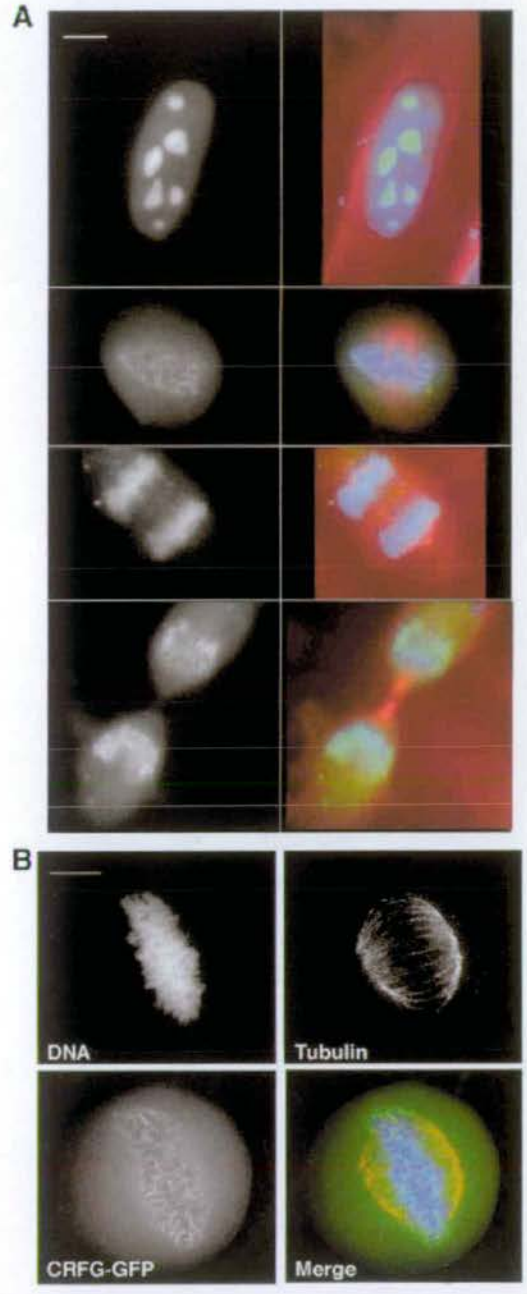

Figure 3. Localisation of NGB/CRFG as a chromosomal protein in mitosis. (**A**) 10^5 HeLa JW cells were transiently transfected with 2 µg pEGFP-C1-CRFG. Cells were fixed 24 h after transfection as described, and were immunostained for α-tubulin and stained with DAPI. Cells in interphase and in different stages of mitosis are shown. Black-and-white images show GFP-CRFG staining, which is shown in green in the merged images. Tubulin staining is shown in red and DNA in blue. Images are of single focal planes. Scale bar is 10 µm. (**B**) Deconvolved image of a transfected cell in metaphase to show the perichromosomal localisation of the GFP-CRFG signal more clearly. Separate channels are shown as indicated and the merged image uses the same colour scheme as in (A).

DISCUSSION

Here we present the first mass spectrometry-driven proteome analysis of metaphase chromosomes prepared from HeLa S3 cells. The preparative method used has been previously used successfully in the identification of CENP-E, DNA topoisomerase II and condensin (28–31), all of which are found in the preparation we describe here. Despite the levels of cytoskeletal and mitochondrial material, the useful percentage of chromosome-associated material found in this preparation makes it an attractive source for further analysis. It is important to note that the relative amount of any given protein in the preparation cannot be assessed by the techniques we used here, as the various peptides from tryptic digests may behave differently during mass spectrometry—indeed, the

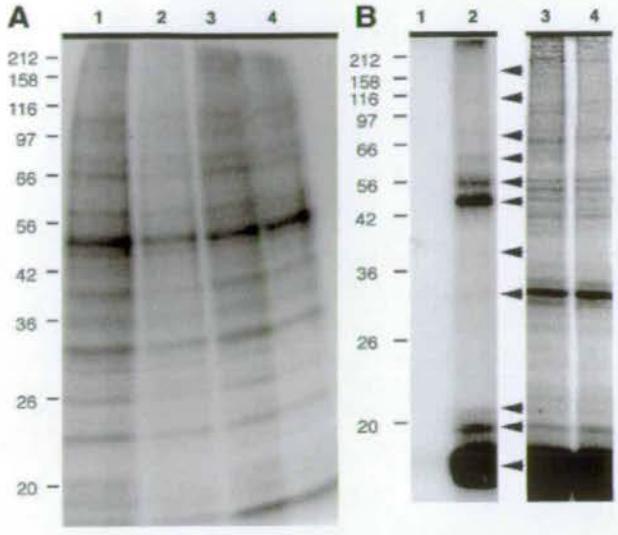

Figure 4. (**A**) Assay for kinase activity in chromosome scaffold fraction. Lanes 1–4 show autoradiographic image of an SDS–polyacrylamide gel used to separate proteins after chromosomes in kinase buffers 1–4, respectively, were incubated with [γ-^{32}P]dATP and then extracted. Apparent molecular masses are shown in kDa on the left. (**B**) Assay for Aurora B kinase substrates in chromosome scaffold fraction. Chromosomes were heat-treated and then incubated in the presence of [γ-^{32}P]dATP without (lanes 1 and 3) or with (lanes 2 and 4) recombinant Aurora B and extracted before being subjected to SDS–PAGE. Lanes 1 and 2 show an autoradiographic image of a 12.5% gel and lanes 3 and 4 show the same gel stained with Coomassie Blue. Arrowheads indicate phosphorylated proteins and apparent molecular masses are shown in kDa on the left.

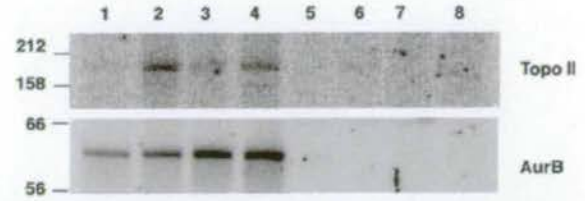

Figure 5. Confirmation of topo IIα as an Aurora B substrate *in vitro*, showing an autoradiograph of an SDS–polyacrylamide gel on which recombinant, heat-treated topo IIα was resolved following incubation with wild-type GST-Aurora B (lanes 1–4) or GST-Aurora B K106R (lanes 5–8) in kinase buffer 1 (lanes 1 and 5), kinase buffer 2 (lanes 2 and 6), kinase buffer 3 (lanes 3 and 7) or kinase buffer 4 (lanes 4 and 8). Apparent molecular masses are shown in kDa on the left.

relatively low scores obtained for the known scaffold component, topoisomerase II, emphasise this point. We attribute the absence of many of the proteins known to be in the scaffold (e.g. the CENP proteins) from the MALDI-TOF profile to their relatively low abundance and to the possibility of their being poor subjects for mass spectrometric analysis. Our observations suggest that the further use of mass spectrometry against a more stringently-extracted scaffold fraction might reveal novel components of the chromosome scaffold that have not been identified by antibodies.

The further characterisation of the unknown and/or poorly-characterised proteins identified in the current screen will require their localisation. This was done for the putative GTP-binding protein NGB/CRFG by fluorescently tagging it and overexpressing it in tissue culture cells. The perichromosomal localisation, seen clearly in metaphase, does not clearly define the likely role of this protein (58–62). It may reflect a nucleolar function for the protein (47), as might be expected from its apparent localisation in interphase (46). However, it may also indicate some role in cell cycle control—a similar mitotic localisation has also been observed for the BCR oncogene product (47,48), which interacts with and activates GTP-binding proteins. The chromosomal localisation of NGB/CRFG we describe here may, therefore, be in some way related to its putative role in renal disease (46), but very little is known about this protein to date.

In the search for new Aurora B substrates, the most likely candidates are those known to have an association with chromosomes or the spindle, such as CAP-C/SMC-4 and topo IIα. Investigation of the *Xenopus* condensin complex showed no mitotic phosphorylation of CAP-C (63). Therefore, topo IIα, which has been well described as a phosphoprotein (49–54), was tested as an Aurora B substrate. Recombinant Aurora B indeed phosphorylated recombinant topo IIα *in vitro*. The functions of DNA topo IIα during mitosis have long been of interest and its phosphorylation, which varies throughout the cell cycle and is regulated by a number of kinases, appears to be of great importance in modulating its activities (64,65). While the localisation of topo IIα during mitosis is somewhat controversial (53,56,66–68), its locations are consistent with its being a potential Aurora B substrate. The localisation of topo IIα at the centromere (69) further enhances the likelihood of the Aurora B interaction being significant, but our inability to specify the target residue(s) by mass spectrometry has

Table 2. Candidate Aurora B substrates identified by MALDI-TOF MS from partially-extracted metaphase chromosomes

Apparent mass (kDa)	Proteins identified
52	Keratin 17
56	ATP synthase, H$^+$ transporting, mitochondrial F1 complex α subunit; ATP synthase, β subunit; keratin 8
62	DEAD/H box polypeptide 30; hypothetical protein FLJ10709
76	GTP-binding protein NGB; NADH-ubiquinone oxidoreductase 75 kDa subunit precursor; BiP protein
170	Topo IIα; chromosome-associated polypeptide C (CAP-C/SMC-4)

Note that additional data are provided for each of these identifications in Table 1; the ProFound analysis refers to these proteins.

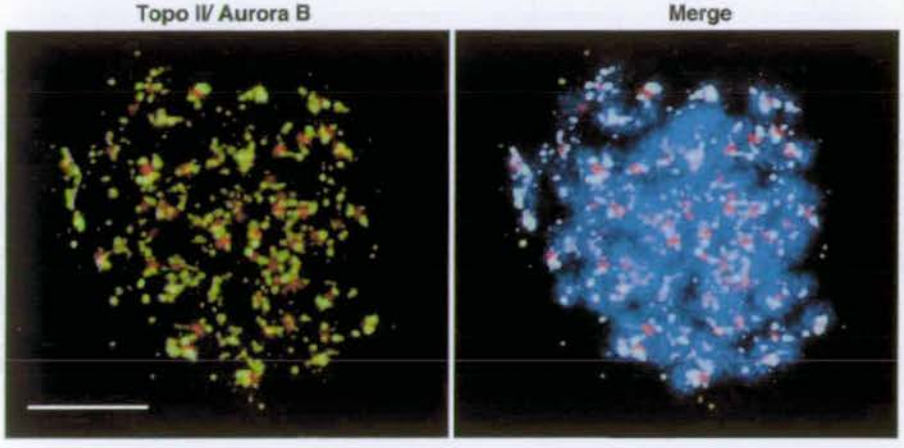

Figure 6. Immunofluorescence localisation of topo IIα and Aurora B. Colcemid-treated, hypotonically swollen HeLa S3 cells were spread and immunostained as described. Deconvolved images show staining for topoisomerase II (green) and Aurora B (red). DNA is shown in blue. Scale bar is 5 μm.

hampered our efforts to define this significance. To date, no consensus Aurora B phosphorylation signal has been described, so we cannot speculate on the potential target residues on topo IIα. While there remain further candidate substrates to be identified, the complexity of the metaphase chromosome fraction may necessitate the use of two-dimensional electrophoresis to resolve phosphorylated proteins sufficiently for their conclusive identification.

In conclusion, we present the proteomic analysis of partially-extracted metaphase chromosomes as a means by which novel mitotic chromosome components may be described and by which chromosomal kinase substrates may be identified. The ability to remove kinase activity endogenous to the preparation by heat treatment means that any kinase may be tested on chromosomes and the more abundant of its potential substrates described.

ACKNOWLEDGEMENTS

We thank Rhys C. Roberts for assistance with phosphopeptide analysis by mass spectrometry and Sally P. Wheatley for help with microscopy. C.M. received an EMBO Long Term Postdoctoral Fellowship during this study. H.D. is the recipient of a Wellcome Trust Prize Studentship. Support was received from the Danish Natural Sciences Research Council to the Danish Biotechnology Instrument Center (O.N.J.). Work in N.O.'s laboratory was supported by NIH grant GM 33944. Work in W.C.E.'s laboratory is supported by the Wellcome Trust, of which he is a Principal Research Fellow.

REFERENCES

1. Nigg,E.A. (2001) Mitotic kinases as regulators of cell division and its checkpoints. *Nature Rev. Mol. Cell Biol.*, **2**, 21–32.
2. Adams,R.R., Maiato,H., Earnshaw,W.C. and Carmena,M. (2001) Essential roles of Drosophila inner centromere protein (INCENP) and aurora B in histone H3 phosphorylation, metaphase chromosome alignment, kinetochore disjunction and chromosome segregation. *J. Cell Biol.*, **153**, 865–880.
3. Giet,R. and Glover,D.M. (2001) Drosophila aurora B kinase is required for histone H3 phosphorylation and condensin recruitment during chromosome condensation and to organize the central spindle during cytokinesis. *J. Cell Biol.*, **152**, 669–682.
4. Kaitna,S., Mendoza,M., Jantsch-Plunger,V. and Glotzer,M. (2000) Incenp and an aurora-like kinase form a complex essential for chromosome segregation and efficient completion of cytokinesis. *Curr. Biol.*, **10**, 1172–1181.
5. Kallio,M.J., McCleland,M.L., Stukenberg,P.T. and Gorbsky,G.J. (2002) Inhibition of aurora B kinase blocks chromosome segregation, overrides the spindle checkpoint, and perturbs microtubule dynamics in mitosis. *Curr. Biol.*, **12**, 900–905.
6. Speliotes,E.K., Uren,A., Vaux,D. and Horvitz,H.R. (2000) The survivin-like *C. elegans* BIR-1 protein acts with the Aurora-like kinase AIR-2 to affect chromosomes and the spindle midzone. *Mol. Cell*, **6**, 211–223.
7. Terada,Y., Tatsuka,M., Suzuki,F., Yasuda,Y., Fujita,S. and Otsu,M. (1998) AIM-1: a mammalian midbody associated protein required for cytokinesis. *EMBO J.*, **17**, 667–676.
8. Adams,R.R., Carmena,M. and Earnshaw,W.C. (2001) Chromosomal passengers and the (aurora) ABCs of mitosis. *Trends Cell. Biol.*, **11**, 49–54.
9. MacCallum,D.E., Losada,A., Kobayashi,R. and Hirano,T. (2002) ISW1 remodeling complexes in Xenopus egg extracts: identification as major chromosomal components that are regulated by INCENP-aurora B. *Mol. Biol. Cell*, **13**, 25–39.
10. Sumara,I., Vorlaufer,E., Stukenberg,P.T., Kelm,O., Redemann,N., Nigg,E.A. and Peters,J.-M. (2002) The dissociation of cohesin from chromosomes in prophase is regulated by polo-like kinase. *Mol. Cell*, **9**, 515–525.
11. Earnshaw,W.C. and Bernat,R.L. (1990) Chromosomal passengers: towards an integrated view of mitosis. *Chromosoma*, **100**, 139–146.
12. Adams,R.R., Wheatley,S.P., Gouldsworthy,A.M., Kandels-Lewis,S.E., Carmena,M., Smythe,C., Gerloff,D.L. and Earnshaw,W.C. (2000) INCENP binds the Aurora-related kinase AIRK2 and is required to target it to chromosomes, the central spindle and cleavage furrow. *Curr. Biol.*, **10**, 1075–1078.
13. Oegema,K., Desai,A., Rybina,S., Kirkham,M. and Hyman,A.A. (2001) Functional analysis of kinetochore assembly in *Caenorhabditis elegans*. *J. Cell Biol.*, **153**, 1209–1226.
14. Uren,A.G., Wong,L., Pakusch,M., Fowler,K.J., Burrows,F.J., Vaux,D.L. and Choo,K.H. (2000) Survivin and the inner centromere protein INCENP show similar cell-cycle localization and gene knockout phenotype. *Curr. Biol.*, **10**, 319–328.
15. Wheatley,S.P., Carvalho,A., Vagnarelli,P. and Earnshaw,W.C. (2001) INCENP is required for proper targeting of Survivin to the centromeres and the anaphase spindle during mitosis. *Curr. Biol.*, **11**, 886–890.

16. Sonoda,E., Matsusaka,T., Morrison,C., Vagnarelli,P., Hoshi,O., Ushiki,T., Nojima,K., Fukagawa,T., Waizenegger,I.C., Peters,J.-M. *et al.* (2001) Scc1/Rad21/Mcd1 is required for sister chromatid cohesion and kinetochore function in vertebrate cells. *Dev. Cell.*, **1**, 759–770.
17. Hsu,J.-Y., Sun,Z.-W., Li,X., Reuben,M., Tatchell,K., Bishop,D.K., Grushcow,J.M., Brame,C.J., Caldwell,J.A., Hunt,D.F. *et al.* (2000) Mitotic phosphorylation of histone H3 is governed by Ipl/ aurora kinase and glc7/PP1 phosphatase in budding yeast and nematodes. *Cell*, **102**, 272–291.
18. Zeitlin,S.G., Shelby,R.D. and Sullivan,K.F. (2001) CENP-A is phosphorylated by Aurora B kinase and plays an unexpected role in completion of cytokinesis. *J. Cell Biol.*, **155**, 1147–1157.
19. Murata-Hori,M., Fumoto,K., Fukuta,Y., Iwasaki,T., Kikuchi,A., Tatsuka,M. and Hosoya,H. (2000) Myosin II regulatory light chain as a novel substrate for AIM-1, an aurora/Ipl1p-related kinase from rat. *J. Biochem. (Tokyo)*, **128**, 903–907.
20. Bishop,J.D. and Schumacher,J.M. (2002) Phosphorylation of the carboxyl terminus of inner centromere protein (INCENP) by the Aurora B kinase stimulates Aurora B kinase activity. *J. Biol. Chem.*, **277**, 27577–27580.
21. Biggins,S., Severin,F.F., Bhalla,N., Sassoon,I., Hyman,A.A. and Murray,A.W. (1999) The conserved protein kinase Ipl1 regulates microtubule binding to kinetochores in budding yeast. *Genes Dev.*, **13**, 532–544.
22. Sassoon,I., Severin,F.F., Andrews,P.D., Taba,M.R., Kaplan,K.B., Ashford,A.J., Stark,M.J., Sorger,P.K. and Hyman,A.A. (1999) Regulation of *Saccharomyces cerevisiae* kinetochores by the type 1 phosphatase Glc7p. *Genes Dev.*, **13**, 545–555.
23. Tanaka,T.U., Rachidi,N., Janke,C., Pereira,G., Galova,M., Schiebel,E., Stark,M.J.R. and Nasmyth,K. (2002) Evidence that the Ipl1-Sli15 (Aurora kinase- INCENP) complex promotes chromosome bi-orientation by altering kinetochore-spindle pole connections. *Cell*, **108**, 317–329.
24. Andersen,J.S., Lyon,C.E., Fox,A.H., Leung,A.K., Lam,Y.W., Steen,H., Mann,M. and Lamond,A.I. (2002) Directed proteomic analysis of the human nucleolus. *Curr. Biol.*, **12**, 1–11.
25. Mann,M., Hendrickson,R.C. and Pandey,A. (2001) Analysis of proteins and proteomes by mass spectrometry. *Annu. Rev. Biochem.*, **70**, 437–473.
26. Mintz,P.J., Patterson,S.D., Neuwald,A.F., Spahr,C.S. and Spector,D.L. (1999) Purification and biochemical characterization of interchromatin granule clusters. *EMBO J.*, **18**, 4308–4320.
27. Lewis,C.D. and Laemmli,U.K. (1982) Higher order metaphase chromosome structure: evidence for metalloprotein interactions. *Cell*, **29**, 171–181.
28. Compton,D.A., Yen,T.J. and Cleveland,D.W. (1991) Identification of novel centromere/kinetochore-associated proteins using monoclonal antibodies generated against human mitotic chromosome scaffolds. *J. Cell Biol.*, **112**, 1083–1097.
29. Earnshaw,W.C., Halligan,B., Cooke,C.A., Heck,M.M. and Liu,L.F. (1985) Topoisomerase II is a structural component of mitotic chromosome scaffolds. *J. Cell Biol.*, **100**, 1706–1715.
30. Fields,A.P. and Shaper,J.H. (1988) A major 62-kD intranuclear matrix polypeptide is a component of metaphase chromosomes. *J. Cell Biol.*, **107**, 833–840.
31. Yen,T.J., Compton,D.A., Wise,D., Zinkowski,R.P., Brinkley,B.R., Earnshaw,W.C. and Cleveland,D.W. (1991) CENP-E, a novel human centromere-associated protein required for progression from metaphase to anaphase. *EMBO J.*, **10**, 1245–1254.
32. Earnshaw,W.C., Halligan,N., Cooke,C. and Rothfield,N. (1984) The kinetochore is part of the metaphase chromosome scaffold. *J. Cell Biol.*, **98**, 352–357.
33. Kingma,P.S., Greider,C.A. and Osheroff,N. (1997) Spontaneous DNA lesions poison human topoisomerase IIalpha and stimulate cleavage proximal to leukemic 11q23 chromosomal breakpoints. *Biochemistry*, **36**, 5934–5939.
34. Wasserman,R.A., Austin,C.A., Fisher,L.M. and Wang,J.C. (1993) Use of yeast in the study of anticancer drugs targeting DNA topoisomerases: expression of a functional recombinant human DNA topoisomerase II alpha in yeast. *Cancer Res.*, **53**, 3591–3596.
35. Adolph,K.W., Cheng,S.M. and Laemmli,U.K. (1977) Role of nonhistone proteins in metaphase chromosome structure. *Cell*, **12**, 805–816.
36. Earnshaw,W.C. and Laemmli,U.K. (1983) Architecture of metaphase chromosomes and chromosome scaffolds. *J. Cell Biol.*, **96**, 84–93.
37. Saitoh,N., Goldberg,I.G., Wood,E.R. and Earnshaw,W.C. (1994) ScII: an abundant chromosome scaffold protein is a member of a family of putative ATPases with an unusual predicted tertiary structure. *J. Cell Biol.*, **127**, 303–318.
38. Earnshaw,W.C. and Rothfield,N. (1985) Identification of a family of human centromere proteins using autoimmune sera from patients with scleroderma. *Chromosoma*, **91**, 313–321.
39. Tomkiel,J.E., Cooke,C.A., Saitoh,H., Bernat,R.L. and Earnshaw,W.C. (1994) CENP-C is required for maintaining proper kinetochore size and for a timely transition to anaphase. *J. Cell Biol.*, **125**, 531–545.
40. Mackay,A.M., Eckley,D.M., Chue,C. and Earnshaw,W.C. (1993) Molecular analysis of the INCENPs (inner centromere proteins): separate domains are required for association with microtubules during interphase and with the central spindle during anaphase. *J. Cell Biol.*, **123**, 373–385.
41. Jensen,O.N., Larsen,M.R. and Roepstorff,P. (1998) Mass spectrometric identification and microcharacterization of proteins from electrophoretic gels: strategies and applications. *Proteins Struct. Func. Genet.*, Suppl **2**, 74–89.
42. Shevchenko,A., Wilm,M., Vorm,O. and Mann,M. (1996) Mass spectrometric sequencing of proteins silver-stained polyacrylamide gels. *Anal. Chem.*, **68**, 850–858.
43. Gobom,J., Nordhoff,E., Mirgorodskaya,E., Ekman,R. and Roepstorff,P. (1999) Sample purification and preparation technique based on nano-scale reversed-phase columns for the sensitive analysis of complex peptide mixtures by matrix-assisted laser desorption/ionization mass spectrometry. *J. Mass Spectrom.*, **34**, 105–116.
44. Zhang,W. and Chait,B.T. (2000) ProFound: an expert system for protein identification using mass spectrometric peptide mapping information. *Anal. Chem.*, **72**, 2482–2489.
45. Pappin,D.J.C., Hojrup,P. and Bleasby,A.J. (1993) Rapid identification of proteins by peptide-mass fingerprinting. *Curr. Biol.*, **3**, 327–332.
46. Laping,N.J., Olson,B.A. and Zhu,Y. (2001) Identification of a novel guanosine triphosphate-binding protein differentially expressed in renal disease. *J. Am. Soc. Nephrol.*, **12**, 883–890.
47. Hernandez-Verdun,D. and Gautier,T. (1994) The chromosome periphery during mitosis. *Bioessays*, **16**, 179–185.
48. Wetzler,M., Talpaz,M., Yee,G., Stass,S.A., Van Etten,R.A., Andreeff,M., Goodacre,A.M., Kleine,H.D., Mahadevia,R.K. and Kurzrock,R. (1995) Cell cycle-related shifts in subcellular localization of BCR: association with mitotic chromosomes and with heterochromatin. *Proc. Natl Acad. Sci. USA*, **92**, 3488–3492.
49. Escargueil,A.E., Plisov,S.Y., Filhol,O., Cochet,C. and Larsen,A.K. (2000) Mitotic phosphorylation of DNA topoisomerase IIα by protein kinase CK2 creates the MPM-2 phosphoepitope on Ser-1469. *J. Biol. Chem.*, **275**, 34710–34718.
50. Heck,M.M., Hittelman,W.N. and Earnshaw,W.C. (1989) *In vivo* phosphorylation of the 170-kDa form of eukaryotic DNA topoisomerase II. Cell cycle analysis. *J. Biol. Chem.*, **264**, 15161–15164.
51. Ishida,R., Iwai,M., Marsh,K.L., Austin,C.A., Yano,T., Shibata,M., Nozaki,N. and Hara,A. (1996) Threonine 1342 in human topoisomerase IIalpha is phosphorylated throughout the cell cycle. *J. Biol. Chem.*, **271**, 30077–30082.
52. Kimura,K., Nozaki,N., Enomoto,T., Tanaka,M. and Kikuchi,A. (1996) Analysis of M phase-specific phosphorylation of DNA topoisomerase II. *J. Biol. Chem.*, **271**, 21439–21445.
53. Taagepera,S., Rao,P.N., Drake,F.H. and Gorbsky,G.J. (1993) DNA topoisomerase IIα is the major chromosome protein recognized by the mitotic phosphoprotein antibody MPM-2. *Proc. Natl Acad. Sci. USA*, **90**, 8407–8411.
54. Wells,N.J., Fry,A.M., Guano,F., Norbury,C. and Hickson,I.D. (1995) Cell cycle phase-specific phosphorylation of human topoisomerase II alpha. Evidence of a role for protein kinase C. *J. Biol. Chem.*, **270**, 28357–28363.
55. Stensballe,A. and Jensen,O.N. (2001) Simplified sample preparation method for protein identification by matrix-assisted laser desorption/ ionization mass spectrometry: in-gel digestion on the probe surface. *Proteomics*, **1**, 955–966.
56. Christensen,M.O., Larsen,M.K., Barthelmes,H.U., Hock,R., Andersen,C.L., Kjeldsen,E., Knudsen,B.R., Westergaard,O., Boege,F. and Mielke,C. (2002) Dynamics of human DNA topoisomerases IIα and IIβ in living cells. *J. Cell Biol.*, **157**, 31–44.

57. Tavormina,P.A., Come,M.G., Hudson,J.R., Mo,Y.Y., Beck,W.T. and Gorbsky,G.J. (2002) Rapid exchange of mammalian topoisomerase II alpha at kinetochores and chromosome arms in mitosis. *J. Cell Biol.*, **158**, 23–29.
58. Chaly,N., Bladon,T., Setterfield,G., Little,J.E., Kaplan,J.G. and Brown,D.L. (1984) Changes in distribution of nuclear matrix antigens during the mitotic cell cycle. *J. Cell Biol.*, **99**, 661–671.
59. Dilworth,S.M. (1991) A perichromosomal region contains proteins phosphorylated during mitosis in *Xenopus laevis* cells. *J. Cell Sci.*, **98**, 309–315.
60. McKeon,F.D., Tuffanelli,D.L., Kobayashi,S. and Kirschner,M.W. (1984) The redistribution of a conserved nuclear envelope protein during the cell cycle suggests a pathway for chromosome condensation. *Cell*, **36**, 83–92.
61. Wataya-Kaneda,M., Kaneda,Y., Sakurai,T., Sugawa,H. and Uchida,T. (1987) A monoclonal antibody against the nucleus reveals the presence of a common protein in the nuclear envelope, the perichromosomal region, and cytoplasmic vesicles. *J. Cell Biol.*, **104**, 1–7.
62. Yasuda,Y. and Maul,G.G. (1990) A nucleolar auto-antigen is part of the major chromosomal surface component. *Chromosoma*, **99**, 152–160.
63. Kimura,K., Hirano,M., Kobayashi,R. and Hirano,T. (1998) Phosphorylation and activation of 13S condensin by Cdc2 *in vitro*. *Science*, **282**, 487–490.
64. Wang,J.C. (1996) DNA topoisomerases. *Annu. Rev. Biochem.*, **65**, 635–692.
65. Warburton,P.E. and Earnshaw,W.C. (1997) Untangling the role of DNA topoisomerase II in mitotic chromosome structure and function. *Bioessays*, **19**, 97–99.
66. Earnshaw,W.C. and Heck,M.M.S. (1985) Localization of topoisomerase II in mitotic chromosomes. *J.Cell Biol.*, **100**, 1716–1725.
67. Sumner,A.T. (1996) The distribution of topoisomerase II on mammalian chromosomes. *Chromosome Res.*, **4**, 5–14.
68. Swedlow,J.R., Sedat,J.W. and Agard,D.A. (1993) Multiple chromosomal populations of topoisomerase II detected *in vivo* by time-lapse, three dimensional wide-field microscopy. *Cell*, **73**, 97–108.
69. Rattner,J.B., Hendzel,M.J., Furbee,C.S., Muller,M.T. and Bazett-Jones,D.P. (1996) Topoisomerase II alpha is associated with the mammalian centromere in a cell cycle- and species-specific manner and is required for proper centromere/kinetochore structure. *J. Cell Biol.*, **134**, 1097–1107.